AD 702 845

PROPELLER-SHAFT THRUST BEARING ANALYSIS-PHASE 1

B. Sternlicht, et al

General Electric Company
Schenectady, New York

May 1959

GENERAL
ENGINEERING
LABORATORY

PROPELLER-SHAFT THRUST BEARING ANALYSIS - PHASE I

by

B. Sternlicht
E. B. Arwas

Report No. 59GL81

May 1, 1959

GENERAL ELECTRIC

PROPELLER SHAFT THRUST BEARING ANALYSIS-PHASE I

Property of The Department of The Navy

Prepared Under Contract Nobs 74682

GENERAL ELECTRIC

General Engineering Laboratory

SCHENECTADY, NEW YORK

TECHNICAL INFORMATION SERIES

AUTHOR	SUBJECT CLASSIFICATION	NO. / DATE
B. Sternlicht E. B. Arwas	Thrust Bearings	59GL81 DATE 5/1/59

TITLE

Propeller-Shaft Thrust Bearing Analysis-Phase I

ABSTRACT

1. An analysis of centrally pivoted tilting pad bearings in the size and speed ranges of propeller shaft application is given. Temperature distribution in the oil film and pad deformation under load are considered. The analysis is made for finite sector shaped pads and moment equilibrium of the pivot is satisfied. 2. A set of design charts which show minimum film thickness, maximum temperature, hydrodynamic oil flow and horsepower loss as functions of unit load and speed for the range of 15" to 36" O.D. bearings is included. 3. The effects of pad subtended angle, pad thickness, radial pivot location and groove mixing temperature on load carrying capacity are considered.

G.E. CLASS	REPRODUCIBLE COPY FILED AT LIBRARY OF GENERAL ENGINEERING LABORATORY SCHENECTADY, NEW YORK	NO. PAGES
I		167
GOV. CLASS. None		

CONCLUSIONS

1. Centrally pivoted pads carry load by virtue of thermal wedge and pad bending. Both these effects must be included to obtain realistic data. 2. Bearing performance is limited by maximum temperature as well as by minimum film thickness. 3. Maximum temperature is an accurate measure of bearing load. It can therefore be used to indicate load and to monitor performance. 4. From the stand point of minimum film thickness, there is an optimum pad angle for each condition of operation. However, within the range studied (30.5° to 51°), maximum temperature decreases with pad angle. 5. Groove mixing temperature has a major effect on bearing performance. 6. Pad thickness and radial pivot location can be optimized for each application.

INFORMATION PREPARED FOR Medium Steam Turbine Generator and Gear Department

TESTS MADE BY

AUTHOR B. Sternlicht *Ben Sternlicht* E. B. Arwas *E. Arwas*

COUNTERSIGNED L. J. Collins *L. J. Collins* H. Apkarian *H. Apkarian* R. O. Fehr *R. O. Fehr*

COMPONENT Bearing and Lubricant Center, Schenectady

5-29-59

GL-16-C

GENERAL ELECTRIC

General Engineering Laboratory

SCHENECTADY, NEW YORK

DISTRIBUTION LIST

TIS REPORT NO 59GL81

Lynn River Works, Medium Steam Turbine, Generator and Gear Department

A. T. Chandonnet	Building 4-64S
L. J. Collins	Building 2-41 (4)
A. Howard	Building 2-64S
O. Pinkus	Building 2-41A
M. A. Prohl	Building 2-64S
C. Rohde	Building 2-64S
N. A. Smith	Building 2-41
H. Spears	Building 2-64S
T. W. Steele	Building 2-41A
F. L. Weaver	Building 5-64S

Washington, D.C., Southeastern District Office, Appartus Sales Division
777 Fourteenth Street, N. W.

T. Hutchins
T. H. Shepard

Fitchburg, Small Steam Turbine Department

H. J. Chase
S. Neal
A. E. Truran

Schenectady, Large Steam Turbine-Generator Department

H. C. Bahr	Building 273-217
R. E. Brandon	Building 69-424
P. G. Ipsen	Building 273-215
R. Sheppard	Building 273-334
G. B. Warren	Building 273-450

Schenectady, Gas Turbine Department

B. O. Buckland	Building 53-420
C. W. George	Building 53
W. J. Leishman	Building 53-420

GL-289

GENERAL ELECTRIC

General Engineering Laboratory

SCHENECTADY, NEW YORK

DISTRIBUTION LIST

TIS REPORT NO. 59GL81

Schenectady, Large Motor and Generator Department

B. L. Goss	Building 41-303
T. C. Johnson	Building 41-324
R. B. McKeeby	Building 41-328
H. D. Snively	Building 273-334

Schenectady, Electric Utility Engineering Department

G. K. Carter	Building 2 - 627
F. J. Maginniss	Building 2 - 621

Schenectady, Medium A. C. Motor Department

E. R. Booser	Building 50-312
M. E. Petersen	Building 46-1
E. R. Summers	Building 50 371
D. H. Ware	Building 18A-5

Schenectady, Small A. C. Motor Department

F. W. Baumann	Building 81-210

Schenectady, General Engineering Laboratory

H. Apkarian,	Building 37-1020 (2)
E. B. Arwas	Building 37-1020
R. C. Elwell	Building 37-1020
R. O. Fehr	Building 37-311
G. R. Fox	Building 37-1020
E. H. Farr	Building 37-248
L. G. Gitzendanner	Building 37-317
E. F. Magnusson	Building 37-248
B. Sternlicht	Building 37-1020
J. F. Young	Building 5-107B

General Engineering Laboratory Library

Reproducible

GL-200

TABLE OF CONTENTS (i)

ACKNOWLEDGEMENTS

The authors would like to acknowledge the assistance of the following personnel of the General Engineering Laboratory:

Dr. E. Farr and Mr. E. F. Magnusson who reprogrammed the numerical solution of the Reynolds and Energy Equations, in order to adapt it to an IBM 650 digital computer with floating decimal point. This greatly reduced the time required for the calculations.

Miss M. E. Haas who performed all the computer calculations.

The authors would also like to acknowledge the assistance of:

Mr. J. C. Reid, Jr. of the Bureau of Ships, who furnished them with considerable technical guidance and data essential to the performance of the work. Mr. Reid also assisted in the selection of bearing sizes for calculation.

Mr. L. J. Collins of the Medium Steam Turbine, Generator and Gear Department who gave them all personal assistance asked of him and who guided and encouraged them in the performance of the work.

Mr. C. Rohde of the Medium Steam Turbine, Generator and Gear Department who authorized publication in this report of the calculated data on the 51-1/2" O. D. x 32" I. D. bearing, which was obtained under a separate contract with his department.

LIST OF TABLES

LIST OF FIGURES

Figure Number	Caption

BACKGROUND AND SCOPE

In 1958 the General Engineering Laboratory made a study of propeller shaft thrust bearing operation and reported its findings in Reference 1. Following this study a comprehensive analytical and experimental program was undertaken, for the purpose of extending present understanding of these bearings and in order to provide a body of design information for use in bearing design and selection. This program, like the preceding introductory study, is being performed under a contract awarded by the Bureau of Ships to General Electric Company's Medium Steam Turbine, Generator and Gear Department.

The program is divided into three phases as follows:

Phase I: Investigate analytically the performance of propeller shaft thrust bearings using the existing Reynolds-Energy Method of solution to provide data necessary in design and selection of these bearings.

Phase II: Extend existing analytical techniques for propeller shaft thrust bearings by including a numerical method of solution of the Elasticity Equation. Review, and where necessary, modify the design data obtained in Phase I, so as to include the effects of pad distortion caused by pressure distribution and thermal gradients.

Phase III: Instrument thrust bearings on two U. S. Navy ships and obtain experimental data on the performance of these bearings. This data is to be obtained in tests carried out at the time of scheduled sea trials. The thrust bearing performance measurements obtained in these sea trials is to be used for correlation with the design data obtained analytically in Phases I and II.

A fourth phase which included the building of a thrust bearing test stand was contemplated but was not included in the present program, since the findings of the program could be used to determine the features of the stand.

The following is our final report on Phase I.

I INTRODUCTION

Virtually all ships in this country, both merchant and combat, use Kingsbury type tilting pad bearings to transmit the propeller thrust to the hull of the vessel. The geometry of these bearings and the principles on which they operate are well known and are described in most texts on lubrication as well as in the catalogues of Kingsbury Machine Works.

Generally, the bearing pads are centrally pivoted, i.e., the spherical pivot back of each pad is located mid-way between the leading and the trailing edges. Central pivot location is required for reversibility, i.e., for operation under either direction of shaft rotation.

Conventional bearing calculations in which temperature variations in the oil film are neglected and in which a converging wedge is formed by the tilting of a flat pad, fail to predict the load carrying capacity of centrally pivoted bearings. The reason for this is illustrated in Figure 1 (a) which shows the hydrodynamic pressure profile that is generated between flat surfaces separated by fluid film that converges slightly in the direction of motion. Under these conditions, calculations show that the resultant of the hydrodynamic pressures lies downstream of the radial centerline of the pad. Since the reaction to these pressures must pass through the pivot, a moment exists which tends to eliminate the convergence and hence load carrying capacity. However, when the temperature variations in the oil film and the deformation of the pad under load are considered in the analysis, the somewhat paradoxical result obtained above is eliminated. Calculations then show that there is a value of pad inclination (generally other than zero) for which the resultant of the hydrodynamic pressures passes through the central pivot as shown in Figure 1 (b).

As the oil flows through the bearing gap, its temperature rises due to the shearing of the film. This rise in temperature produces a "thermal wedge" action which accounts for part of the load carrying capacity of the bearing (provided that the viscosity and mass density of the lubricant decrease with temperature rise, which is the case for all known oils). Early in the program, calculations were made to determine the magnitude of the thermal wedge effect in a centrally pivoted finite pad. A sector shaped pad of a 31" 8-shoe bearing was analyzed, first with the pivot in optimum position and then with the pivot centrally located. In both cases, the pad was assumed to remain flat and the other operating conditions were:

Speed - 320 RPM
Minimum Film Thickness - 0.001"
Oil - 2190T
Oil Temperature at Pad Inlet - 130°F

The results are shown in Figures 2 (a) and 2 (b). It is seen that the thermal wedge effect allows the flat centrally pivoted pad to carry approximately 56% of the load carried by the pad with optimum pivot. At the same time, the maximum temperature reached with the flat centrally pivoted pads is 25°F higher than that reached in the pad with optimum pivot. Experience, however, suggests that the difference in performance between central and optimum pivot locations is not so severe. It was, therefore, decided at that time that, in order to make a more realistic analysis in Phase I, it should be extended to incorporate a simplified elasticity approach which allows pad deformation to be approximated and included in the calculation. Figure 2 (c) shows the load and maximum temperature of the 31" 8-shoe centrally pivoted bearing pad under the same operating conditions but with pad deformation included. Comparison of Figures 2 (a) and 2 (c) now show that the centrally pivoted pad is capable of carrying approximately 92% of the load carried by the flat pad with optimum pivot. Its maximum temperature is 6°F higher than that of the flat pad with optimum pivot. These results are in better agreement with experimental evidence and the method of analysis which includes a simplified elasticity solution has been used in all succeeding calculations.

(To the extent that pad deformation was included in the Phase I calculations the results presented in this report have anticipated those to be obtained in Phase II. In the latter phase, the Elasticity Equation is more rigorously solved and includes, in addition, thermal deformation of the pad. However, it requires a considerably more elaborate digital computer program. It may be expected that comparison between the two sets of results will suggest modifications of the Phase I approach to yield a simple yet sufficiently rigorous method of solution.)

The conflict between the isothermal, flat pad method of solution and experience with centrally pivoted pads has been realized, since the time that Albert Kingsbury accomplished his pioneering work on slider bearing performance (Ref. 2). More recently, interest in the effects of thermal wedge and of pad deformation has resulted in analytical studies of infinitely wide bearings, some of which are reported in References 3, 4 and 5. For the case of the finite bearings, the importance of including the effects of temperature variations in the oil film has been studied by one of the authors of this report and it is explained in Reference 6. To the best knowledge of the authors, the present report is the first published study of finite centrally pivoted pad bearings in which the effects of radial and tangential inclinations, temperature variations in the oil film, and pad deformation are all considered. The results obtained have shown good agreement with experience. They have indicated that pad deformations are of the order of the minimum film thicknesses and they have explained such test results as:

1. bearing failures caused by high pad temperatures.

2. occurrence of bearing failures in the vicinity of the pivot.
3. insensitivity of trailing edge film thicknesses at high loads.

In order to make the Phase I study as complete as possible, approximately 70% more cases were analyzed than were called for in the contract for this phase. In all, 262 operating points were calculated. At each operating point, the values of radial and tangential pad inclination which satisfied equilibrium of moments were obtained using a trial and error procedure. This procedure required an average of 5 solutions of the Reynolds and Energy Equations for each operating point, so that the total number of solutions exceeded 1300.

The studies were conducted as follows:

1. Eight standard bearings were analyzed which scanned the range of present day propeller shaft bearing sizes (19" O. D. to 50" O. D.) and propeller speeds (100 R. P. M. to 320 R. P. M.). Each bearing was analyzed at two speeds and with 6, 8 and 10 pad geometries. Calculations were made at three values of minimum film thicknesses, at each speed and geometry. These calculations have yielded the value and location of the minimum film thickness, the temperature and pressure distributions, the oil flow and horsepower loss as functions of bearing size, number of pads, unit load and speed. In particular, they have shown the optimum number of pads as a function of bearing size, unit load and speed.

2. The ahead bearing of DD933 (U. S. S. Barry) was analyzed at the full speed ahead conditions. Its astern bearing was similarly analyzed at full speed astern condition. (The U. S. S. Barry was earlier selected by the Bureau of Ships to be the first ship for sea trial thrust bearing tests under Phase III of the program. The thrust bearings of the starboard shaft of this ship were instrumented and the tests at sea have just been completed.)

3. The ahead bearing of DL1 (U. S. S. Norfolk) was analyzed under full speed ahead operation. This bearing was selected for analysis because of the past history of several successive failures.

4. A 31" O. D. x 15-1/2" I. D. bearing was extensively analyzed in order to investigate the effects of pad thickness and radial pivot location on bearing performance.

5. A 31" O. D. x 15-1/2" I. D. and the 39" O. D. x 19-1/2" I. D. bearing were further analyzed to determine the effect of pad inlet oil temperature on bearing performance. In particular the effect of pad inlet temperature on load carrying capacity and maximum temperature were investigated.

6. Additional bearing sizes ranging up to 100" O. D. were analyzed to investigate the relationship between bearing size, pad thickness and unit loading.

7. A 51-1/2" O. D. x 32" I. D. bearing with 10 and 12 shoe geometries was analyzed at 200 R. P. M. and at 400 R. P. M. These analyses were made under separate contract with General Electric Company's Medium Steam Turbine, Generator and Gear Department who authorized their inclusion in the present report. They are of interest because the upper speed is quite high and the results illustrate some of the thrust bearing operating characteristics that will be encountered as propeller speeds are raised.

II ANALYSIS AND METHOD OF CALCULATION

The important considerations in thrust bearing analysis are:

1. Pressure distribution and hence load carrying capacity
2. Temperature distribution
3. Location of the center of pressure
4. Oil flow
5. Horsepower loss

all as functions of the bearing geometry, film shape and speed.

In this section, the equations from which these quantities can be calculated are given. The film shape which includes the effects of pad inclinations and deformation is discussed, as are the groove mixing temperature and the viscosity-temperature relation. Before proceeding to these, however, it is necessary to point out here the principal limitations of the analysis.

1. The analysis applies only to steady state conditions. It does not supply any information on the transient conditions that occur during start up and shut down. It also does not apply to dynamic load conditions (such as crash ahead and crash astern) when relative axial motion between the runner and the bearing introduces squeeze film effects.

2. Laminar conditions prevail in the oil film. Actually the Reynolds Number in present day propeller shaft thrust bearings is small enough for this condition to be satisfied under steady state operation. This is illustrated by the following calculation for an extreme case:

$$
\begin{aligned}
D &= 50'' \\
N &= 320 \text{ RPM} \\
h &= 0.002'' \\
\mu &= 1 \times 10^{-6} \text{ lb.-sec/in.}^2 \\
\rho &= 0.803 \times 10^{-4} \text{ lb.-sec.}^2/\text{in.}^4 \\
U_{max} &= 840 \text{ in./sec.}
\end{aligned}
$$

$$\text{Reynolds Number (Maximum)} = \frac{\rho \, U_{max} \, h}{\mu} = 135$$

3. Oil inertia effects are negligible. At the relatively low surface speeds of propeller shaft thrust bearings, this assumption too is quite valid.

4. The fluid is incompressible.

5. Variation of the specific heat of the oil with temperature are neglected.

A. Reynolds and Energy Equations and Their Boundary Conditions

The Reynolds Equation describes the hydrodynamic pressures generated in the oil film of a bearing. These pressures separate the bearing and runner surfaces when there is a relative motion between them. For a finite pad, the Reynolds Equation in polar coordinates is (Ref. 7):

$$\frac{\partial}{\partial r}\left(\frac{rh^3}{\mu}\frac{\partial p}{\partial r}\right)+\frac{\partial}{\partial\theta}\left(\frac{h^3}{\mu r}\frac{\partial p}{\partial\theta}\right) = 6\,\omega r\,\frac{\partial h}{\partial\theta} \qquad (1)$$

The boundary conditions that are needed for the solution of this equation arise from the fact that the pressure falls to zero at the pad perimeter.

With the coordinate system shown in Figure 3, the boundary conditions are then:

$$p_{(r,\,0)} = p_{(R-L,\,\theta)} = p_{(r,\theta_T)} = p_{(R,\,\theta)} = 0 \qquad (2)$$

Because the oil film may break down in diverging regions in the bearing, it is necessary to impose an additional condition which states that the pad pressures never fall below atmospheric.

In order to include in the analysis the effects of temperature (and hence viscosity) variations in the oil film, the Energy Equation has to be solved together with the Reynolds Equation. The Energy Equation can be written (Ref. 7):

$$\frac{\mu}{h}(\omega r)^2 + \frac{h^3}{12\mu}\left[\frac{\partial p}{r\partial\theta}^{2} + \left(\frac{\partial p}{\partial r}\right)^2\right] - C_p\,\rho\, g\, J\left[\left(\frac{r\omega h}{2} - \frac{h^3}{12\mu}\frac{\partial p}{r\partial\theta}\right)\frac{\partial T}{r\partial\theta} - \frac{h^3}{12\mu}\frac{\partial p}{\partial r}\frac{\partial T}{\partial r}\right] = 0 \qquad (3)$$

In Equation (3) it is assumed that the oil flow through the clearance space is adiabatic. All the heat generated within the fluid due to fluid shear is considered to be carried away by the mass transfer of the fluid and no heat is gained, or lost through the bearing surfaces. This is a comparatively good assumption, for the heat transfer coefficient at the fluid boundaries is very small. (Reference 8)

The boundary conditions used for the solution of Equation 3 are that

a) the pad inlet oil is at the groove temperature and

b) the radial temperature gradient is zero along the inner and outer circumferences to the pad because of the cooling effect of the surrounding oil.

Thus:

$$T_{(r,o)} = T_{GR} \tag{4}$$

$$\left(\frac{\partial T}{\partial r}\right)_{(R-L\ \theta)} = \left(\frac{\partial T}{\partial r}\right)_{(R,\ \theta)} = 0$$

With the introduction of the proper film shape, the solutions of Equations (1) and (3) yield the pressure and temperature distributions on the bearing pads.

B. Load Carrying Capacity

The total reaction of each bearing pad and hence the load it carries is given by the integral of the hydrodynamic pressures over the pad area. Thus:

$$W = \int_{R-L}^{R} \int_{0}^{\theta_T} p\ r\ dr\ d\theta \tag{5}$$

C. Oil Flow

Oil is introduced into each pad through the clearance space at its leading edge, by the motion of the runner. Part of this oil leaves the clearance space in the same manner from the trailing edge. The remaining part of the oil is forced out from all edges by the pressure gradients that are built up over the bearing surface. Referring to Figure 3, the oil flow (in G. P. M.) through the four edges is:

Flow into the pad:

$$\frac{231}{60}\ Q_1 = \int_{R-L}^{R} \left(\frac{\omega r h}{2}\right)_{\theta=0} dr - \int_{R-L}^{R} \left(\frac{h^3}{\mu r}\ \frac{\partial p}{\partial \theta}\right)_{\theta=0} dr \tag{6}$$

Flow out of the pad:

$$\frac{231}{60}\ Q_2 = \int_{0}^{\theta_T} \left(\frac{h^3 r}{\mu}\ \frac{\partial p}{\partial r}\right)_{r=R-L} d\theta \tag{7}$$

$$\frac{231}{60}\, Q_3 = \int_{R-L}^{R} \left(\frac{\omega r h}{2}\right)_{\theta = \theta_T} dr + \int_{R-L}^{R} \left(\frac{h^3}{\mu r}\, \frac{\partial p}{\partial \theta}\right)_{\theta = \theta_T} dr \tag{7}$$

$$\frac{231}{60}\, Q_4 = \int_{0}^{\theta_T} \left(\frac{h^3 r}{\mu}\, \frac{\partial p}{\partial r}\right)_{r = R} d\theta$$

It is seen that the flow through the leading and trailing edges is made of two components. The first of these is independent of the pressure gradients and it is referred to as the "Shear Flow". The second component depends on the pressure gradients and it is referred to as the "Pressure Gradient Flow".

Since there is no relative radial motion between the runner and the bearing pads, there is only "Pressure Gradient Flow" out of the inner and outer circumferential boundaries of the bearing pads.

D. Horsepower Loss

It is assumed that all of the heat generated in the oil film goes into temperature rise of the oil. Thus, the horsepower loss can be computed from the oil flow through the bearing pads and its temperature rise. Thus:

$$HP_2 = \frac{C_p \rho g}{0.707} \int_{0}^{\theta_T} \left[\frac{h^3 r}{\mu}\, \frac{\partial p}{\partial r}\, (T - T_{GR})\right]_{r = R-L} d\theta$$

$$HP_3 = \frac{C_p \rho g}{0.707} \left\{ \int_{R-L}^{R} \left[\frac{\omega r h}{2}\, (T - T_{GR})\right]_{\theta = \theta_T} dr + \int_{R-L}^{R} \left(\frac{h^3}{\mu r}\, \frac{\partial p}{\partial \theta}\, (T - T_{GR})\right)_{\theta = \theta_T} dr \right\} \tag{8}$$

$$HP_4 = \frac{C_p \rho g}{0.707} \int_{0}^{\theta_T} \left[\frac{h^3 r}{\mu}\, \frac{\partial p}{\partial r}\, (T - T_{GR})\right]_{r = R} d\theta$$

1 the total horsepower loss per pad is

$$HP = HP_2 + HP_3 \quad HP_4 \tag{9}$$

E. Center of Pressure

The point on the pad surface through which the resultant of the hydrodynamic pressures acts is called the center of pressure. Its coordinates are given by:

$$r_{cp} = \frac{\left\{\left[\int_{R-L}^{R}\int_{0}^{\theta_T} p\, r^2 \cos\theta \, dr\, d\theta\right]^2 + \left[\int_{R-L}^{R}\int_{0}^{\theta_T} p\, r^2 \sin\theta \, dr\, d\theta\right]^2\right\}^{1/2}}{W}$$

$$\theta_{cp} = \tan^{-1}\left\{\frac{\int_{R-L}^{R}\int_{0}^{\theta_T} p\, r^2 \sin\theta \, dr\, d\theta}{\int_{R-L}^{R}\int_{0}^{\theta_T} p\, r^2 \cos\theta \, dr\, d\theta}\right\} \tag{10}$$

F. Film Shape

Under the hydrodynamic pressures and the pivot reaction, each pad bends so that the bearing surface becomes slightly convex, as shown in Figure 1 (b). The shape that the pad assumes under load can be calculated from a solution of the Elasticity Equation and this is done in Phase II. For the present, however, it is assumed that the bearing surface becomes very slightly spherical. In accordance with plate theory, the bending deflections are taken to be proportional to load and inversely proportional to the pad thickness cubed. Since the pads are ball seated, they also tilt in both radial and tangential directions, till moment equilibrium is satisfied.

The film shape is then (see Appendix):

$$h = h_a + m_\theta\left[r_a \sin\left(\theta_a - \frac{\theta_T}{2}\right) - r \sin\left(\theta - \frac{\theta_T}{2}\right)\right] - m_r\left[r_a \cos\left(\theta_a - \frac{\theta_T}{2}\right) - r\cos\left(\theta - \frac{\theta_T}{2}\right)\right]$$
$$+ \frac{1}{2R_c}\left[r^2 - r_a^2 - 2\, r\, r_p \cos(\theta - \theta_p) + 2\, r_a r_p \cos(\theta_a - \theta_p)\right] \tag{11}$$

For cases where loads are light and the bending deflections are small, it is convenient to use as reference, the point at the inside radius and trailing edge of the pad. Equation (11) then becomes (for a centrally pivoted pad):

$$h = h_1 + m_\theta\left[(R-L)\sin\frac{\theta_T}{2} - r\sin\left(\theta - \frac{\theta_T}{2}\right)\right] - m_r\left[(R-L)\cos\frac{\theta_T}{2} - r\cos\left(\theta - \frac{\theta_T}{2}\right)\right]$$
$$+ \frac{1}{2R_c}\left[r^2 - (R-L)^2 + 2(R-L)\,r_p\cos\frac{\theta_T}{2} - 2\,r\,r_p\cos\left(\theta - \frac{\theta_T}{2}\right)\right] \tag{12}$$

For cases where the loads are large and the bending deflections are of the same order as the minimum film thickness, the point of minimum film thickness may fall within the pad boundary. It is then more convenient to use this point as reference. Its coordinates can be obtained by differentiating Equation (11) and setting:

$$\frac{\partial h}{\partial r} = 0 \qquad \text{and} \qquad \frac{\partial h}{\partial \theta} = 0$$

The coordinates of the point of minimum film thickness are then found to be:

$$r_m = R_c\left[m_\theta^2 + \left(\frac{r_p}{R_c} - m_r\right)^2\right]^{1/2}$$
$$\theta_m = \frac{\theta_T}{2} + \tan^{-1}\left(\frac{m_\theta}{\frac{r_p}{R_c} - m_r}\right) \tag{13}$$

Substituting Equation (13) into Equation (11), the film thickness profile becomes (for a centrally pivoted pad):

$$h = h_{min} + \frac{R_c}{2}\left[m_\theta^2 + \left(\frac{r_p}{R_c} - m_r\right)^2\right] + r\left[m_\theta\sin\left(\theta - \frac{\theta_T}{2}\right) + \left(\frac{r_p}{R_c} - m_r\right)\cos\left(\theta - \frac{\theta_T}{2}\right) - \frac{r}{2R_c}\right] \tag{14}$$

In Equations 11 through 14 above, R_c is the radius of curvature of the bent pad. In the present analysis, it is calculated from the load and pad thickness (see Appendix) using the relation:

$$\frac{1}{2R_c} = 0.75 \times 10^{-8}\,\frac{W}{t^3_{avg}} \tag{15}$$

where W is the load per pad

t_{avg} is the mean thickness of the pad

G. Oil Groove Temperature

The temperature at which the oil enters the clearance space between the runner and the pads has an important effect on the load carrying capacity of the bearing. It is introduced in the analysis as one of the boundary conditions of Equation (3).

In general, the temperature of the oil in the feed grooves between the pads is several degrees higher than at the housing inlet ports. This difference is largely due to the mixing in each groove with hot oil discharged from the trailing edge of the downstream pad. It is, therefore, significantly affected by such factors as:

a) quantity of oil admitted to the housing (this is generally several times the amount that flows through the clearance spaces.)

b) extent of the grooves

c) pad discharge temperature

In the Phase I calculations, the pad groove temperatures are obtained from the experimental data of several investigators. The experimental points are plotted in Figure 4 and a representative curve is drawn through them. This curve shows the feed groove temperature as a function of the unit load carried by the bearing, when the oil temperature at housing inlet is 115 F.

Figure 4 is, of course, an average curve. In the experimental work on which it is based, the oil flow through the bearing housing was four to five times the clearance flow and the total area of the grooves was 15% of the effective runner area.

Different values of these quantities or the location of major heat sources or sinks near the bearing housing would be expected to affect the groove temperature.

H. Viscosity-Temperature Relation

The viscosity-temperature relation of the lubricant is required in the simultaneous solution of Equations (1) and (3). In all the Phase I calculations, the lubricant properties used were those of 2190T oil.

The absolute viscosity versus temperature plot for 2190T oil is shown in Figure 5.

I. Numerical Solution of the Reynolds and Energy Equations

A finite difference procedure was used to solve the Reynolds and Energy Equations. These, however, were first put in dimensionless form (Equations A-2 and A-5 of the Appendix) in order to facilitate comparison between geometrically similar bearings.

The finite difference form of the dimensionless Reynolds and Energy Equations are given by Equations A-4 and A-7 of the Appendix. These are two sets of algebraic equations that can be solved on a digital computer using an iterative procedure. Their solutions yield the pressure and temperature profiles over the pad surface.

Figure 6 is a typical thrust bearing sector pad, divided into a mesh of m x n sections. Referring to Equation A-4 and Figure 6, it is seen that the dimensionless pressure $\bar{p}_{i,j}$ at any point is expressed in terms of the corresponding dimensionless pressures, viscosities and film thicknesses. The boundary condition states that the pressure is zero around the periphery of the sector. In order to meet this condition, the pressures at fictitious image points outside the boundary are set equal in magnitude but opposite in sign to the pressures at the corresponding points inside the boundary. By employing a process of iteration the m x n equations represented by Equation A-4 are solved on the computer and the pressures $\bar{p}_{i,j}$ are determined at each mesh centerpoint. The process of iteration is continued until the difference between successive values of the sum of the pressures converges to within a prescribed error. In this analysis, the error is specified to be less than 0.1%, i.e.

$$\text{Error} = \frac{\sum_{j=1}^{m} \sum_{i=1}^{n} \left[(\bar{p}_{i,j})_k - (\bar{p}_{i,j})_{k-1} \right]}{\sum_{j=1}^{m} \sum_{i=1}^{n} (\bar{p}_{i,j})_k} < 0.001 \qquad (16)$$

The load carrying capacity of a bearing is greatly influenced by the oil viscosity. The temperature (hence the viscosities) at each mesh point are obtained from the solution of Equation A-7 . The boundary conditions for this equation are introduced by setting: a) the temperature, along the inlet edge equal to the groove temperature and b) the temperatures at fictitious image points outside the inner and outer circumferential boundaries equal in magnitude and sign to those at the corresponding points inside the boundaries.

The steps for the simultaneous solution of the Reynolds and Energy Equations are then performed in the following manner:

(1) The value of the film thickness at every point is determined.

(2) $\bar{p}_{i,j}$ is assumed equal to zero and the known value of inlet temperature is assigned to $\bar{T}_{i,j}$

(3) The values of $\bar{T}_{i,j}$ are then determined at every point from equation A-7

(4) The values of $\bar{\mu}_{i,j}$ are calculated from values of $\bar{T}_{i,j}$

(5) Having the values of $\bar{\mu}_{i,j}$, $\bar{h}_{i,j}$ and $\bar{p}_{i,j}$, the first approximation of the pressure field is determined from equation A-4 and improved several times by iteration.

(6) The value of the pressure field thus obtained is used to recalculate the temperature distribution from which a new set of $\bar{\mu}_{i,j}$ values is determined.

(7) A second approximation of the pressure field is now obtained. This cycle of pressure and temperature iterations is continued until the error, which is the difference between successive values of the pressure field, falls within the limit prescribed in equation 16.

(8) The final value of the pressure field is then used to compute the final value of the temperature field.

(9) The total pad load, oil flow, horsepower loss and the coordinates of the center of pressure are calculated by means of Equations A-8, A-10, A-15 and A-16.

J. Trial and Error Procedure for Pivoted Pad Bearings

At each operating point, the pad deformation has to be related to the pad load in accordance with Equation 15. The film shape which depends on this deformation and on the inclinations of the pad has to be such that the resulting center of pressure passes through the pivot. Finally, the groove temperature used has to be related to the unit loading in accordance with Figure 4. In order to meet these requirements, the following trial and error procedure was used:

(1) For the bearing geometry being studied, select a value of minimum film thickness.

(2) Estimate the corresponding unit load and hence the groove temperature (T_{GR}) and the bending coefficient ($K = 1/2R_c$).

(3) Select values of radial and tangential inclinations (m_θ and m_r respectively).

(4) Introduce the above as input data and obtain the corresponding computer solution.

(5) From the computer output data determine the coordinates of the center of pressure and the actual unit load (and hence the actual groove temperature and bending coefficient). Check whether these agree with the estimated ones within the following error limits:

$$
\begin{aligned}
&\text{a)} \quad \left|(T_{GR})_{actual} - (T_{GR})_{estimated}\right| \leq 2^{\circ}F \\
&\text{b)} \quad \left|(K)_{actual} - (K)_{estimated}\right| \leq 2 \times 10^{-6}\ \text{in.}^{-1} \\
&\text{c)} \quad \left|r_{cp}\,\% - r_p\,\%\right| \leq 0.5\% \\
&\text{d)} \quad \left|\theta_{cp}\,\% - \theta_p\,\%\right| \leq 0.5\%
\end{aligned}
\qquad (17)
$$

If any of the conditions, a through d of Equation 17, are not satisfied, steps 2 through 5 are repeated until all errors are within the specified limits.

This procedure was found to require an average of 5 trial computer solutions for each operating point obtained.

K. Estimate of Errors

A 7 x 7 mesh was used in the numerical solution of the Reynolds and Energy Equations. This was the finest mesh size that could be accommodated with an IBM 650 computer for the present program. Previous experience of the authors has indicated that satisfactory accuracy can be achieved with the 7 x 7 mesh, provided there are no sharp inflexion points in the film thickness profile. As an additional check, the calculations for one case were repeated on a larger computing machine, using a 13 x 13 mesh. The results agreed with those obtained using the 7 x 7 mesh within 1%.

The error limits defined in Equation 17 were set up in order to limit the number of iterations required for each solution. On the basis of calculations carried out with smaller allowable errors, the effects of the limits set in Equation 17 are estimated to be:

Error in calculated maximum temperature $\leq$ 5°F
Error in calculated minimum film thickness $\leq$ 0.0001"

In the calculation of the hydrodynamic oil flow and the horsepower loss, additional errors are introduced in the numerical calculation of the pressure gradients at the pad edges (see equations A-13 and A-15). Particularly at high loads, where the pad bending deflections are correspondingly large, errors in the calculated values of hydrodynamic oil flow and horsepower loss may be as high as 20%.

III RESULTS

1. Eight bearings ranging in size from 19" to 50" diameter were analyzed, each at two speeds in the range 100 to 320 RPM. These were:

BEARING SIZE (O.D." x I.D.")	SPEEDS (RPM)
19 x 9-1/2	160 and 310
25 x 12-1/2	120 and 240
31 x 15-1/2	180 and 320
37 x 18-1/2	180 and 320
39 x 19-1/2	150 and 200
41 x 20-1/2	100 and 200
45 x 22-1/2	100 and 170
50 x 25	100 and 170

These bearings were all geometrically similar, with the following properties:

$$\frac{L}{R} = \frac{1}{2} \qquad k = 0.85$$

$$\frac{t_{avg}}{R} = 0.154 \qquad r_p\% = \theta_p\% = 50$$

In all cases, 6, 8, and 10 pad geometries were analyzed. The results are given in Tables 1 through 8 and plotted in Figures 7 through 46.

2. The ahead and astern bearings of the USS Barry (DD933) and the ahead bearing of the USS Norfolk (DL1) were studied at their full speed condition. These are:

	SIZE (O.D." x I.D.")	NUMBER OF PADS	SPEED (RPM)
Astern Bearing USS Barry*	26 x 17-1/2	8	160
Ahead Bearing USS Barry	31 x 16-1/2	8	320
Ahead Bearing USS Norfolk	35 x 18-1/2	8	170

The results are given in Tables 9 through 11 and plotted in Figures 48 through 56.

- - - - - - - - - - -

* In the case of the astern bearing of DD933, Figure 47 was used to determine T_{GR}. This is because the grooves between the pads of the bearing amounted to approximately 35% of the effective runner area, as compared with about 15% in the other bearings. In the absence of data for this size groove, Figure 47 was obtained from Figure 4, considering the groove temperature rise to be inversely proportional to the extent of the grooves

3. In order to estimate the effects of pad thickness, radial pivot location, groove temperature and bearing size, several additional calculations were made varying these parameters one at a time. The calculations were made for the following:

Bearing Size (O. D." x I. D.")	No. of Pads	Speeds (RPM)	$\frac{t_{avg}}{R}$	r_p%	T_{GR}
31 x 15-1/2	6, 8 and 10	180 and 320	0.130	50	Per Figure 4
31 x 15-1/2	6, 8 and 10	180 and 320	0.193	50	Per Figure 4
31 x 15-1/2	6, 8 and 10	180 and 320	0.154	53	Per Figure 4
31 x 15-1/2	6, 8 and 10	180 and 320	0.154	47	Per Figure 4
31 x 15-1/2	8	180 and 320	0.154	50	130°F
39 x 19-1/2	8	150 and 200	0.154	50	130°F
19 x 9-1/2	6, 8 and 10	100	0.154	50	Per Figure 4
75 x 37-1/2	6, 8 and 10	100	0.154	50	Per Figure 4
100 x 50	6, 8 and 10	100	0.154	50	Per Figure 4
19 x 9-1/2	6	100	0.130	50	Per Figure 4
45 x 27-1/2	6	100	0.130	50	Per Figure 4
75 x 37-1/2	6	100	0.130	50	Per Figure 4
100 x 50	6	100	0.130	50	Per Figure 4

The results are given in Tables 12 through 21 and plotted in Figures 57 through 81.

4. A 51-1/2" O. D. x 32" I. D. bearing that was analyzed under separate contract with M. S. T. G. &G. Dept. has also been included in this report. The geometry and operating conditions were:

Bearing Size (O. D. x I. D.)	No. of Pads	Speeds (RPM)	$\frac{t_{avg}}{R}$	r_p%	T_{GR}
51-1/2 x 32	10 and 12	200 and 400	0. 117	52. 6	Per Figure 4

The results are given in Table 22 and plotted in Figures 82 through 86.

IV DESIGN CHARTS

In order to facilitate design and selection of thrust bearings, where the outer diameter is roughly twice the inner diameter, the data in Tables 1 through 8 was used to arrive at a set of design charts. These are given in Figures 87 through 98. Note that in these charts (as in the other figures in this report) solid lines represent data within the range of calculations and dashed lines indicate extrapolated values.

When the oil film temperatures in Tables 1 through 8 are plotted, it is seen that both the maximum and the average temperatures are, with good accuracy, functions only of the unit load, number of shoes and pad inlet temperature. This allows the maximum and average temperature to be represented on a single chart, Figure 87. The accuracy of this chart, up to $T_{max} = 235^oF$, is $\pm 5^oF$. Above $T_{max} = 235^oF$, the accuracy is $\pm 10^oF$.

The minimum film thickness is a function of bearing size and speed as well as unit loading, number of shoes and pad inlet temperature. It is represented here as a function of these variables, in the set of nine charts, Figures 88 through 96. The accuracy of these charts is $\pm$ 0.0001" within the calculated regions. In the extrapolated regions, errors may be somewhat larger.

The hydrodynamic oil flow per pad is plotted in Figure 97, as a function of the dimensionless parameter $\left(\frac{\mu_{avg} U_{avg}}{p_{avg} B}\right)$ As was pointed out earlier, the oil flow calculations are subject to significant error (in some cases as high as 20%), in part because of the numerical approximation of the pressure gradient at the pad edges. It is also necessary to keep in mind that the oil flow given by Figure 97 is only that which flows through the clearance spaces between the runner and the bearing pads. The total flow furnished to the bearing should be several times this quantity.

The friction horsepower loss per pad is plotted in Figure 98, also as a function of the dimensionless parameter $\left(\frac{\mu_{avg} U_{avg}}{p_{avg} B}\right)$ This horsepower loss is dependent on the calculated oil flow and is thus subject to the same errors. In addition, it should be noted that Figure 98 shows only the horsepower loss due to fluid shear in the oil film. There are additional losses in the bearing, such as those due to turbulence in the oil grooves.

The example below illustrates the use of the charts.

Example: Compare the performance of 6 8 and 10 pad geometries for a 35" O. D. x 17-1/2" I. D. bearing at a speed of 280 RPM and a unit load of 650 psi. (Oil 2190T, k = 0.85 in all cases)

	6 Pad	8 Pad	10 Pad
p_{avg} at h_{min} = 0.0010" (Per Figures 88, 91 and 94)	528	520	453
p_{avg} at h_{min} = 0.0008" (Per Figures 89, 92 and 95)	623	663	620
p_{avg} at h_{min} = 0.0006" (Per Figures 90, 93 and 96)	745	832	815
$\therefore$ h_{min} at p_{avg} = 650 psi (by interpolation)	0.0075"	0.0082"	0.0077"
T_{max} at 650 psi (Per Figure 87) - °F	237	215	207
T_{avg} at 650 psi (Per Figure 87) - °F	185	185	184
μ_{avg} (Per Figure 5)	1.8×10^{-6}	1.8×10^{-6}	1.8×10^{-6}
$U_{avg} = 2\pi (R - L/2) N$ - in/sec	385	385	385
$B = (R - L/2)\,\theta_T = (R - L/2)\,\frac{2k\pi}{n}$ - in.	11.7	8.76	7.01
$\left(\frac{\mu_{avg}\, U_{avg}}{p_{avg}\, B}\right) \times 10^6$	0.091	0.122	0.152
$\left(\frac{Q}{B\, L\, U_{avg}}\right) \times 10^6$ (Per Figure 97)	24.9	24.7	24.6
Q GPM	0.98	0.73	0.58
Q_{tot} GPM (= n x Q)	5.9	5.8	5.8
$f \times 10^3$ (Per Figure 98)	0.97	1.01	1.12
$HP = \frac{f\, B\, L\, p_{avg}\, U_{avg}}{6600}$	3.77	2.94	2.61
HP_{tot} (= n x HP)	22.6	23.5	26.1

V DISCUSSION AND CONCLUSIONS

1. The two principal criteria of thrust bearing performance are the minimum film thickness and the maximum temperature. The present analysis, which was limited to 6, 8 and 10 pad bearings, showed that:

   a) For each condition of operation (bearing size, load and speed), there is an optimum number of pads, from the standpoint of minimum film thickness. This can be seen by comparing the design charts, Figures 88 through 96.

   b) The maximum temperature can be decreased by increasing the number of pads in the bearing. This gain is greatest in the critical high load regions as shown in Figure 87.

   Note also from Figure 87 that the maximum temperature is a very sensitive indicator of bearing load. This is in contrast to the oil temperature which is little influenced by load changes.

2. At low loads, the minimum film thickness occurs at the inside radius of the trailing edge. However, as the bearing load (and hence the pad deformation) increases, the point of minimum film thickness moves toward the pivot, as shown in Figure 99. This figure shows that the radial location of the point of minimum film thickness moves quite rapidly towards the center region of the pad. It can be concluded from this that failures which result from small dirt particles in the oil film are most likely to occur near the pivot. This is borne out by experience.

   Figure 99 also shows that the location of the point of minimum film thickness is dependent on the pad subtended angle. Thus, it moves inward from the trailing edge most rapidly in the case of the 6 pad bearing.

   The marked divergence, at high loads, between the minimum film thickness and the film thickness at the inside radius of the trailing edge is also shown in Figure 100. In fact this figure shows that at high loads, the film thickness at the inside radius of the trailing edge becomes almost insensitive to load changes.

3. The effect of pad thickness is illustrated in Figures 101. Note that there is an optimum pad thickness at each specific load, from both the standpoints of minimum film thickness and maximum temperature. At low loads, thinner pads are preferable for the deformation there allows a more favorable film shape. At high loads, on the other hand, deformations become excessive and reduce load carrying capacity.

4. Since propeller shaft bearings are required to operate under either direction of rotation, the pivot location can be varied only radially. Figure 102 shows the effect of radial pivot location on minimum film thickness and maximum temperature, for several values of unit loading. Both these sets of curves indicate that there is an optimum pivot location, that varies with unit loading. The optimum locations obtained from the two sets of curves are, however, different. Thus, from the standpoint of minimum film thickness, the optimum pivot location approaches the mean radius from the outer circumference, as the unit loading increases. From the standpoint of maximum temperature on the other hand, the optimum pivot location approaches the mean radius from the inner circumference, also as the unit load increases.

5. The groove mixing temperature plays a very important role in bearing performance. Figure 103 shows the reduction in load carrying capacity that accompanies a rise in the groove temperature. This reduction is a major one, as indicated in the following table (obtained from Figure 103):

h_{min} "	T_{GR} °F	p_{avg} psi	T_{max} °F
0.0006	130	1030	220
0.0006	158	800	235

Thus, for a constant minimum film thickness, a reduction of 28°F in groove temperature achieves an increase of 28% in unit load, together with a reduction of 15°F in the maximum temperature.

6. For a geometrically similar series of bearings, the unit loading will increase with bearing size (at a given angular speed and minimum film thickness) as shown, for example, in Figure 81. This is of course due to the higher surface speed of the larger bearings. Note however, that the slope of the curve decreases quite rapidly due to the rise in groove mixing temperature and bending deflections. This points up again the importance of these two factors on bearing performance.

7. Early in this report, it was pointed out that the inclusion of thermal wedge and pad bending in the analysis explains the load carrying capacity of centrally pivoted pads. The load carrying capacities of a flat pad bearing with optimum pivot location and of a centrally pivoted pad were then compared in Figure 2, for a particular pad geometry. It should be noted, however, that the hydrodynamic pressure profiles differ markedly in the two cases, as shown in Figure 104.

8. In the present analysis, heat conduction was neglected. Thus, the calculated maximum film temperatures are somewhat higher than those which occur in practice. (The calculated values are therefore conservative.) Furthermore, whereas the calculated maximum temperatures are at the trailing edge, in practice they will occur at a small distance inward, also because of conduction.

V. RECOMMENDATIONS

1. The simplified analysis that was used here has shown that several aspects of bearing geometry, such as number of pads, pad thickness and radial pivot location, have a significant effect on load carrying capacity. The effect of number of pads was studied for a large range of bearing sizes. The effects of the other factors were studied for a 31" O.D. x 15-1/2" I.D. bearing. It is desirable to:

   a) Verify the results using a more rigorous elasticity analysis (as is being done in Phase II).

   b) Extend the results obtained to bearings with different L/R ratios.

   c) Obtain experimental verification (PhaseIII and contemplated thrust bearing test machine.)

2. Groove mixing temperature plays a very important role in determining the load carrying capacity of thrust bearings. Gains in load capacity on the order of 25% can be achieved if mixing in the grooves can be inhibited, thus lowering the pad inlet temperature of the oil. This suggests an investigation aimed at developing suitable baffles in the oil grooves which would reduce the carry over of hot oil from the downstream pad. (A reduction in the oil temperature at housing inlets also serves to improve performance.)

3. The major importance of pad geometry and groove mixing temperature on bearing performance indicate that design modifications can be made to greatly increase the load carrying capacity of tilting pad bearings. In such designs, consideration should be given to multi-point supports and to shaped pad surfaces as well as to the other aspects of bearing geometry studied in this report. Advantage should also be taken of the elasticity of the pads in optimizing the bearing design.

4. The present analysis was limited to steady state conditions. Analytical and experimental investigations are necessary in order to arrive at means of predicting bearing performance under transient conditions, such as acceleration, crash maneuvers, start up under load (as in a submerged submarine) and others.

5. Metallurgical work is badly needed to-day to set up operating temperature limits of the various babbitts in use as well as to develop alternative materials.

6. In future analytical work, the effect of thermal conduction should be studied.

7. The extent of misalignment present in thrust bearing installations on board ship needs to be investigated. In parallel with this, the degree of load equalization between pads and the load carrying capacity of the bearings under misalignment should be analyzed.

APPENDIX

APPENDIX

1. Finite Difference Equations

The numerical solution of the Reynolds and Energy Equations by means of finite differences is described in Reference 11. Here a brief outline of the procedure is given.

For convenience of comparison between geometrically similar pads, the Reynolds and Energy Equations are first put in dimensionless form.

Let
$$r = R\,\bar{r} \qquad p = 12\pi N' \mu_{GR}\,\bar{p}\left[\text{where } N' = \left(\frac{R}{h_a}\right)^2 N\right]$$
$$h = h_a\,\bar{h}$$
$$\theta = \bar{\theta} \tag{A-1}$$
$$\mu = \mu_{GR}\,\bar{\mu} \qquad T = \frac{12\pi N' \mu_{GR}}{\rho\, g\, J\, C_p}\,\bar{T}$$

Introducing Equation (A-1) into Equation (1) of the text, we obtain the Reynolds Equation in dimensionless form:

$$\frac{\partial}{\partial \bar{r}}\left(\frac{\bar{r}\bar{h}^3}{\bar{\mu}}\frac{\partial \bar{p}}{\partial \bar{r}}\right) + \frac{\partial}{\bar{r}\partial \bar{\theta}}\left(\frac{\bar{h}^3}{\bar{\mu}}\frac{\partial \bar{p}}{\partial \bar{\theta}}\right) - \frac{\bar{r}\partial \bar{h}}{\partial \bar{\theta}} = 0 \tag{A-2}$$

Referring to Figure 6, we can write

$$\frac{\partial}{\partial \bar{r}}\left(\frac{\bar{r}\bar{h}^3}{\bar{\mu}}\frac{\partial \bar{p}}{\partial \bar{r}}\right) = \frac{\left.\frac{\bar{r}\bar{h}^3}{\bar{\mu}}\right|_{i+1/2,j}\left(\frac{\bar{p}_{i+1,j}-\bar{p}_{i,j}}{\Delta \bar{r}}\right) - \left.\frac{\bar{r}\bar{h}^3}{\bar{\mu}}\right|_{i-1/2,j}\left(\frac{\bar{p}_{i,j}-\bar{p}_{i-1,j}}{\Delta \bar{r}}\right)}{\Delta \bar{r}}$$

$$\frac{\partial}{\bar{r}\partial \bar{\theta}}\left(\frac{\bar{h}^3}{\bar{\mu}}\frac{\partial \bar{p}}{\partial \bar{\theta}}\right) = \frac{\left.\frac{\bar{h}^3}{\bar{\mu}}\right|_{i,j+1/2}\left(\frac{\bar{p}_{i,j+1}-\bar{p}_{i,j}}{\Delta \bar{\theta}}\right) - \left.\frac{\bar{h}^3}{\bar{\mu}}\right|_{i,j-1/2}\left(\frac{\bar{p}_{i,j}-\bar{p}_{i,j-1}}{\Delta \bar{\theta}}\right)}{\bar{r}_{i,j}\Delta \bar{\theta}} \tag{A-3}$$

$$\frac{\bar{r}\partial \bar{h}}{\partial \bar{\theta}} = \frac{\bar{r}_{i,j}\left(\bar{h}_{i,j+1/2}-\bar{h}_{i,j-1/2}\right)}{\Delta \bar{\theta}}$$

And, introducing Equation (A-3) into Equation (A-2) and solving for $\bar{p}_{i,j}$ we obtain

$$\bar{p}_{i,j} = \frac{\left(\left.\frac{\bar{r}\bar{h}^3}{\bar{\mu}}\right|_{i+1/2,j}\frac{\bar{p}_{i+1,j}}{\Delta \bar{r}^2}\right) + \left(\left.\frac{\bar{r}\bar{h}^3}{\bar{\mu}}\right|_{i-1/2,j}\frac{\bar{p}_{i-1,j}}{\Delta \bar{r}^2}\right) + \left(\left.\frac{\bar{h}^3}{\bar{\mu}\bar{r}}\right|_{i,j+1/2}\frac{\bar{p}_{i,j+1}}{\Delta \bar{\theta}^2}\right)}{\left(\left.\frac{\bar{r}\bar{h}^3}{\bar{\mu}}\right|_{i+1/2,j} + \left.\frac{\bar{r}\bar{h}^3}{\bar{\mu}}\right|_{i-1/2,j}\right)\frac{1}{\Delta \bar{r}^2} + \left(\left.\frac{\bar{h}^3}{\bar{r}\bar{\mu}}\right|_{i,j+1/2} + \left.\frac{\bar{h}^3}{\bar{r}\bar{\mu}}\right|_{i,j-1/2}\right)\frac{1}{\Delta \bar{\theta}^2}}$$
$$+ \frac{\left(\left.\frac{\bar{h}^3}{\bar{\mu}\bar{r}}\right|_{i,j-1/2}\frac{\bar{p}_{i,j-1}}{\Delta \bar{\theta}^2}\right) + r_{ij}\frac{\left(\bar{h}_{i,j-1/2}-\bar{h}_{i,j+1/2}\right)}{\Delta \bar{\theta}}}{\left(\left.\frac{\bar{r}\bar{h}^3}{\bar{\mu}}\right|_{i+1/2,j} + \left.\frac{\bar{r}\bar{h}^3}{\bar{\mu}}\right|_{i-1/2,j}\right)\frac{1}{\Delta \bar{r}^2} + \left(\left.\frac{\bar{h}^3}{\bar{r}\bar{\mu}}\right|_{i,j+1/2} + \left.\frac{\bar{h}^3}{\bar{r}\bar{\mu}}\right|_{i,j-1/2}\right)\frac{1}{\Delta \bar{\theta}^2}} \tag{A-4}$$

Similarly, from Equations (A-1) and Equation (2) of the text, we obtain the Energy Equation in dimensionless form:

$$\frac{\overline{\mu}\overline{r}^2}{3\overline{h}} + \frac{\overline{h}^3}{\overline{\mu}}\left[\left(\frac{\partial\overline{p}}{\overline{r}\partial\theta}\right)^2 + \left(\frac{\partial\overline{p}}{\partial\overline{r}}\right)^2\right] = \left[\overline{h} - \frac{\overline{h}^3}{\overline{\mu}\overline{r}^2}\frac{\partial\overline{p}}{\partial\theta}\right]\frac{\partial\overline{T}}{\partial\theta} - \left(\frac{\overline{h}^3}{\overline{\mu}}\frac{\partial\overline{p}}{\partial\overline{r}}\right)\frac{\partial\overline{T}}{\partial\overline{r}} \qquad \text{(A-5)}$$

Referring to Figure 6, the above equation can be reduced to a difference equation:

$$\begin{aligned}
&\frac{\overline{\mu}\overline{r}^2}{3\overline{h}}\bigg|_{i,j} + \frac{\overline{h}^3}{\overline{\mu}}\bigg|_{i,j}\left[\left(\frac{\overline{p}_{i,j+1} - \overline{p}_{i,j-1}}{2\overline{r}\Delta\theta}\right)^2 + \left(\frac{\overline{p}_{i+1,j} - \overline{p}_{i-1,j}}{2\Delta\overline{r}}\right)^2\right] \\
&= \left[\overline{h}\Big|_{i,j} - \frac{\overline{h}^3}{\overline{\mu}\overline{r}^2}\bigg|_{i,j}\frac{\overline{p}_{i,j+1} - \overline{p}_{i,j-1}}{2\Delta\theta}\right]\frac{\overline{T}_{i,j+1} - \overline{T}_{i,j-1}}{2\Delta\theta} \\
&\quad - \frac{\overline{h}}{\overline{\mu}}\bigg|_{i,j}\left(\frac{\overline{p}_{i+1,j} - \overline{p}_{i-1,j}}{2\Delta\overline{r}}\right)\left(\frac{\overline{T}_{i+1,j} - \overline{T}_{i-1,j}}{2\Delta\overline{r}}\right)
\end{aligned} \qquad \text{(A-6)}$$

Now solving for $\overline{T}_{i,j+1}$, we obtain

$$\begin{aligned}
\overline{T}_{i,j+1} &= \frac{2\Delta\theta\left[\frac{\overline{\mu}\overline{r}^2}{3\overline{h}}\Big|_{i,j} + \frac{\overline{h}^3}{\overline{\mu}}\Big|_{i,j}\left\{\left(\frac{\overline{p}_{i,j+1} - \overline{p}_{i,j-1}}{2\overline{r}\Delta\theta}\right)^2 + \left(\frac{\overline{p}_{i+1,j} - \overline{p}_{i-1,j}}{2\Delta\overline{r}}\right)^2\right\}\right.}{\left[\overline{h}\Big|_{i,j} - \frac{\overline{h}^3}{\overline{\mu}\overline{r}^2}\Big|_{i,j}\left(\frac{\overline{p}_{i,j+1} - \overline{p}_{i,j-1}}{2\Delta\theta}\right)\right]} \qquad \text{(A-7)} \\
&+ \frac{+\frac{\overline{h}^3}{\overline{\mu}}\Big|_{i,j}\left(\frac{\overline{p}_{i+1,j} - \overline{p}_{i-1,j}}{2\Delta\overline{r}}\right)\left(\frac{\overline{T}_{i+1,j} - \overline{T}_{i-1,j}}{2\Delta\overline{r}}\right) + \left\{\overline{h}\Big|_{i,j}\right.}{\left[\overline{h}\Big|_{i,j} - \frac{\overline{h}^3}{\overline{\mu}\overline{r}^2}\Big|_{i,j}\left(\frac{\overline{p}_{i,j+1} - \overline{p}_{i,j-1}}{2\Delta\theta}\right)\right]} \\
&- \frac{\left.-\frac{\overline{h}^3}{\overline{\mu}\overline{r}^2}\Big|_{i,j}\left(\frac{\overline{p}_{i,j+1} - \overline{p}_{i,j-1}}{2\Delta\theta}\right)\right\}\frac{\overline{T}_{i,j-1}}{2\Delta\theta}\right]}{\left[\overline{h}\Big|_{i,j} - \frac{\overline{h}^3}{\overline{\mu}\overline{r}^2}\Big|_{i,j}\left(\frac{\overline{p}_{i,j+1} - \overline{p}_{i,j-1}}{2\Delta\theta}\right)\right]}
\end{aligned}$$

The pressure and temperature profiles are obtained by the numerical solution of the two sets of Equations (A-4) and (A-7) using the iterative procedure described on Page 13.

The load carried by each bearing pad (Equation 5 of the text) is obtained by a numerical integration of the pressure field over the pad surface.

$$\bar{W} = \Delta\bar{\theta}\,\Delta\bar{r} \sum_{j=1}^{m} \sum_{i=1}^{n} (\bar{p}_{i,j})_k\, \bar{r}_{i,j} \tag{A-8}$$

The oil flow out of each pad is given in Equations 7 of the text. In order to generalize the solutions, a dimensionless factor is used:

$$\bar{Q} = \frac{231\,Q}{60\,\pi NRL\,h_a} \tag{A-9}$$

Equations (A-1) and (A-9) are introduced into Equation 7 and four point approximations are used for the pressure gradients at the pad edges (Reference 12). Noting that the pressure is zero along the edges, the numerical form of the flow equations becomes:

$$\bar{Q}_2 = \frac{R}{L}\frac{\Delta\bar{\theta}}{\Delta\bar{r}} \sum_{j=1}^{m} \left(\frac{\bar{h}^3}{\mu\bar{r}}\right)_{1/2,j} (3.000\,\bar{p}_{1,j} - 1.500\bar{p}_{1-1/2,j} + 0.333\,\bar{p}_{2,j})$$

$$\bar{Q}_3 = \frac{R}{L}\Delta\bar{r} \sum_{i=1}^{n} (\bar{r}\,\bar{h})_{i,\,m+1/2} \tag{A-10}$$

$$+ \frac{R}{L}\frac{\Delta\bar{r}}{\Delta\bar{\theta}} \sum_{i=1}^{n} \left(\frac{\bar{h}^3}{\mu\bar{r}}\right)_{i,\,m+1/2} (3.000\,\bar{p}_{i,m} - 1.500\,\bar{p}_{i,m-1/2} + 0.333\bar{p}_{i,m-1})$$

$$\bar{Q}_4 = \frac{R}{L}\frac{\Delta\theta}{\Delta\bar{r}} \sum_{j=1}^{m} \left(\frac{\bar{h}^3}{\mu\bar{r}}\right)_{n+1/2,\,j} (3.000\bar{p}_{n,j} - 1.500\,\bar{p}_{n-1/2} + 0.333\,\bar{p}_{n-1,j})$$

The total flow out of the bearing is given by

$$\bar{Q} = \bar{Q}_2 + \bar{Q}_3 + \bar{Q}_4 \tag{A-11}$$

The horsepower loss by fluid shear in each bearing pad was written in Equation 8 of the text in the form

$$HP = \frac{231}{60} \times \frac{C_p \rho g}{0.707} \times Q \Delta T \qquad \text{(A-12)}$$

In dimensionless form this is:

$$\overline{HP} = \overline{Q} \, \Delta \overline{T} \qquad \text{(A-13)}$$

where, from Equations (A-1), (A-9) and (A-12):

$$\overline{HP} = \frac{0.707}{12 \pi^2} \frac{J h_a}{N^2 R^3 \mu_{GR} L} \qquad \text{(A-14)}$$

In numerical form the horsepower loss is then given by:

$$\overline{HP}_2 = \frac{R}{L} \frac{\Delta \overline{\theta}}{\Delta \overline{r}} \sum_{j=1}^{m} \left(\frac{\overline{h}^3}{\overline{\mu}\,\overline{r}}\right)_{1/2,j} (3.000\,\overline{p}_{1,j} - 1.500\,\overline{p}_{1-1/2,j} + 0.333\,\overline{p}_{2,j})(\overline{T}_{1/2,j} - \overline{T}_{GR})$$

$$\overline{HP}_3 = \frac{R}{L} \Delta \overline{r} \sum_{i=1}^{n} (\overline{r}\,\overline{h})_{i,m+1/2} (\overline{T}_{i,m+1/2} - \overline{T}_{GR})$$

$$+ \frac{R}{L} \frac{\Delta \overline{r}}{\Delta \overline{\theta}} \sum_{i=1}^{n} \left(\frac{\overline{h}^3}{\overline{\mu}\,\overline{r}}\right)_{i,m+1/2} (3.000\,\overline{p}_{i,m} - 1.500\,\overline{p}_{i,m-1/2} + 0.333\,\overline{p}_{i,m-1})(\overline{T}_{i,m+1/2} - \overline{T}_{GR})$$

(A-15)

$$\overline{HP}_4 = \frac{R}{L} \frac{\Delta \overline{\theta}}{\Delta \overline{r}} \sum_{j=1}^{m} \left(\frac{\overline{h}^3}{\overline{\mu}\,\overline{r}}\right)_{n+1/2,j} (3.000\,\overline{p}_{n,j} - 1.500\,\overline{p}_{n-1/2} + 0.333\,\overline{p}_{n-1,j})(\overline{T}_{n+1/2,j} - \overline{T}_{GR})$$

and the total horsepower loss in each bearing pad is:

$$\overline{HP} = \overline{HP}_2 + \overline{HP}_3 + \overline{HP}_4$$

The equations for the center of pressure (Equations 10 of the text) are in numerical form:

$$\bar{x} = \frac{\Delta\theta\,\Delta\bar{r}\,\sum_{j=1}^{m}\sum_{i=1}^{n}\bar{r}^2_{i,j}\,\sin\theta_{i,j}\,(\bar{p}_{i,j})_k}{W}$$

(A-16)

$$\bar{y} = \frac{\Delta\theta\,\Delta\bar{r}\sum\bar{r}^2_{i,j}\,\cos\bar{\theta}_{i,j}\,\bar{p}_{i,j})_k}{W}$$

Hence: $r_p\% = 100\left\{1 - \frac{R}{L}\left[1 - (\bar{x}^2 + \bar{y}^2)\right]^{\frac{1}{2}}\right\}$

(A-17)

and $\theta_p\% = \dfrac{100\tan^{-1}(\bar{x}/\bar{y})}{\theta_T}$

2. Film Shape

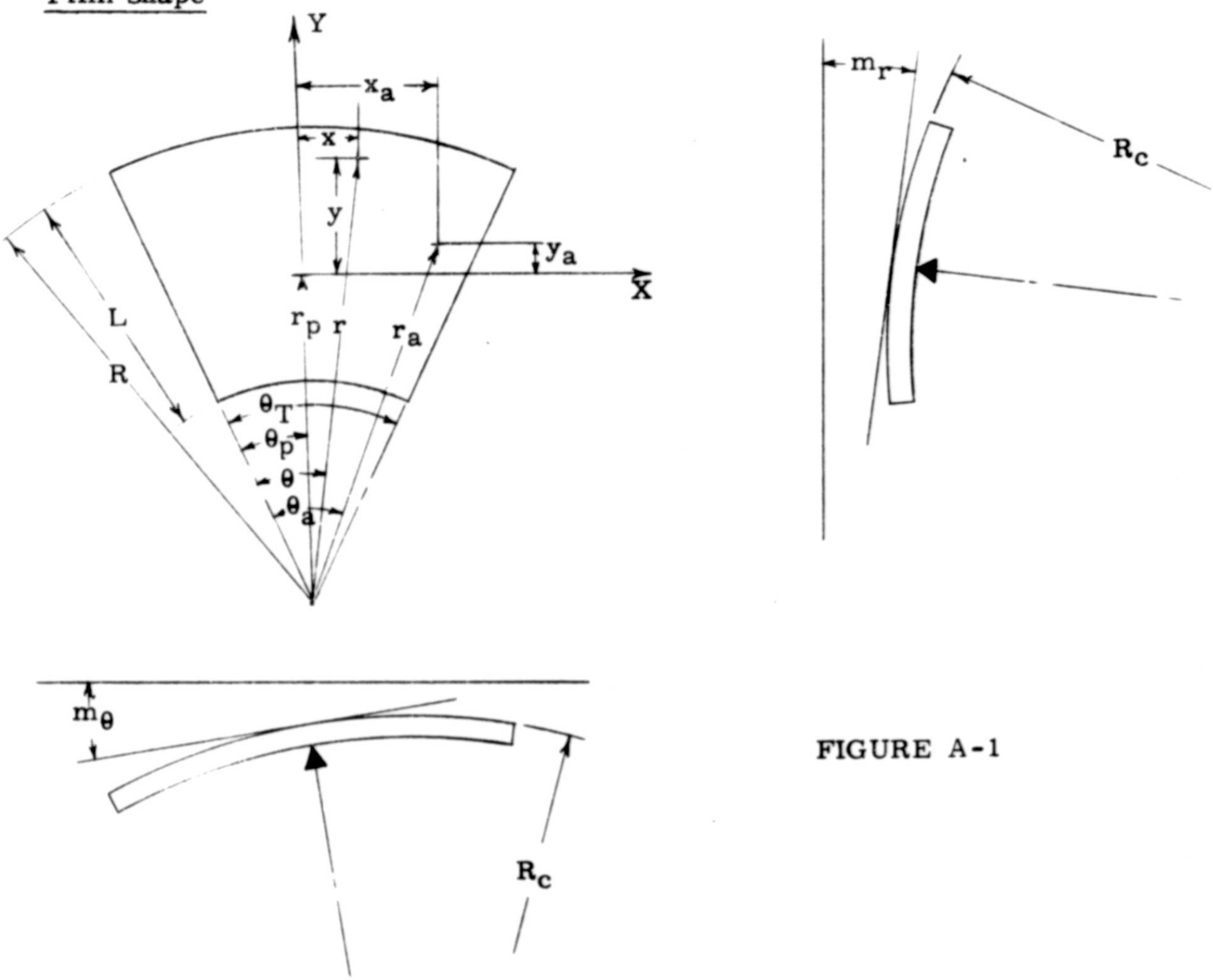

FIGURE A-1

We consider that the convex shape to which the pad bends under load may be represented by part of a spherical surface whose radius of curvature is R_c, as shown in Figure A-1. In all cases considered here, R_c is very large, greater than 10^4 inches. In addition, the pad inclines, so that its tangent plane directly above the pivot point has slopes m_θ (circumferentially) and m_r (radially), with respect to the plane of the runner, as shown in Figure A-1. The pad inclinations are small so that

$$
\begin{aligned}
\sin m_\theta &= \tan m_\theta = m_\theta \\
\cos m_\theta &= 1 \\
\sin m_r &= \tan m_r = m_r \\
\cos m_r &= 1
\end{aligned}
\qquad \text{(A-18)}
$$

Let the film thickness at a reference point (x_a, y_a) on the pad surface be h_a. The film thickness at any other point (x, y) can then be written:

$$h = h_a - m_\theta (x - x_a) + m_r (y - y_a) + R_c \left[\left(1 - \frac{x_a^2 + y_a^2}{R_c^2}\right)^{\frac{1}{2}} - \left(1 - \frac{x^2 + y^2}{R_c^2}\right)^{\frac{1}{2}} \right] \qquad \text{(A-19)}$$

Since R_c is very large, powers of the ratio $\left(\frac{r^2}{R_c^2}\right)$ are neglected. Equation (A-19) then becomes:

$$h = h_a - m_\theta (x - x_a) + m_r (y - y_a) + \frac{(x^2 + y^2) - (x_a^2 + y_a^2)}{2 R_c} \qquad \text{(A-20)}$$

This equation can be converted from the x, y co-ordinate system to the r, θ coordinate system of Figure A-1 by means of the relations:

$$\begin{aligned} x &= r \sin\left(\theta - \frac{\theta_T}{2}\right) - r_p \sin\left(\theta_p - \frac{\theta_T}{2}\right) \\ y &= r \cos\left(\theta - \frac{\theta_T}{2}\right) - r_p \cos\left(\theta_p - \frac{\theta_T}{2}\right) \end{aligned} \qquad \text{(A-21)}$$

The general equation for the film shape in polar coordinates is then:

$$h = h_a + m_\theta \left[r_a \sin\left(\theta_a - \frac{\theta_T}{2}\right) - r \sin\left(\theta - \frac{\theta_T}{2}\right) \right] - m_r \left[r_a \cos\left(\theta_a - \frac{\theta_T}{2}\right) - r \cos\left(\theta - \frac{\theta_T}{2}\right) \right] + \frac{1}{2 R_c} \left[r^2 - r_a^2 - 2 r r_p \cos(\theta - \theta_p) + 2 r_a r_p \cos(\theta_a - \theta_p) \right] \qquad \text{(A-22)}$$

(note that Equation A-22 can also be used to describe the film shape for flat pads. In such cases, R_c is infinite, thus eliminating the fourth term on the right hand side of the equation.)

3. Bending Coefficient

Equation A-20 and Figure A-1 show that (with the simplified elasticity approach used here), the bending deflection along a point on the pad surface is proportional to the square of its distance from the pivot, i.e.

$$\delta = K (x^2 + y^2) \qquad \text{(A-23)}$$

where $K = 1/(2R_c)$ (A-24)

The value of the bending coefficient K was obtained by calculating the deflection at the rim of an equivalent circular plate point supported at the center of its lower face and carrying a conically distributed load on its upper face. A circular plate was used because a closed solution for its bending deflections is available (Reference 11). A conical load distribution was selected because the ratio of peak to average pressure (3:1) is similar to that in an actual bearing pad.

Integrating Equation 57 of Reference 11, for a steel circular plate (radius "a" and thickness "t_{avg}") under the loading and support described above, the deflection at the rim is found to be:

$$\delta = 0.75 \times 10^{-8} \frac{W a^2}{t_{avg}^3} \qquad \text{(A-25)}$$

From equations A-23 and A-25, the relation between the bending coefficient and the pad load is:

$$K = 0.75 \times 10^{-8} \frac{W}{t_{avg}^3} \qquad \text{(A-26)}$$

This relation was used in all the Phase I solutions.

REFERENCES

1. "Feasibility Study for Propeller Shaft Thrust Bearing Program", B. Sternlicht and E. B. Arwas, T. I. S. Report No. 58GL147.

2. "On Problems on the Theory of Fluid Film Lubrication with an Experimental Method of Solution", A. Kingsbury, Trans. A. S. M. E., Vol. 53.

3. "The Influence of Surface Profile on the Load Capacity of Thrust Bearings with Centrally Pivoted Pads", A. A. Raimondi and J. Boyd, Trans. A. S. M. E. April 1955.

4. "Theory for Slider Bearings with a Convex Pad Surface, Side Leakage Neglected" S. Abramovitz, Franklin Institute Journal.

5. "The Effect of Bearing Deformation in Slider Bearing Lubrication", F. Osterle and E. Saibel, A. S. L. E. Preprint No. 57AM2B-2.

6. "Reynolds and Energy Considerations in Thrust Bearing Analysis", B. Sternlicht I. M. E. Paper 21, London Conference on Lubrication and Wear, Oct. 1957.

7. "The Hydrodynamical Theory of Film Lubrication", W. F. Cope, Proc. Royal Society of London, Vol. 197, p. 201, 1949.

8. "Heat Transfer in Bearing from the Lubrication of the Gliding Surfaces", G. Vogelpohl, Forschungsh, Ver. dtsch. lug., p. 425, July-August 1949.

9. "Application of Digital Computers to Bearing Design", B. Sternlicht and F. J. Maginniss, A. S. M. E. Paper No. 56A73.

10. N. A. C. A. Technical Note 2214, Chung-Hua Wu.

11. "Theory of Plates and Shells", S. Timoshenko, McGraw Hill Book Co., 1940.

TABLES

MARINE THRUST BEARING PROGRAM - PHASE I

TABLE NO. 1

19" O.D. x 9 1/2" I.D. THRUST BEARING $\left(\frac{L}{R} = 0.5\right)$

Effective Bearing Area - 181 Sq. In. (k = 0.85)

Average Pad Thickness - 1.462 In. $\left(\frac{t_{avg.}}{R} = 0.154\right)$

Pivot Pitch Diameter - 14.25 In. (r_p% = 50; θ_p% = 50)

Oil - 2190 T at 115°F Inlet

Case No.	θ_T Deg.	No. of Pads	N RPM	$m_\theta \times 10^6$ in/in	$m_r \times 10^6$ in/in	$K = \frac{1}{2R_c}$ 10^{-6} in^{-1}	h_{min} in	r_m%	θ_m%	h_1 in	T_{GR} °F	T_{AVG} °F	T_{MAX} °F	P_{AVG} psi	P_{MAX} psi	$W_{TOT} \times 10^{-3}$ lbs	Q_{TOT} gpm	$H.P._{TOT}$
1	51	6	160	75	27	5	0.00132	50	100	0.00135	125	136	150	67	142	12	0.816	1.34
2	51	6	160	143	19	25	0.0006	54	95	0.00077	132	155	184	353	899	64.7	0.575	1.56
3	51	6	160	170	19	38	0.0004	52	85.2	0.00065	142	171	209	517	1529	93.3	0.510	1.46
4	51	6	310	130	24	13	0.00124	64.3	100	0.00136	126	144	165	168	370	30.3	1.78	4.29
5	51	6	310	190	21	36	0.0006	54	91.4	0.00085	140	170	207	518	1372	93.5	1.25	4.00
6	51	6	310	210	23	49	0.0004	52	83.8	0.000732	152	189	239	682	2099	123.0	1.13	3.90
7	38.25	8	160	98	40	16	0.0006	35.7	100	0.000667	130	154	173	302	685	54.4	0.60	1.76
8	38.25	8	160	122	35	29	0.0004	44	96.7	0.000529	144	175	200	528	1355	95.5	0.48	1.61
9	38.25	8	160	129	30	36	0.0003	46	89	0.000479	152	190	222	682	1920	123.0	0.412	1.5
10	38.25	8	310	113	70	12	0.00101	14.3	100	0.00102	127	147	164	201	435	36.3	1.77	4.7
11	38.25	8	310	135	44	26	0.000604	42.8	100	0.00071	140	172	195	481	1142	86.9	1.27	4.66
12	38.25	8	310	155	39	38	0.0004	45	94.8	0.00058	154	195	226	744	1944	134.0	1.03	4.2
13	30.6	10	160	69	76	8	0.000744	35.7	100	0.00099	126	143	155	140	301	25.3	0.769	1.76
14	30.6	10	160	95	53	21	0.000409	28.6	100	0.00045	140	171	188	458	1073	82.6	0.517	1.80
15	30.6	10	160	103	42	28	0.000301	42.8	100	0.00040	150	189	211	670	1686	120.7	0.43	1.71
16	30.6	10	310	115	79	16	0.00068	14.3	100	0.00069	133	159	176	341	747	61.6	1.55	5.09
17	30.6	10	310	128	51	31	0.000404	42.8	100	0.00051	153	193	215	688	1672	124.0	1.09	4.58
18	30.6	10	310	140	40	40	0.0003	44	98.2	0.00048	163	212	242	933	2448	169.7	0.94	4.39

MARINE THRUST BEARING PROGRAM - PHASE I

TABLE NO. 2

25" O.D. x 12.5" I.D. THRUST BEARING $\left(\frac{L}{R} = 0.5\right)$

Effective Bearing Area - 312 Sq. In. (k = 0.85)

Average Pad Thickness - 1.025 In. $\left(\frac{t_{avg.}}{R} = 0.154\right)$

Pivot Pitch Diameter - 18.75 In. ($r_p\%$ = 50 ; $\theta_p\%$ = 50)

Oil - 2190 T at 115°F Inlet

Case No.	θ_T Deg.	No. of Pads	N RPM	$m_\theta \times 10^6$ in/in	$m_r \times 10^6$ in/in	$K = \frac{1}{2R_c}$ 10^{-6} in^{-1}	h_{min} in	$r_m\%$	$\theta_m\%$	h_1 in	T_{GR} °F	T_{AVG} °F	T_{MAX} °F	P_{AVG} psi	P_{MAX} psi	$W_{TOT} \times 10^{-3}$ lbs	Q_{TOT} gpm	H.P.$_{TOT}$
19	51	6	120	[illegible]	30	6	0.00126	42.8	100	0.00130	125	139	155	110	241	34.5	1.12	2.16
20	51	6	120	144	22	22	0.0006	51	89.7	0.00084	135	159	190	410	1104	127.8	0.828	2.12
21	51	6	120	161	22	30	0.0004	50	82.5	0.00074	144	174	217	558	1777	174.1	0.77	2.22
22	51	6	240	138	26	14	0.00121	57.1	100	0.00138	128	148	173	246	563	77.0	2.59	6.70
23	51	6	240	188	24	31	0.0006	52	86.5	0.000951	144	176	216	562	1622	175.2	1.94	5.9
24	51	6	240	201	25	40	0.0004	50	80.4	0.000869	153	194	253	718	2410	224.0	1.82	6.35
25	38.25	8	120	90	54	7	0.00099	14.3	100	0.000995	125	141	155	150	327	46.8	1.14	2.38
26	38.25	8	120	107	42	17	0.0006	42.9	100	0.000705	134	159	179	383	923	119.6	0.86	2.47
27	38.25	8	120	119	33	24	0.0004	44	91.4	0.000590	146	180	207	600	1636	187.4	0.69	2.30
28	38.25	8	240	108	62	9	0.00132	21.4	100	0.00134	126	[illegible]	160	168	364	52.3	3.04	6.9
29	38.25	8	240	134	42	23	0.0006	43	99.5	0.00077	145	[illegible]	205	577	1442	180.0	1.86	6.9
30	38.25	8	240	153	34	33	0.0004	46	94.2	0.00069	158	201	239	802	2293	250.3	1.55	6.13
31	30.6	10	120	80	52	11	0.00063	21.4	100	0.00065	130	155	169	296	659	91.3	0.94	2.67
32	30.6	10	120	96	41	19	0.0004	35.7	100	0.00051	144	179	199	564	1391	174.8	0.72	2.53
33	30.6	10	120	104	32	24	0.0003	43	95.5	0.00048	156	196	222	759	2024	235.2	0.62	2.39
34	30.6	10	240	93	79	7	0.00106	0	100	0.00106	126	147	160	170	363	52.8	2.95	7.57
35	30.6	10	240	108	56	16	0.00062	28.6	100	0.00069	140	173	191	504	1150	156.1	2.03	7.74
36	30.6	10	240	125	46	26	0.0004	42.8	100	0.00057	159	201	227	809	2040	250.1	1.60	6.85

MARINE THRUST BEARING PROGRAM - PHASE I

TABLE NO. 3

31" O.D. x 15.5" I.D. THRUST BEARING $\left(\frac{L}{R} = 0.5\right)$

Effective Bearing Area - 480 Sq. In. (k = 0.85)

Average Pad Thickness - 2.385 In. $\left(\frac{t_{avg.}}{R} = 0.154\right)$

Pivot Pitch Diameter - 23.25 In. ($r_p\%$ = 50; $\theta_p\%$ = 50)

Oil - 2190 T at 115°F Inlet

Case No.	θ_T Deg.	No. of Pads	N RPM	$m_\theta x10^6$ in/in	$m_r x10^6$ in/in	$K=\frac{1}{2R_c}$ 10^{-6} in^{-1}	h_{min} in	$r_m\%$	$\theta_m\%$	h_1 in	T_{GR} °F	T_{AVG} °F	T_{MAX} °F	P_{AVG} psi	P_{MAX} psi	$W_{TOT}x10^{-3}$ lbs	Q_{TOT} gpm	$H.P._{TOT}$
37	51	6	180	139	27	14	0.00111	52	99	0.00133	130	153	180	321	779	154.2	3.02	8.18
38	51	6	180	177	21	25	0.0006	52	84.4	0.00104	146	176	219	593	1802	284.5	2.48	7.48
39	51	6	180	193	24	32	0.0004	50	79.5	0.00098	154	194	258	721	2520	346.0	2.45	7.44
40	51	6	320	176	24	18	0.0012	55	97.2	0.00153	136	162	195	423	1046	213.1	6.2	19.6
41	51	6	320	216	24	32	0.0006	53	82.7	0.00118	154	193	249	730	2304	350.4	5.05	18.0
42	51	6	320	222	24	39	0.0004	50	77.6	0.00114	163	211	294	887	3492	425.0	4.85	20.2
43	38.25	8	180	95	58	8	0.00127	21.4	100	0.00129	127	147	162	207	456	99.5	3.48	8.34
44	38.25	8	180	134	38	20	0.0006	44	95.5	0.00838	143	181	209	619	1618	289.0	2.34	8.24
45	38.25	8	180	147	34	27	0.0004	46	86.3	0.00076	158	202	244	811	2440	382.0	1.98	7.53
46	38.25	8	320	122	58	12	0.00124	35.7	100	0.00132	132	161	181	345	783	166.8	6.5	21.3
47	38.25	8	320	161	38	26	0.0006	46	91.4	0.00094	158	200	235	900	2172	384.0	4.47	18.5
48	38.25	8	320	173	34	33	0.0004	47	84.7	0.00087	165	221	273	1058	3323	508.0	3.94	18.9
49	30.6	10	180	74	88	5	0.00115	0	100	0.00115	125	144	156	153	3278	73.5	3.88	9.23
50	30.6	10	180	107	50	15	0.00061	36.5	100	0.00073	144	179	198	562	1344	269.8	2.47	9.09
51	30.6	10	180	118	37	22	0.0004	43.5	95.5	0.00065	160	205	234	858	2298	411.8	1.95	8.35
52	30.6	10	320	95	95	5	0.00132	0	100	0.00132	127	149	164	213	453	100.2	8.00	23.5
53	30.6	10	320	126	51	20	0.000603	42.8	100	0.00079	156	200	222	772	1899	370.5	4.6	20.3
54	30.6	10	320	143	39	29	0.0004	44.5	92.7	0.00076	165	224	264	1138	3153	546.3	3.86	19.3

MARINE THRUST BEARING PROGRAM - PHASE I

TABLE NO. 4

37" O.D. x 18.5 " I.D. THRUST BEARING $\left(\frac{L}{R} = 0.5\right)$

Effective Bearing Area - 685 Sq. In. (k = 0.85)

Average Pad Thickness - 2.85 In. $\left(\frac{t_{avg.}}{R} = 0.154\right)$

Pivot Pitch Diameter - 27.75 In. (r_p% = 50 ; θ_p% = 50)

Oil - 2190 T at 115°F Inlet

Case No.	θ_T Deg.	No. of Pads	N RPM	$m_\theta \times 10^6$ in/in	$m_r \times 10^6$ in/in	$K=\frac{1}{2R_c}$ 10^{-6} in^{-1}	h_{min} in	r_m%	θ_m%	h_1 in	T_{GR} °F	T_{AVG} °F	T_{MAX} °F	P_{AVG} psi	P_{MAX} psi	$W_{TOT} \times 10^{-3}$ lbs	Q_{TOT} gpm	$H.P._{TOT}$
55	51	6	180	150	26	14	0.0012	53	94	0.00152	133	157	185	368	934	252.2	4.92	13.4
56	51	6	180	185	25	24	0.0006	50	81.5	0.0012	149	184	234	642	2101	439.7	4.15	13.4
57	51	6	180	194	25	29	0.0004	50	77.3	0.00116	156	201	275	773	3135	529.8	4.02	14.6
58	51	6	320	183	26	18	0.0012	52.5	91.5	0.00163	140	171	206	507	1342	347.4	9.5	31.0
59	51	6	320	220	25	30	0.0006	50	80	0.00139	157	201	268	798	2767	546.9	8.46	33.2
60	51	6	320	230	24	35	0.0004	50	76.8	0.00136	163	218	317	946	4241	647.8	8.47	38.6
61	38.25	8	180	95	50	7	0.00126	28.6	100	0.00131	130	154	172	285	636	195.5	5.21	14.9
62	38.25	8	180	134	26	19	0.0006	47.5	89	0.00098	153	192	226	709	1995	485.6	3.52	13.1
63	38.25	8	180	156	28	25	0.0004	48	84.4	0.00092	161	210	263	910	2980	623.2	3.29	13.3
64	38.25	8	320	135	56	13	0.00121	35.7	100	0.00138	137	169	191	474	1113	324.6	10.02	35.7
65	38.25	8	320	175	26	25	0.0006	49	88.3	0.00113	161	209	254	918	2634	628.5	7.15	30.7
66	38.25	8	320	190	27	32	0.0004	49	82.5	0.00111	165	227	303	1148	4115	786.5	6.77	33.5
67	30.6	10	180	43	89	3	0.00156	0	100	0.00156	125	142	153	75	160	51.5	6.83	14.7
68	30.6	10	180	110	40	15	0.0006	42.8	100	0.00082	152	191	214	693	1748	474.9	3.7	14.4
69	30.6	10	180	126	34	22	0.0004	45	90.2	0.00079	164	215	254	957	2709	655.4	3.11	13.7
70	30.6	10	320	90	77	6	0.00137	0	100	0.00137	130	158	175	285	617	195.3	11.6	39.6
71	30.6	10	320	134	40	20	0.0006	44	97.5	0.000929	163	213	242	916	2384	627.5	7.09	32.8
72	30.6	10	320	153	34	28	0.0004	46	88	0.000931	165	234	288	1291	3907	884.5	6.13	34.2

MARINE THRUST BEARING PROGRAM - PHASE I

TABLE NO. 5

39" O.D. x 19.5" I.D. THRUST BEARING $\left(\frac{L}{R} = 0.5\right)$

Effective Bearing Area - 760 Sq. In. (k = 0.85)

Average Pad Thickness - 3.00 In. $\left(\frac{t_{avg.}}{R} = 0.154\right)$

Pivot Pitch Diameter - 29.25 In. ($r_p\%$ = 50 ; $\theta_p\%$ = 50)

Oil - 2190 T at 115°F Inlet

Case No.	θ_T Deg.	No. of Pads	N RPM	$m_\theta x10^6$ in/in	$m_r x10^6$ in/in	$K=\frac{1}{2R_c}$ 10^{-6} in^{-1}	h_{min} in	$r_m\%$	$\theta_m\%$	h_1 in	T_{GR} °F	T_{AVG} °F	T_{MAX} °F	P_{AVG} psi	P_{MAX} psi	$W_{TOT}x10^{-3}$ lbs	Q_{TOT} gpm	$H.P._{TOT}$
73	51	6	150	147	20	13	0.0012	53	85.4	0.00156	133	155	183	351	894	266.7	4.60	11.8
74	51	6	150	179	22	22	0.0006	51	81.4	0.00122	148	181	230	614	2037	466.4	3.88	11.7
75	51	6	150	187	22	26	0.0004	50	77.9	0.00117	155	197	271	749	3063	568.9	3.74	12.9
76	51	6	200	160	20	14	0.0012	54	93.7	0.0016	135	160	193	423	1081	321.7	6.40	18.6
77	51	6	200	193	21	24	0.0006	51	81	0.0013	152	190	246	693	2340	526.9	5.47	18.2
78	51	6	200	207	23	30	0.0004	50	76.6	0.0013	160	206	288	784	3434	595.5	5.61	21.5
79	38.25	8	150	93	45	7	0.00124	35.7	100	0.00132	128	152	170	294	658	224.0	4.78	14.2
80	38.25	8	150	135	31	18	0.0006	46	89.8	0.00098	151	188	220	681	1920	517.7	3.37	11.8
81	38.25	8	150	151	27	23	0.0004	48	84.4	0.00094	161	206	258	855	2843	650.0	3.08	11.7
82	38.25	8	200	106	48	9	0.00122	35.7	100	0.00133	131	159	180	373	853	283.4	6.55	22.0
83	38.25	8	200	148	31	20	0.0006	47	99	0.00103	156	197	234	771	2193	586.0	4.69	17.7
84	38.25	8	200	165	27	26	0.0004	48	83	0.00102	164	215	276	951	3296	722.5	4.4	18.4
85	30.6	10	150	87	56	7	0.00097	21.4	100	0.0010	132	159	175	364	809	276.4	4.57	14.9
86	30.6	10	150	110	38	14	0.0006	42.8	100	0.00083	150	187	210	678	1711	515.0	3.51	13.4
87	30.6	10	150	121	31	20	0.0004	45	90.4	0.0008	163	212	249	917	2662	697.0	2.89	12.1
88	30.6	10	200	94	51	8	0.00096	28.6	100	0.00102	137	169	188	455	1027	345.8	6.39	22.9
89	30.6	10	200	116	37	16	0.0006	43	99	0.00088	157	199	224	763	1965	579.5	4.73	19.7
90	30.6	10	200	131	32	22	0.0004	46	89.5	0.00085	164	221	264	1072	3146	816.0	4.01	19.1

MARINE THRUST BEARING PROGRAM - PHASE I

TABLE NO. 6

41" O.D. x 20.5" I.D. THRUST BEARING $\left(\frac{L}{R} = 0.5\right)$

Effective Bearing Area - 840 Sq. In. (k = 0.85)

Average Pad Thickness - 3.16 In. $\left(\frac{t_{avg.}}{R} = 0.154\right)$

Pivot Pitch Diameter - 30.75 In. (r_p% = 50 ; θ_p% = 50)

Oil - 2190 T at 115°F Inlet

Case No.	θ_T Deg.	No. of Pads	N RPM	$m_\theta x10^6$ in/in	$m_r x10^6$ in/in	$K=\frac{1}{2R_c}$ 10^{-6} in^{-1}	h_{min} in	r_m%	θ_m%	h_1 in	T_{GR} °F	T_{AVG} °F	T_{MAX} °F	P_{AVG} psi	P_{MAX} psi	$W_{TOT}x10^{-3}$ lbs	Q_{TOT} gpm	$H.P._{TOT}$
91	51	6	100	114	17	9	0.0012	53.5	96.4	0.00147	129	149	175	291	715	244.0	3.14	7.72
92	51	6	100	159	20	18	0.0006	51	82.5	0.00116	143	172	216	546	1781	458.0	2.72	7.45
93	51	6	100	167	20	22	0.0004	50	78	0.00111	150	188	251	667	2667	560.0	2.60	8.15
94	51	6	200	156	18	14	0.0012	53.5	90.5	0.00164	136	163	197	444	1172	373.0	7.02	21.0
95	51	6	200	196	20	24	0.0006	51	89	0.00138	154	192	252	695	2425	583.0	6.4	21.3
96	51	6	200	203	23	28	0.0004	50	76.6	0.00133	159	208	294	833	3683	700.0	6.37	25.7
97	38.25	8	100	85	44	6	0.00125	28.6	100	0.00131	127	146	162	232	518	194.0	3.5	8.49
98	38.25	8	100	119	30	15	0.0006	45	90.3	0.00093	146	178	207	590	1646	496.0	2.4	7.59
99	38.25	8	100	130	26	19	0.0004	47	84.2	0.00088	156	197	241	757	2426	635.0	2.15	7.5
100	38.25	8	200	115	42	10	0.00121	42.8	100	0.00139	135	163	185	407	954	341.9	7.45	24.6
101	38.25	8	200	152	29	20	0.0006	47.5	88	0.00110	158	199	239	787	2285	661.0	5.42	20.4
102	38.25	8	200	165	27	25	0.0004	48	82.6	0.00106	164	218	283	987	3500	829.4	5.05	21.8
103	30.6	10	100	70	57	50	0.00099	7.1	100	0.00099	128	150	164	260	571	218.8	3.35	9.26
104	30.6	10	100	94	37	12	0.0006	42.8	100	0.00080	145	178	199	571	1451	480.0	2.48	8.57
105	30.6	10	100	101	29	16	0.0004	44.5	90	0.00074	158	202	233	802	2309	673.7	2.0	7.81
106	30.6	10	200	105	50	10	0.00093	35.7	100	0.00105	140	173	193	520	1210	436.7	6.89	25.97
107	30.6	10	200	120	37	16	0.0006	43	88.5	0.00092	158	201	228	804	2097	675.6	5.41	22.78
108	30.6	10	200	131	32	22	0.0004	49	87.4	0.0009	165	224	272	1088	3303	913.9	4.59	22.18

MARINE THRUST BEARING PROGRAM - PHASE I

TABLE NO. 7

45" O.D. x 22.5" I.D. THRUST BEARING $\left(\frac{L}{R} = 0.5\right)$

Effective Bearing Area - 1012 Sq. In. (k = 0.85)
Average Pad Thickness - 3.46 In. $\left(\frac{t_{avg.}}{R} = 0.154\right)$
Pivot Pitch Diameter - 33.75 In. (r_p% = 50; θ_p% = 50)
Oil - 2190 T at 115°F Inlet

Case No.	θ_T Deg.	No. of Pads	N RPM	$m_\theta x10^6$ in/in	$m_r x10^6$ in/in	$K=\frac{1}{2R_c}$ 10^{-6} in^{-1}	h_{min} in	r_m%	θ_m%	h_1 in	T_{GR} °F	T_{AVG} °F	T_{MAX} °F	P_{AVG} psi	P_{MAX} psi	$W_{TOT}x10^{-3}$ lbs	Q_{TOT} gpm	$H.P._{TOT}$
109	51	6	100	118	170	9	0.0012	53	93.8	0.00153	130	152	179	334	842	337.6	3.96	11.8
110	51	6	100	162	20	18	0.0006	50	80.3	0.00129	146	177	223	555	1911	562.1	3.62	10.0
111	51	6	100	168	19	21	0.0004	50	76.9	0.00124	151	191	260	684	2895	692.4	3.52	11.7
112	51	6	170	156	18	13	0.0012	53.5	89.8	0.00169	136	162	197	450	1205	455.1	7.49	21.5
113	51	6	170	185	20	21	0.0006	51	79.5	0.00142	152	191	252	703	2494	711.6	6.77	22.7
114	51	6	170	200	23	25	0.0004	50	76.9	0.0014	158	206	295	816	3774	825.4	6.91	26.8
115	38.25	8	100	73	46	4	0.0013	21.4	100	0.00132	126	147	164	236	517	238.8	4.35	11.7
116	38.25	8	100	116	28	14	0.0006	46	88.2	0.000988	148	183	214	638	1837	654.4	2.98	9.96
117	38.25	8	100	130	27	18	0.0004	47	83	0.00094	156	201	250	806	2687	815.7	2.77	10.2
118	38.25	8	170	114	42	9	0.00121	42.8	100	0.0014	134	161	184	426	1000	430.7	7.9	25.8
119	38.25	8	170	143	29	18	0.0006	47	87.4	0.00113	157	198	239	788	2305	797.1	5.76	21.2
120	38.25	8	170	155	27	22	0.0004	48	81.8	0.0011	163	217	284	979	3533	990.9	5.33	22.9
121	30.6	10	100	63	57	3	0.0011	0	100	0.0011	126	148	162	230	494	232.7	4.5	12.4
122	30.6	10	100	95	36	12	0.0006	41	97	0.00086	149	184	207	614	1616	621.8	3.09	10.9
123	30.6	10	100	102	28	15	0.0004	45	89.3	0.00079	160	207	242	865	2542	875.4	2.54	10.3
124	30.6	10	170	104	50	9	0.00093	35.7	100	0.00106	140	172	192	533	1243	539.0	7.32	26.8
125	30.6	10	170	118	37	15	0.0006	43	96.1	0.00096	158	201	228	801	2140	810.9	5.73	23.3
126	30.6	10	170	131	31	20	0.0004	46	87.5	0.00095	165	222	272	1069	3337	1082.2	4.94	22.8

MARINE THRUST BEARING PROGRAM - PHASE I

TABLE NO. 8

50" O.D. x 25" I.D. THRUST BEARING $\left(\frac{L}{R} = 0.5\right)$

Effective Bearing Area - 1250 Sq. In. ([illegible].85)

Average Pad Thickness - 3.85 In. ([illegible] 0.154)

Pivot Pitch Diameter - 37.5 In. ([illegible] ; θ_p% = 50)

Oil - 2190 T at 115°F Inlet

Case No.	θ_T Deg.	No. of Pads	N RPM	$m_\theta x10^6$ in/in	$m_r x10^6$ in/in	$K=\frac{1}{2R_c}$ 10^{-6} in^{-1}	h_{min} in	r_m%	θ_m%	h_1 in	T_{GR} °F	T_{AVG} °F	T_{MAX} °F	P_{AVG} psi	P_{MAX} psi	$W_{TOT}x10^{-3}$ lbs	Q_{TOT} gpm	$H.P._{TOT}$
127	51	6	100	136	16	10	0.[illegible]	53.5	90.6	0.00166	133	155	184	374	990	467.4	5.38	13.2
128	51	6	100	163	19	17	0.[illegible]	50	73.8	0.00142	147	180	231	593	2137	740.9	4.89	14.2
129	51	6	100	169	18	19	0.[illegible]	50	76.7	0.00134	153	196	272	722	3244	902.8	4.73	16.5
130	51	6	170	164	18	13	0.[illegible]	53	87.7	0.00181	139	167	204	490	1370	611.9	10.01	29.2
131	51	6	170	186	20	20	0.[illegible]	50.5	78	0.00158	154	196	262	728	2730	909.9	9.2	32.1
132	51	6	170	200	20	23	0.[illegible]	50.5	76.2	0.00156	160	211	309	839	4189	1048.5	9.75	41.3
133	38.25	8	100	91	37	6	0.[illegible]	35.7	100	0.00136	130	153	173	342	787	426.9	5.57	16.0
134	38.25	8	100	125	25	14	0.[illegible]	47	86.6	0.00111	151	188	223	678	2036	847.5	4.05	13.5
135	38.25	8	100	131	26	17	0.[illegible]	47	81.5	0.00105	159	206	263	835	2951	1044.3	3.74	14.1
136	38.25	8	170	114	41	9	0.[illegible]	42.8	100	0.00144	138	168	192	481	1166	601.5	10.0	34.5
137	38.25	8	170	148	27	17	0.[illegible]	48	85.5	0.00124	159	204	249	840	2577	1050.1	7.64	29.6
138	38.25	8	170	152	26	20	0.[illegible]	48	81	0.00119	164	223	299	1048	3951	1316.6	7.07	32.4
139	30.6	10	100	87	40	8	0.[illegible]	35.7	100	0.00098	127	172	190	520	1262	389.6	4.69	16.3
140	30.6	10	100	97	32	11	0.[illegible]	43	96.5	0.00091	151	189	214	699	1863	874.3	4.00	15.0
141	30.6	10	100	106	25	15	0.[illegible]	46	86.4	0.00091	162	213	254	907	2827	1133.2	3.39	14.0
142	30.6	10	170	103	47	9	0.[illegible]	35.7	100	0.0011	144	180	200	608	1457	760.6	9.21	35.9
143	30.6	10	170	115	35	14	0.[illegible]	43.5	93.2	0.00104	160	208	239	883	2427	1103.2	7.32	31.9
144	30.6	10	170	127	28	18	0.[illegible]	46.5	86.2	0.00103	165	229	286	1175	3787	1468.7	6.42	32.2

MARINE THRUST BEARING PROGRAM - PHASE I

TABLE NO. 9

26" O.D. x 17 1/2" I.D. THRUST BEARING $\left(\frac{L}{R} = 0.327\right)$

Effective Bearing Area - 184 Sq. In. (k = 0.631)

Average Pad Thickness - 1.47 In. $\left(\frac{t_{avg.}}{R} = 0.113\right)$

Pivot Pitch Diameter - 21.75 In. (r_p% = 50 ; θ_p% = 50)

Oil - 2190 T at 115°F Inlet

Case No.	θ_T Deg.	No. of Pads	N RPM	$m_\theta \times 10^6$ in/in	$m_r \times 10^6$ in/in	$K = \frac{1}{2R_c}$ 10^{-6} in^{-1}	h_{min} in	r_m%	θ_m%	h_1 in	T_{GR} °F	T_{AVG} °F	T_{MAX} °F	P_{AVG} psi	P_{MAX} psi	$W_{TOT} \times 10^{-3}$ lbs	Q_{TOT} gpm	$H.P._{TOT}$
145	28.4	8	160	135	16	19	0.00072	50	100	0.00081	128	154	177	350	788	63.8	1.10	3.47
146	28.4	8	160	155	10	29	0.00050	53.7	99	0.00065	137	169	200	570	1394	103.7	0.92	3.35
147	28.4	8	160	177	15	46	0.00030	50	85.9	0.00053	149	194	243	864	2535	157.7	0.75	3.02

TABLE NO. 10

31" O.D. x 16 1/2" I.D. THRUST BEARING $\left(\frac{L}{R} = 0.468\right)$

Effective Bearing Area - 459 Sq. In. ($k = 0.85$)

Average Pad Thickness - 2.20 In. $\left(\frac{t_{avg.}}{R} = 0.142\right)$

Pivot Pitch Diameter - 24 In. ($r_p\% = 51.7$; $\theta_p\% = 50$)

Oil - 2190 T at 115°F Inlet

Case No.	θ_T Deg.	No. of Pads	N RPM	$m_\theta \times 10^6$ in/in	$m_r \times 10^6$ in/in	$K = \frac{1}{2R_c}$ 10^{-6} in^{-1}	h_{min} in	$r_m\%$	$\theta_m\%$	h_1 in	T_{GR} °F	T_{AVG} °F	T_{MAX} °F	P_{AVG} psi	P_{MAX} psi	$F_{TOT} \times 10^{-3}$ lbs	Q_{TOT} gpm	$H.P._{TOT}$
148	38.25	8	320	150	14	15	0.00121	57.2	100	0.00149	134	161	187	392	908	181.0	6.60	21.0
149	38.25	8	320	190	10	31	0.00060	55	87.8	0.00111	157	197	241	783	2221	361.0	4.67	13.2
150	38.25	8	320	210	21	40	0.00040	52	83	0.00102	164	216	283	982	3172	453.0	4.36	13.0

MARINE THRUST BEARING PROGRAM - PHASE I

TABLE NO. 11

35" O.D. x 18 1/2" I.D. THRUST BEARING $\left(\frac{L}{R} = 0.471\right)$

Effective Bearing Area - 591 Sq. In. (k = 0.85)

Average Pad Thickness - 2.33 In. $\left(\frac{t_{avg.}}{R} = 0.133\right)$

Pivot Pitch Diameter - 27 In. (r_p% =51.5; θ_p% = 50)

Oil - 2190 T at 115°F Inlet

Case No.	θ_T Deg.	No. of Pads	N RPM	$m_\theta x10^6$ in/in	$m_r x10^6$ in/in	$K=\frac{1}{2R_c}$ 10^{-6} in^{-1}	h_{min} in	r_m%	θ_m%	h_1 in	T_{GR} °F	T_{AVG} °F	T_{MAX} °F	P_{AVG} psi	P_{MAX} psi	$W_{TOT}x10^{-3}$ lbs	Q_{TOT} gpm	$H.P._{TOT}$
151	38.25	8	170	135	15	13	0.00120	57.2	100	0.00149	131	151	174	314	738	185.2	4.43	11.7
152	38.25	8	170	174	19	27	0.00060	52	86	0.00113	148	172	218	629	1573	371.0	3.24	10.3
153	38.25	8	170	189	21	34	0.00040	51.3	81	0.00108	156	200	256	773	2731	457.0	3.03	10.7

TABLE NO. 12

31" O.D. x 15 1/2" I.D. THRUST BEARING $\left(\frac{L}{R} = 0.5\right)$

Effective Bearing Area - 480 Sq. In. (k = 0.85)

Average Pad Thickness - 2.01 In. $\left(\frac{t_{avg.}}{R} = 0.130\right)$

Pivot Pitch Diameter - 23.25 In. (r_p% = 50 ; θ_p% = 50)

Oil - 2190 T at 115°F Inlet

Case No.	θ_T Deg.	No. of Pads	N RPM	$m_\theta \times 10^6$ in/in	$m_r \times 10^6$ in/in	$K=\frac{1}{2R_c}$ 10^{-6} in^{-1}	h_{min} in	r_m%	θ_m%	h_1 in	T_{GR} °F	T_{AVG} °F	T_{MAX} °F	P_{AVG} psi	P_{MAX} psi	$W_{TOT} \times 10^{-3}$ lbs	Q_{TOT} gpm	$H.P._{TOT}$
154	51	6	180	199	29	24	0.00111	52.0	93.0	0.00151	130	150	176	332	878	158.9	3.4	7.5
155	51	6	180	229	28	37	0.00060	50.0	80.0	0.00127	144	172	216	512	1757	245.8	3.03	7.88
156	51	6	180	250	27	46	0.00040	50.0	76.4	0.00128	148	185	245	615	2690	295.0	3.12	9.64
157	51	6	320	238	28	30	0.00120	53	88.3	0.00173	136	160	191	408	1120	196.0	6.58	17.7
158	51	6	320	280	27	46	0.00060	51	79.5	0.00147	149	185	243	662	2412	317.8	6.21	19.4
159	51	6	320	300	28	56	0.00040	51	76	0.00150	156	201	284	734	3516	352.5	6.65	25.2
160	38.25	8	180	120	58	12	0.00124	35.7	100	0.00132	130	148	164	236	535	113.2	3.63	5.45
161	38.25	8	180	182	42	32	0.00060	46	88	0.00103	146	177	207	572	1674	274.3	2.64	7.74
162	38.25	8	180	202	34	41	0.00040	48	82	0.00102	155	194	241	704	2475	338.2	2.46	14.2
163	38.25	8	320	165	58	20	0.00121	42.8	100	0.00141	133	159	180	402	955	192.9	6.93	21.4
164	38.25	8	320	224	42	41	0.00060	48	96	0.00119	154	193	232	728	2223	350.0	5.31	13.2
165	38.25	8	320	237	37	50	0.00040	48	81	0.00117	161	211	275	991	3325	427.0	5.09	19.5
166	30.6	10	180	80	96	7	0.00135	0	100	0.00135	126	141	151	120	259	57.4	4.38	8.62
167	30.6	10	180	140	50	25	0.00060	42	98	0.00096	145	178	199	532	1525	279.3	2.65	8.77
168	30.6	10	180	158	37	34	0.00040	46	88.8	0.00084	158	200	233	775	2335	372.1	2.22	7.91
169	30.6	10	320	127	89	13	0.00128	21.4	100	0.00131	130	154	167	270	641	138.7	7.97	2.27
170	30.6	10	320	173	53	33	0.00060	44	94.5	0.00099	155	196	223	[illegible]	2062	363.[illegible]	5.13	1.09
171	30.6	10	320	198	39	44	0.00040	47	[illegible]	0.00101	163	216	264	[illegible]	[illegible]	[illegible]	4.59	1.91

MARINE THRUST BEARING PROGRAM - PHASE I

TABLE NO. 13

31" O.D. x 151/2" I.D. THRUST BEARING $\left(\frac{L}{R} = 0.5\right)$

Effective Bearing Area - 480 Sq. In. (k = 0.85)

Average Pad Thickness - 2.99 In. $\left(\frac{t_{AVG}}{R} = 0.193\right)$

Pivot Pitch Diameter - 23.25 In. (r_p% = 50 ; θ_p% = 50)

Oil - 2190 T at 115°F Inlet

Case No.	θ_T Deg.	No. of Pads	N RPM	$m_\theta x10^6$ in/in	$m_r x10^6$ in/in	$K = \frac{1}{2R_c}$ 10^{-6} in^{-1}	h_{min} in	r_m%	θ_m%	h_1 in	T_{GR} °F	T_{AVG} °F	T_{MAX} °F	P_{AVG} psi	P_{MAX} psi	$W_{TOT}x10^{-3}$ lbs	Q_{TOT} gpm	H.P.$_{TOT}$
172	51	6	180	90	22	6	0.00115	57.1	100	0.00126	129	154	181	270	997	129.8	2.74	[illegible]
173	51	6	180	120	15	14	0.00060	53	91.4	0.00085	148	185	226	633	1676	304.0	1.97	[illegible]
174	51	6	180	130	16	18	0.00040	52	85	0.00072	159	205	265	862	2563	414.0	1.76	7.45
175	51	6	320	120	18	9	0.00122	64.2	100	0.00142	134	165	198	379	860	192.1	5.61	[illegible]
176	51	6	320	145	15	18	0.00060	54	88.8	0.00093	158	203	258	819	2222	393.7	[illegible]	[illegible]
177	51	6	320	160	16	24	0.00040	52	62.3	0.00084	165	222	305	1085	3537	521.5	3.66	[illegible]
178	38.25	8	180	75	58	4	0.00142	0	100	0.00142	127	144	199	138	296	66.2	3.66	[illegible]
179	38.25	8	180	90	30	10	0.00060	42.8	100	0.00072	146	195	210	603	1417	290.0	[illegible]	8.02
180	38.25	8	180	96	23	14	0.00040	46.4	96	0.00058	161	212	249	935	2387	448.4	1.62	8.14
181	38.25	8	320	80	58	5	0.00136	7.1	100	0.00136	130	158	178	232	499	111.8	[illegible]	22.4
182	38.25	8	320	115	34	14	0.00060	42.8	100	0.00077	158	205	237	918	1954	392.9	4.04	[illegible]
183	38.25	8	320	120	27	20	0.00040	46.5	90	0.00067	165	232	284	1243	3390	596.0	3.16	19.2
184	30.6	10	180	60	55	30	0.0092	0	100	0.00092	127	155	170	234	501	113.5	2.98	[illegible]
185	30.6	10	180	75	48	7	0.00066	21.4	100	0.00068	139	174	193	465	1027	223.1	2.39	[illegible]
186	30.6	10	180	82	32	12	0.00041	42.8	100	0.00052	160	210	234	964	2071	414.7	1.73	8.77
187	30.6	10	320	68	98	30	0.00160	0	100	0.00160	127	145	153	107	227	[illegible]	8.86	[illegible]
188	30.6	10	320	90	46	9	0.00065	28.6	100	0.00067	151	193	217	671	1496	[illegible]	4.39	[illegible]
189	30.6	10	320	98	34	15	0.00040	42.8	100	0.00056	165	233	263	1237	2999	[illegible]	[illegible]	21.4

MARINE THRUST BEARING PROGRAM - PHASE I

TABLE NO. 14

31" O.D. x 15 1/2" I.D. THRUST BEARING $\left(\frac{L}{R} = 0.5\right)$

Effective Bearing Area - 480 Sq. In. (k = 0.85)

Average Pad Thickness - 2.385 In. $\left(\frac{t_{avg.}}{R} = 0.154\right)$

Pivot Pitch Diameter - 23.72 In. ($r_p\%$ = 53 ; $\theta_p\%$ = 50)

Oil - 2190 T at 115°F Inlet

Case No.	θ_T Deg.	No. of Pads	N RPM	$m_\theta x10^6$ in/in	$m_r x10^6$ in/in	$K=\frac{1}{2R_c}$ 10^{-6} in^{-1}	h_{min} in	r_m%	θ_m%	h_1 in	T_{GR} °F	T_{AVG} °F	T_{MAX} °F	P_{AVG} psi	P_{MAX} psi	$W_{TOT}x10^{-3}$ lbs	Q_{TOT} gpm	H.P.$_{TOT}$
190	51	6	180	154	-37	14	0.00111	84	94.4	0.00171	131	151	186	308	747	148.0	3.22	7.09
191	51	6	180	188	-15	26	0.00060	63.5	82.5	0.00129	145	176	226	571	1745	274.0	2.62	7.85
192	51	6	180	195	-8	32	0.00040	59.5	77.8	0.00120	154	193	264	713	2531	342.2	2.46	8.48
193	51	6	320	184	-53	15	0.00140	93	100		132	153	189	317	745	152.0	7.25	19.4
194	51	6	320	220	-15	32	0.00060	62	81	0.00143	154	193	258	724	2278	347.5	5.21	18.7
195	51	6	320	231	-7	39	0.00040	59	77.4	0.00136	161	210	303	884	3393	424.0	5.02	21.0
196	38.25	8	180	109	-2	8	0.00125	71.4	100	0.00152	127	147	170	246	541	118.0	3.52	9.15
197	38.25	8	180	139	2	21	0.00060	58.2	91	0.00104	149	183	217	618	1654	297.0	2.30	8.01
198	38.25	8	180	155	3	27	0.00040	56.8	85.6	0.00095	159	202	251	831	2476	399.0	2.02	7.78
199	38.25	8	320	134	-2	12	0.00122	71.4	100	0.00157	134	161	189	380	861	175.3	6.55	22.0
200	38.25	8	320	168	0	27	0.00060	58.2	88.3	0.00116	159	201	245	793	2195	380.6	4.46	18.2
201	38.25	8	320	193	6	36	0.00040	56	83.5	0.00112	164	219	286	1030	3336	494.0	4.16	19.1
202	30.6	10	180	96	23	8	0.00097	50	100	0.00109	136	155	177	332	731	159.5	3.17	10.01
203	30.6	10	180	114	15	16	0.00060	57.1	100	0.00088	148	182	206	600	1464	288.9	2.45	8.96
204	30.6	10	180	122	11	23	0.00040	53.3	91.9	0.00080	161	207	242	971	2375	417.6	1.91	8.26
205	30.6	10	320	126	22	12	0.00096	57.1	100	0.00117	140	172	196	494	1116	237.9	6.04	22.0
206	30.6	10	320	138	15	22	0.00060	54	99.6	0.00099	158	202	232	807	2027	387.4	4.58	20.5
207	30.6	10	320	154	12	31	0.00040	54	89	0.00095	165	225	273	1120	3273	551.5	3.30	19.5

MARINE THRUST BEARING PROGRAM - PHASE I

TABLE NO. 15

31" O.D. x 151/2" I.D. THRUST BEARING $\left(\frac{L}{R} = 0.5\right)$

Effective Bearing Area	- 480	Sq. In. (k = 0.85)
Average Pad Thickness	- 2.385	In. $\left(\frac{t_{avg.}}{R} = 0.154\right)$
Pivot Pitch Diameter	- 22.78	In. (r_p% = 47 ; θ_p% = 50)

Oil - 2190 T at 115°F Inlet

Case No.	θ_T Deg.	No. of Pads	N RPM	$m_\theta x10^6$ in/in	$m_r x10^6$ in/in	$K=\frac{1}{2R_c}$ 10^{-6} in^{-1}	h_{min} in	r_m%	θ_m%	h_1 in	T_{GR} °F	T_{AVG} °F	T_{MAX} °F	P_{AVG} psi	P_{MAX} psi	$W_{TOT}x10^{-3}$ lbs	Q_{TOT} gpm	$H.P._{TOT}$
203	51	6	180	130	72	14	0.00111	28.6	100	0.00118	130	152	172	288	684	138.2	3.08	8.10
209	51	6	180	169	57	25	0.00060	39	85.7	0.00086	145	177	210	558	1651	268.0	2.45	7.35
210	51	6	180	180	48	31	0.00040	42	80	0.00081	153	193	252	716	2443	343.5	2.32	7.[illegible]
211	51	6	320	164	79	18	0.00120	35.7	100	0.00131	135	162	186	382	922	183.5	6.28	19.5
212	51	6	320	213	56	32	0.00060	42.2	84.5	0.00100	154	192	241	707	2200	339.0	5.34	17.[illegible]
213	51	6	320	218	53	39	0.00040	42.7	78.6	0.00095	161	210	289	867	3275	416.0	4.33	19.2
214	38.25	8	180	80	100	7	0.00090	0	100	0.00090	127	152	166	256	576	122.7	3.[illegible]	9.47
215	38.25	8	180	124	69	19	0.0006	30.5	99.2	0.00071	145	178	201	569	1490	272.6	2.4[illegible]	8.34
216	38.25	8	180	137	55	26	0.0004	37.5	87.2	0.00064	157	201	239	790	2371	379.0	1.99	7.57
217	38.25	8	320	72	138	6	0.00120	0	100	0.00120	125	152	165	183	408	87.9	6.33	22.8
218	38.25	8	320	155	69	25	0.00060	35	95	0.00079	156	198	228	756	2030	363.0	4.63	18.6
219	38.25	8	320	169	62	33	0.00040	38.7	86	0.00072	164	218	272	1005	3107	453.0	4.[illegible]	18.3
220	30.6	10	180	88	100	9	0.00076	0	100	0.00076	132	158	169	307	710	147.8	3.15	9.51
221	30.6	10	180	96	85	13	0.00063	14.3	100	0.00064	138	171	187	454	1103	218.0	2.6[illegible]	9.26
222	30.6	10	180	105	62	20	0.00040	31.2	98.6	0.00052	156	201	226	795	2160	381.6	2.[illegible]1	8.52
223	30.6	10	320	88	120	9	0.00078	0	100	0.00078	132	167	182	382	883	183.1	6.[illegible]	24.4
224	30.6	10	320	120	83	18	0.00061	21.4	100	0.00068	152	193	213	678	1690	325.6	4.93	21.[illegible]
225	30.6	10	320	139	63	27	0.00040	36	96	0.00061	164	220	257	1024	2991	520.6	3.00	19.[illegible]

MARINE THRUST BEARING PROGRAM - PHASE I

TABLE NO. 16

31" O.D. x 15 1/2" I.D. THRUST BEARING $\left(\frac{L}{R} = 0.5\right)$

Effective Bearing Area - 480 Sq. In. (k = 0.85)

Average Pad Thickness - 2.385 In. $\left(\frac{t_{avg.}}{R} = 0.154\right)$

Pivot Pitch Diameter - In. ($r_p\%$ = 50 ; $\theta_p\%$ = 50)

Oil - 2190 T at 115°F Inlet

Case No.	θ_T Deg.	No. of Pads	N RPM	$m_\theta x10^6$ in/in	$m_r x10^6$ in/in	$K=\frac{1}{2R_c}$ 10^{-6} in^{-1}	h_{min} in	$r_m\%$	$\theta_m\%$	h_1 in	T_{GR} °F	T_{AVG} °F	T_{MAX} °F	P_{AVG} psi	P_{MAX} psi	$W_{TOT}x10^{-3}$ lbs	Q_{TOT} gpm	$H.P._{TOT}$
226	38.25	8	180	92	61	7	0.00130	14.3	100	0.00131	130	148	163	182	399	87.5	3.55	3.40
227	38.25	8	180	155	36	24	0.00060	46.3	93.1	0.00091	130	171	201	754	2007	362.0	2.49	9.76
228	38.25	8	180	182	36	33	0.00040	47.3	86.6	0.00087	130	185	230	1047	3196	503.0	2.26	9.[illegible]
229	38.25	8	320	135	58	12	0.00126	35.7	100	0.00136	130	157	178	366	919	175.5	6.85	22.6
230	38.25	8	320	204	40	33	0.00060	47.8	90.9	0.00106	130	184	221	1031	2847	495.0	5.07	23.6
231	38.25	8	320	236	35	43	0.00040	49	85.9	0.00105	130	200	262	1342	4407	645.0	4.79	24.4

TABLE NO. 17

39" O.D. x 191/2" I.D. THRUST BEARING $\left(\frac{L}{R} = 0.5\right)$

Effective Bearing Area - 760 Sq. In. (k = 0.85)

Average Pad Thickness - 3.00 In. $\left(\frac{t_{avg.}}{R} = 0.154\right)$

Pivot Pitch Diameter - 29.25 In. (r_p% = 50 ; θ_p% = 50)

Oil - 2190 T at 115°F Inlet

Case No.	θ_T Deg.	No. of Pads	N RPM	$m_\theta x10^6$ in/in	$m_r x10^6$ in/in	$K=\frac{1}{2R_c}$ 10^{-6} in^{-1}	h_{min} in	r_m%	θ_m%	h_1 in	T_{GR} °F	T_{AVG} °F	T_{MAX} °F	P_{AVG} psi	P_{MAX} psi	$W_{TOT}x10^{-3}$ lbs	Q_{TOT} gpm	$H.P._{TOT}$
232	38.25	8	150	102	46	8	0.00124	35.7	100	0.00133	130	153	170	298	677	266.7	4.90	13.7
233	38.25	8	150	158	32	21	0.00060	47.2	89.7	0.00106	130	175	210	848	2396	644.0	3.67	14.5
234	38.25	8	150	186	29	29	0.00040	48.5	83.4	0.00110	130	189	245	1071	3682	814.0	3.60	15.6
235	38.25	8	200	119	48	10	0.00123	35.7	100	0.00137	130	157	178	393	905	298.5	6.83	22.2
236	38.25	8	200	183	35	25	0.00060	47.5	88.5	0.00116	130	181	221	971	2811	738.0	5.33	22.6
237	38.25	8	200	204	28	31	0.00040	49.1	84.2	0.00116	130	197	261	1245	4335	947.0	5.08	24.3

TABLE NO. 18

19" O.D. x 9 1/2" I.D. THRUST BEARING $\left(\frac{L}{R} = 0.5\right)$

Effective Bearing Area - 181 Sq. In. ($k = 0.85$)

Average Pad Thickness - 1.462 In. $\left(\frac{t_{avg.}}{R} = 0.154\right)$

Pivot Pitch Diameter - 14.25 In. ($r_p\% = 50$; $\theta_p\% = 50$)

Oil - 2190 T at 115°F Inlet

Case No.	θ_T Deg.	No. of Pads	N RPM	$m_\theta x10^6$ in/in	$m_r x10^6$ in/in	$K = \frac{1}{2R_c}$ 10^{-6} in^{-1}	h_{min} in	$r_m\%$	$\theta_m\%$	h_1 in	T_{GR} °F	T_{AVG} °F	T_{MAX} °F	P_{AVG} psi	P_{MAX} psi	$W_{TOT}x10^{-3}$ lbs	Q_{TOT} gpm	H.P.$_{TOT}$
238	51	6	100	113	18	19	0.00060	53.1	97.2	0.00072	129	147	171	254	621	45.9	0.33	0.75
239	51	6	100	147	18	31	0.00040	52.1	87.4	0.00060	136	159	192	416	1171	75.2	0.29	0.72
240	51	6	100	150	20	37	0.00030	50.2	82.2	0.00054	141	170	210	520	1653	93.7	0.27	0.75
241	38.25	8	100	83	44	12	0.00063	28.6	100	0.00065	127	144	159	195	435	35.2	0.37	0.81
242	38.25	8	100	106	34	23	0.00040	42.8	100	0.00050	136	161	182	414	1021	74.7	0.29	0.83
243	38.25	8	100	112	28	29	0.00030	45.2	92.1		144	175	202	599	1513	101.0	0.24	0.78
244	30.6	10	100	44	68	4	0.00069	0	100	0.00069	125	141	152	964	2058	17.4	0.40	0.85
245	30.6	10	100	82	54	16	0.00042	21.4	100	0.00044	133	156	170	324	736	58.4	0.32	0.88
246	30.6	10	100	85	40	22	0.00030	35.7	100	0.00037	141	174	192	522	1283	94.3	0.25	0.88

MARINE THRUST BEARING PROGRAM - PHASE I

TABLE NO. 19

75" O.D. x 371/2" I.D. THRUST BEARING $\left(\frac{L}{R} = 0.5\right)$

Effective Bearing Area - 2810 Sq. In. ($k = 0.85$)

Average Pad Thickness - 5.77 In. $\left(\frac{t_{avg.}}{R} = 0.154\right)$

Pivot Pitch Diameter - 56.25 In. ($r_p\% = 50$; $\theta_p\% = 50$)

Oil - 2190 T at 115°F Inlet

Case No.	θ_T Deg.	No. of Pads	N RPM	$m_\theta x10^6$ in/in	$m_r x10^6$ in/in	$K=\frac{1}{2R_c}$ 10^{-6} in^{-1}	h_{min} in	$r_m\%$	$\theta_m\%$	h_1 in	T_{GR} °F	T_{AVG} °F	T_{MAX} °F	P_{AVG} psi	P_{MAX} psi	$W_{TOT}x10^{-3}$ lbs	Q_{TOT} gpm	$H.P._{TOT}$
247	51	6	100	170	20	13	0.00060	50	76.3	0.00205	153	196	272	706	3203	1985.0	16.0	53.1
248	51	6	100	183	22	15	0.00040	49.8	74.6	0.00210	157	210	318	783	4390	2200.0	16.7	61.8
249	38.25	8	100	137	25	12	0.00060	47.5	81.0	0.00166	160	206	263	802	2927	2260.0	13.1	47.3
250	38.25	8	100	136	21	13	0.00040	48.1	78.3	0.00161	163	225	319	1004	4517	2825.0	12.2	53.6
251	30.6	10	100	106	26	10	0.00060	45.5	86.5	0.00137	162	213	254	902	2819	2544.0	11.5	47.3
252	30.6	10	100	115	25	12	0.00040	46.6	82.8	0.00137	165	232	306	1128	4311	3180.2	10.9	51.4

MARINE THRUST BEARING PROGRAM - PHASE I

TABLE NO. 20

100" O.D. x 50" I.D. THRUST BEARING $\left(\frac{L}{R} = 0.5\right)$

Effective Bearing Area - 5000 Sq. In. (k = 0.85)

Average Pad Thickness - 7.70 In. $\left(\frac{t_{avg.}}{R} = 0.154\right)$

Pivot Pitch Diameter - 75 In. (r_p% = 50 ; θ_p% = 50)

Oil - 2190 T at 115°F Inlet

Case No.	θ_T Deg.	No. of Pads	N RPM	$m_\theta x10^6$ in/in	$m_r x10^6$ in/in	$K=\frac{1}{2R_c}$ 10^{-6} in^{-1}	h_{min} in	r_m%	θ_m%	h_1 in	T_{GR} °F	T_{AVG} °F	T_{MAX} °F	P_{AVG} psi	P_{MAX} psi	$W_{TOT}x10^{-3}$ lbs	Q_{TOT} gpm	$H.P._{TOT}$
253	51	6	100	179	20	11	0.00060	49.8	74.5	0.00284	156	206	305	745	4268	3730	39.2	142
254	51	6	100	175	22	12	0.00040	49	72.1	0.00290	160	226	352	876	6451	4380	47.8	171
255	38.25	8	100	130	22	9	0.00060	47.8	79.4	0.00205	163	221	301	977	3995	4890	28.2	121
256	38.25	8	100	146	21	11	0.00040	48.5	76.8	0.00226	165	237	367	1055	5939	5280	27.4	138
257	30.6	10	100	116	24	9	0.00060	46.7	83.0	0.00191	165	226	289	1028	3758	5151	26.7	118
258	30.6	10	100	122	22	10	0.00040	47.4	81.1	0.00191	165	248	353	1296	5862	6493	25.7	132

MARINE THRUST BEARING - Phase I

Table No. 21

Oil - 2190 TEP at 115°F Inlet

R in.	9.5	22.5	37.5	50
L in.	4.75	11.25	18.75	25
t_{avg} in.	1.236	2.924	4.88	6.50
θ_T - degrees	51	51	51	51
n	6	6	6	6
r_p %	50	50	50	50
θ_p %	50	50	50	50
N - RPM	100	100	100	100
$m_\theta \times 10^{-6}$ in/in	187	228	215	211
$m_r \times 10^{-6}$ in/in	25	27	25	23
$K \times 10^{-6}$ in^{-1}	47	30	21	17
h_{min} - in.	0.00040	0.00040	0.00040	0.00040
r_m %	50.2	46.5	49.2	49.0
θ_m %	81.7	75.5	70.7	68.7
T_{GR} - °F	134	145	151	154
T_{AVG} - °F	155	181	204	220
T_{MAX} - °F	188	251	286	300
P_{AVG} - P.S.I.	377	565	666	704
P_{MAX} - P.S.I.	1203	3004	4625	5682
$W_{TOT} \times 10^{-3}$ - Lbs.	68.1	572.0	1870	3520

MARINE THRUST BEARING PROGRAM - PHASE I

TABLE NO. 22

51 1/2 " O.D. x 32 " I.D. THRUST BEARING $\left(\frac{L}{R} = 0.379\right)$

Effective Bearing Area - 1,085 Sq. In. (k = 0.85)

Average Pad Thickness - 3.00 In. $\left(\frac{t_{avg.}}{R} = 0.117\right)$

Pivot Pitch Diameter - 42.25" In. (r_p% =52.6; θ_p% = 50)

Oil - 2190 T at 115°F Inlet

Case No.	θ_T Deg.	No. of Pads	N RPM	$m_\theta x10^6$ in/in	$m_r x10^6$ in/in	$K=\frac{1}{2R_c}$ 10^{-6} in^{-1}	h_{min} in	r_m%	θ_m%	h_1 in	T_{GR} °F	T_{AVG} °F	T_{MAX} °F	P_{AVG} psi	P_{MAX} psi	$W_{TOT}x10^{-3}$ lbs	Q_{TOT} gpm	$H.P._{TOT}$
263	30.6	10	200	155	-35	9	0.00242				130	150	174	274	610	296.9	19.0	47.5
264	30.6	10	200	154	-28	12	0.00151				135	162	194	433	1019	469.1	15.3	48.9
265	30.6	10	200	170	-20	15	0.00120				140	169	202	514	1267	557.6	14.4	46.8
266	30.6	10	200	198	-20	26	0.00060				160	204	262	844	2663	916.1	11.1	42.5
267	30.6	10	200	208	-30	31	0.00040				164	222	312	1058	4111	1147.6	10.5	47.7
268	30.6	10	400	185	-39	9	0.00292				130	155	182	334	732	362.3	46.8	145
269	30.6	10	400	215	-23	21	0.00120				152	190	231	718	1841	779.3	31.8	125
270	30.6	10	400	210	-22	22	0.00112				154	195	240	765	2011	830.5	29.8	122
271	30.6	10	400	242	-6	33	0.00060				165	225	310	1165	3939	1264	25.8	130
272	30.6	10	400	266	-30	42	0.00040				165	245	374	1360	5935	1475	26.2	152
273	25.5	12	200	132	-5	6	0.00246				128	145	162	198	429	215.0	21.4	42.8
274	25.5	12	200	125	-5	8	0.00189				130	155	176	319	707	346.1	17.2	52.0
275	25.5	12	200	145	-3	13	0.00131				141	170	196	488	1155	529.8	14.6	49.2
276	25.5	12	200	170	-2	24	0.00060				163	209	254	894	2574	969.9	10.5	42.3
277	25.5	12	200	176	-2	29	0.00040				165	230	302	1172	4005	1271	9.3	47.1
278	25.5	12	400	164	-15	6	0.00297				128	150	172	265	566	287.6	52.1	148
279	25.5	12	400	175	-14	15	0.00140				146	182	212	609	1425	661.0	34.9	141
280	25.5	12	400	183	-8	18	0.00116				153	194	223	708	1713	767.6	32.1	134
281	25.5	12	400	212	0	31	0.00060				165	231	297	1281	3873	1390	23.6	130
282	25.5	12	400	225	10	38	0.00040				165	256	361	1602	5431	1740	22.2	146

FIGURES

Figure 1
MOMENT EQUILIBRIUM

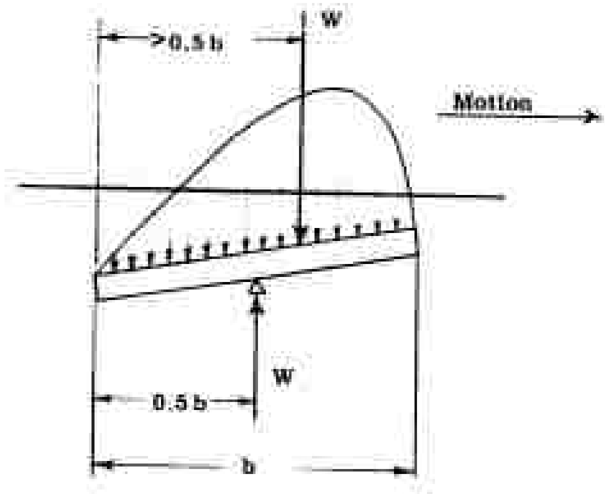

Restoring Moment: $M \neq 0$

(a)

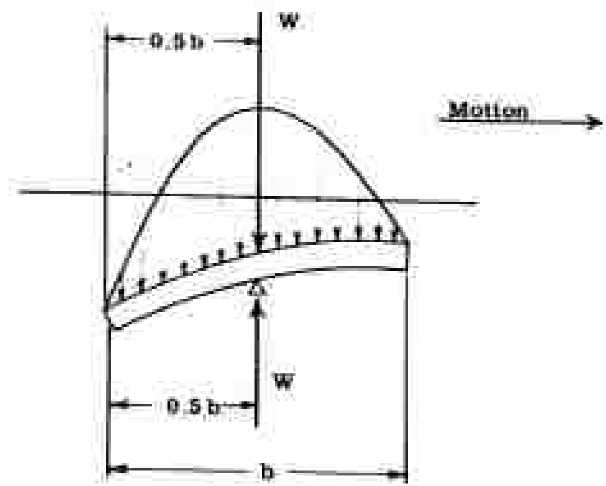

Restoring Moment: $M = 0$

(b)

Bearing Pad: 31" OD, $15\frac{1}{2}$" ID, $38\frac{1}{4}^{o}$ Subtended Angle   Speed: 320 RPM

Oil: 2190T, 130°F at Pad Inlet   Minimum Film Thickness: .001"

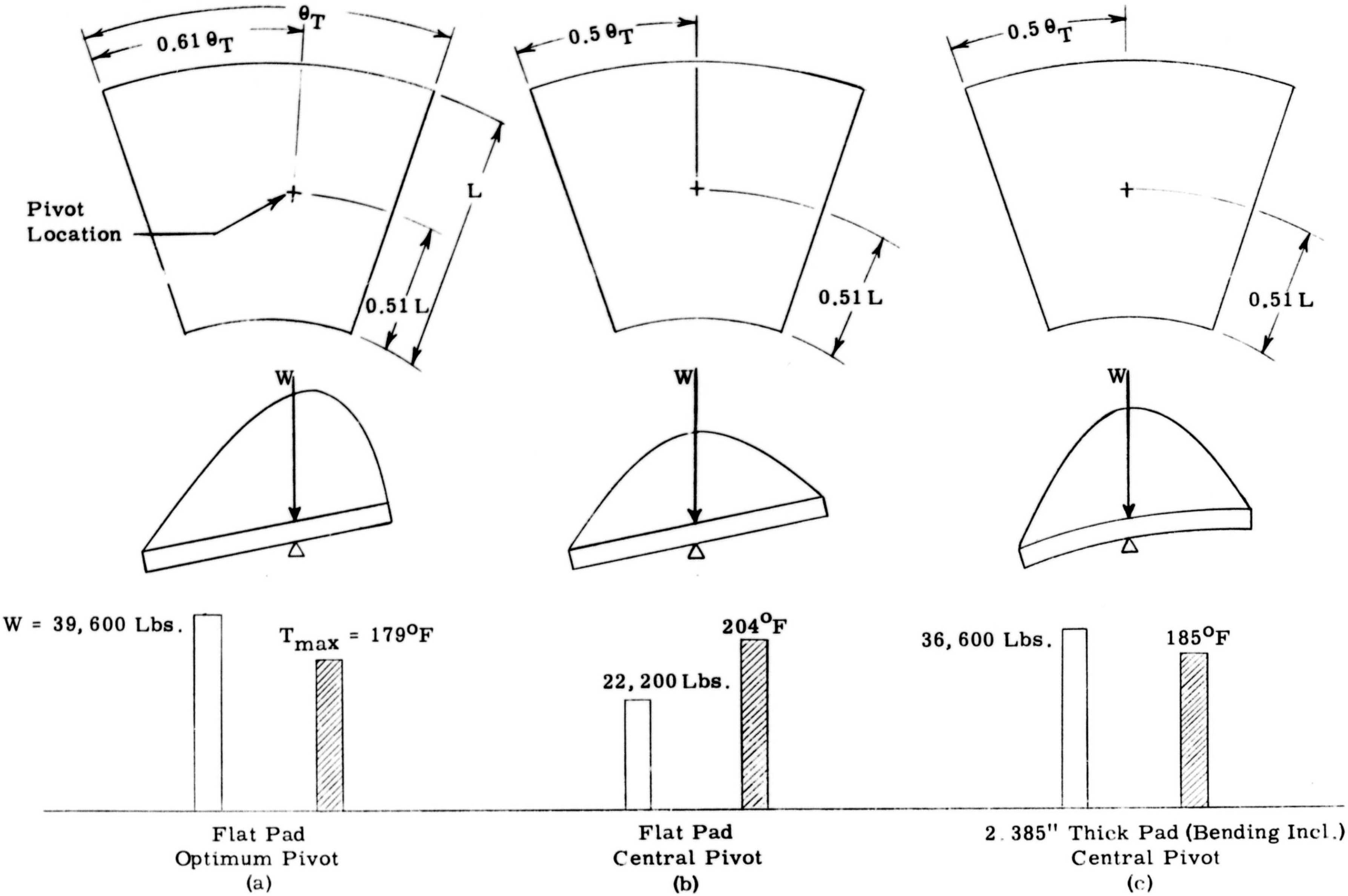

Figure 2

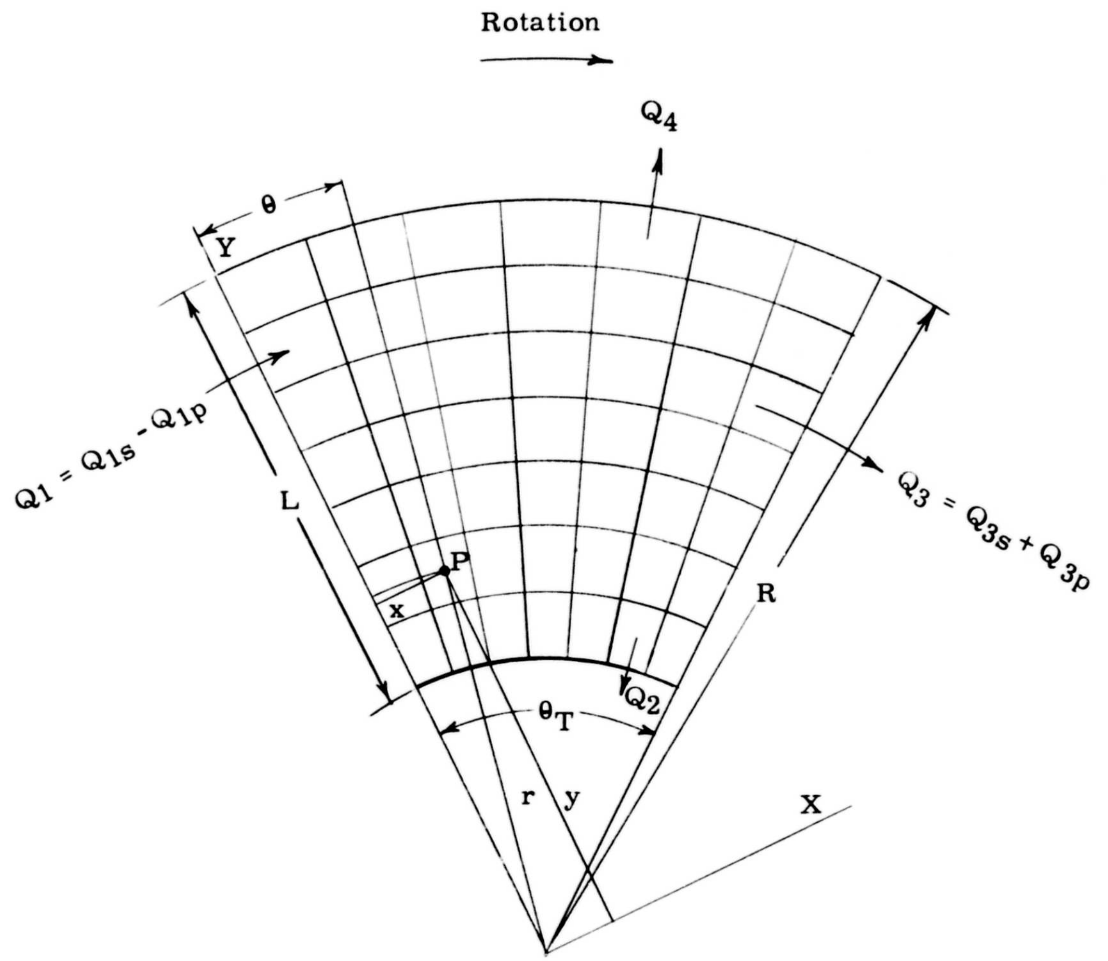

Figure 3

Co-ordinate System

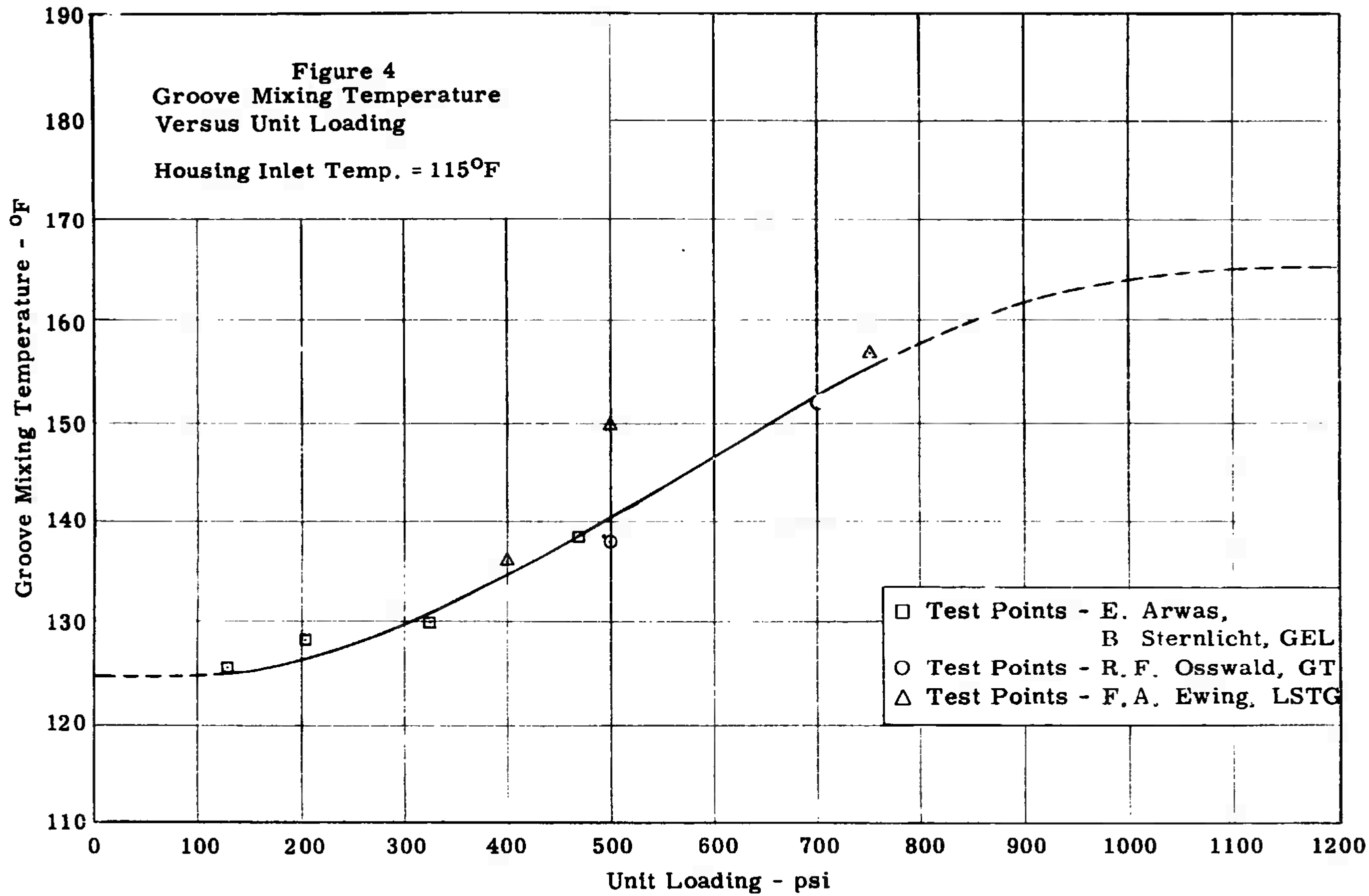

Figure 4
Groove Mixing Temperature
Versus Unit Loading
Housing Inlet Temp. = 115°F
190
180
170
160
150
140
130
120
110
Groove Mixing Temperature - °F
0
100
200
300
400
500
600
700
800
900
1000
1100
1200
Unit Loading - psi
□ Test Points - E. Arwas,
B Sternlicht, GEL
O Test Points - R.F. Osswald, GT
Δ Test Points - F.A. Ewing, LSTG

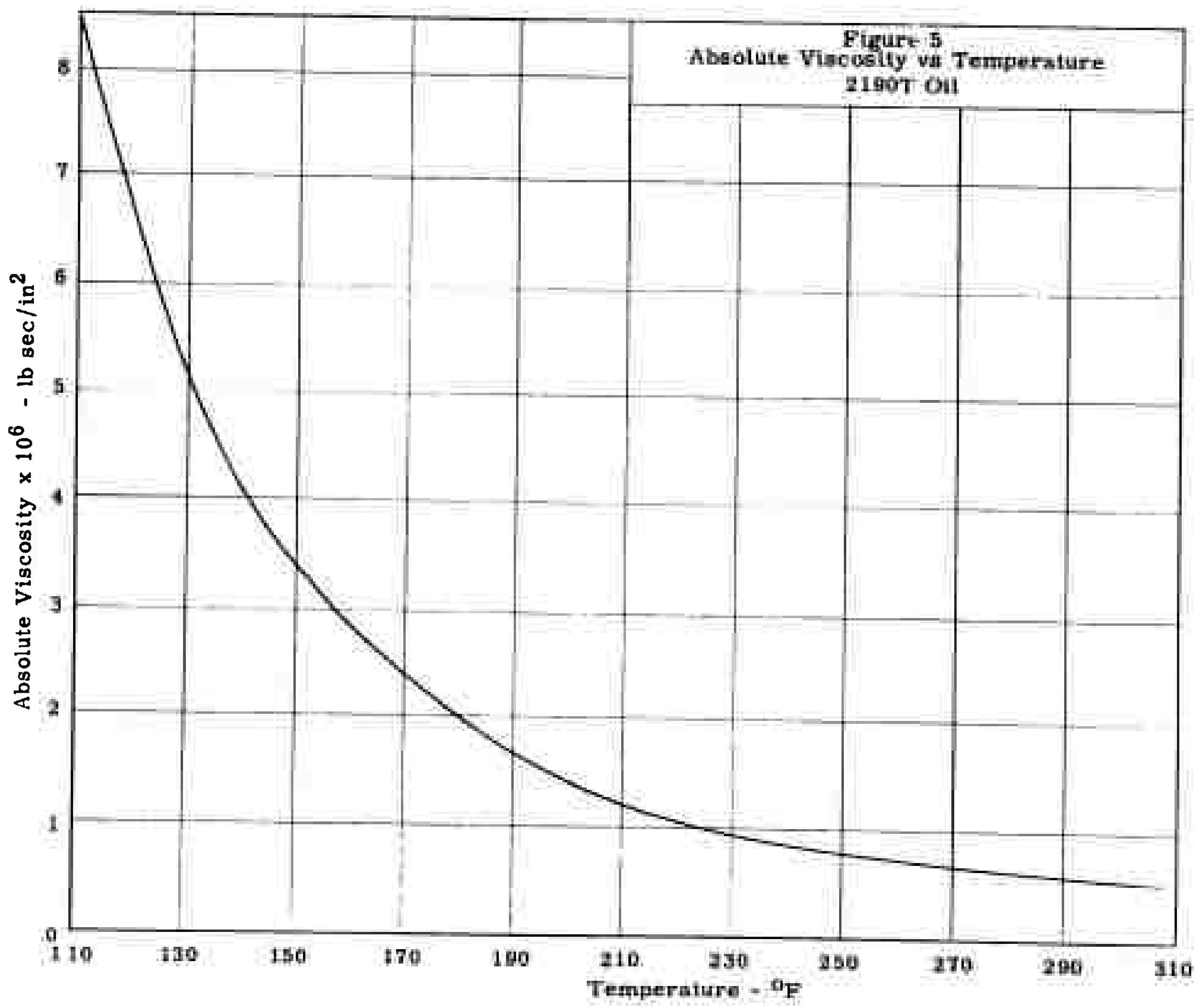

Figure 5
Absolute Viscosity vs Temperature
2190T Oil

Figure 6
MESH NOTATION

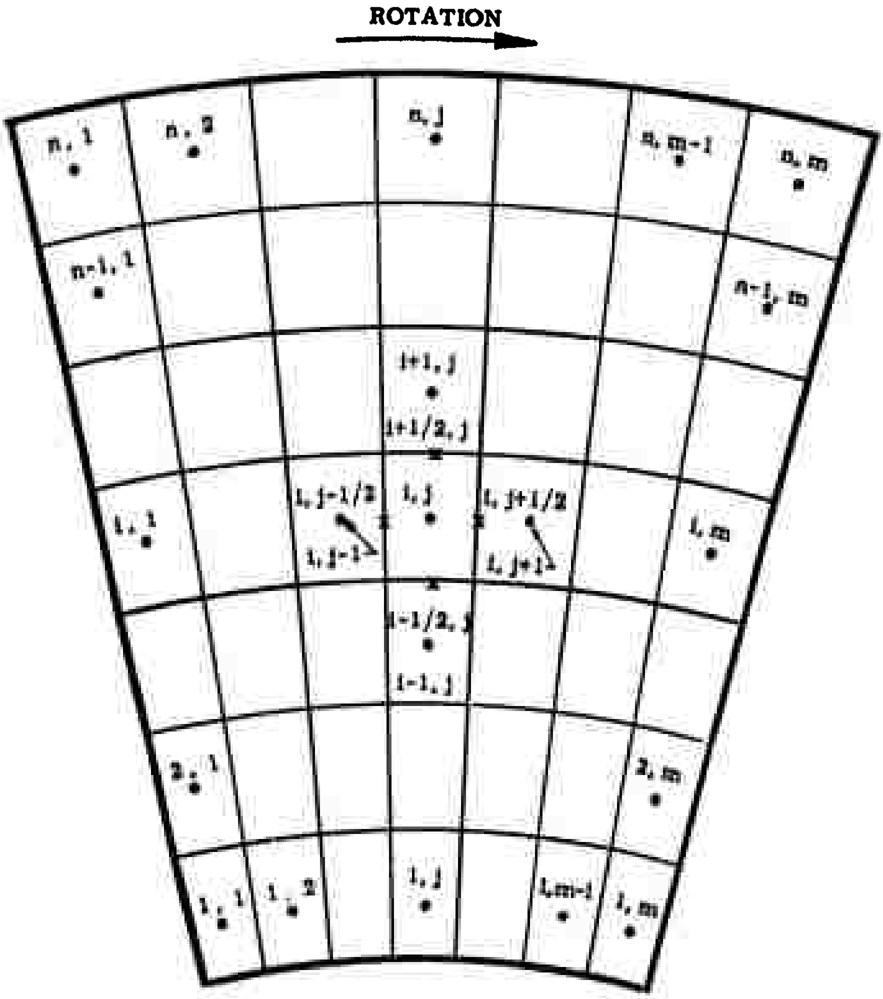

Figure 6

160 x 220   29/64 In. Div.

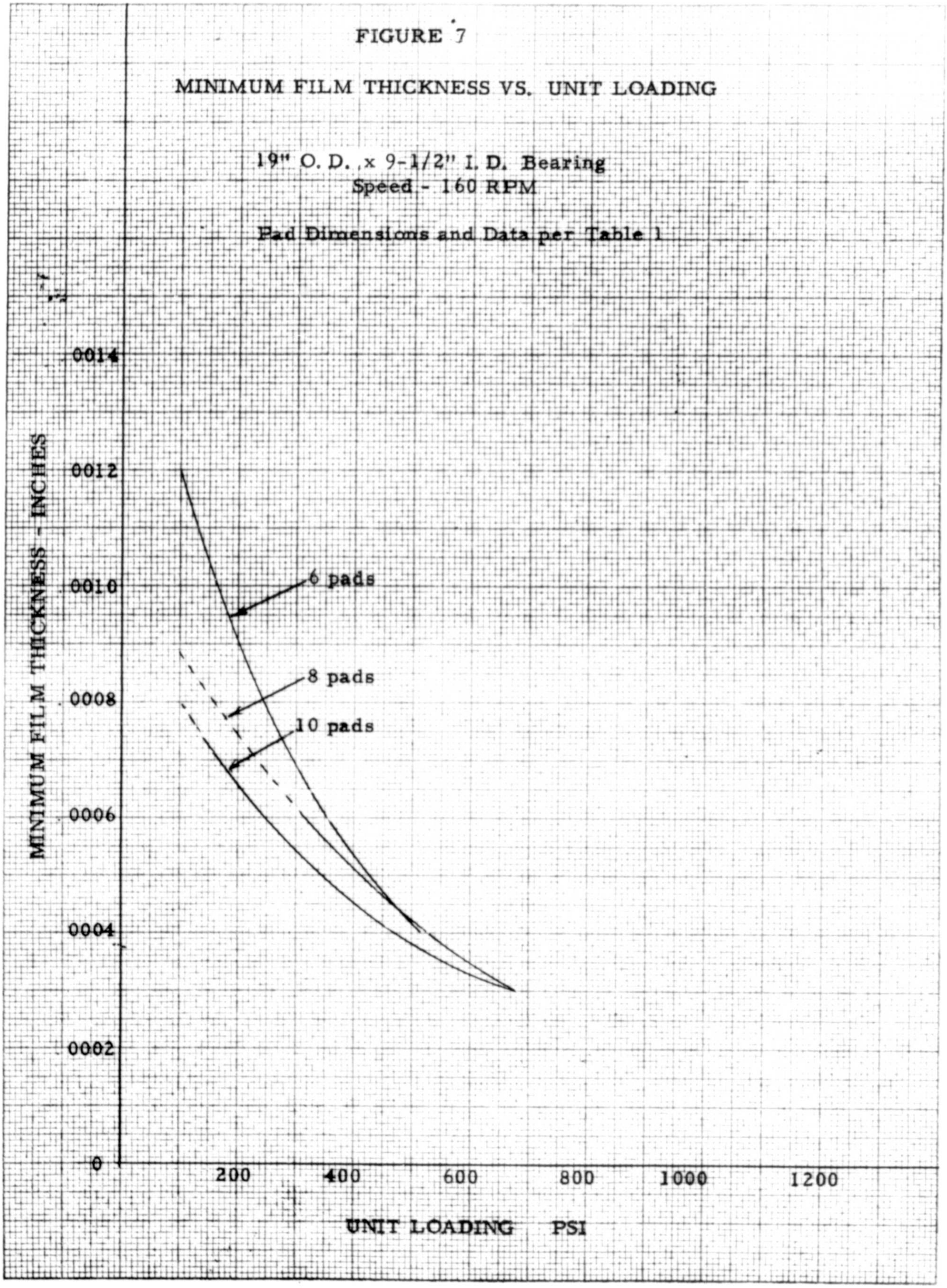

FIGURE 8

MINIMUM FILM THICKNESS VS. UNIT LOADING

19" O. D. x 9-1/2" I. D. Bearing
Speed - 310 RPM

Pad Dimensions and Data per Table 1

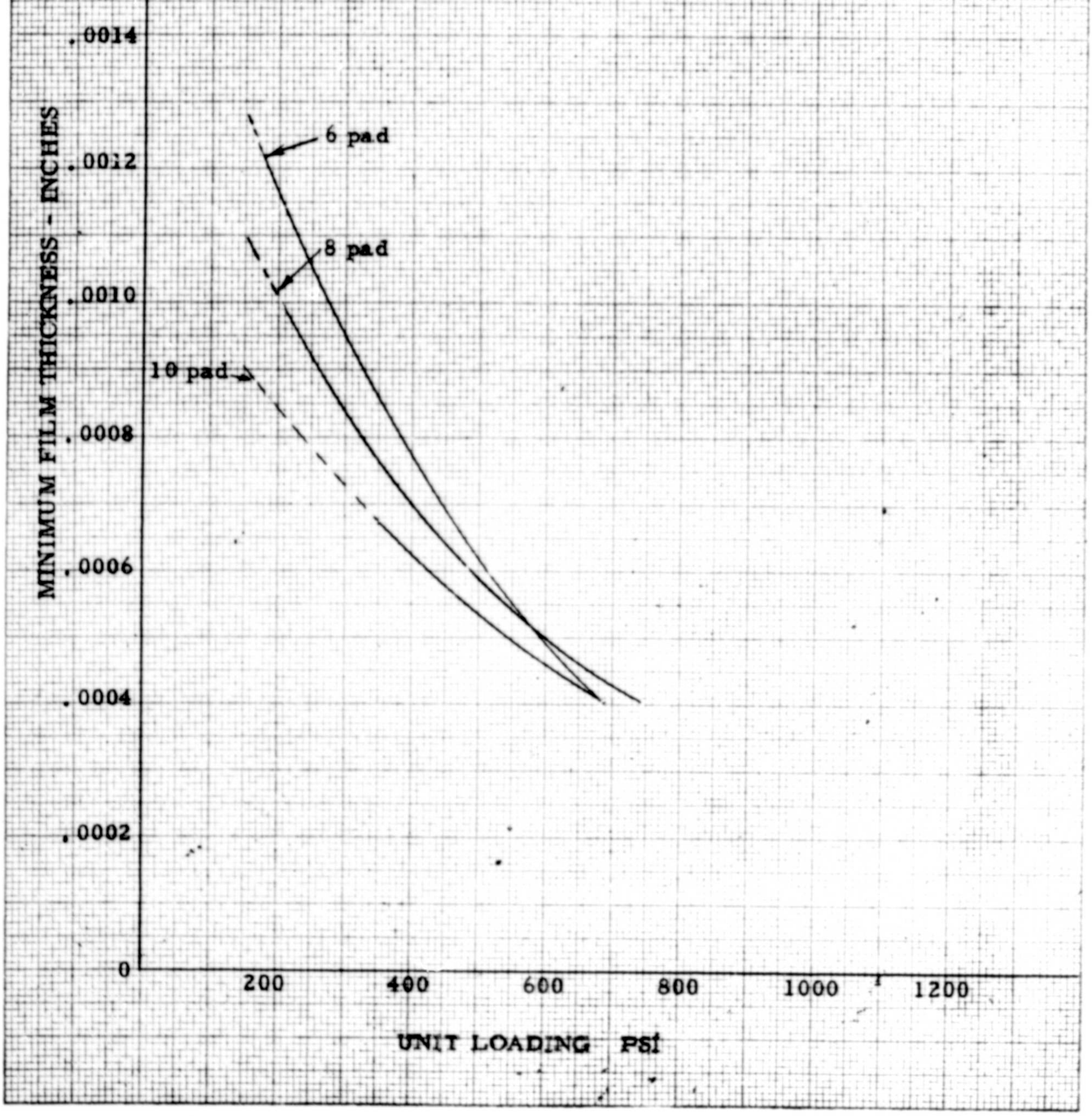

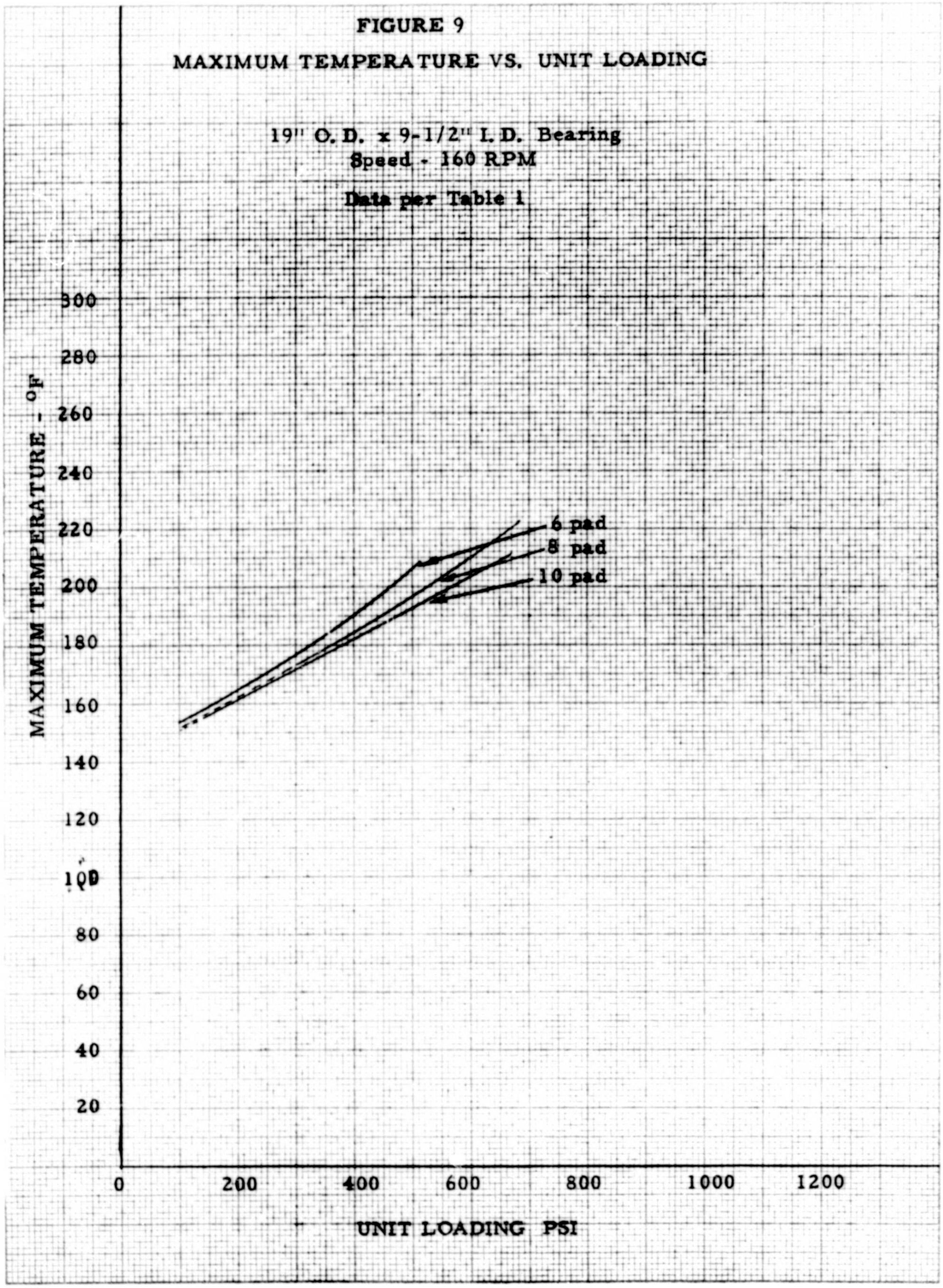

160 x 220   29/64 In. Div.

FIGURE 10

MAXIMUM TEMPERATURE VS. UNIT LOADING

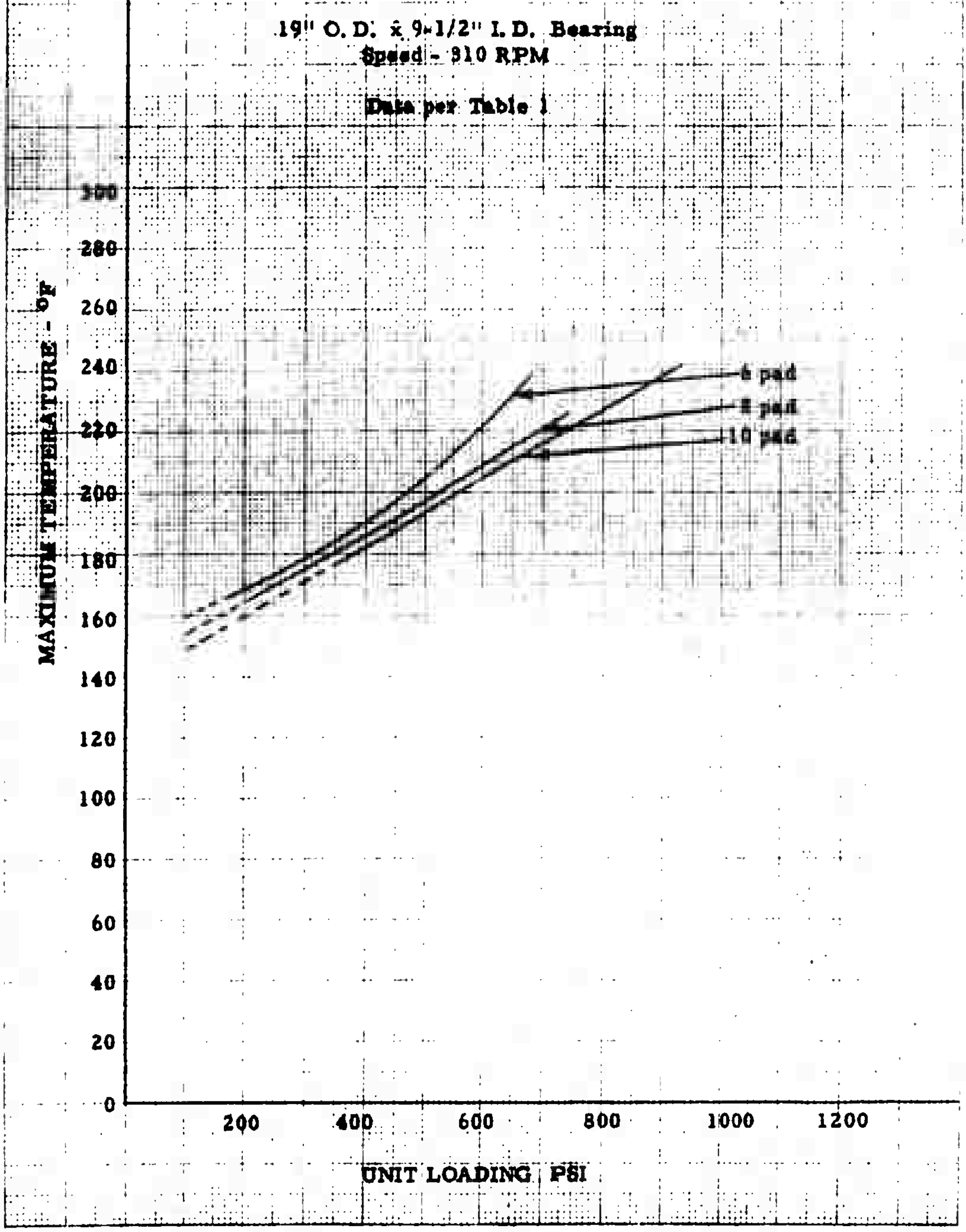

FIGURE 11

HYDRODYNAMIC OIL FLOW VERSUS UNIT LOADING

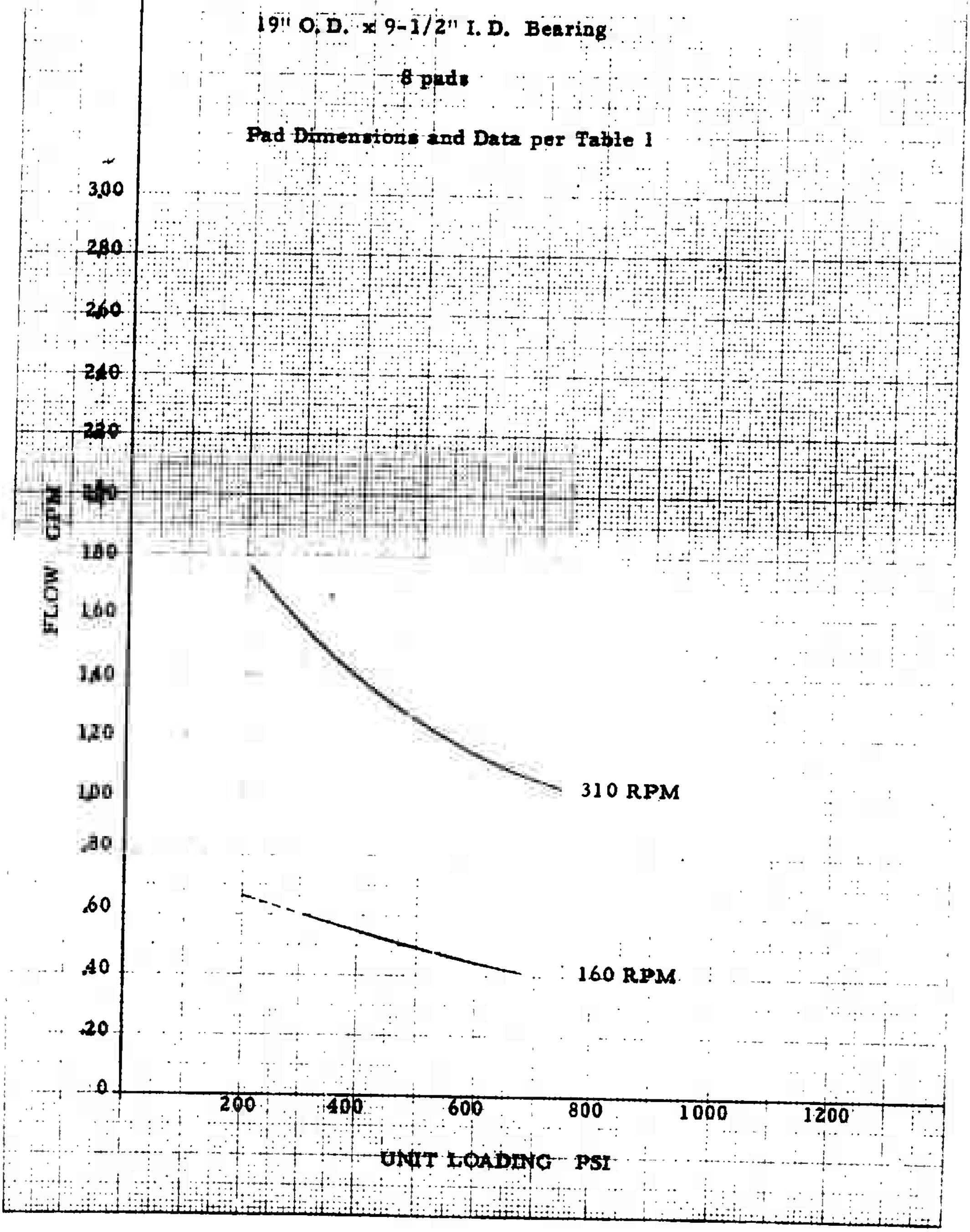

160 x 220 29/64 In. Div.

FIGURE 12

MINIMUM FILM THICKNESS VS. UNIT LOADING

25" O.D. x 12-1/2" I.D. Bearing
Speed - 120 RPM

Pad Dimensions and Data per Table 2

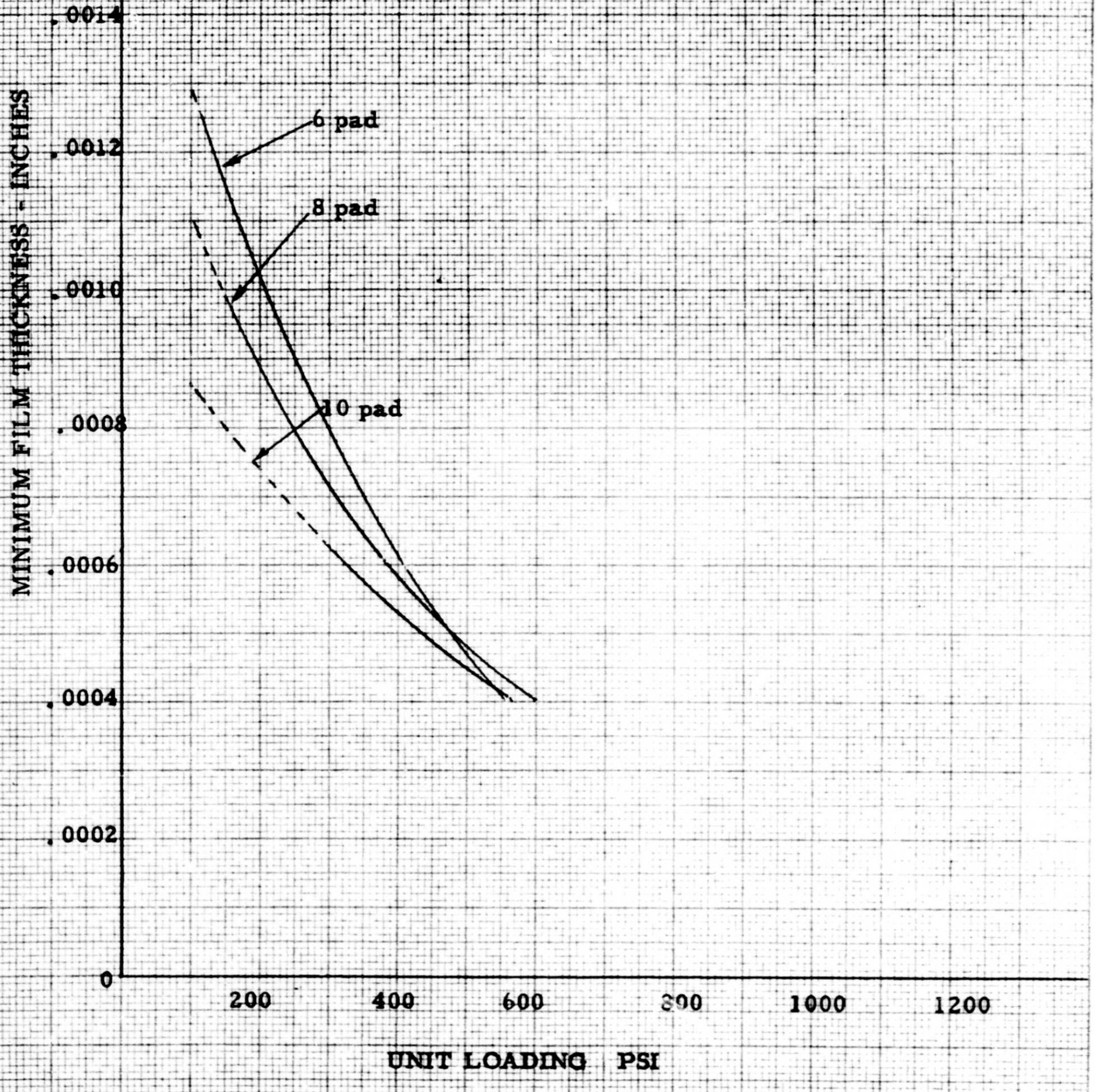

FIGURE 13

MINIMUM FILM THICKNESS VS. UNIT LOADING

25" O.D. x 12-1/2" I.D. Bearing
Speed - 240 RPM

Pad Dimensions and Data per Table 2

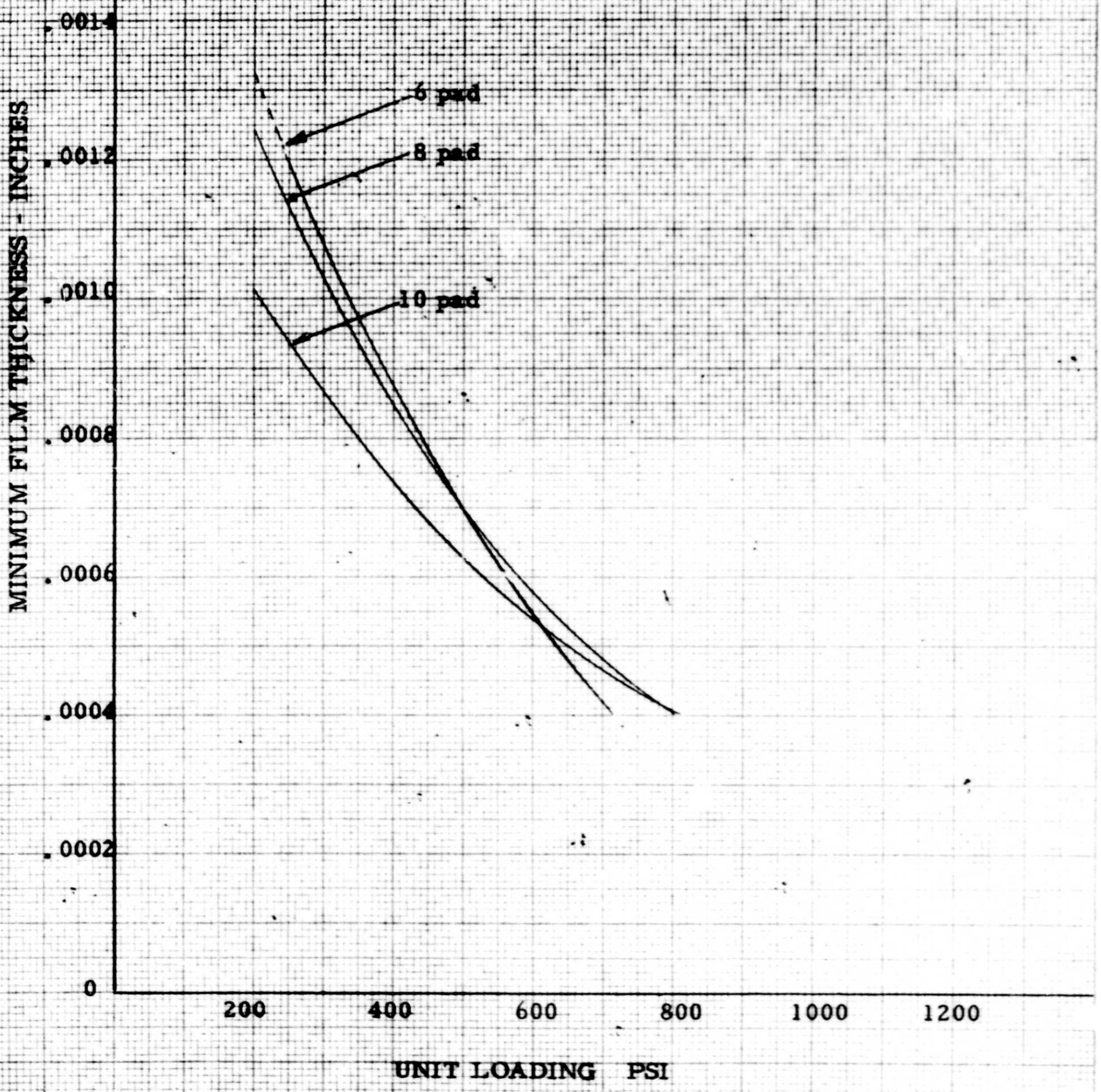

160 x 220 29/64 In. Div.

FIGURE 14

MAXIMUM TEMPERATURE VS. UNIT LOADING

25" O.D. x 12-1/2" I.D. Bearing
Speed - 120 RPM

Data per Table 2

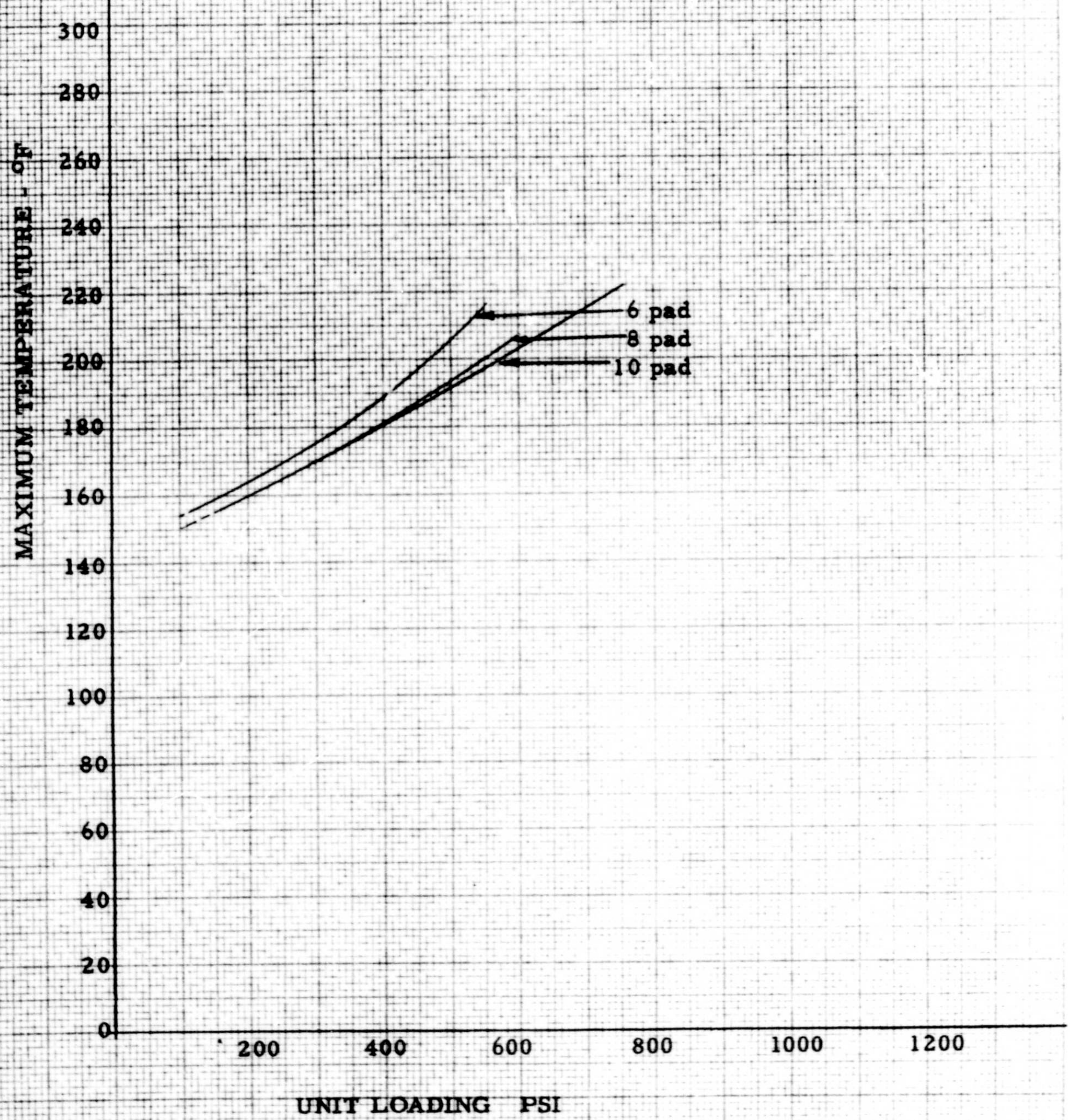

FIGURE 15

MAXIMUM TEMPERATURE VS. UNIT LOADING

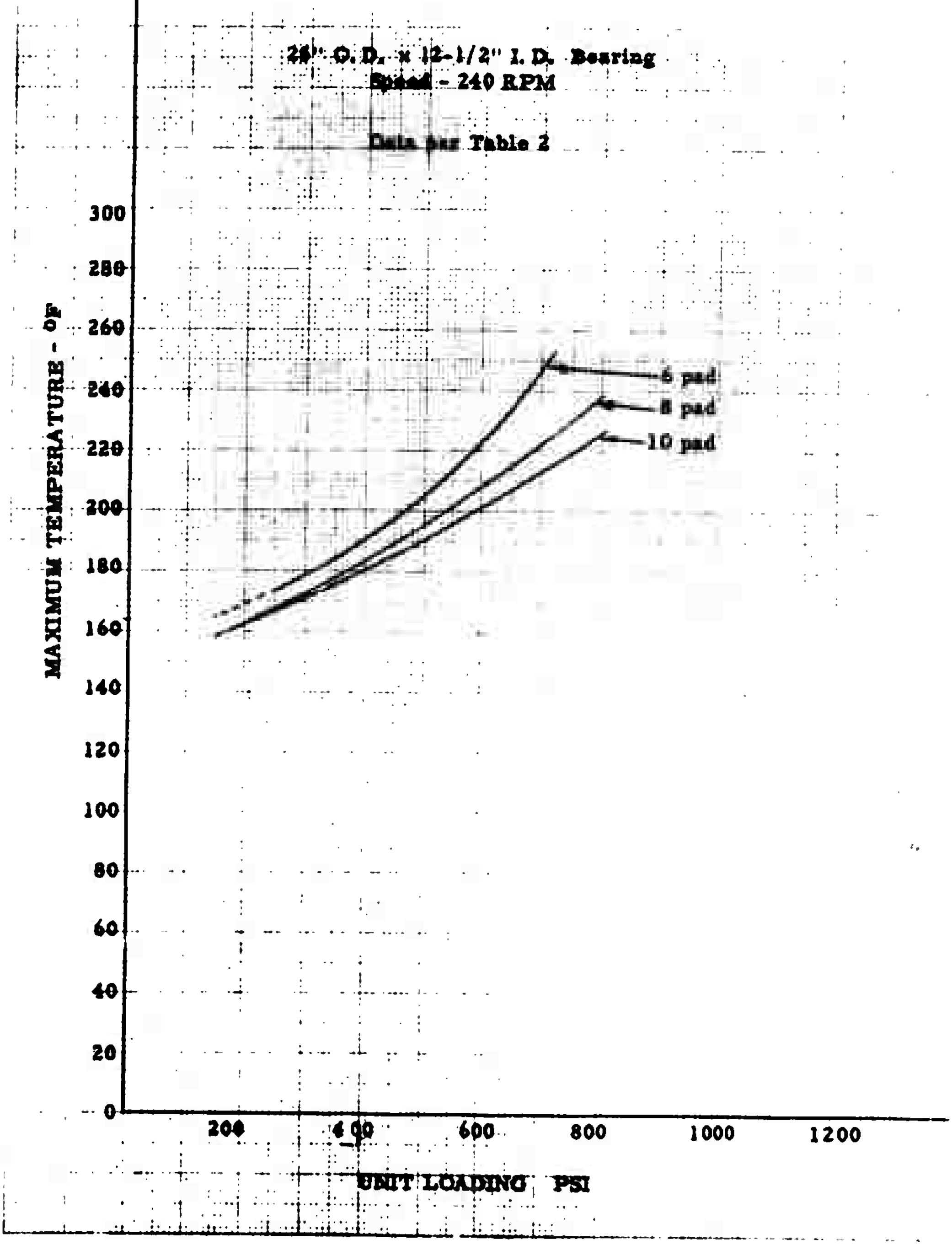

160 x 220   29/64 In. Div.

FIGURE 16

HYDRODYNAMIC OIL FLOW VERSUS UNIT LOADING

25" O.D. x 12-1/2" I.D. Bearing

8 Pads

Pad Dimensions and Data per Table 2

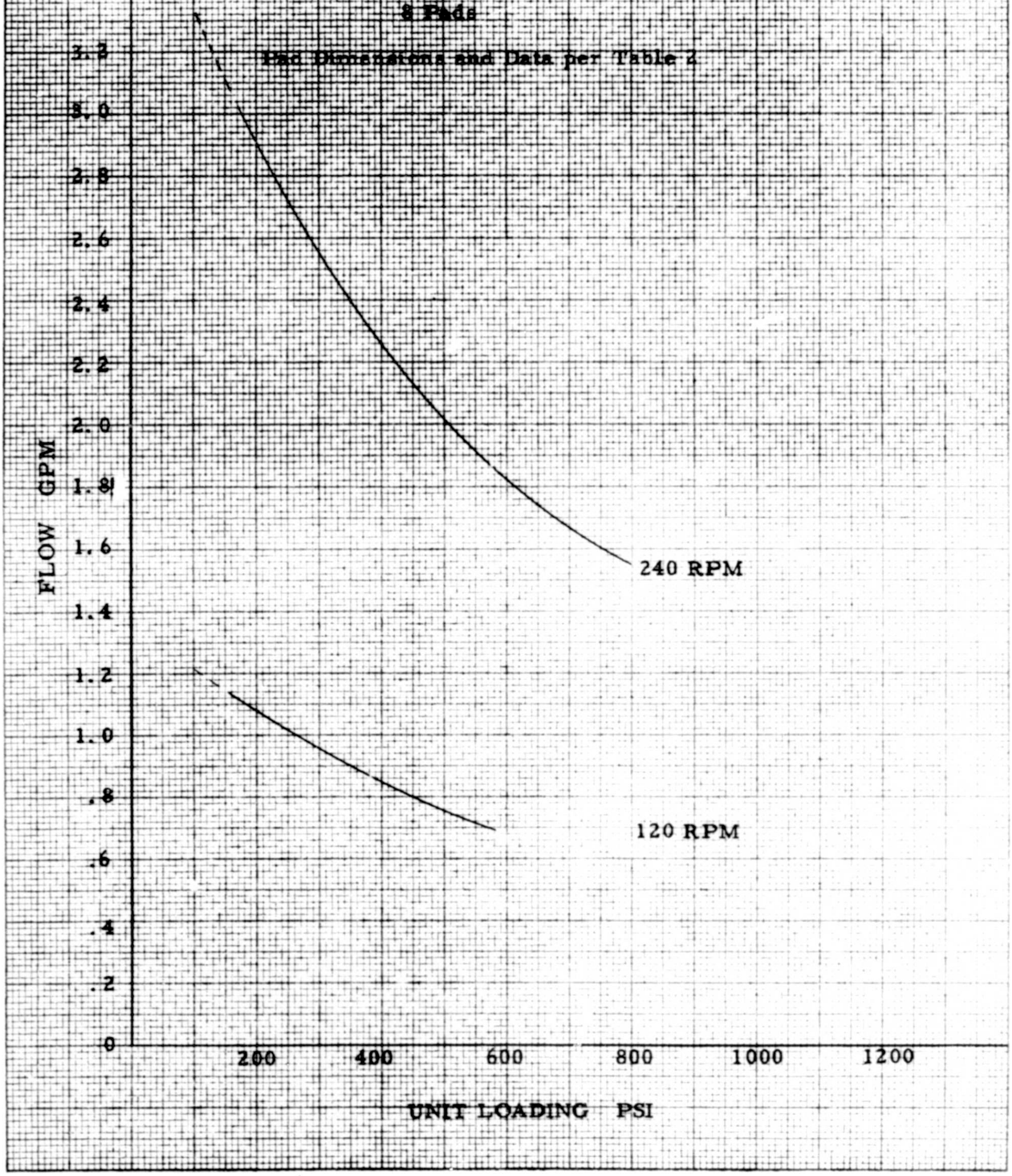

FIGURE 17

MINIMUM FILM THICKNESS VS. UNIT LOADING

31" O.D. x 15-1/2" I.D. Bearing
Speed - 180 RPM

Pad Dimensions and Data per Table 3

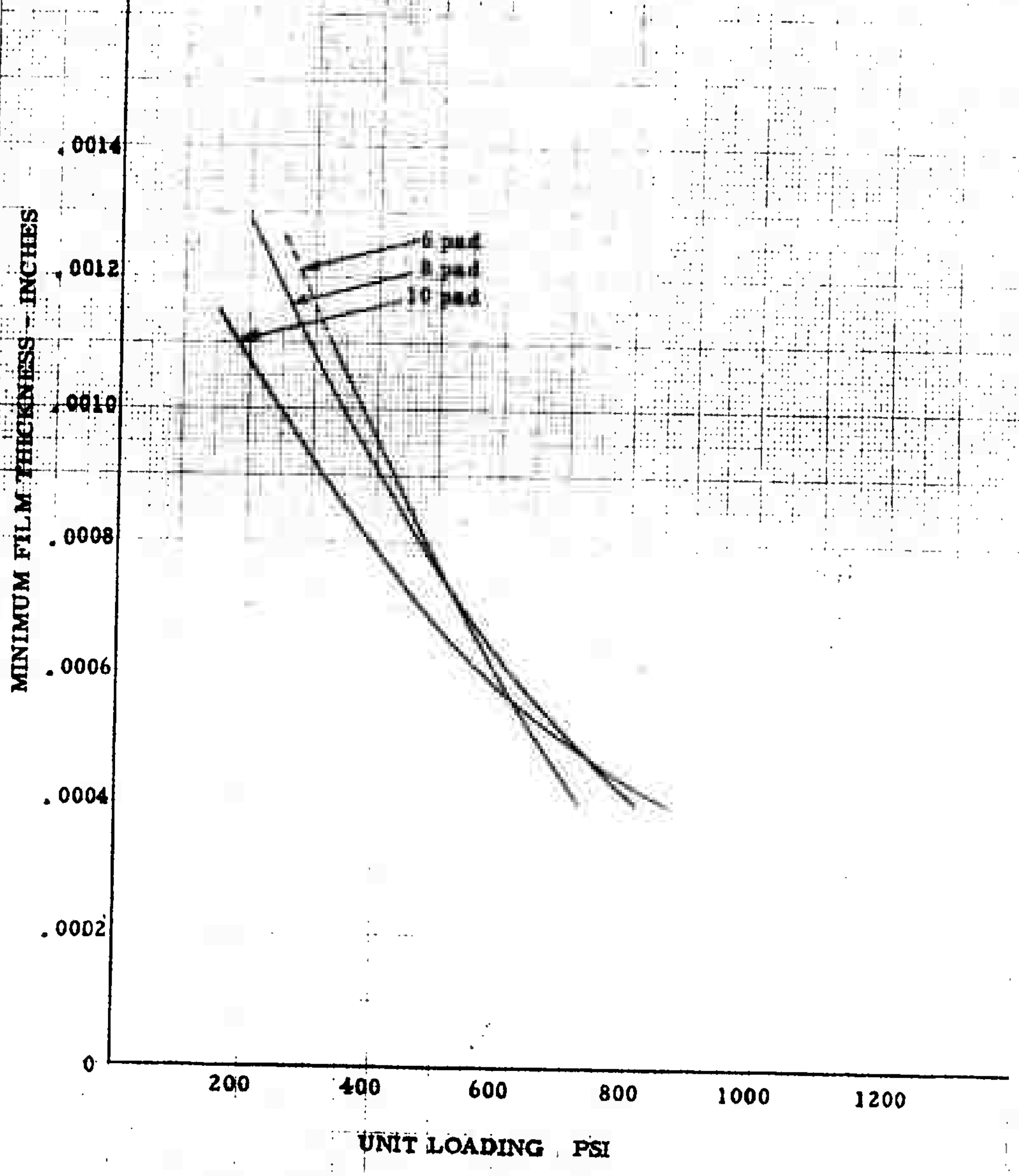

FIGURE 18

MINIMUM FILM THICKNESS VS. UNIT LOADING

31" O.D. x 15-1/2" I.D. Bearing
Speed - 320 RPM

Pad Dimensions and Data per Table 3

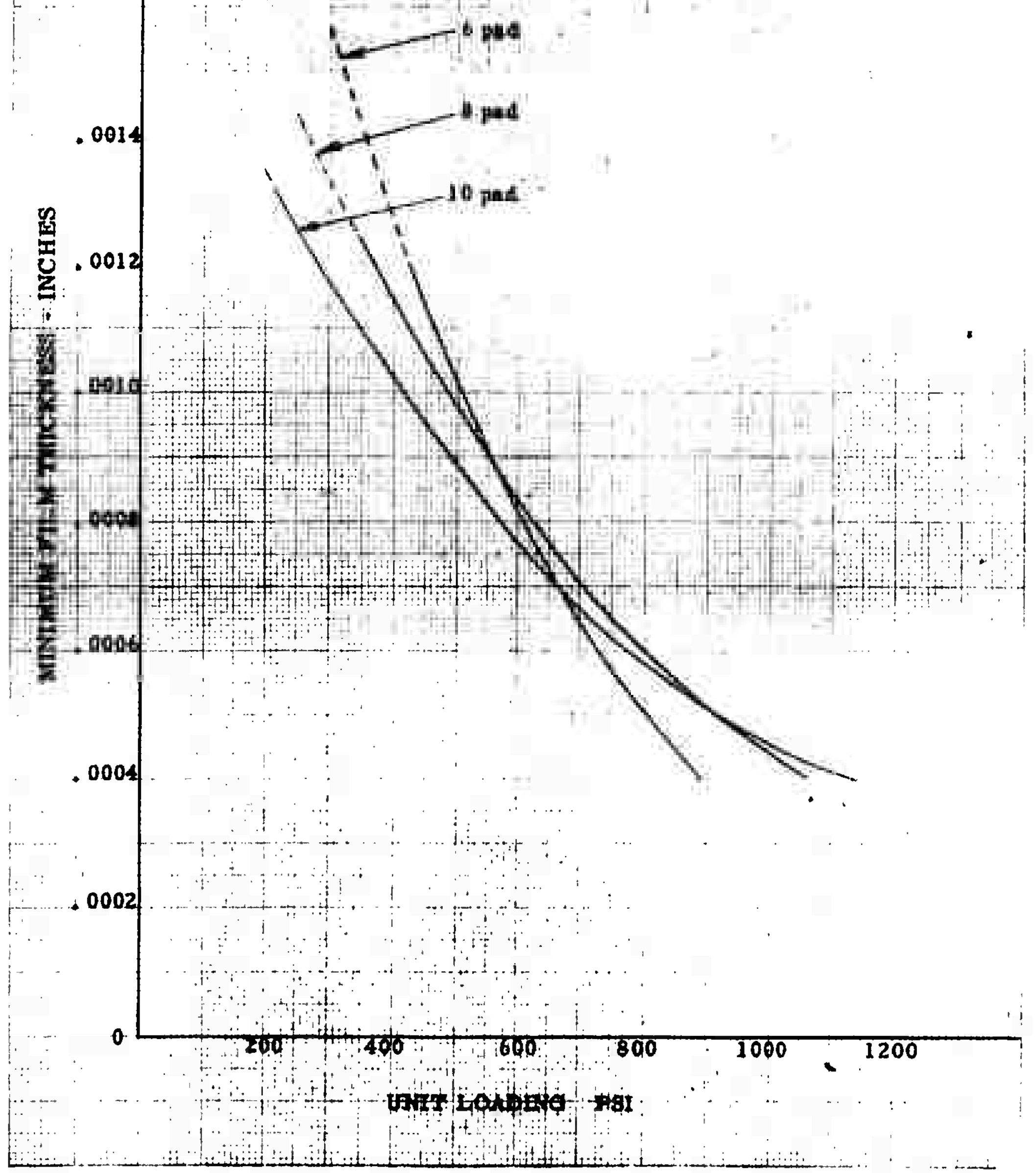

FIGURE 19

MAXIMUM TEMPERATURE VS. UNIT LOADING

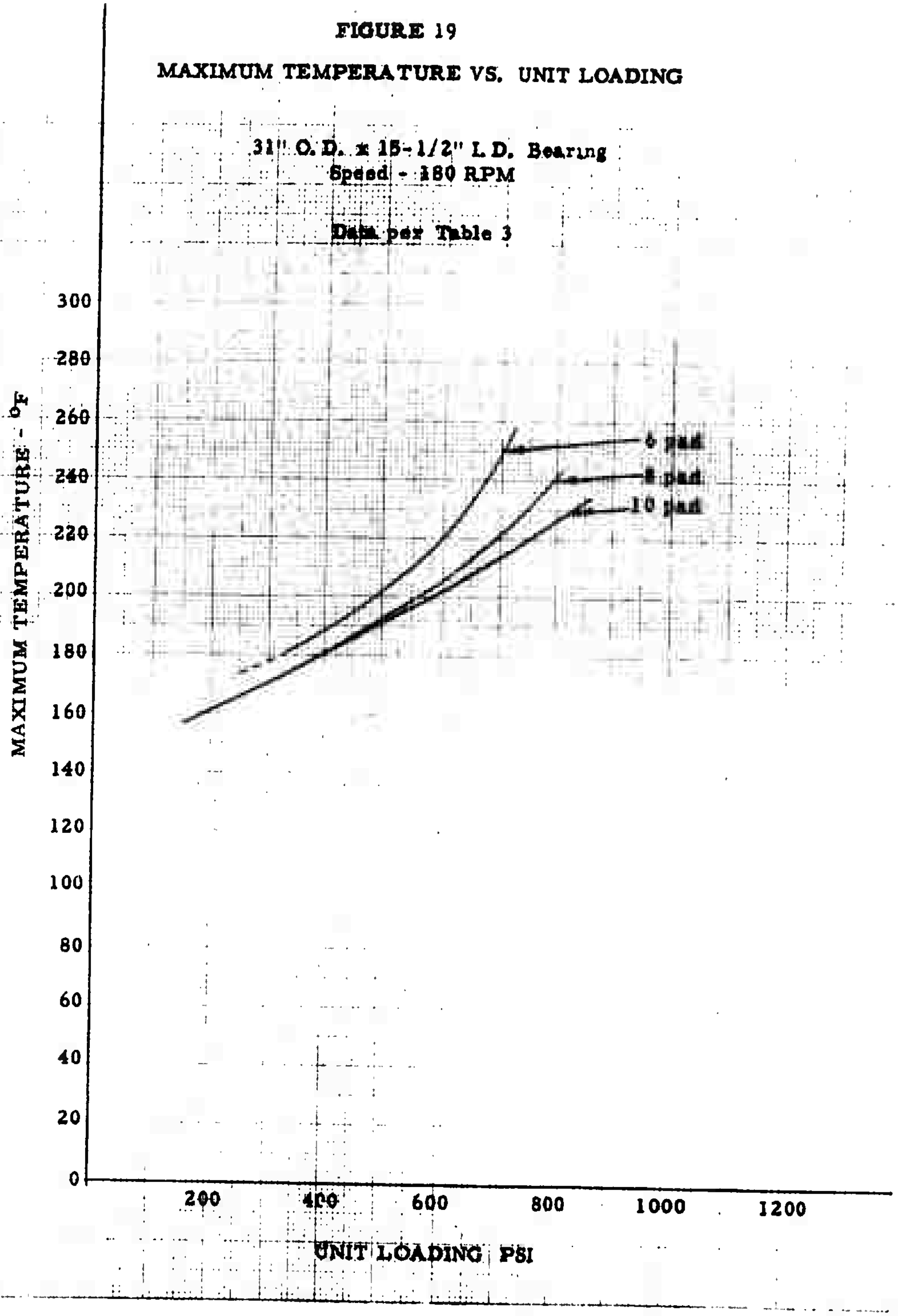

FIGURE 20
MAXIMUM TEMPERATURE VS. UNIT LOADING

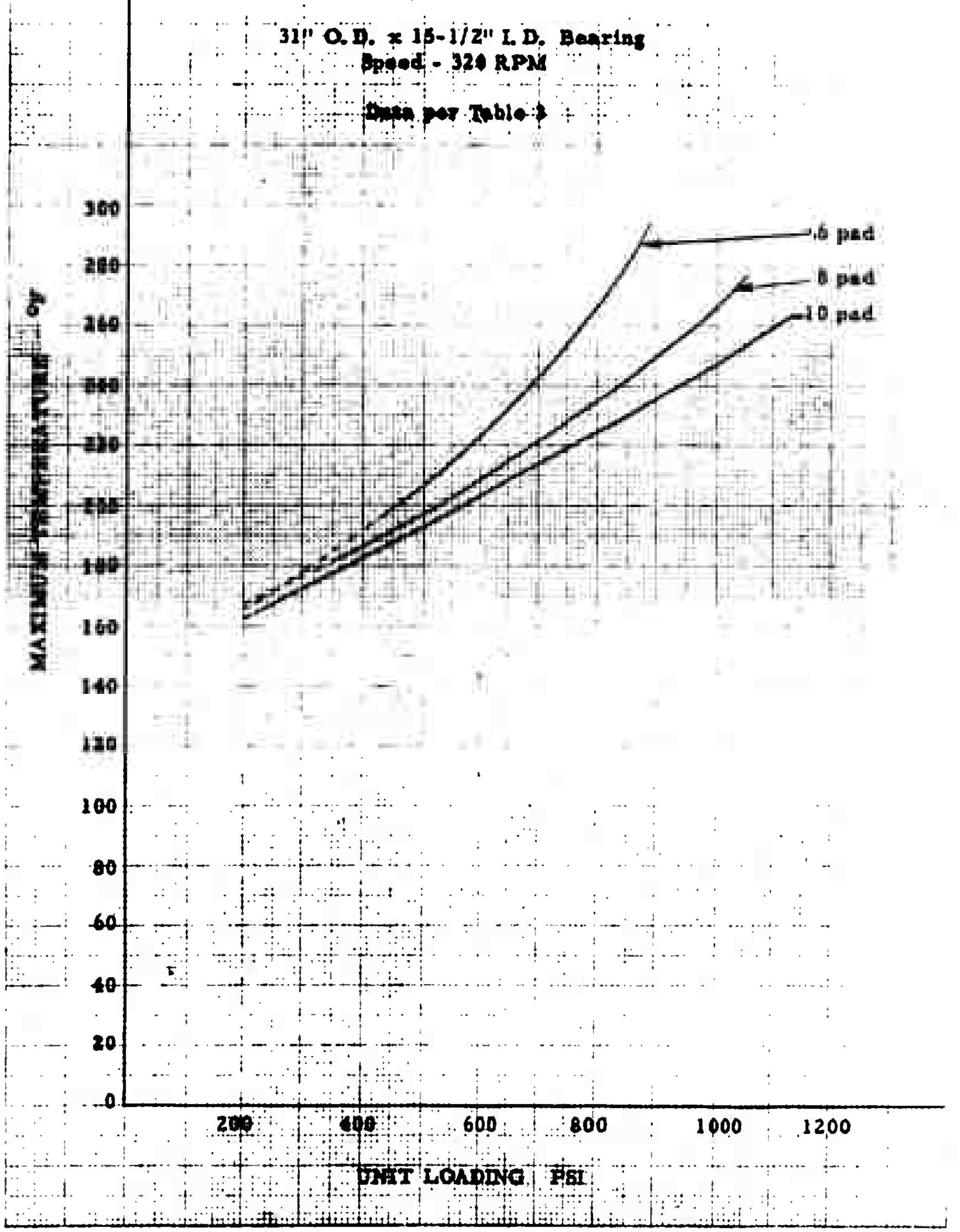

FIGURE 21

HYDRODYNAMIC OIL FLOW VERSUS UNIT LOADING

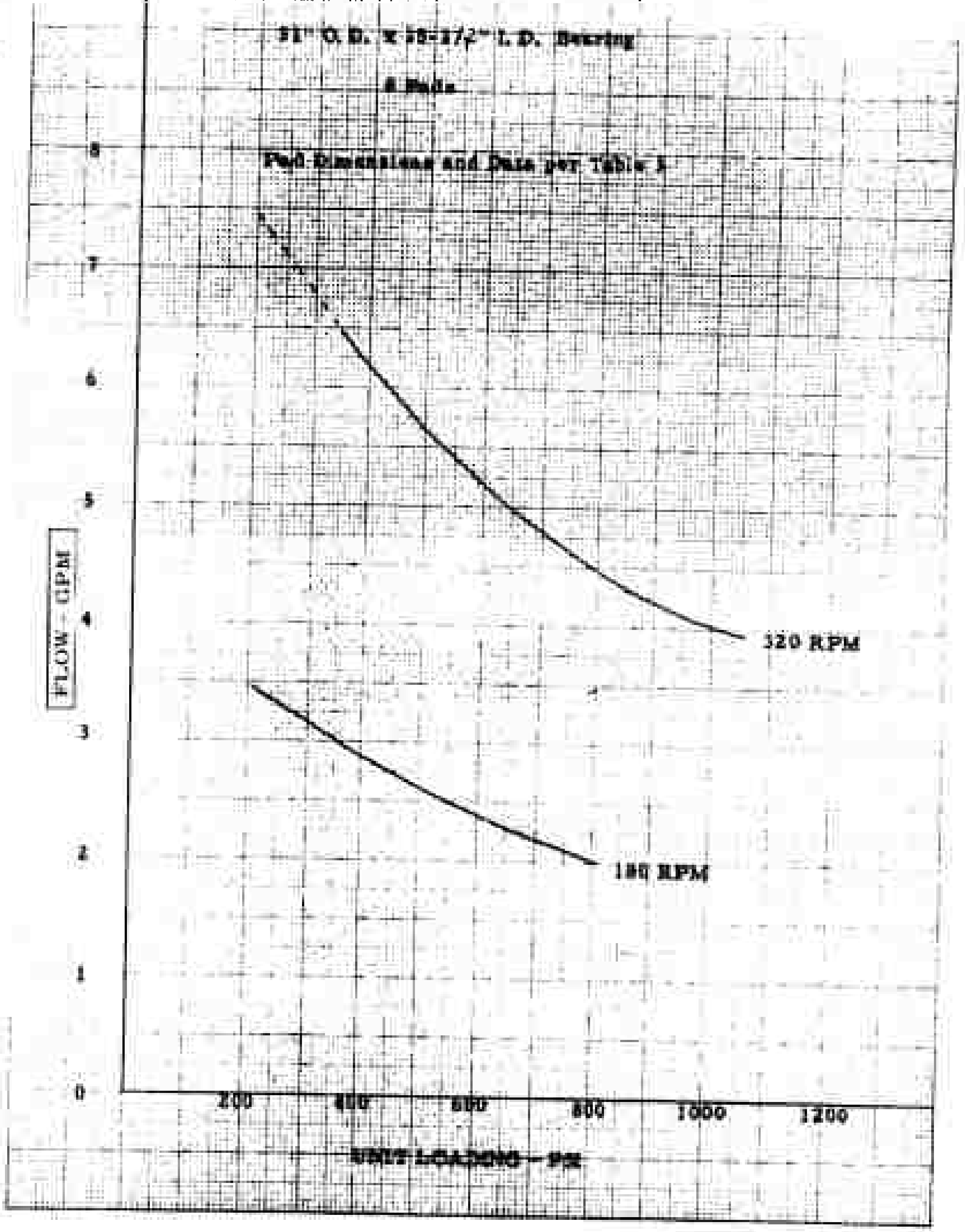

FIGURE 22

MINIMUM FILM THICKNESS VS. UNIT LOADING

37" O. D. x 18-1/2" I. D. Bearing
Speed - 180 RPM

Data per Table 4

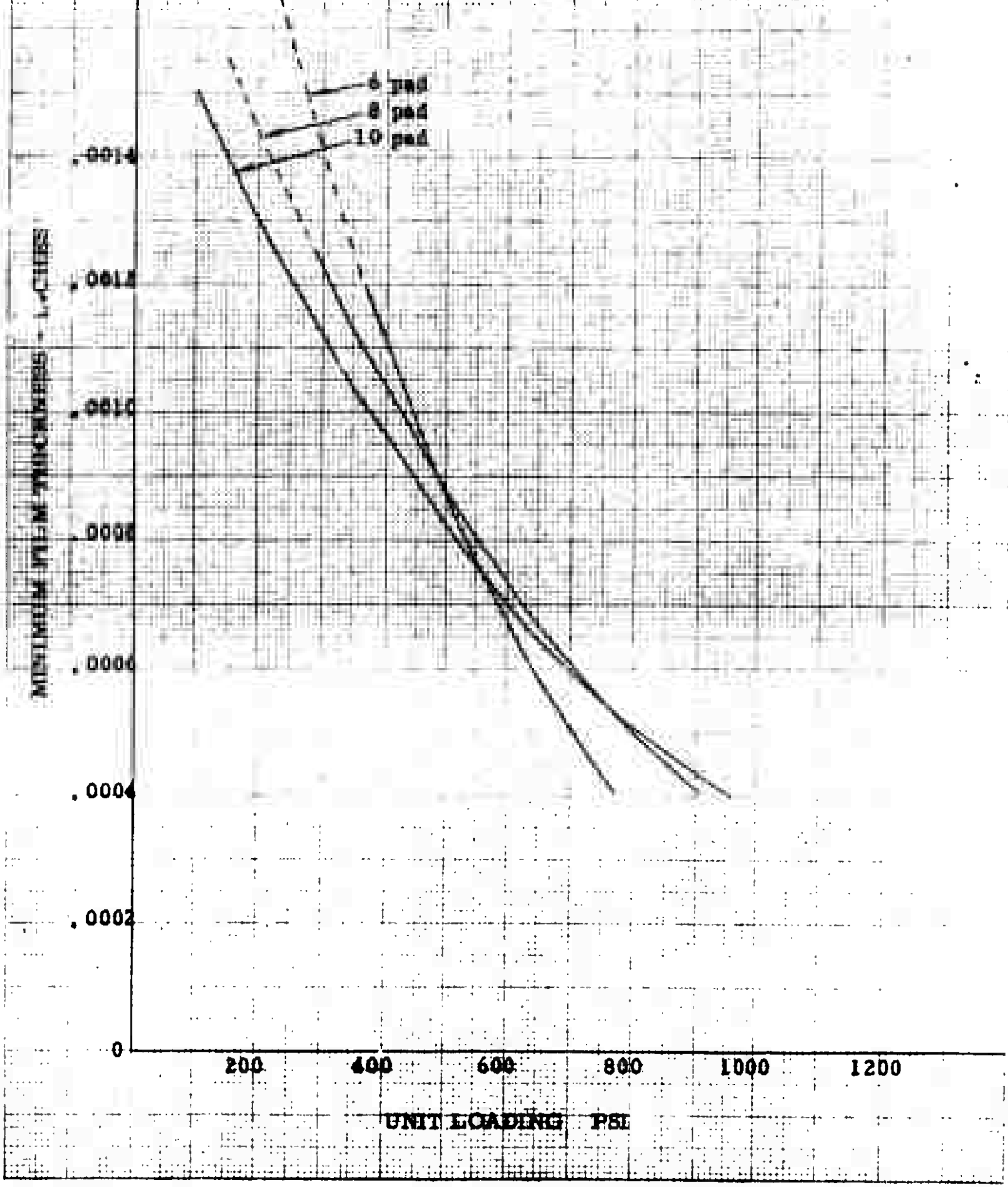

FIGURE 23

MINIMUM FILM THICKNESS VS. UNIT LOADING

37" O.D. x 18-1/2" I.D. Bearing
Speed - 320 RPM

Pad Dimensions and Data per Table 4

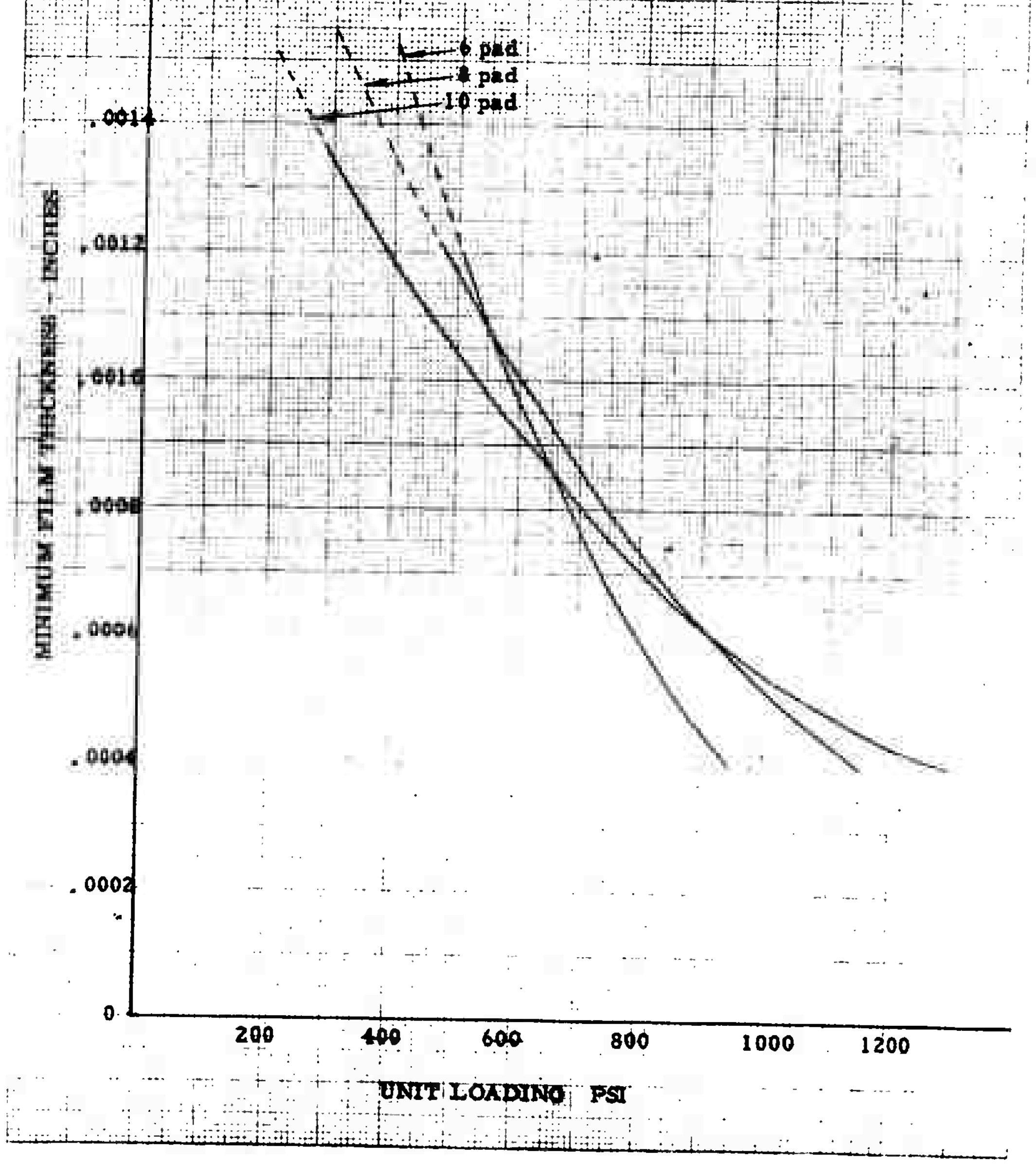

FIGURE 24

MAXIMUM TEMPERATURE VS. UNIT LOADING

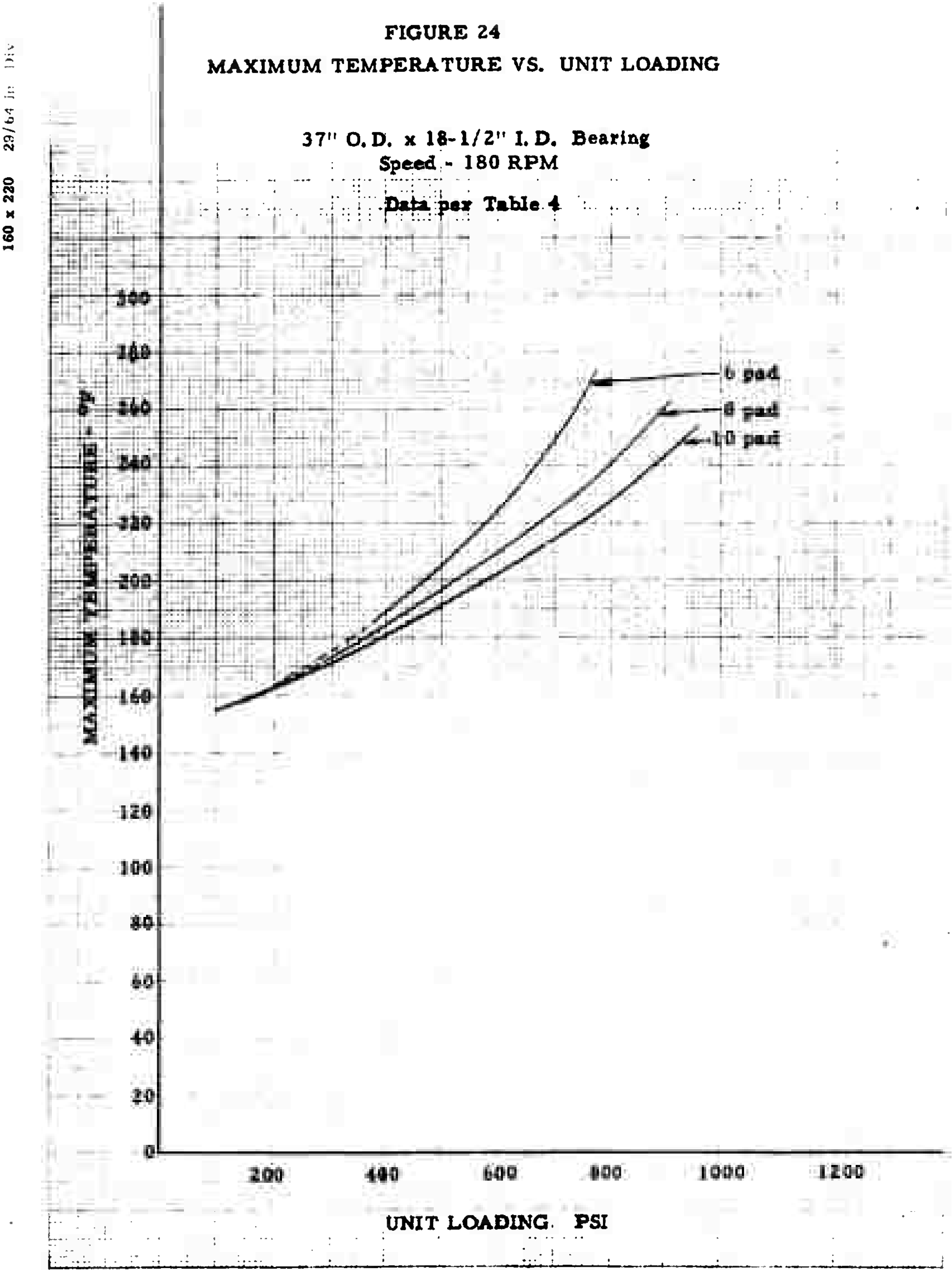

FIGURE 25

MAXIMUM TEMPERATURE VS. UNIT LOADING

37" O. D. x 18-1/2" I. D. Bearing
Speed - 320 RPM

Data per Table 4

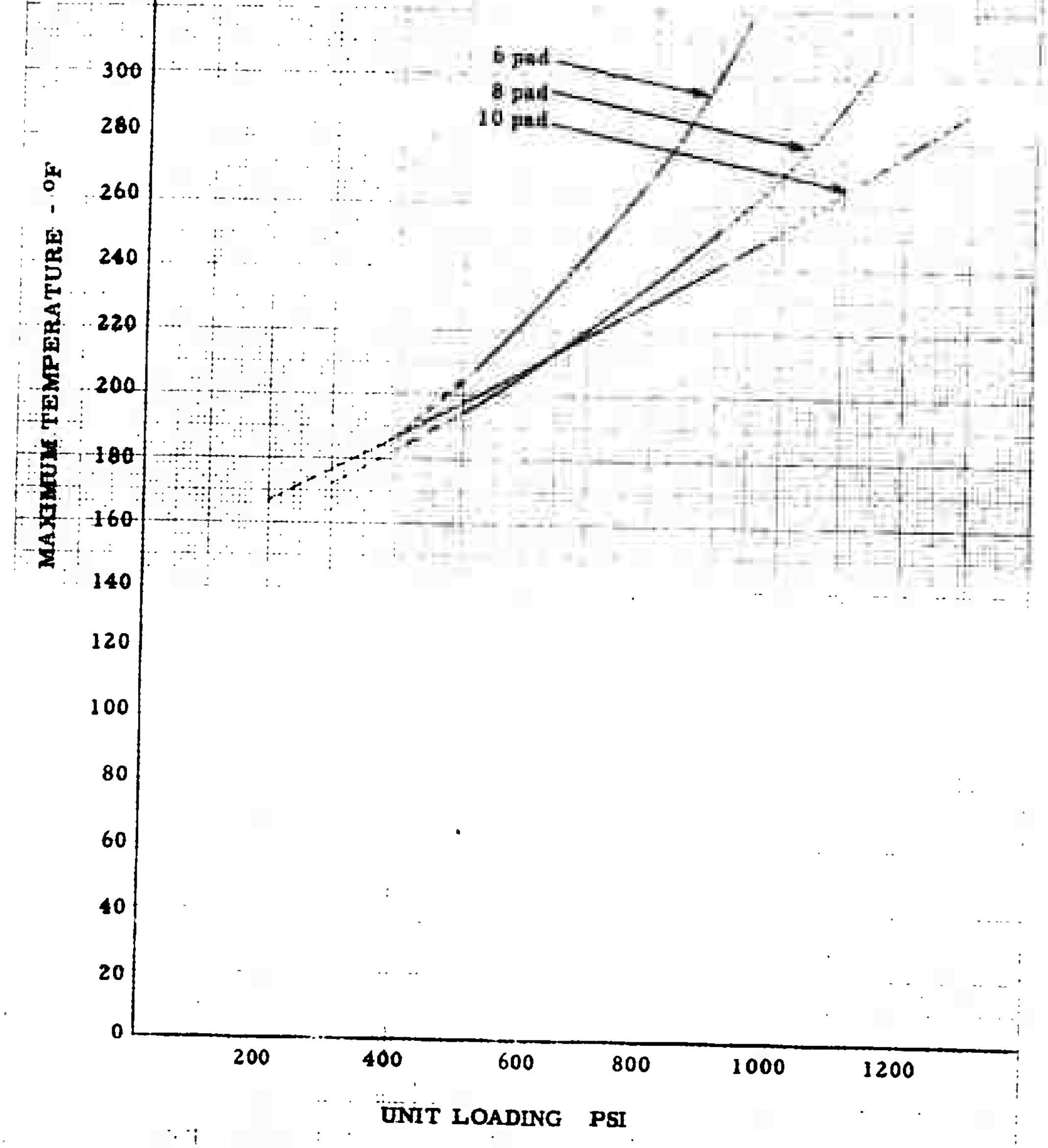

FIGURE 26

HYDRODYNAMIC OIL FLOW VERSUS UNIT LOADING

37" O.D. x 18-1/2" I.D. Bearing

8 pads

Pad Dimensions and Data per Table 4

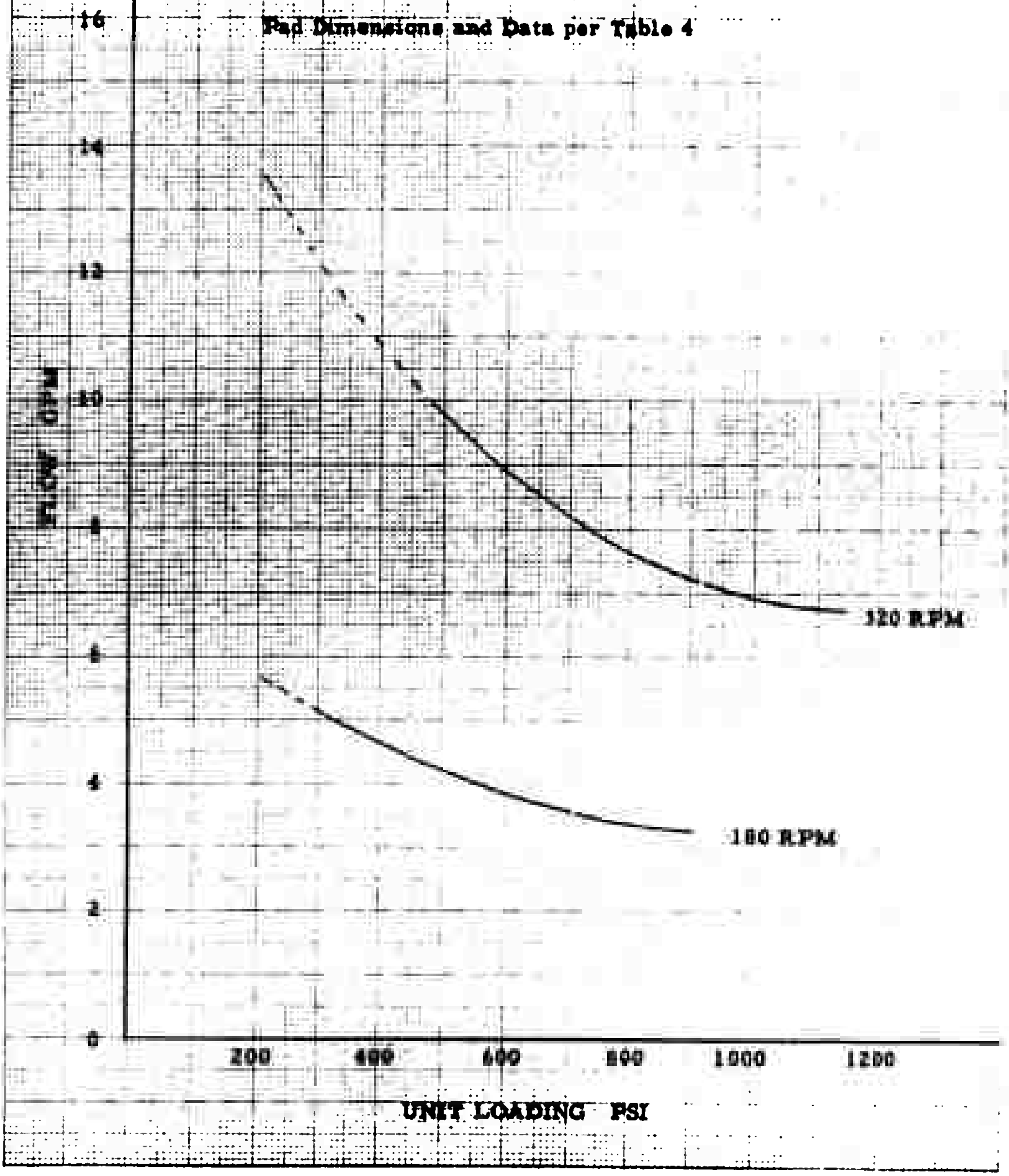

FIGURE 27

MINIMUM FILM THICKNESS VS. UNIT LOADING

39" O.D. x 19-1/2" I.D. Bearing
Speed - 150 RPM

Data per Table 5

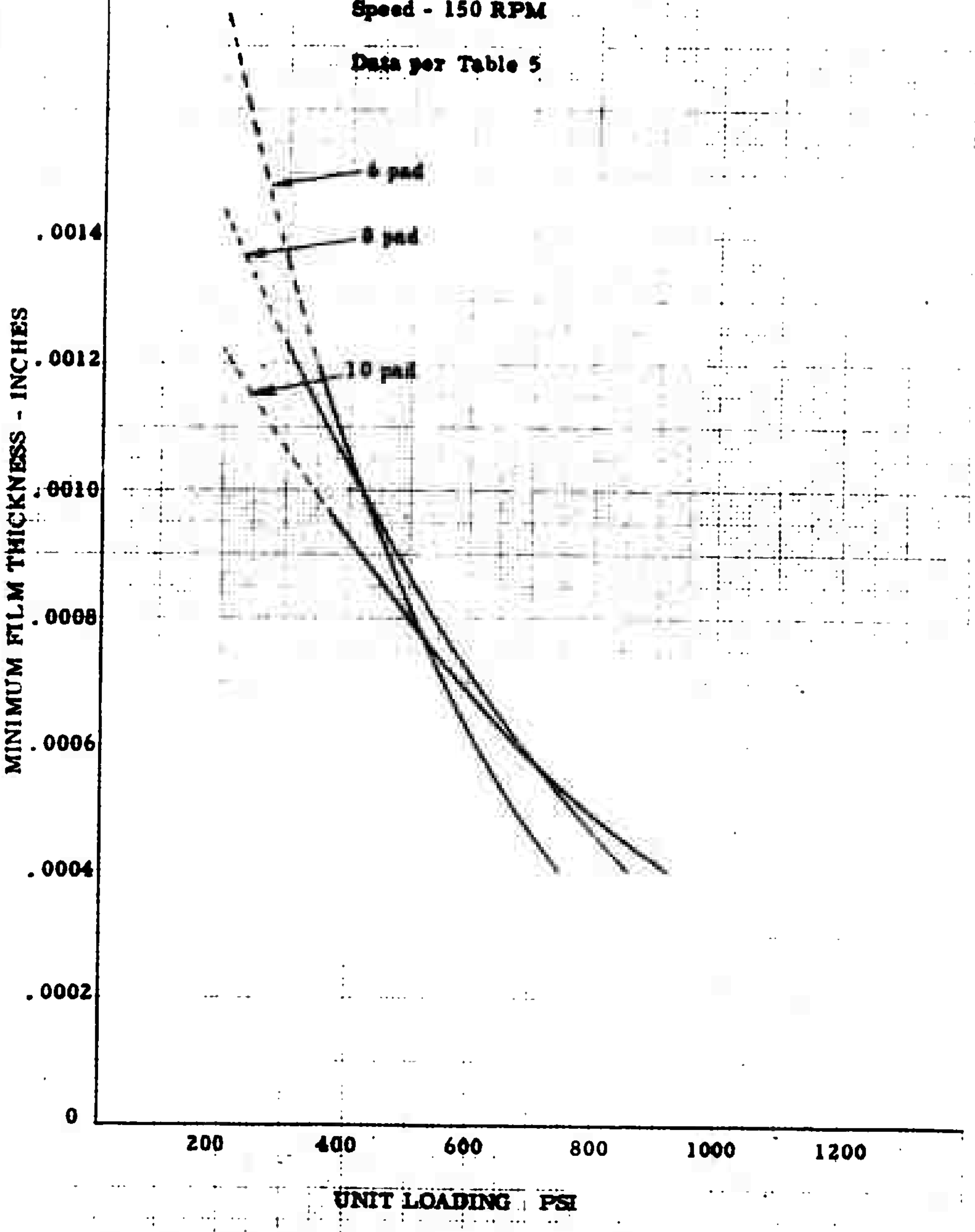

FIGURE 28

MINIMUM FILM THICKNESS VS. UNIT LOADING

39" O.D. x 19-1/2" I.D. Bearing
Speed - 200 RPM

Pad Dimensions and Data per Table 5

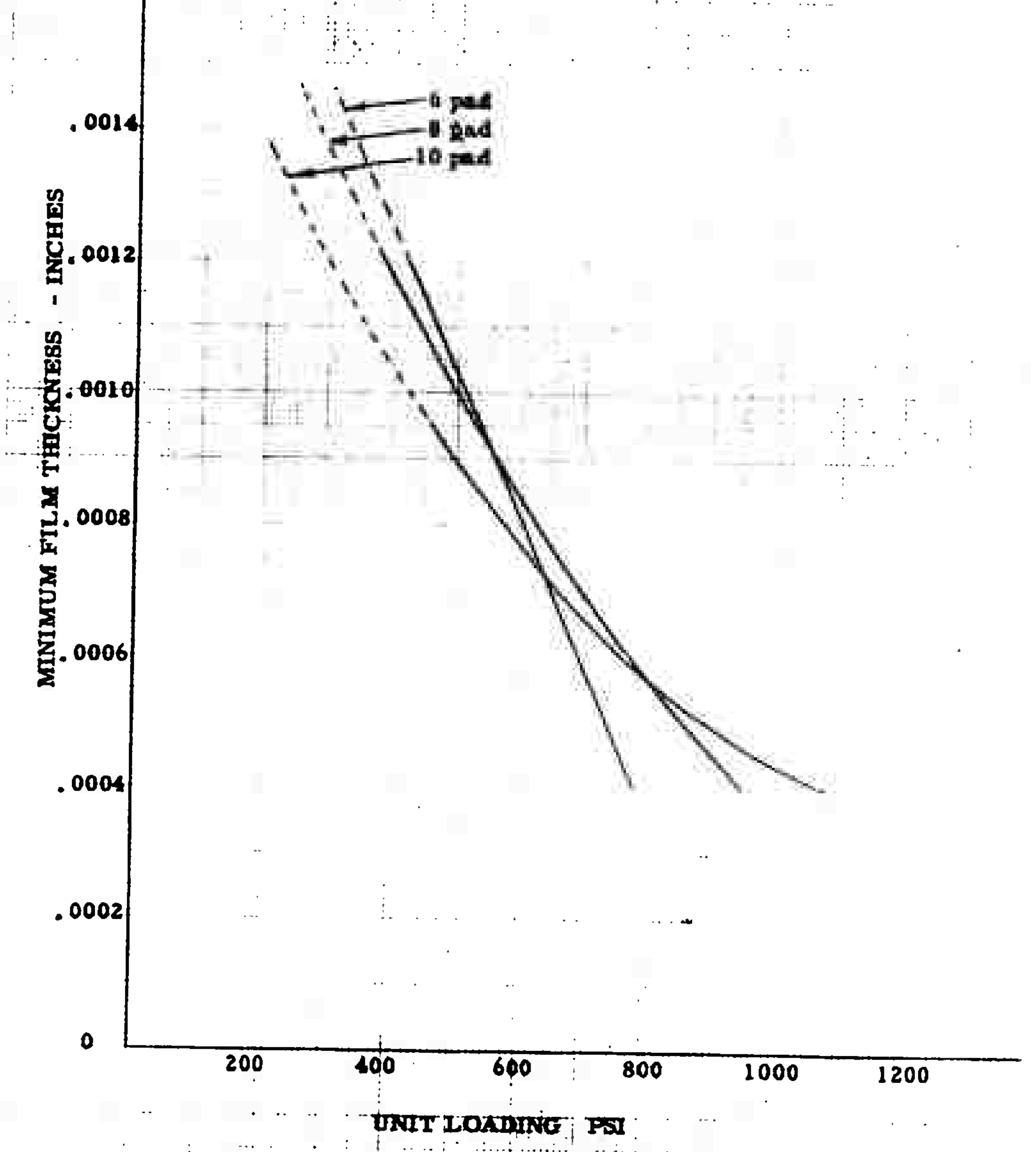

FIGURE 29

MAXIMUM TEMPERATURE VS. UNIT LOADING

39" O.D. x 19-1/2" I.D. Bearing
Speed - 150 RPM

Data per Table 5

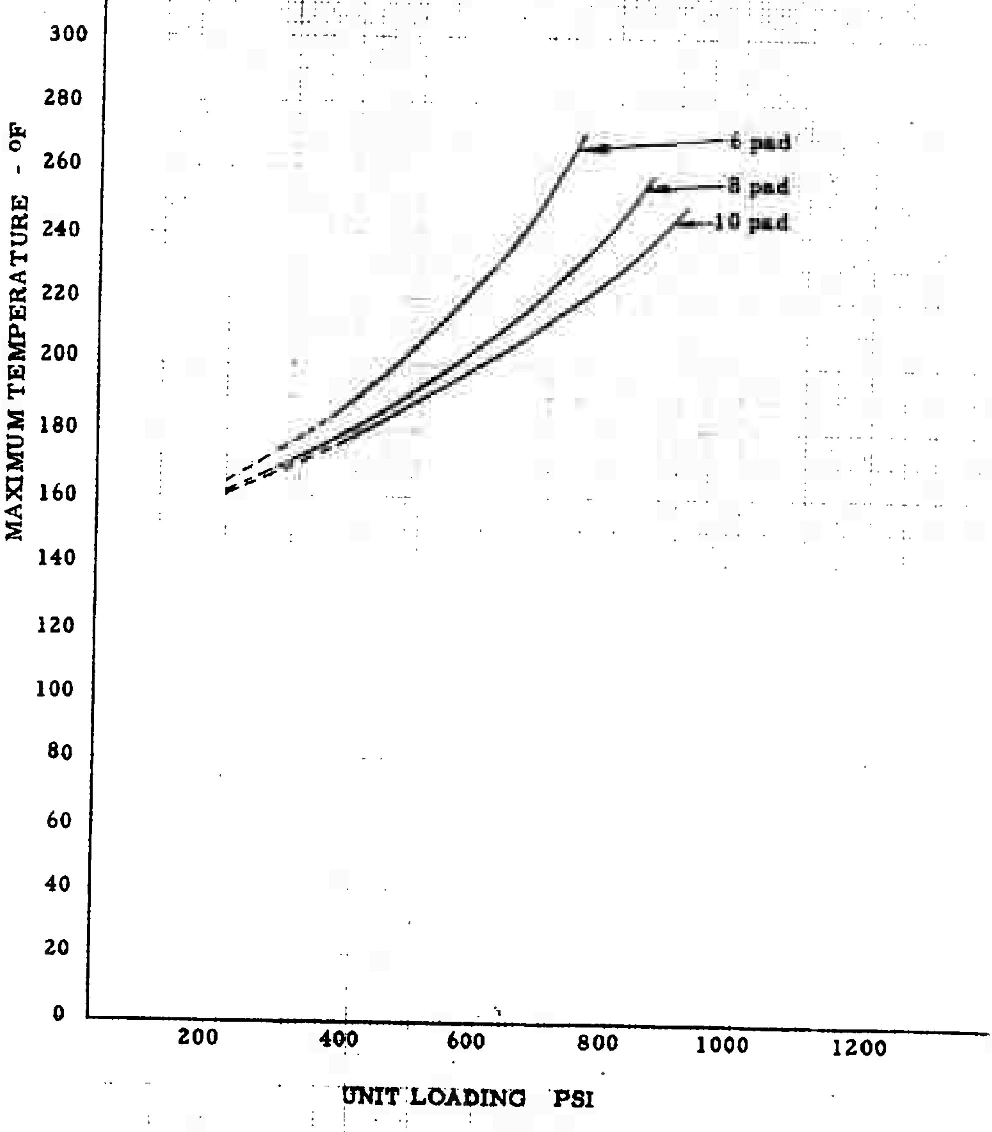

FIGURE 30

MAXIMUM TEMPERATURE VS. UNIT LOADING

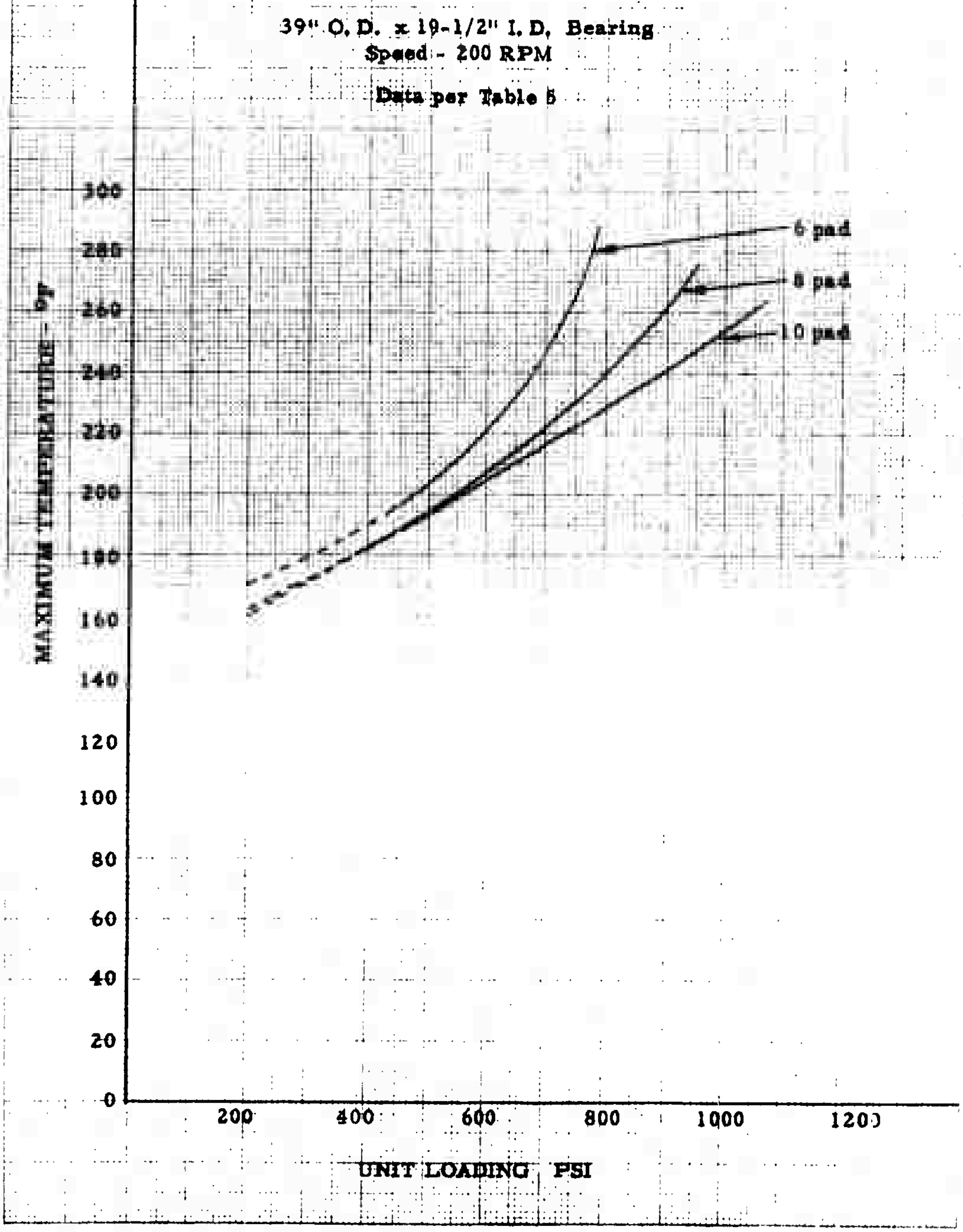

TABLE 31

HYDRODYNAMIC OIL FLOW VERSUS UNIT LOADING

39" O.D. x 19-1/2" I.D. Bearing

8 pads

Pad Dimensions and Data per Table 5

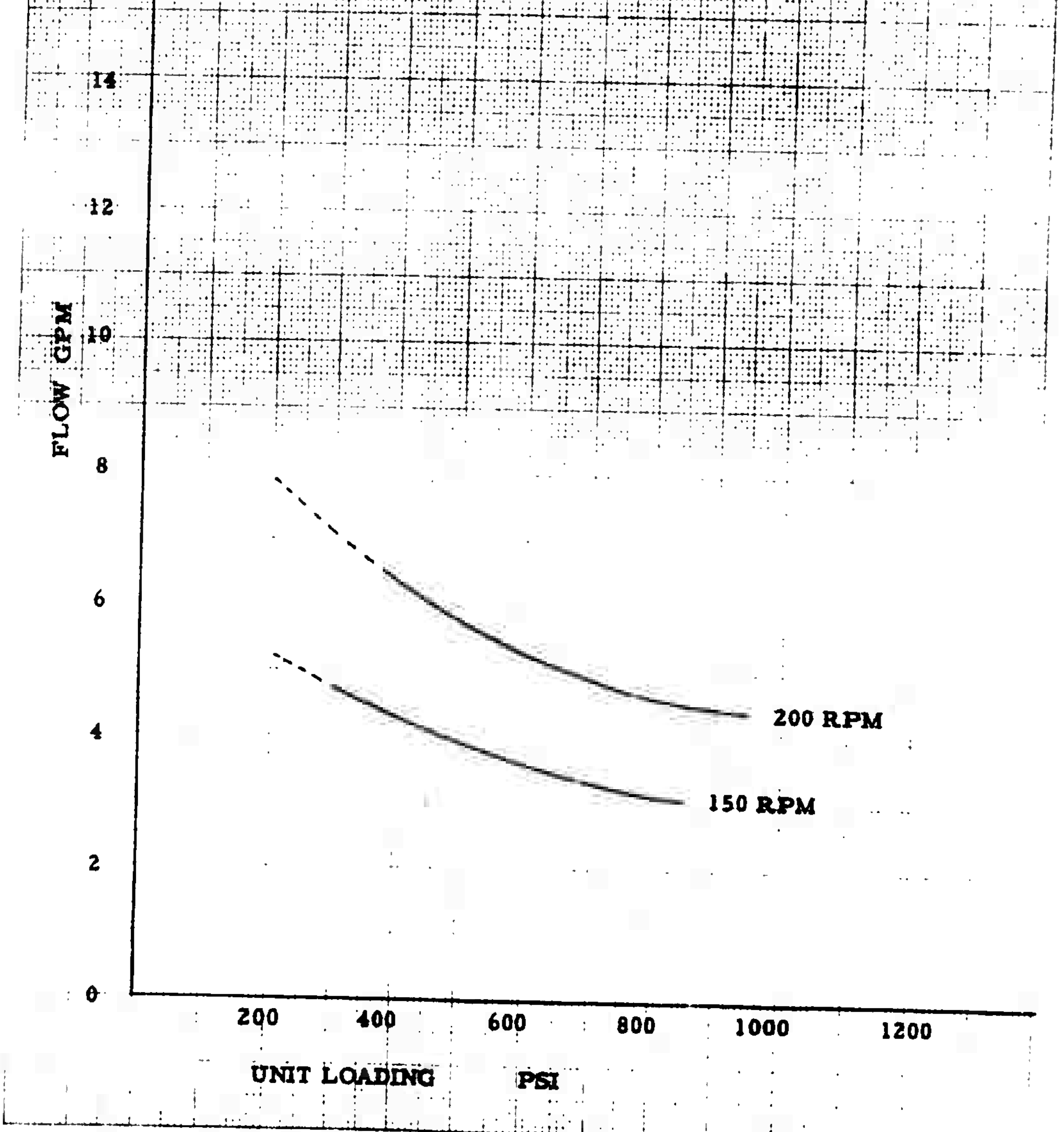

FIGURE 32

MINIMUM FILM THICKNESS VS. UNIT LOADING

41" O. D. x 20-1/2" I. D. Bearing
Speed - 100 RPM

Pad Dimensions and data per Table 6

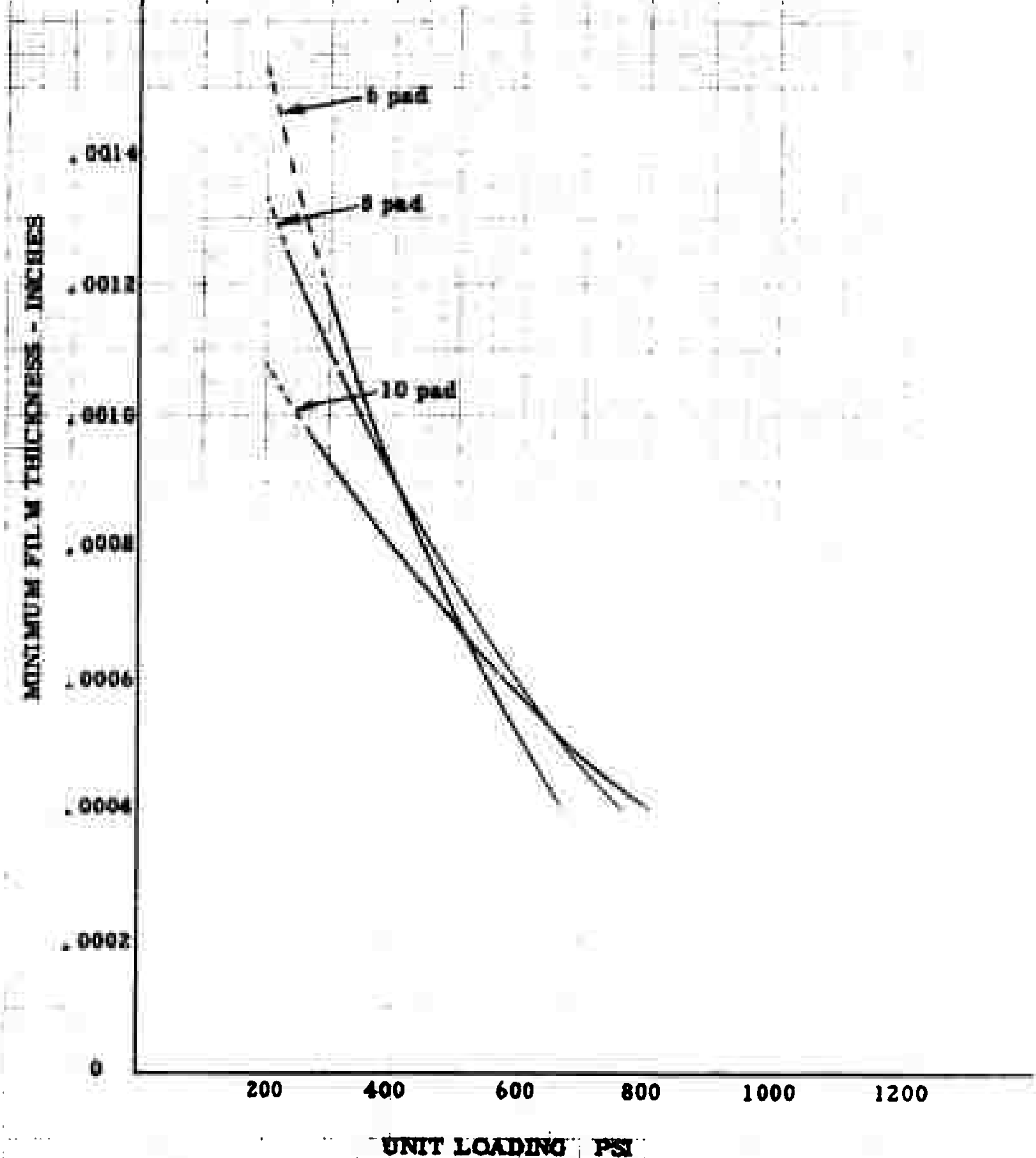

FIGURE 33

MINIMUM FILM THICKNESS VS. UNIT LOADING

41" O. D. x 20-1/2" I. D. Bearing
Speed - 200 RPM

Pad Dimensions and Data per Table 6

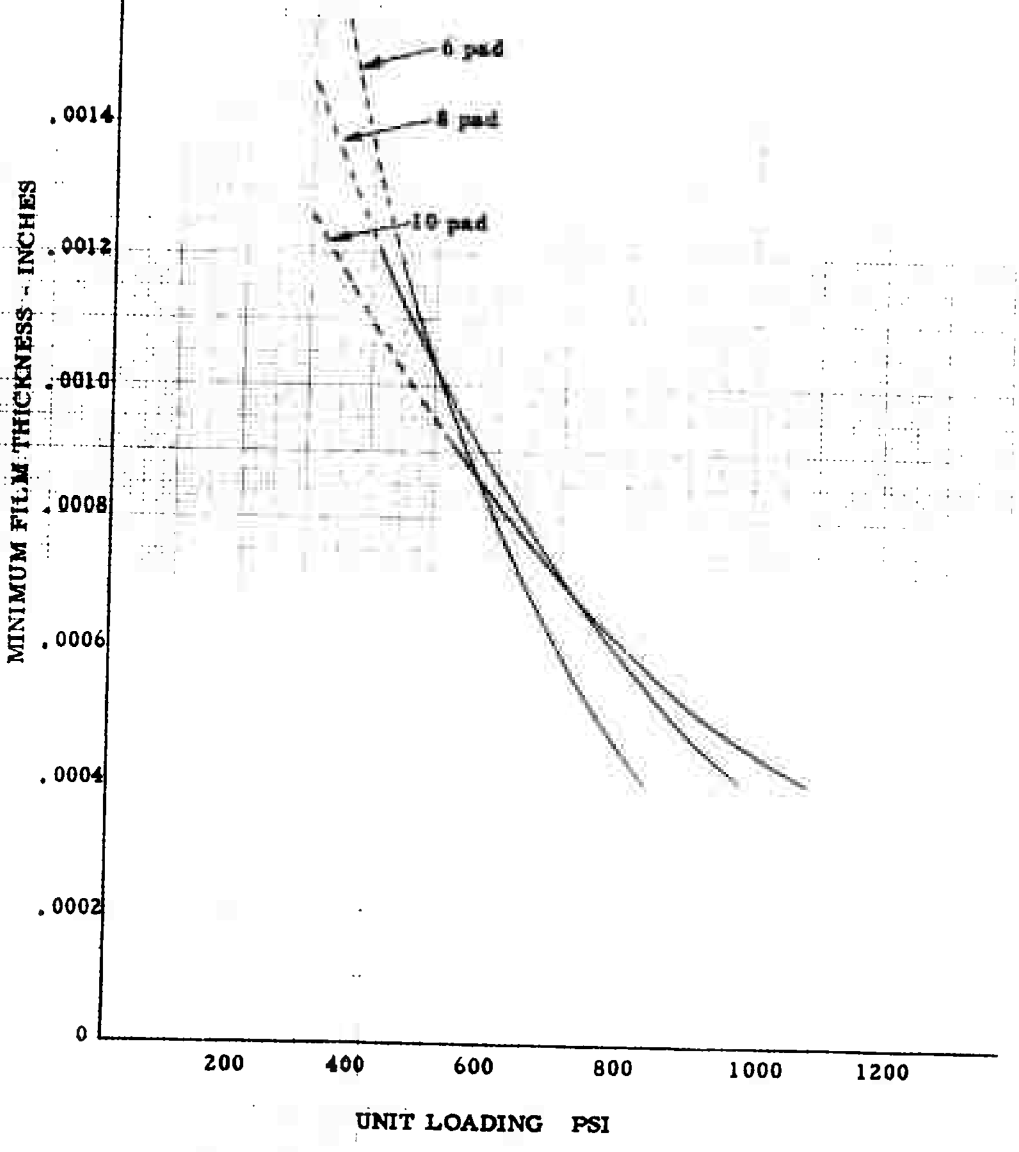

FIGURE 34

MAXIMUM TEMPERATURE VS. UNIT LOADING

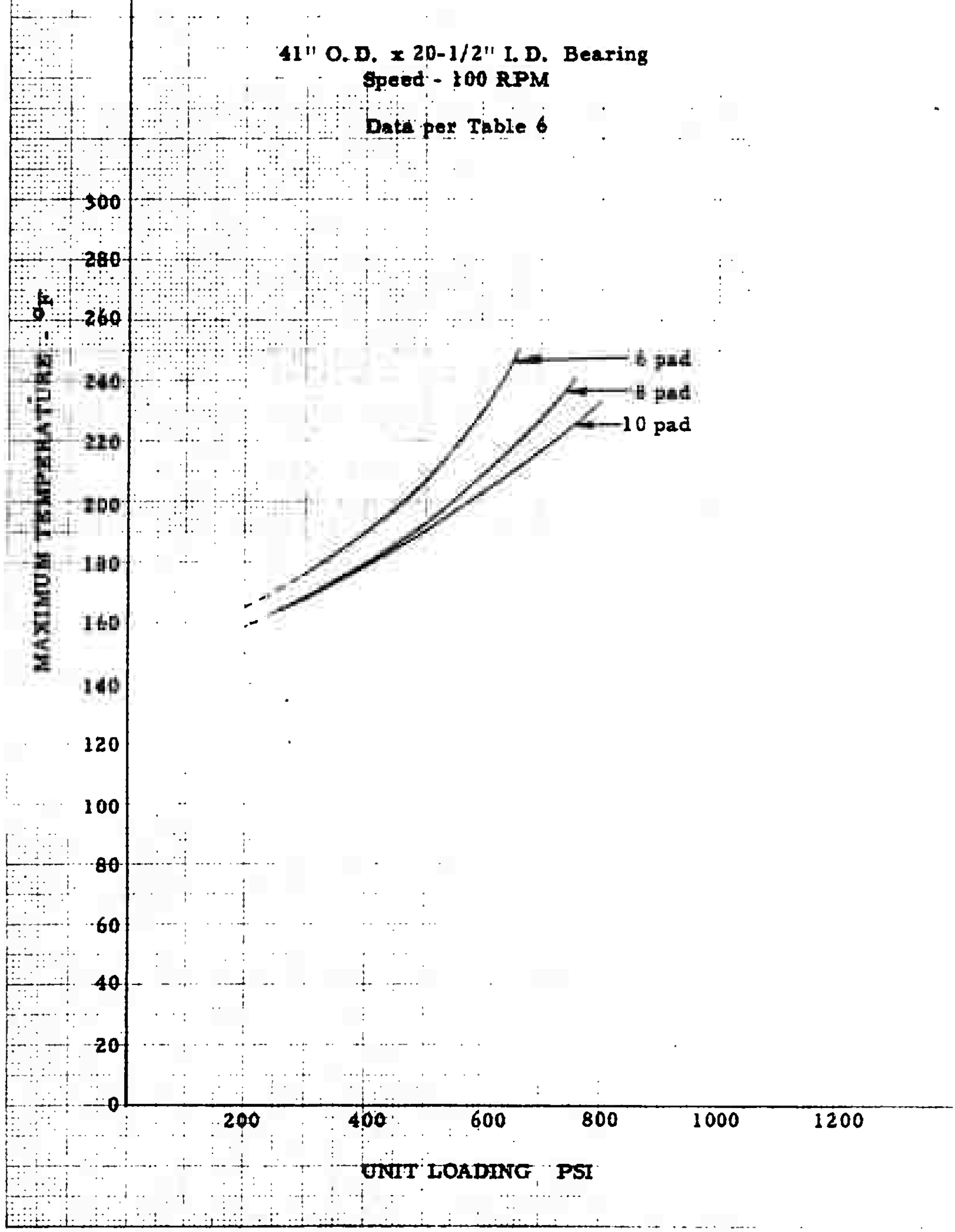

FIGURE 35

MAXIMUM TEMPERATURE VS. UNIT LOADING

41" O. D. x 20-1/2" I. D. Bearing
Speed - 200 RPM

Data per Table 6

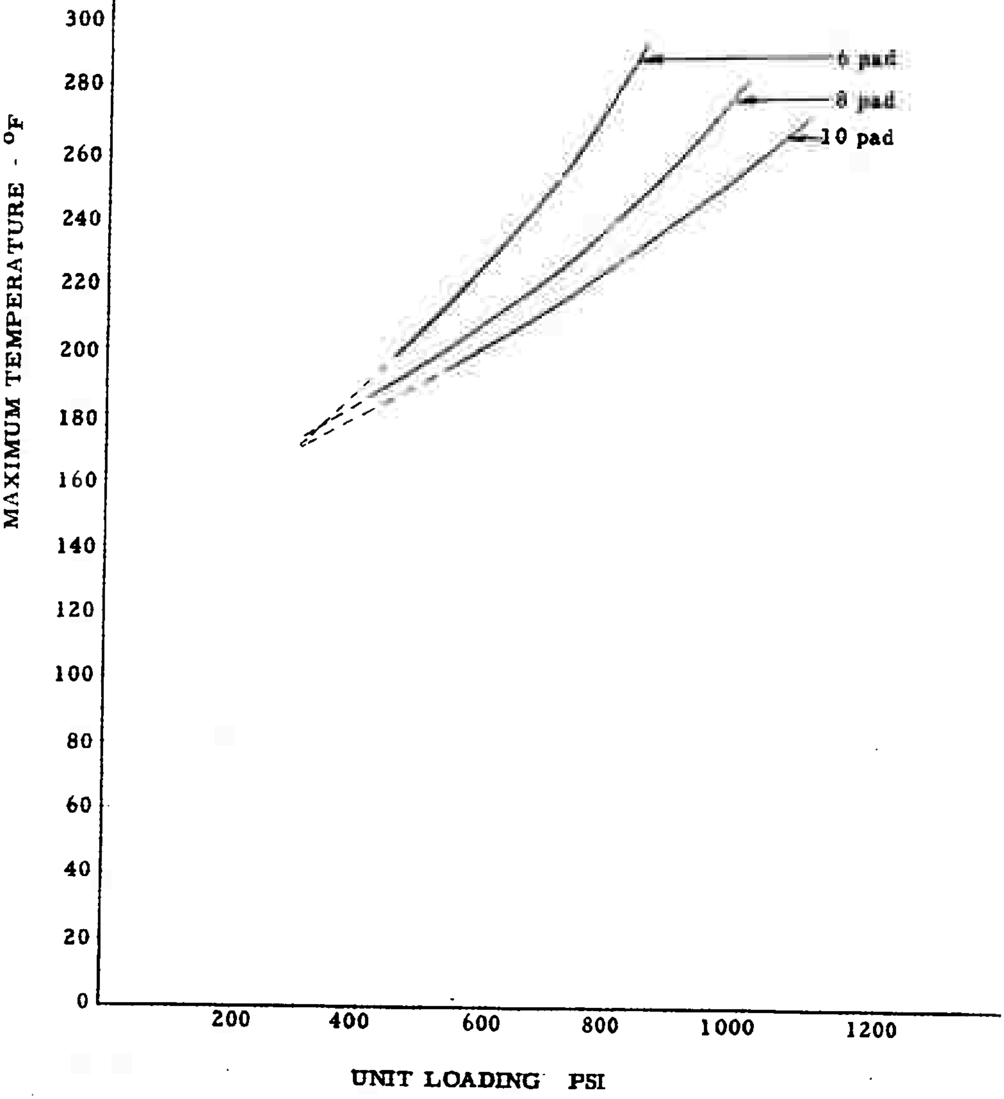

FIGURE 36

HYDRODYNAMIC OIL FLOW VERSUS UNIT LOADING

41" O.D. x 20-1/2" I.D. Bearing

8 pads

Pad Dimensions and Data per Table 6

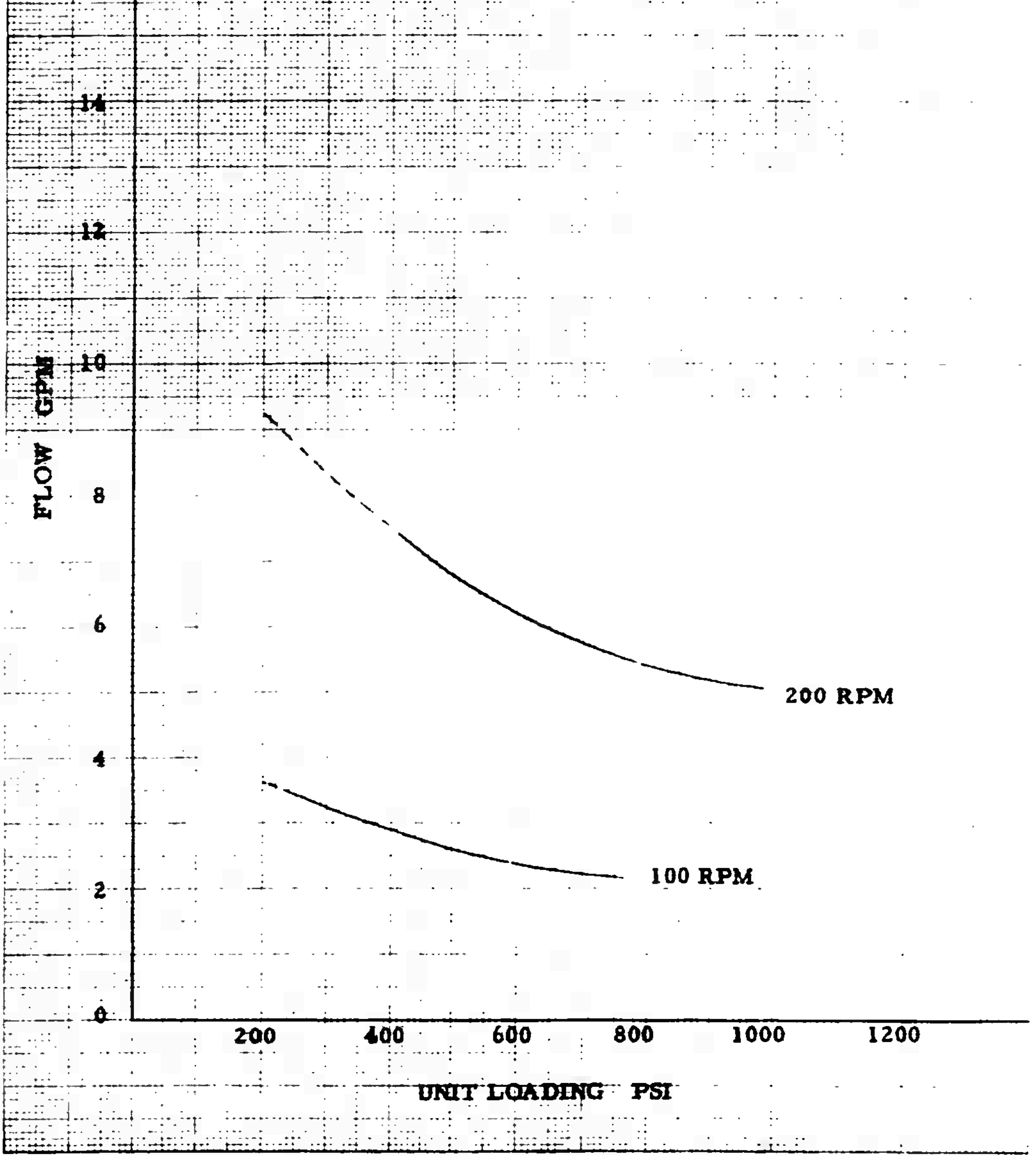

FIGURE 37

MINIMUM FILM THICKNESS VS. UNIT LOADING

45" O. D. x 22-1/2" I. D. Bearing
Speed - 100 RPM

Pad Dimensions and Data per Table 7

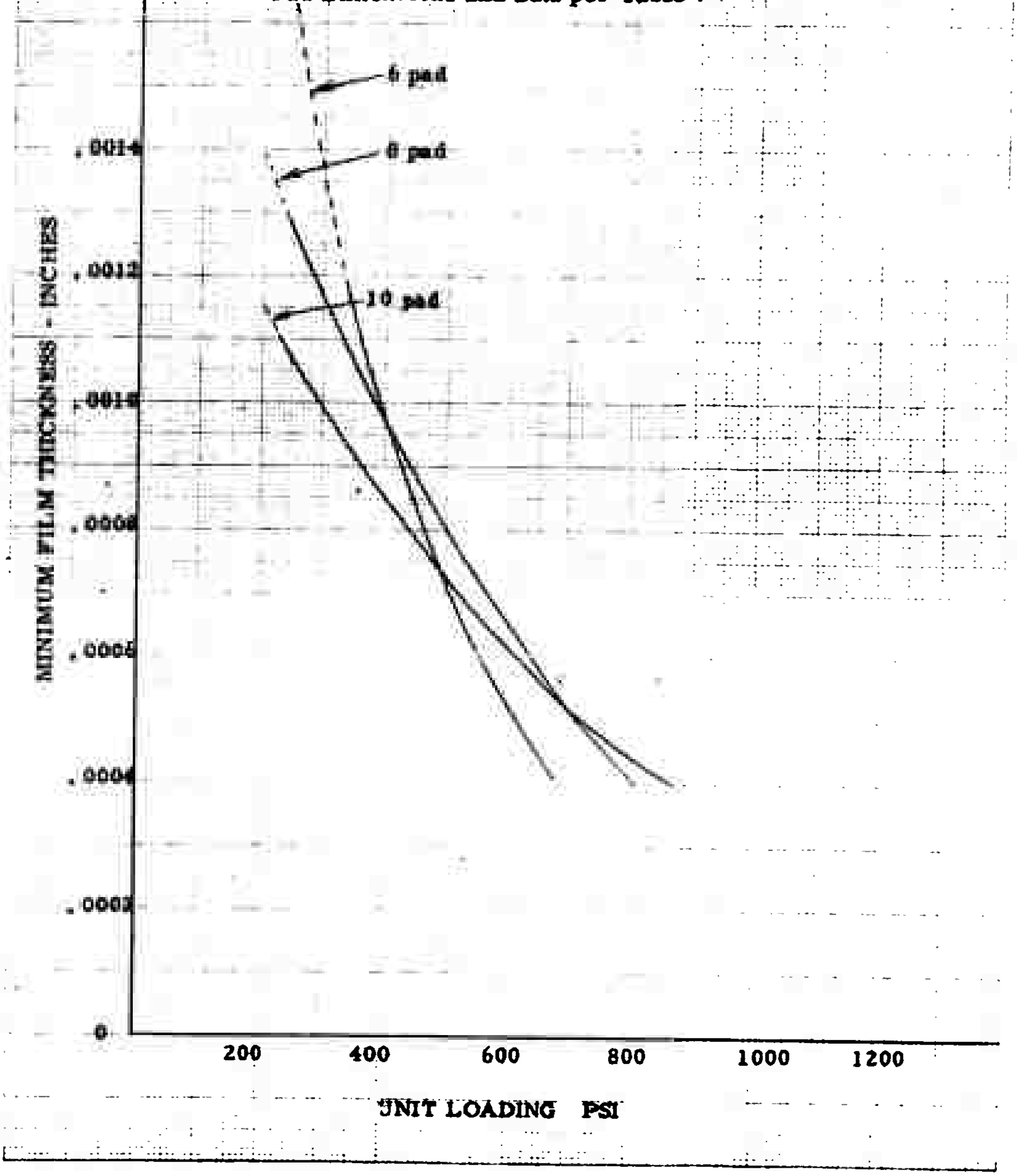

FIGURE 38

MINIMUM FILM THICKNESS VS. UNIT LOADING

45" O.D. x 22-1/2" I.D. Bearing
Speed — 170 RPM

Pad Dimensions and Data per Table 7

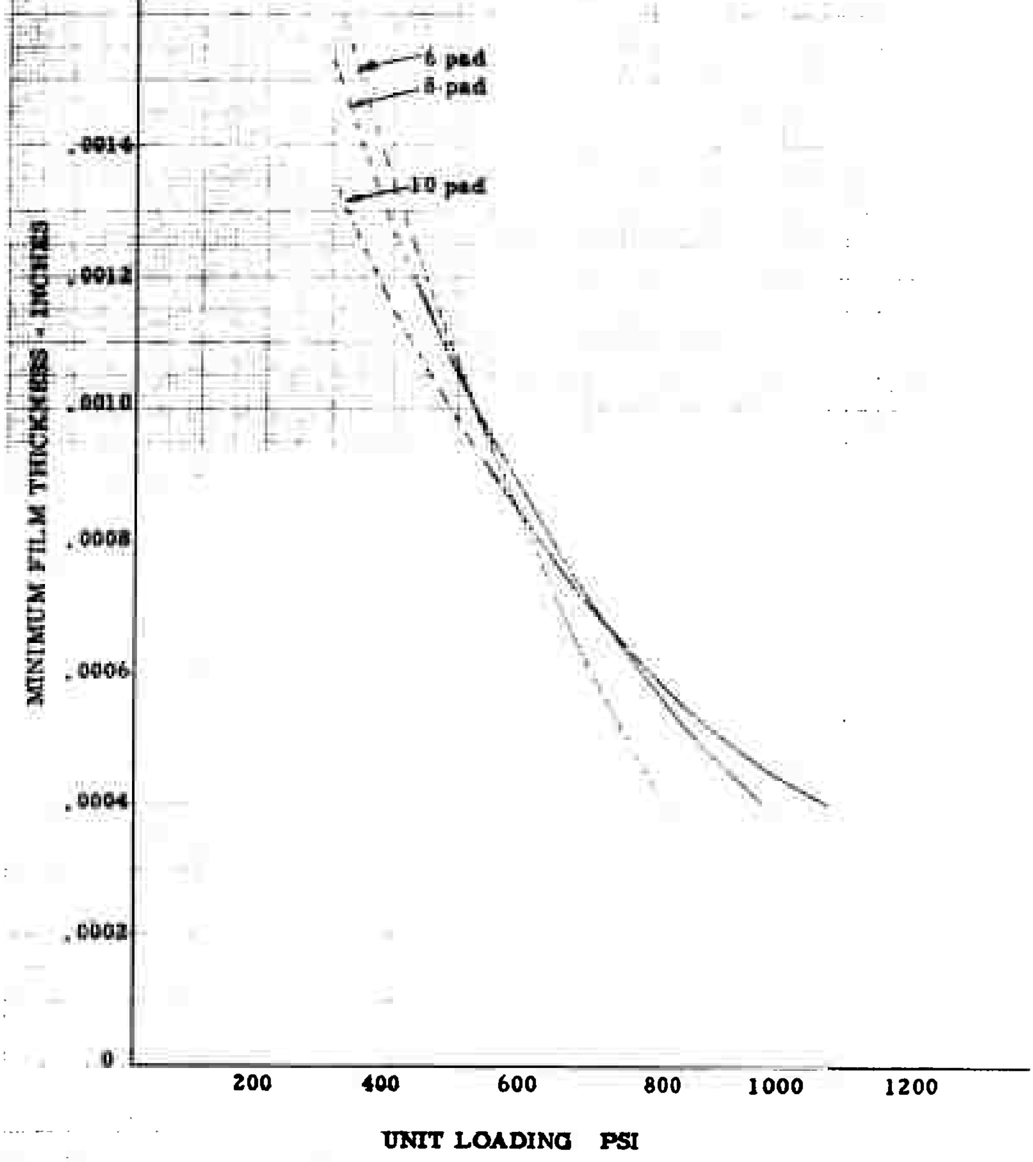

FIGURE 39
MAXIMUM TEMPERATURE VS. UNIT LOADING

45" O. D. x 22-1/2" I. D. Bearing
Speed - 100 RPM

Data per Table 7

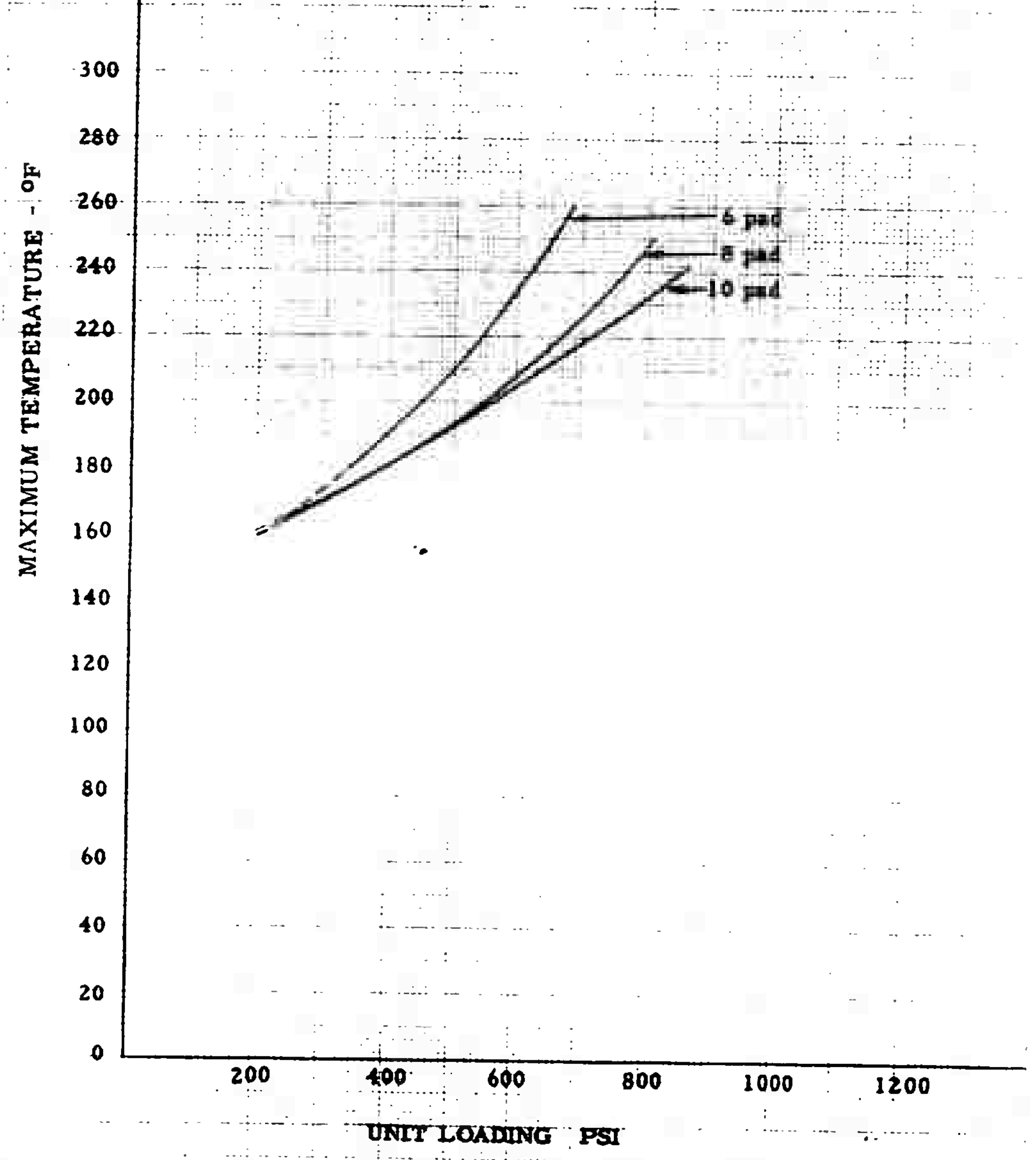

FIGURE 40

MAXIMUM TEMPERATURE VS. UNIT LOADING

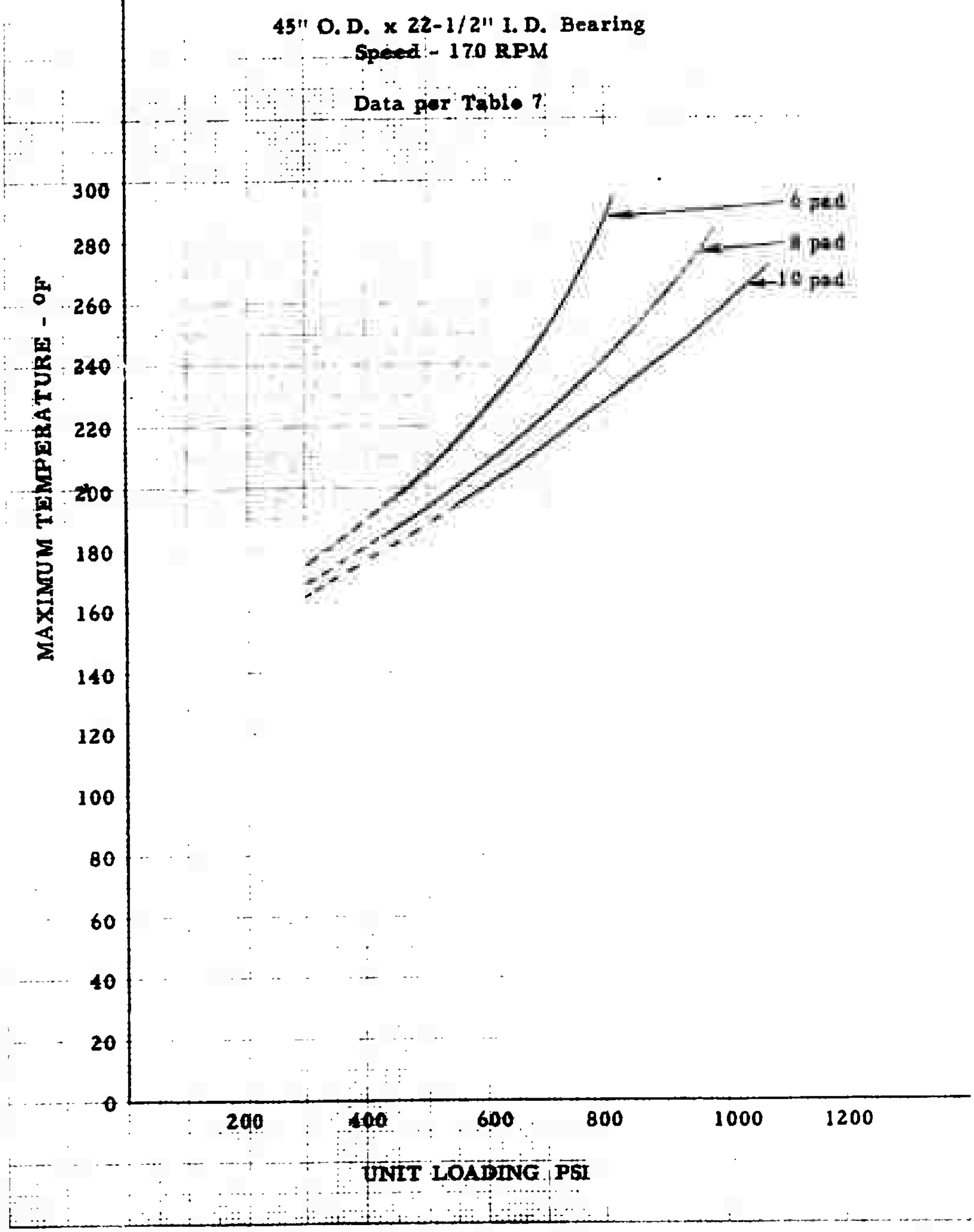

FIGURE 41

HYDRODYNAMIC OIL FLOW VERSUS UNIT LOADING

45" O.D. x 22-1/2" I.D. Bearing

8 pads

Pad Dimensions and Data per Table 7

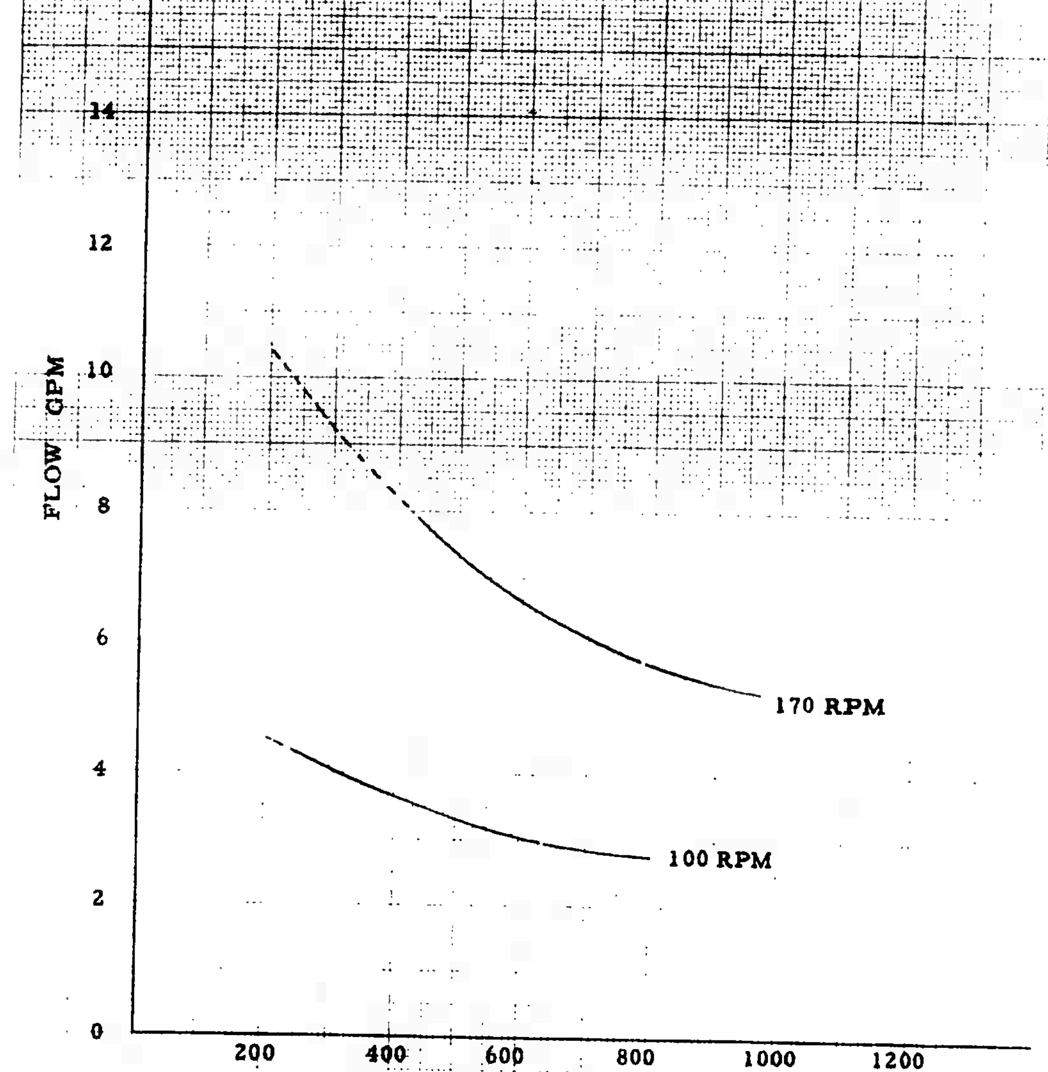

FIGURE 42

MINIMUM FILM THICKNESS VS. UNIT LOADING

50" O. D. x 25" I. D. Bearing
Speed - 100 RPM

Pad Dimensions and Data per Table 8

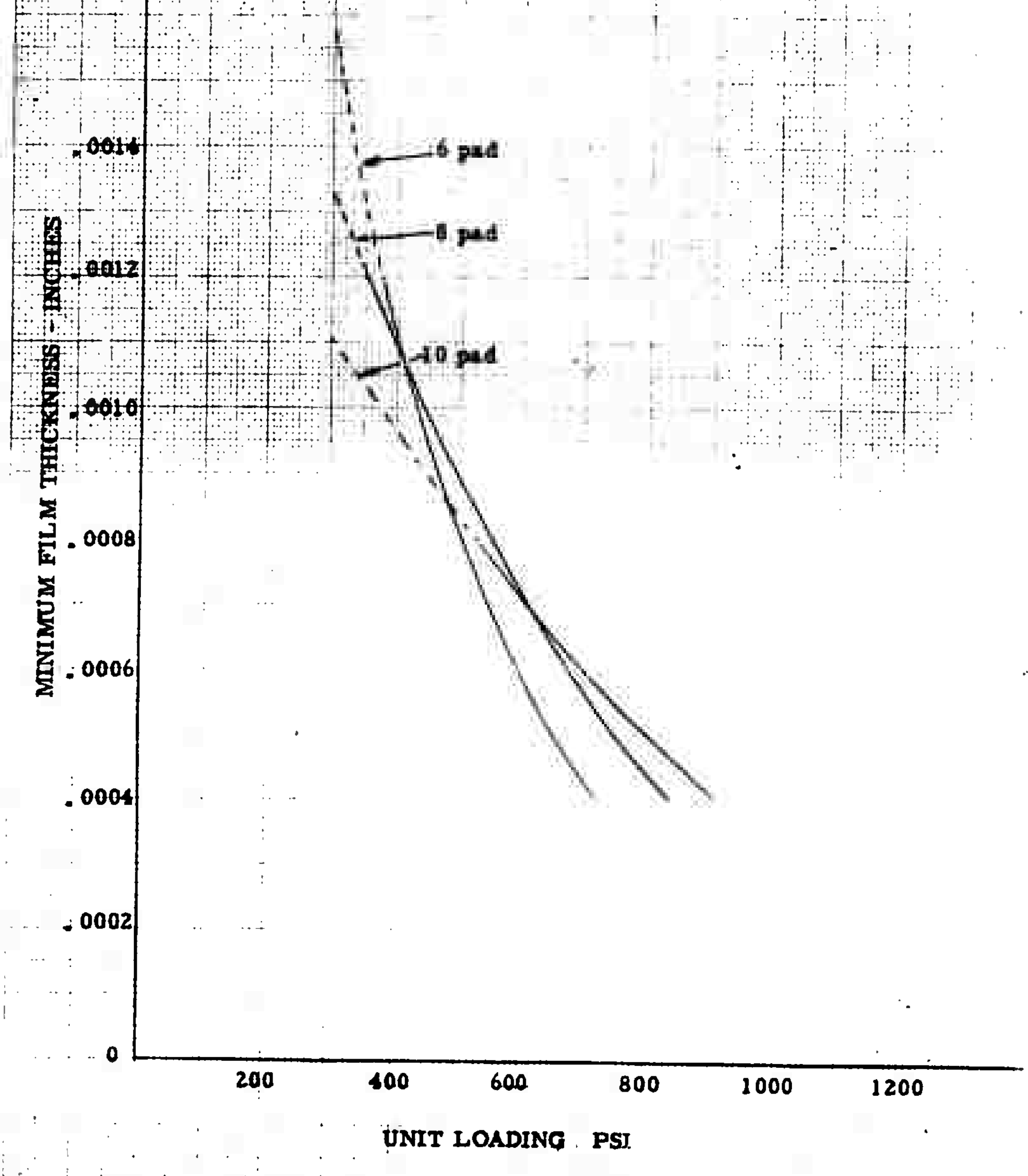

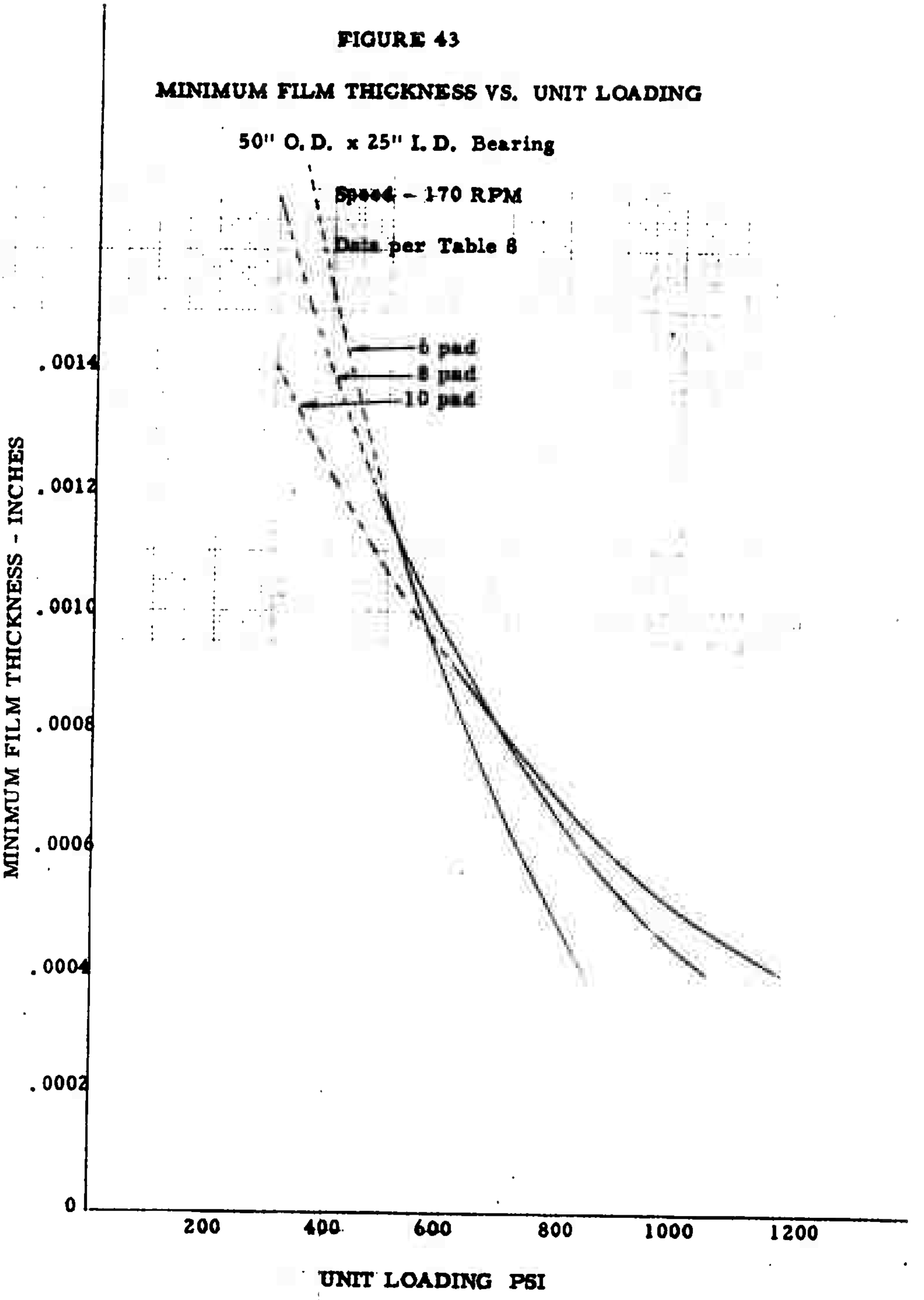
FIGURE 43
MINIMUM FILM THICKNESS VS. UNIT LOADING
50" O.D. x 25" I.D. Bearing
Speed - 170 RPM
Data per Table 8
6 pad
8 pad
10 pad
MINIMUM FILM THICKNESS - INCHES
.0014
.0012
.0010
.0008
.0006
.0004
.0002
0
200
400
600
800
1000
1200
UNIT LOADING PSI

FIGURE 44

MAXIMUM TEMPERATURE VS. UNIT LOADING

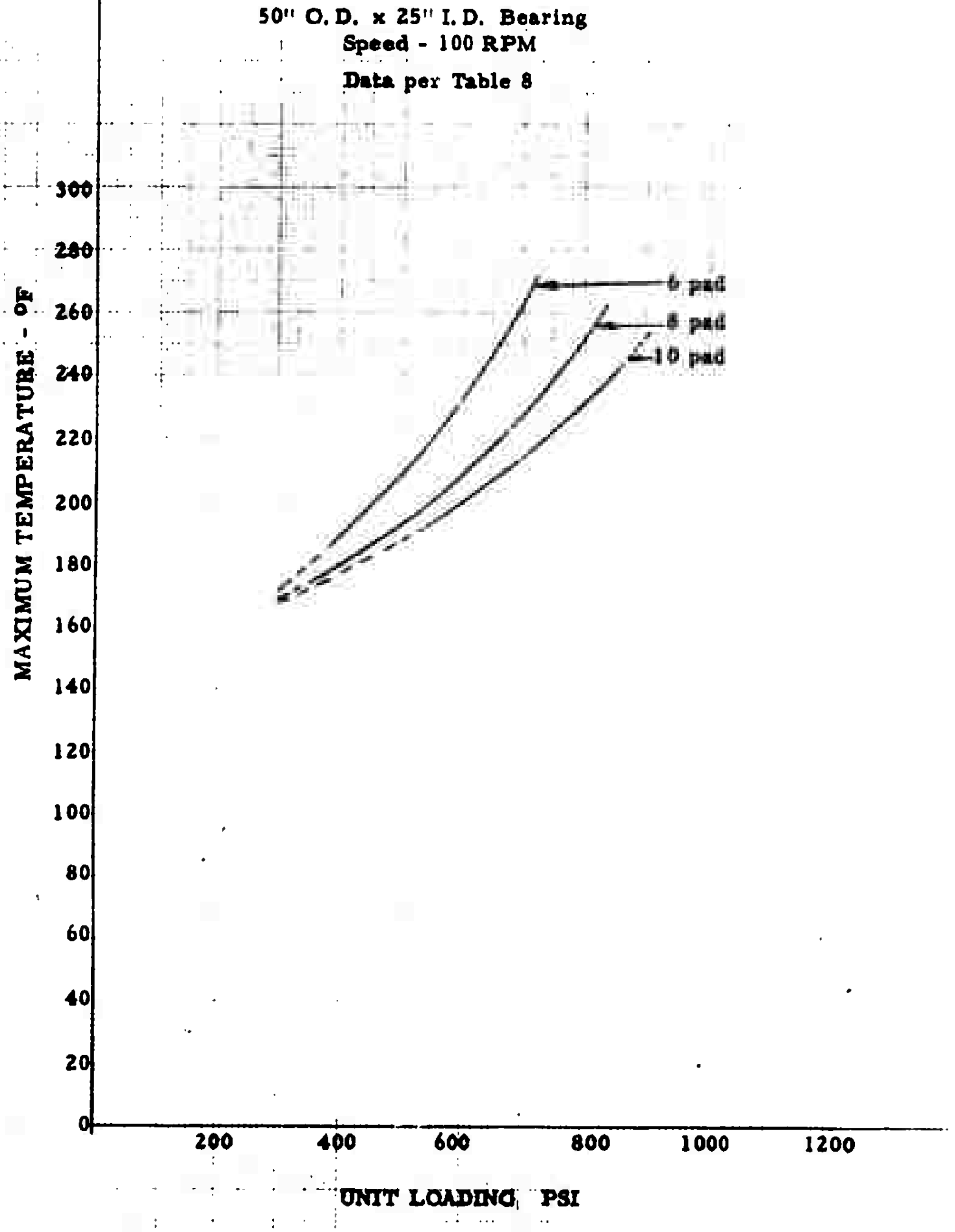

FIGURE 45

MAXIMUM TEMPERATURE VS. UNIT LOADING

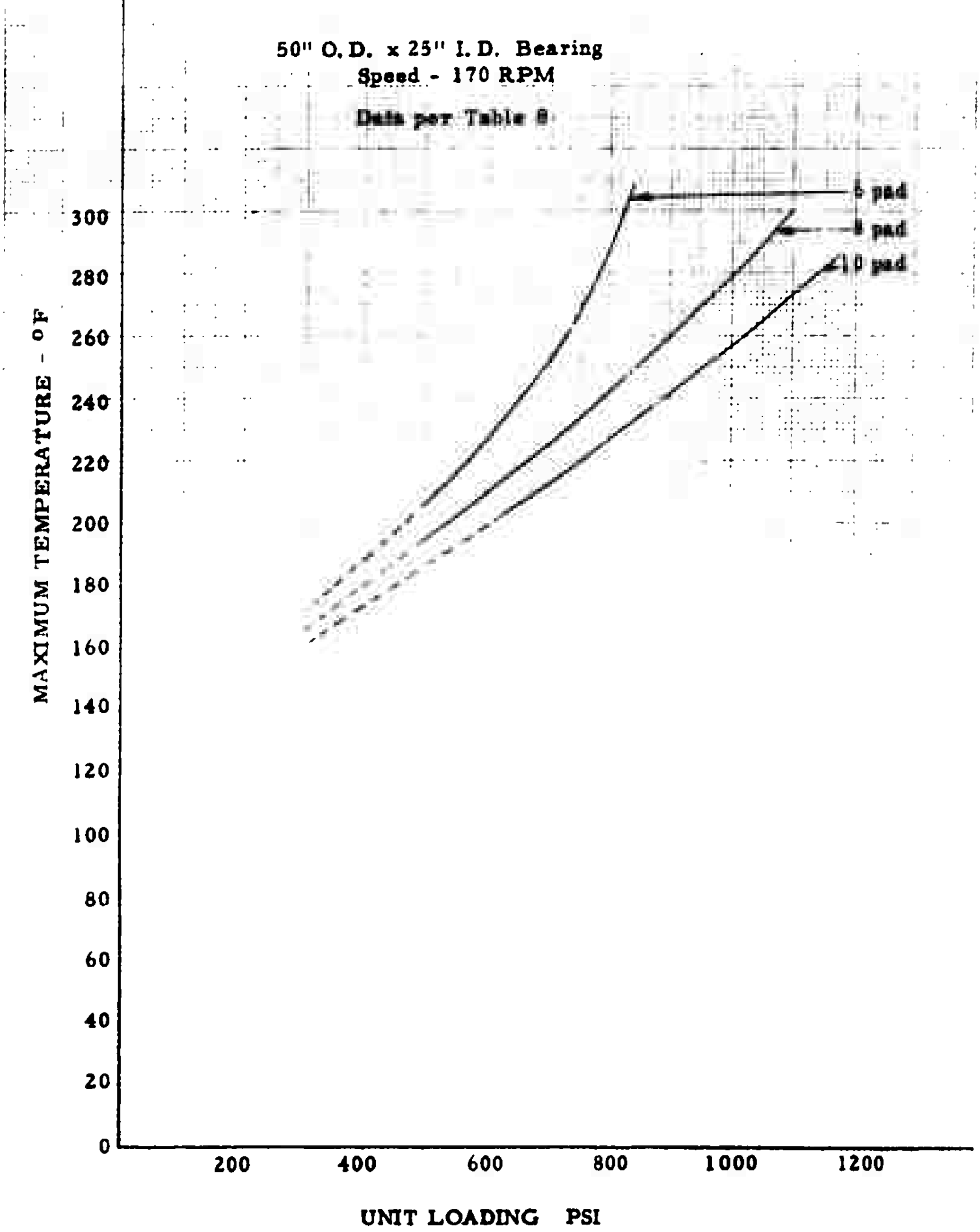

FIGURE 46

HYDRODYNAMIC OIL FLOW VERSUS UNIT LOADING

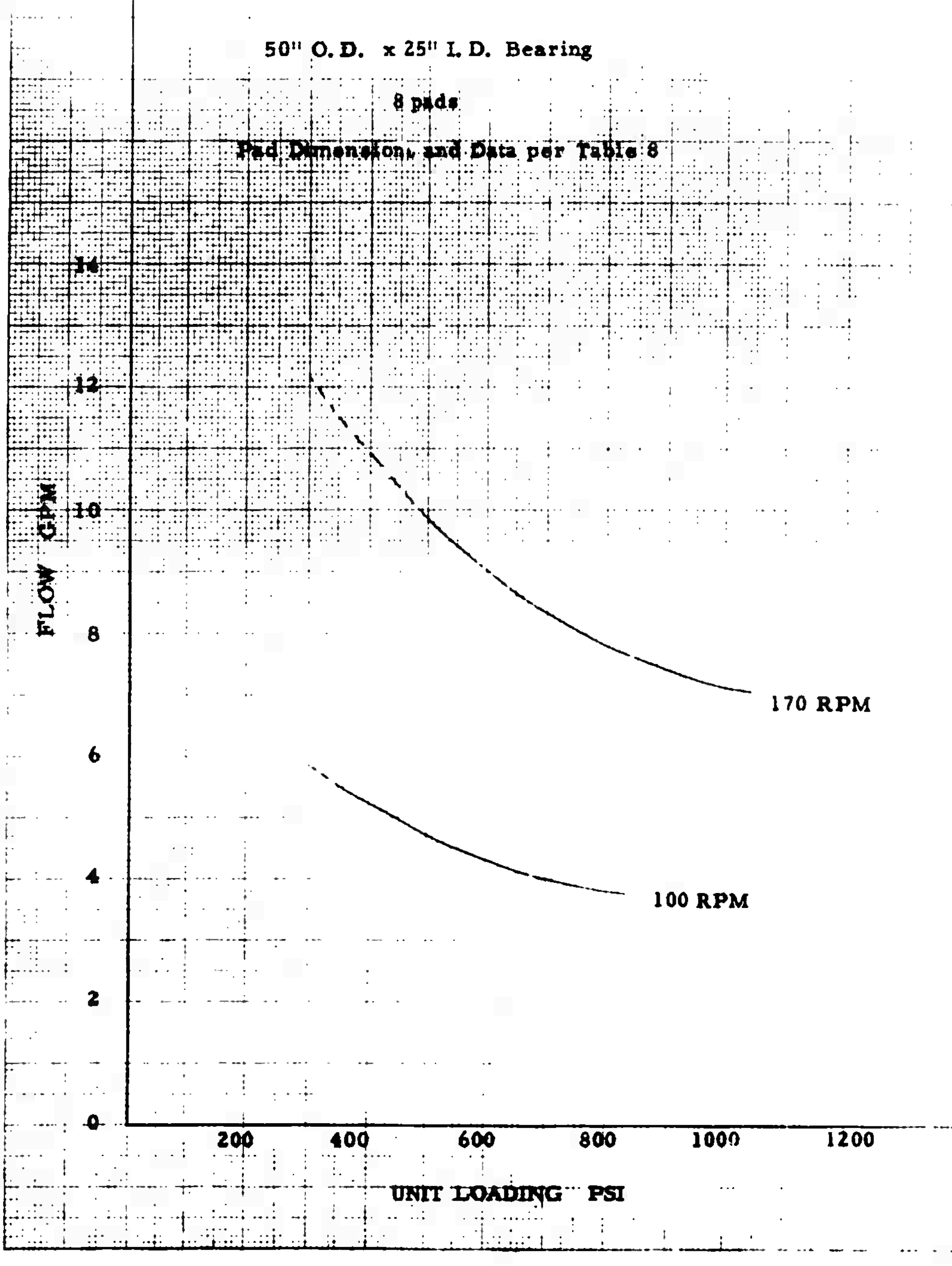

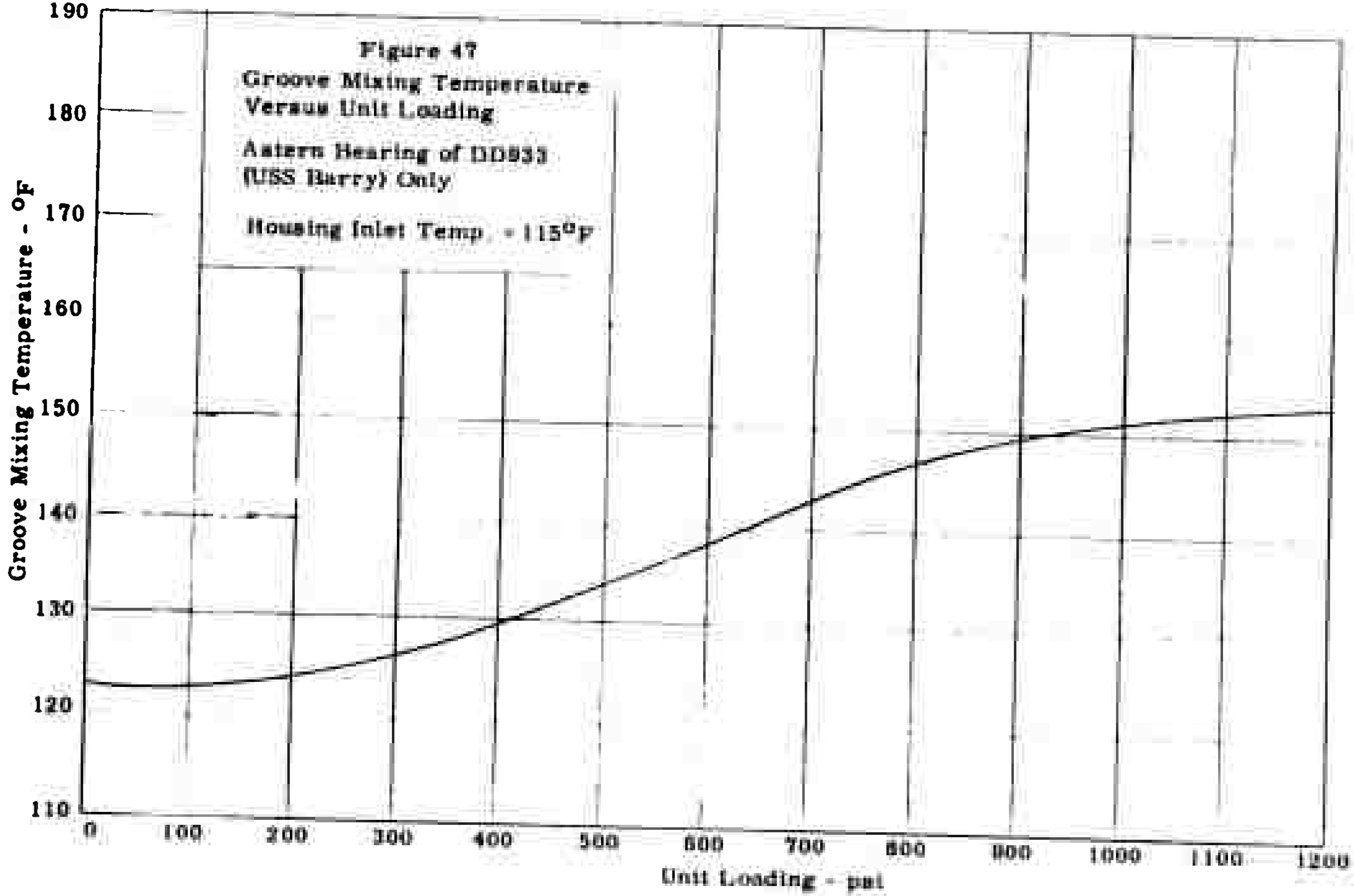

Figure 47
Groove Mixing Temperature Versus Unit Loading

Astern Bearing of DD933 (USS Barry) Only

Housing Inlet Temp. = 115°F

FIGURE 48

MINIMUM FILM THICKNESS VS. UNIT LOADING

26" O.D. x 17-1/2" I.D. Bearing
Speed - 160 RPM

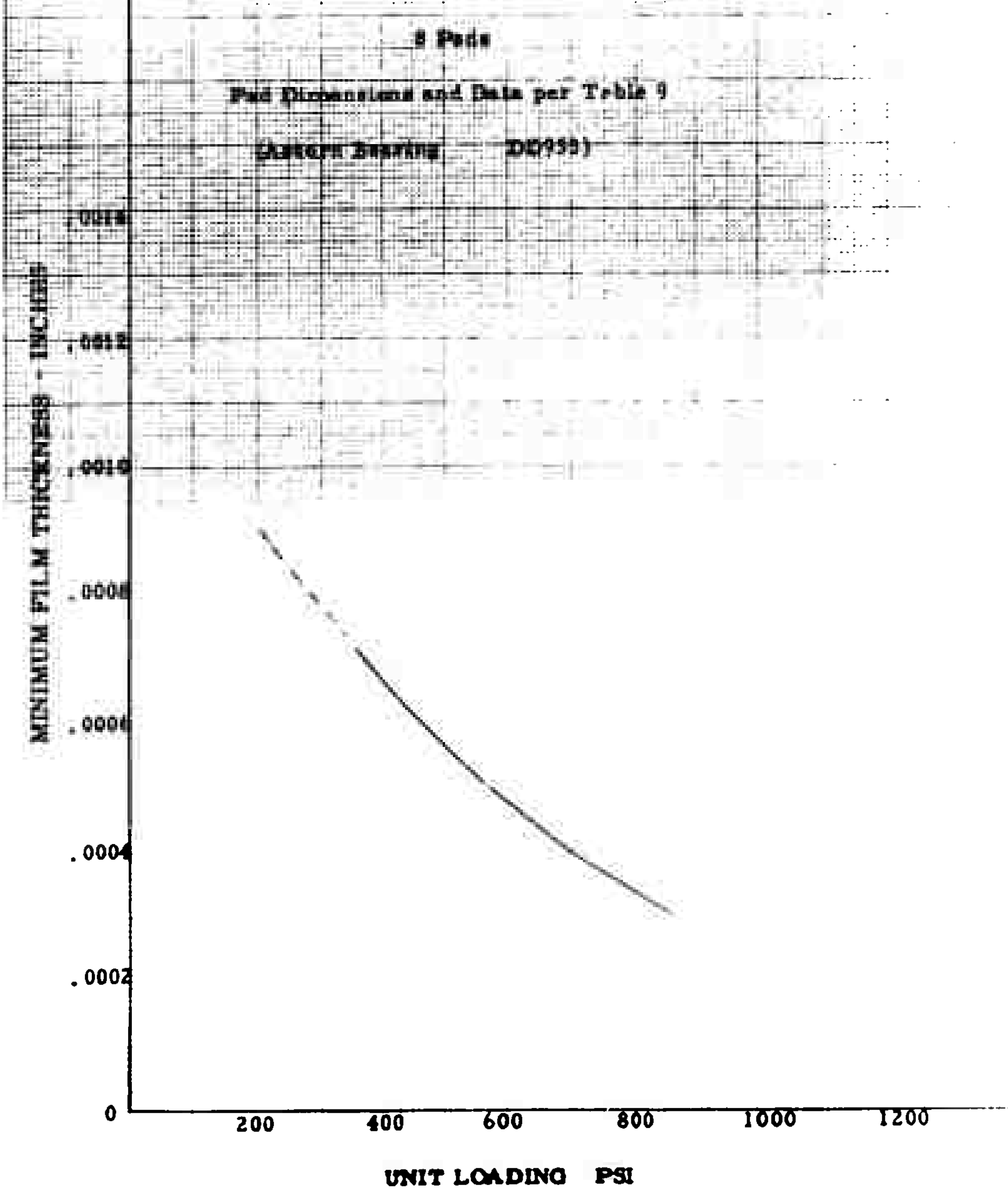

FIGURE 49

MAXIMUM TEMPERATURE VS. UNIT LOADING

26" O.D. x 17-1/2" I.D. Bearing
Speed - 160 RPM

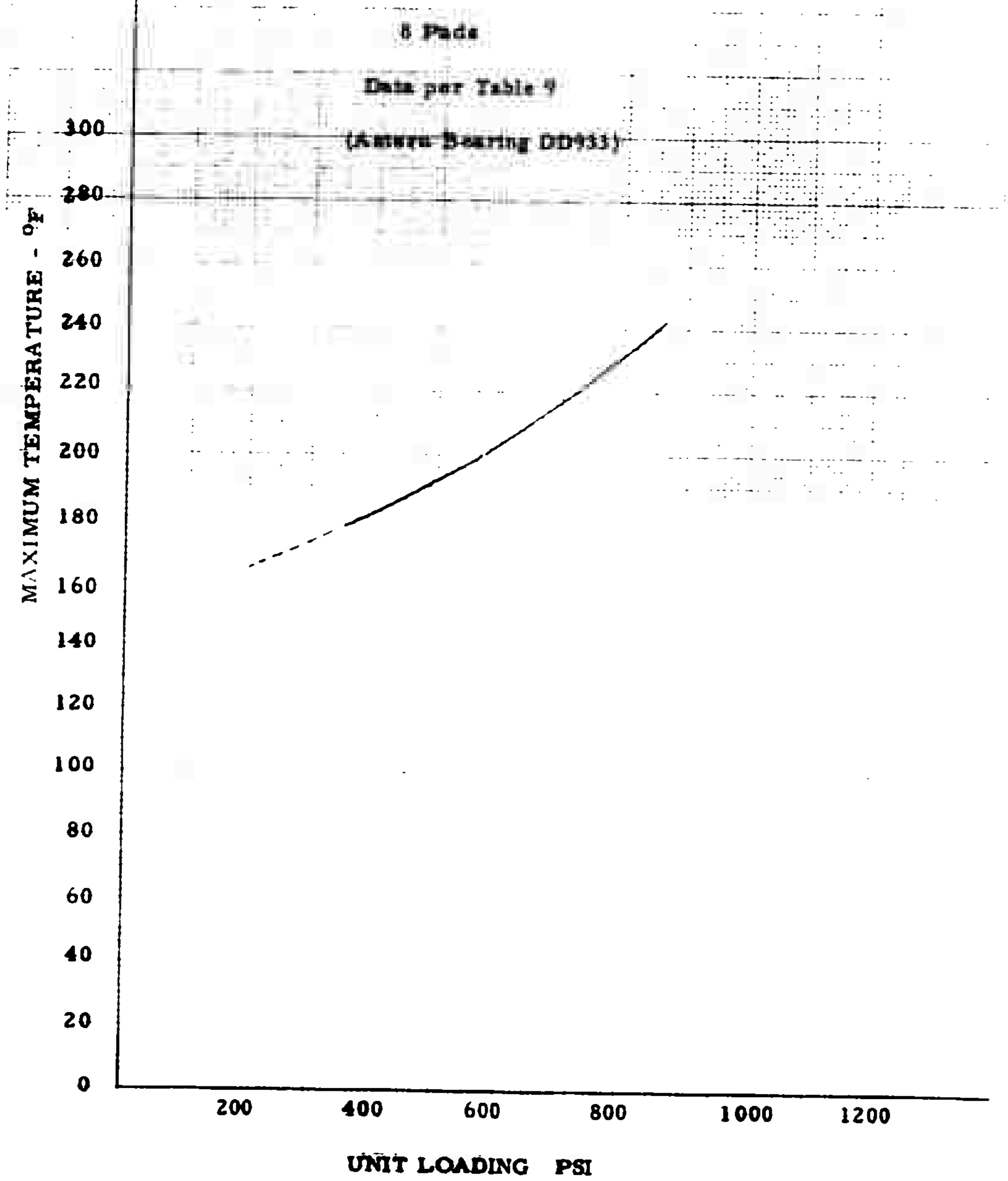

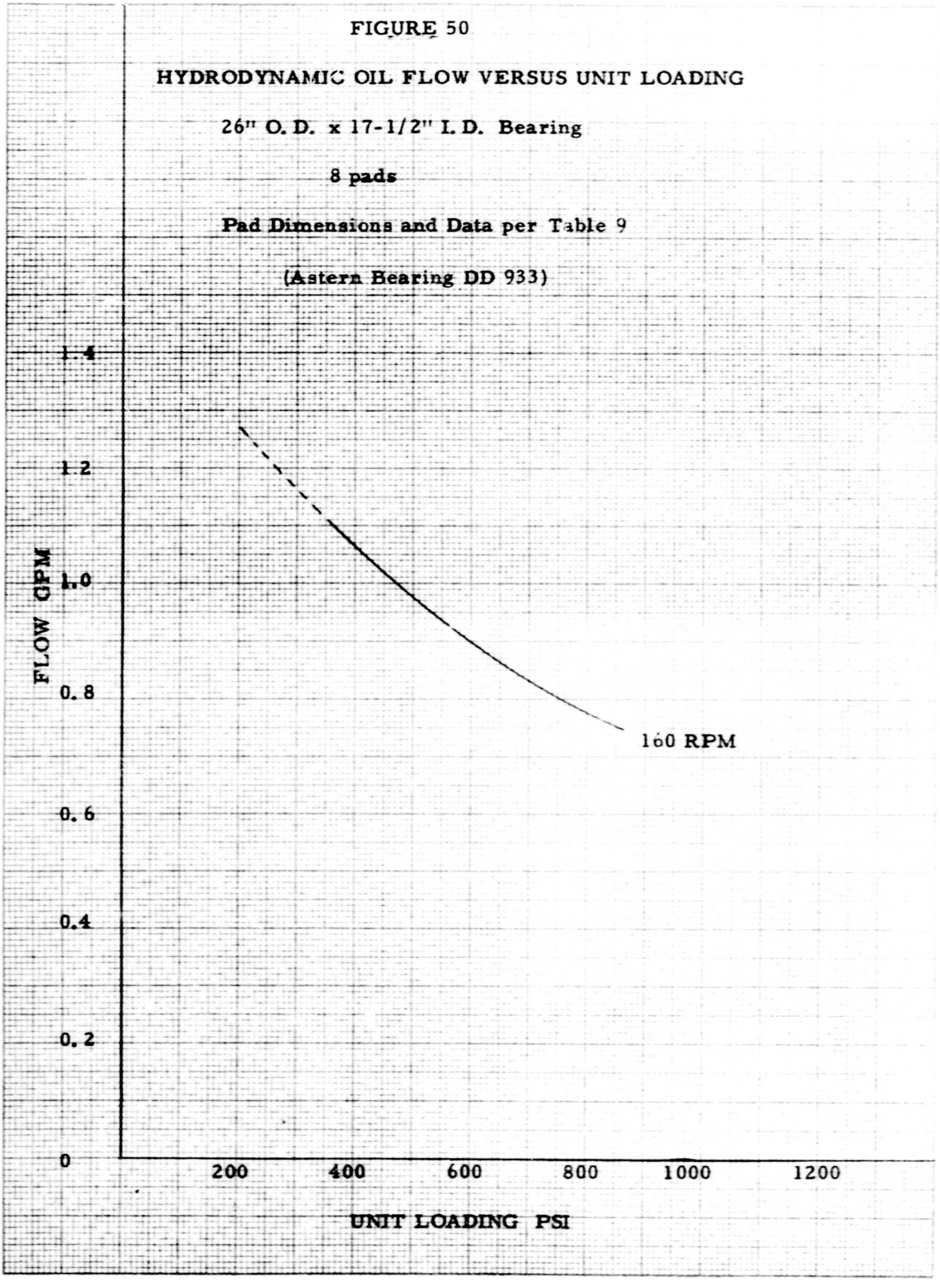
FIGURE 50
HYDRODYNAMIC OIL FLOW VERSUS UNIT LOADING
26" O. D. x 17-1/2" I. D. Bearing
8 pads
Pad Dimensions and Data per Table 9
(Astern Bearing DD 933)
FLOW GPM
1.4
1.2
1.0
0.8
0.6
0.4
0.2
0
200
400
600
800
1000
1200
UNIT LOADING PSI
160 RPM

TABLE 51

MINIMUM FILM THICKNESS VS. UNIT LOADING

31" O.D. x 16-1/2" I.D. Bearing
Speed - 320 RPM

8 Pads

Pad Dimensions and Data per Table 10

(Ahead Bearing DD933)

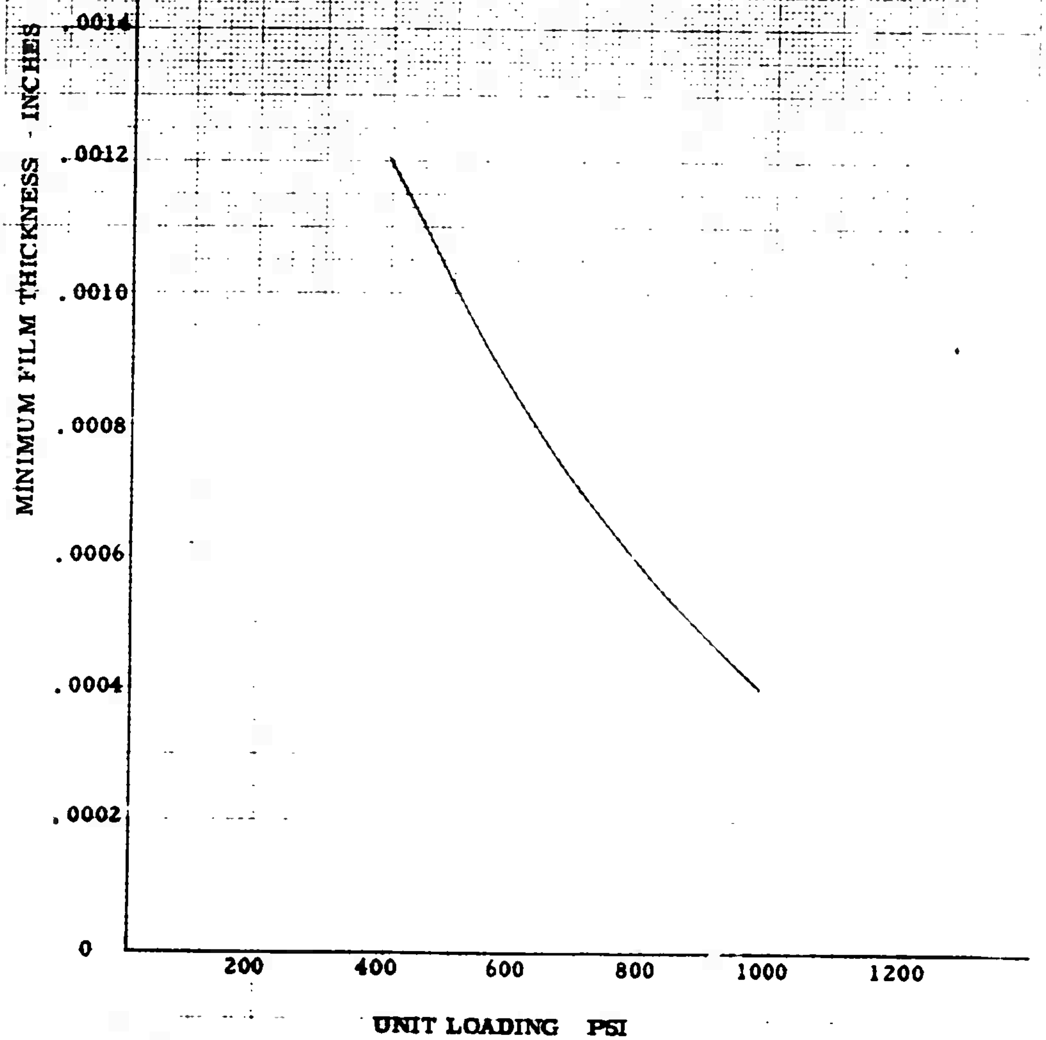

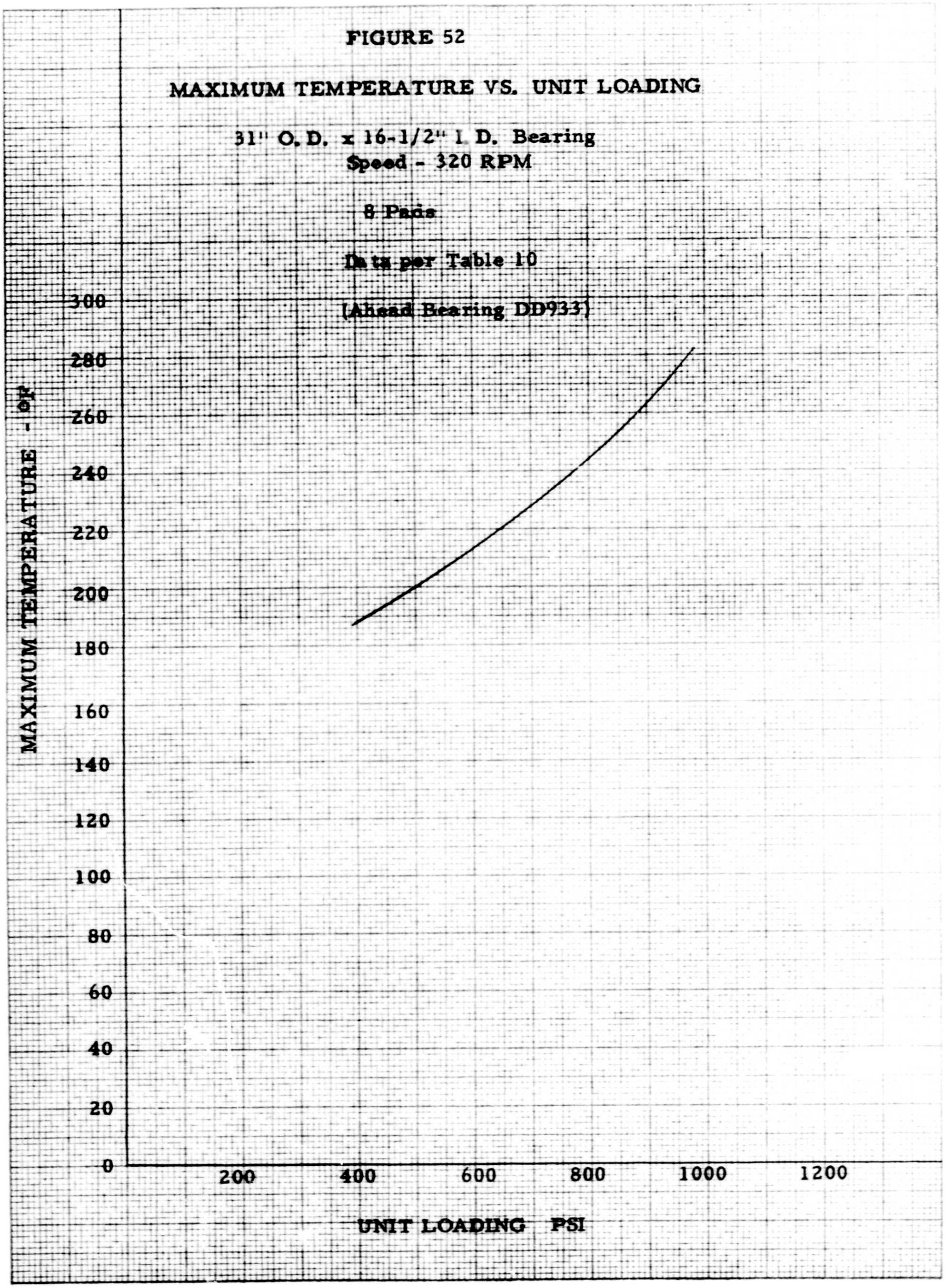
FIGURE 52
MAXIMUM TEMPERATURE VS. UNIT LOADING
31" O.D. x 16-1/2" I.D. Bearing
Speed - 320 RPM
8 Pads
Data per Table 10
(Ahead Bearing DD933)
MAXIMUM TEMPERATURE - °F
0
20
40
60
80
100
120
140
160
180
200
220
240
260
280
300
200
400
600
800
1000
1200
UNIT LOADING PSI

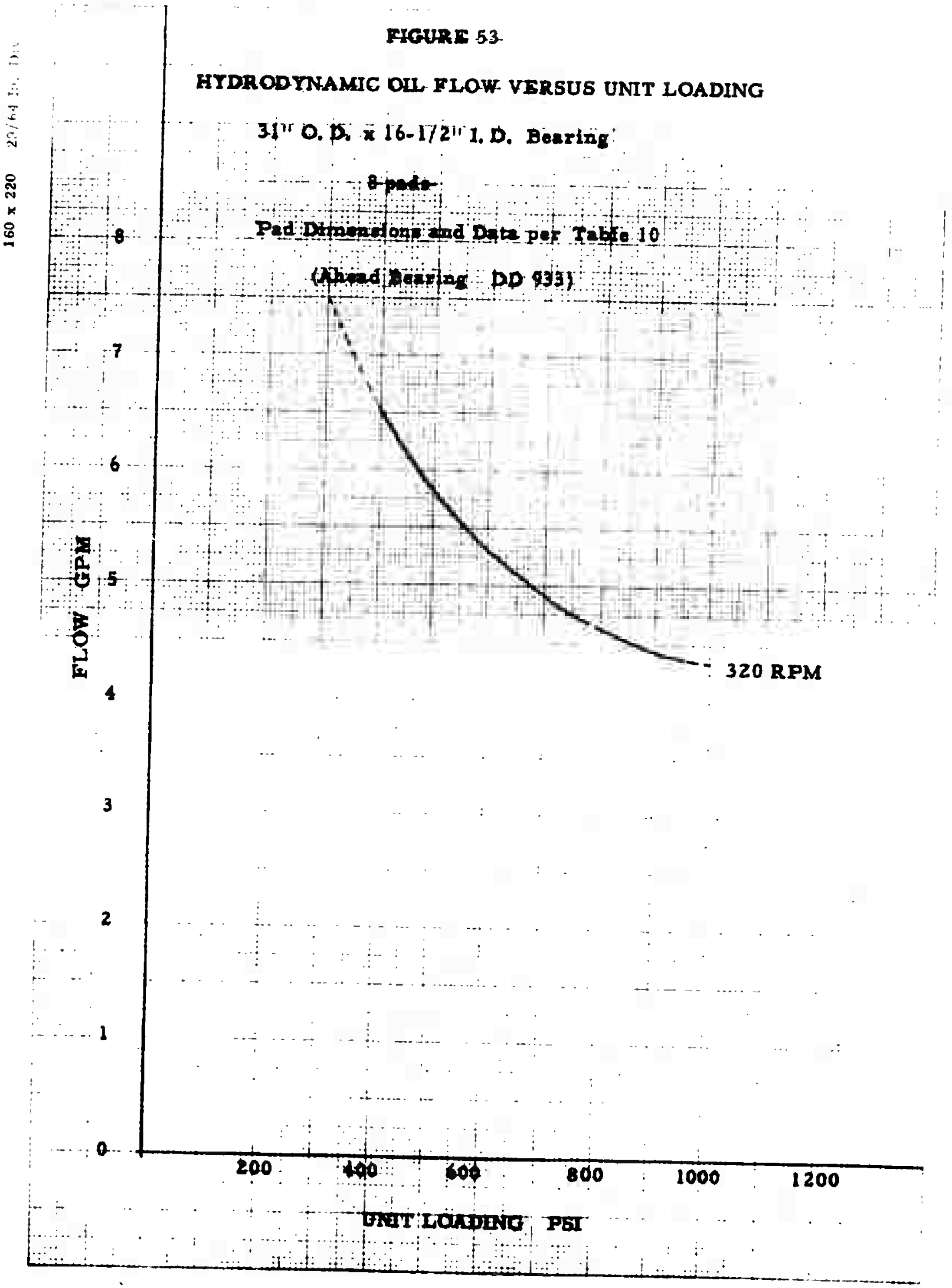
FIGURE 53
HYDRODYNAMIC OIL FLOW VERSUS UNIT LOADING
31" O. D. x 16-1/2" I. D. Bearing
8 pads
Pad Dimensions and Data per Table 10
(Ahead Bearing DD 933)
FLOW GPM
8
7
6
5
4
3
2
1
0
320 RPM
200
400
600
800
1000
1200
UNIT LOADING PSI
160 x 220

FIGURE 54

MINIMUM FILM THICKNESS VS. UNIT LOADING

35" O. D. x 18-1/2" I. D. Bearing
Speed - 170 RPM

8 Pads

Pad Dimensions and Data per Table II

(Ahead Bearing — DL1)

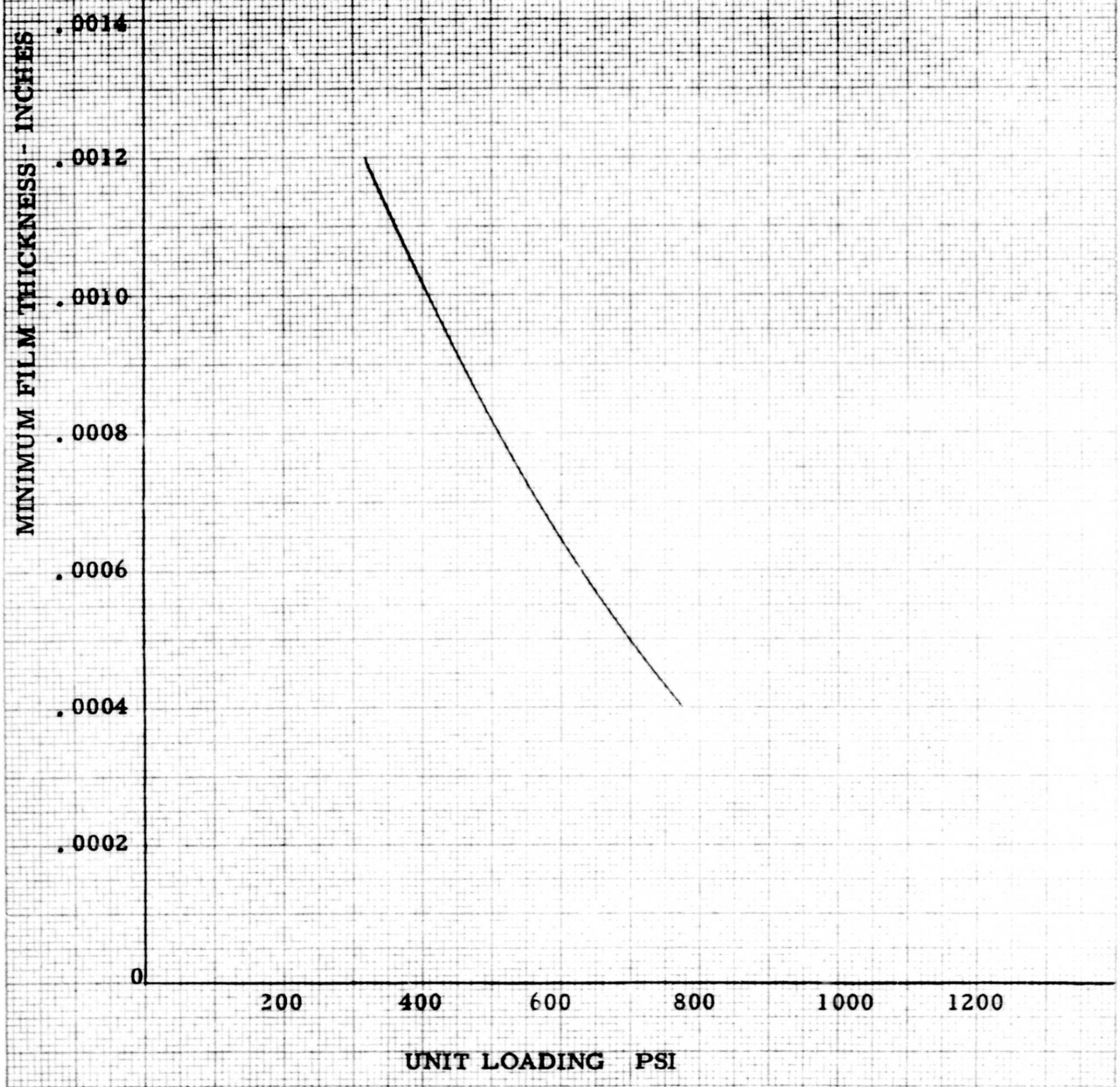

FIGURE 55

MAXIMUM TEMPERATURE VS. UNIT LOADING

35" O. D. x 18-1/2" I. D. Bearing
Speed - 170 RPM

8 Pads

Data per Table II

(Ahead Bearing DL1)

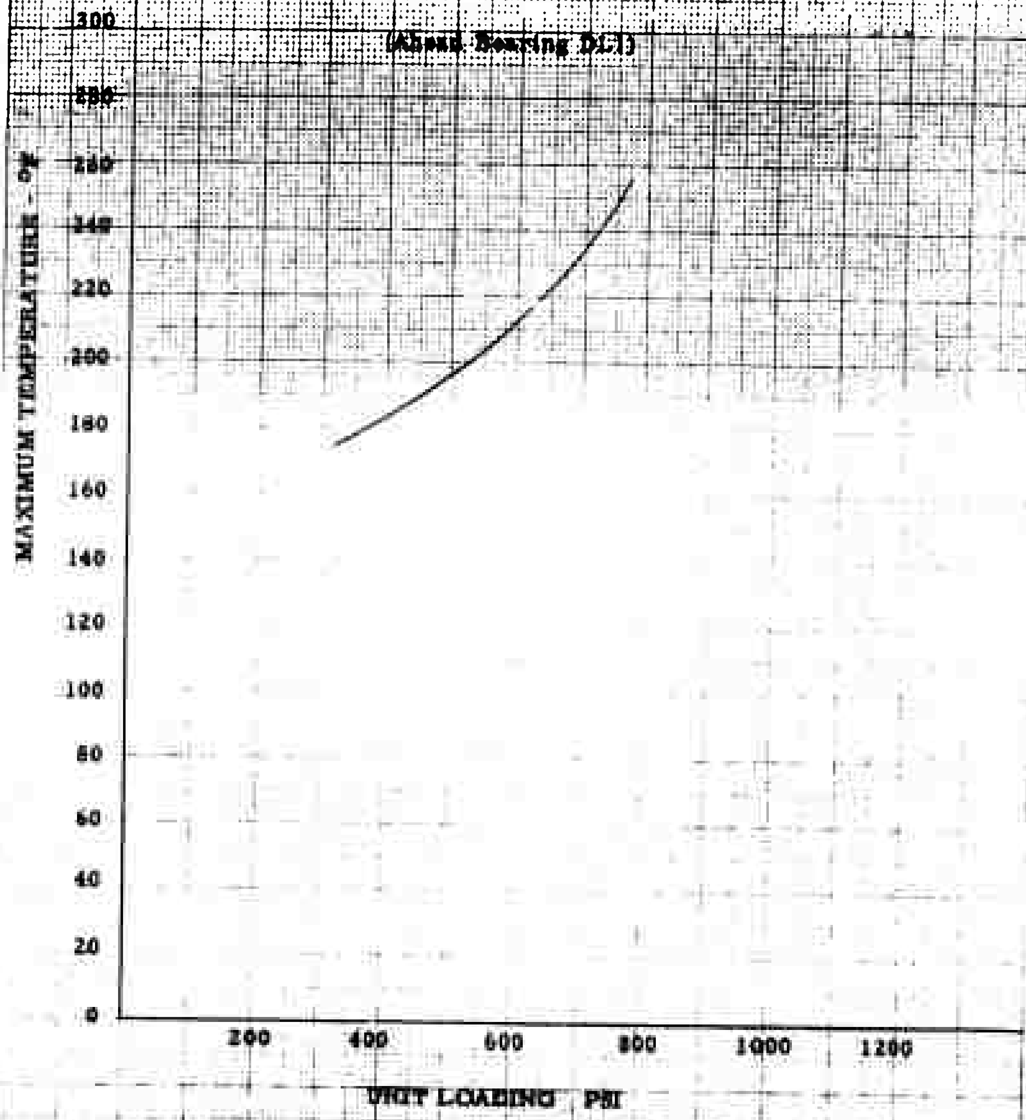

160 x 220

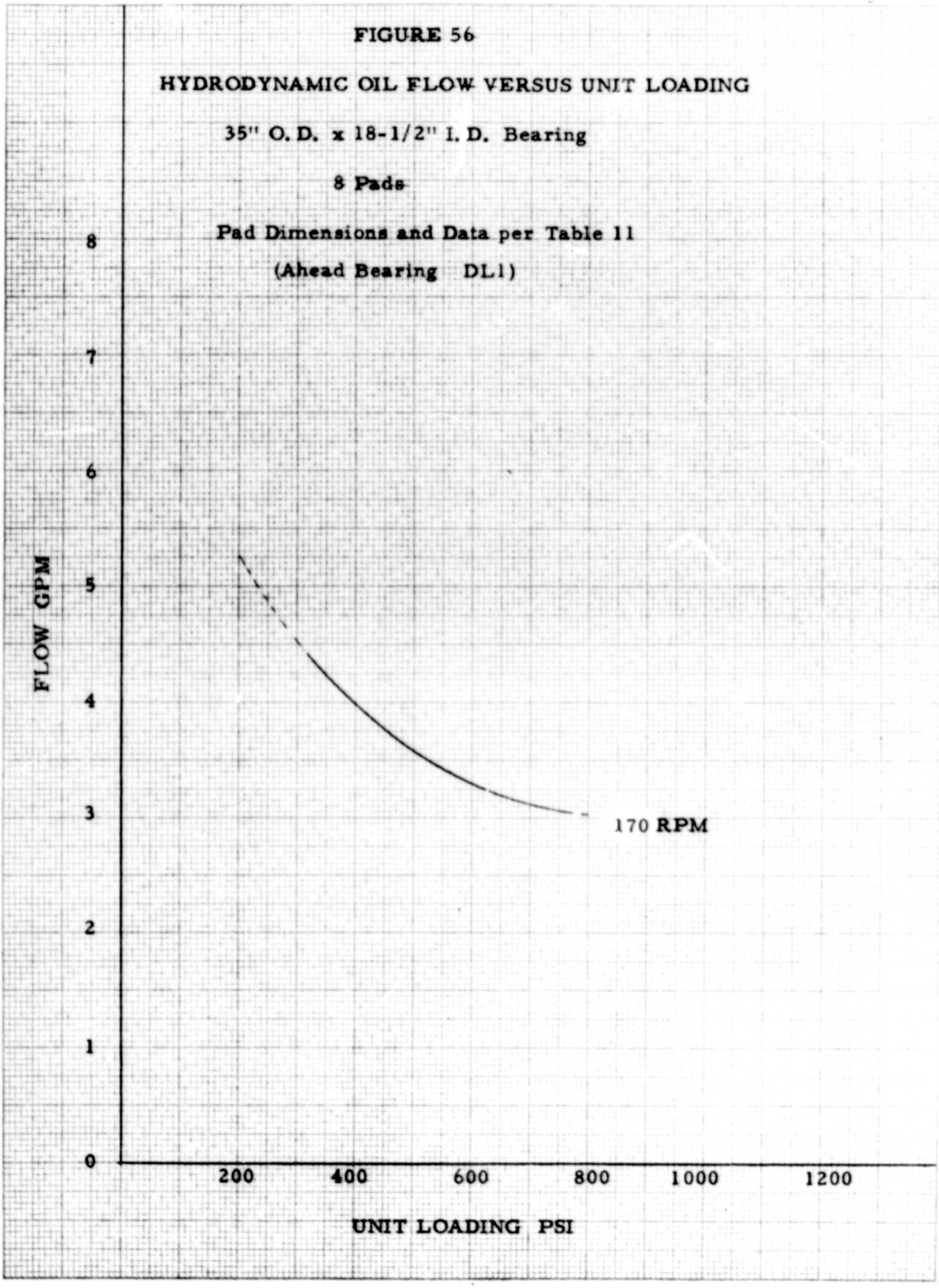

FIGURE 56

HYDRODYNAMIC OIL FLOW VERSUS UNIT LOADING

35" O.D. x 18-1/2" I.D. Bearing

8 Pads

Pad Dimensions and Data per Table 11

(Ahead Bearing DL1)

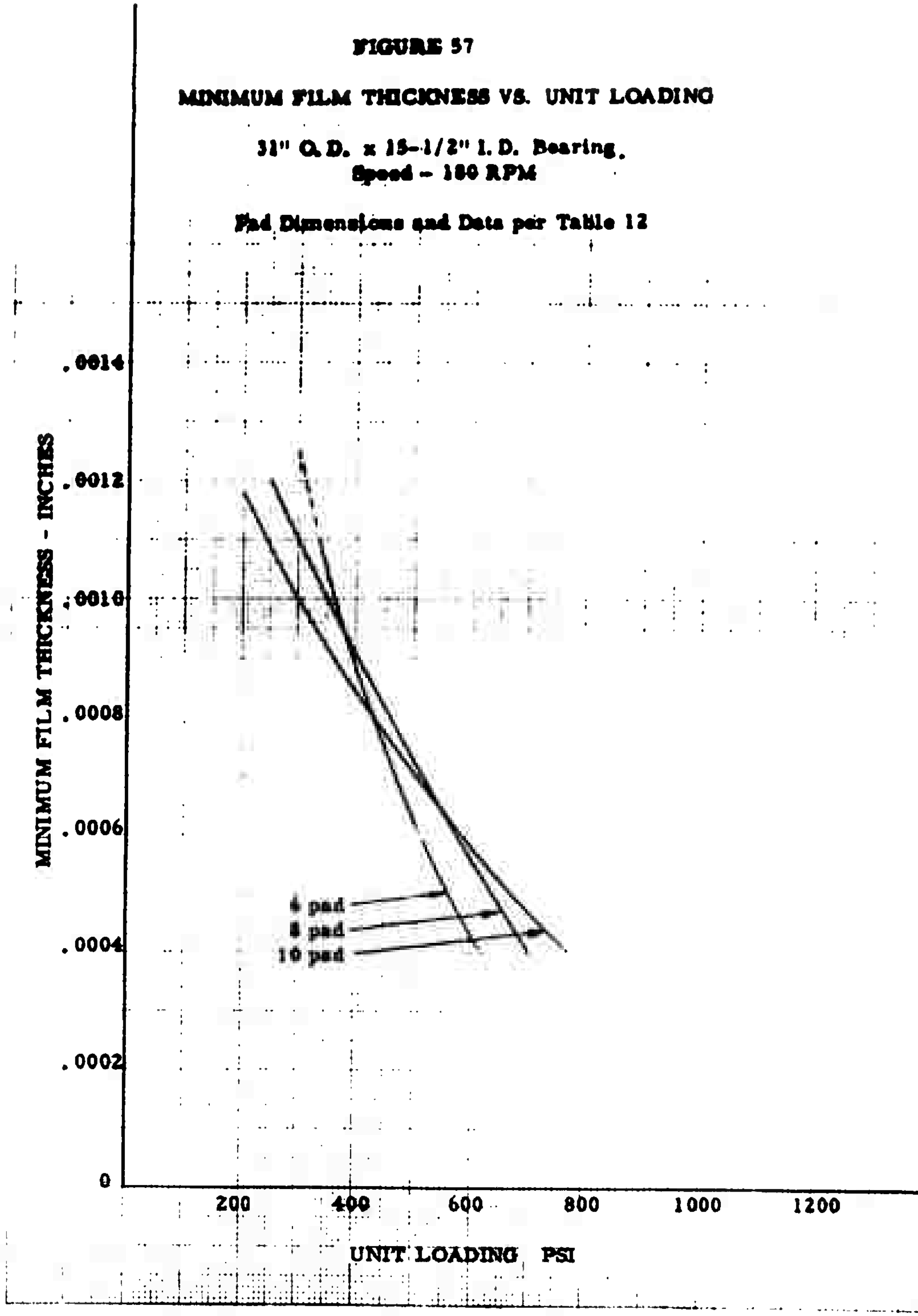
FIGURE 57
MINIMUM FILM THICKNESS VS. UNIT LOADING
31" O.D. x 15-1/2" I.D. Bearing.
Speed - 180 RPM
Pad Dimensions and Data per Table 12
MINIMUM FILM THICKNESS - INCHES
.0014
.0012
.0010
.0008
.0006
.0004
.0002
0
6 pad
8 pad
10 pad
200
400
600
800
1000
1200
UNIT LOADING PSI

160 x 220   29/64 In. Div.

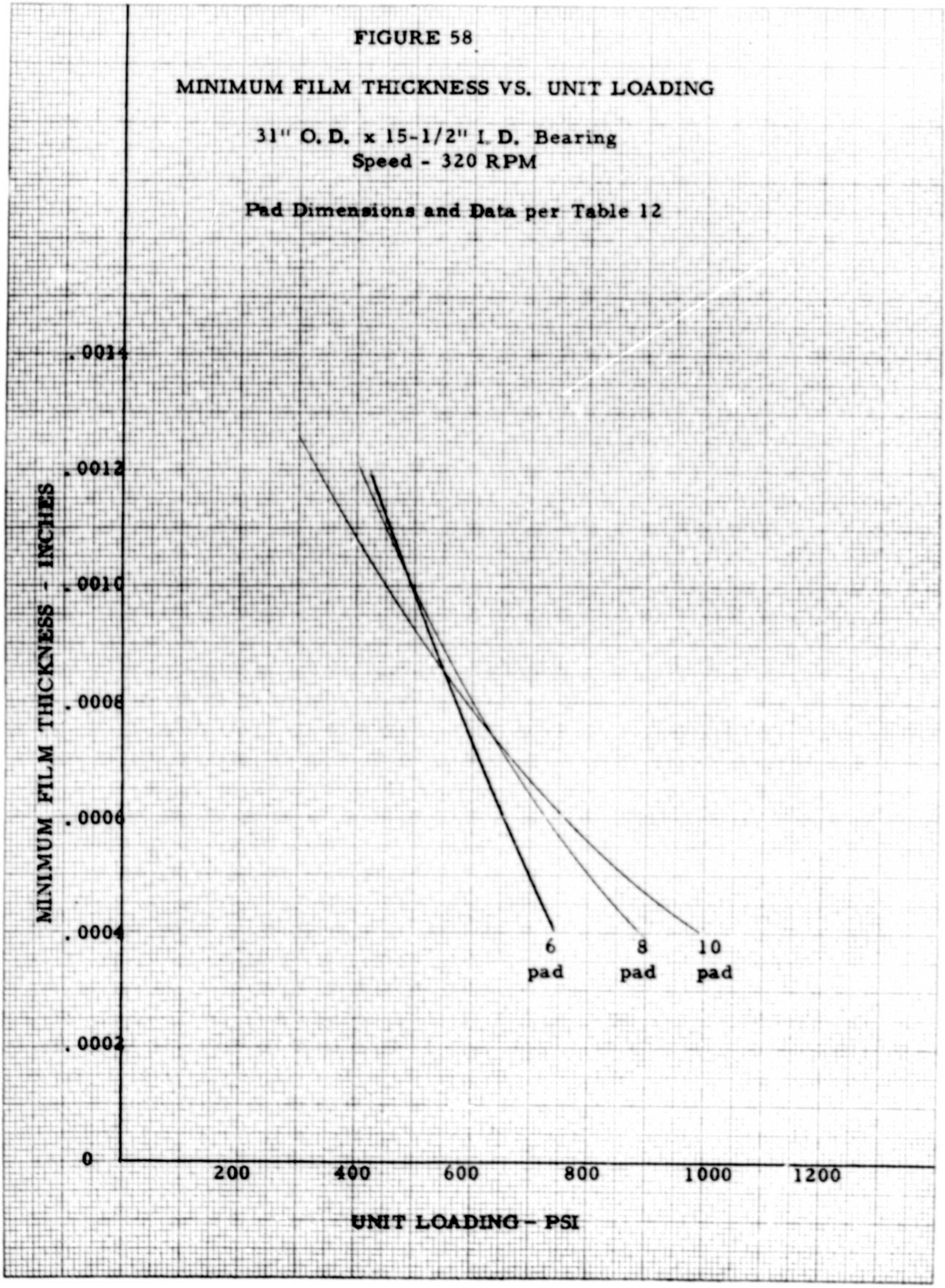

FIGURE 59

MAXIMUM TEMPERATURE VS. UNIT LOADING

31" O. D. x 15-1/2" I. D. Bearing
Speed - 180 RPM

Data per Table 12

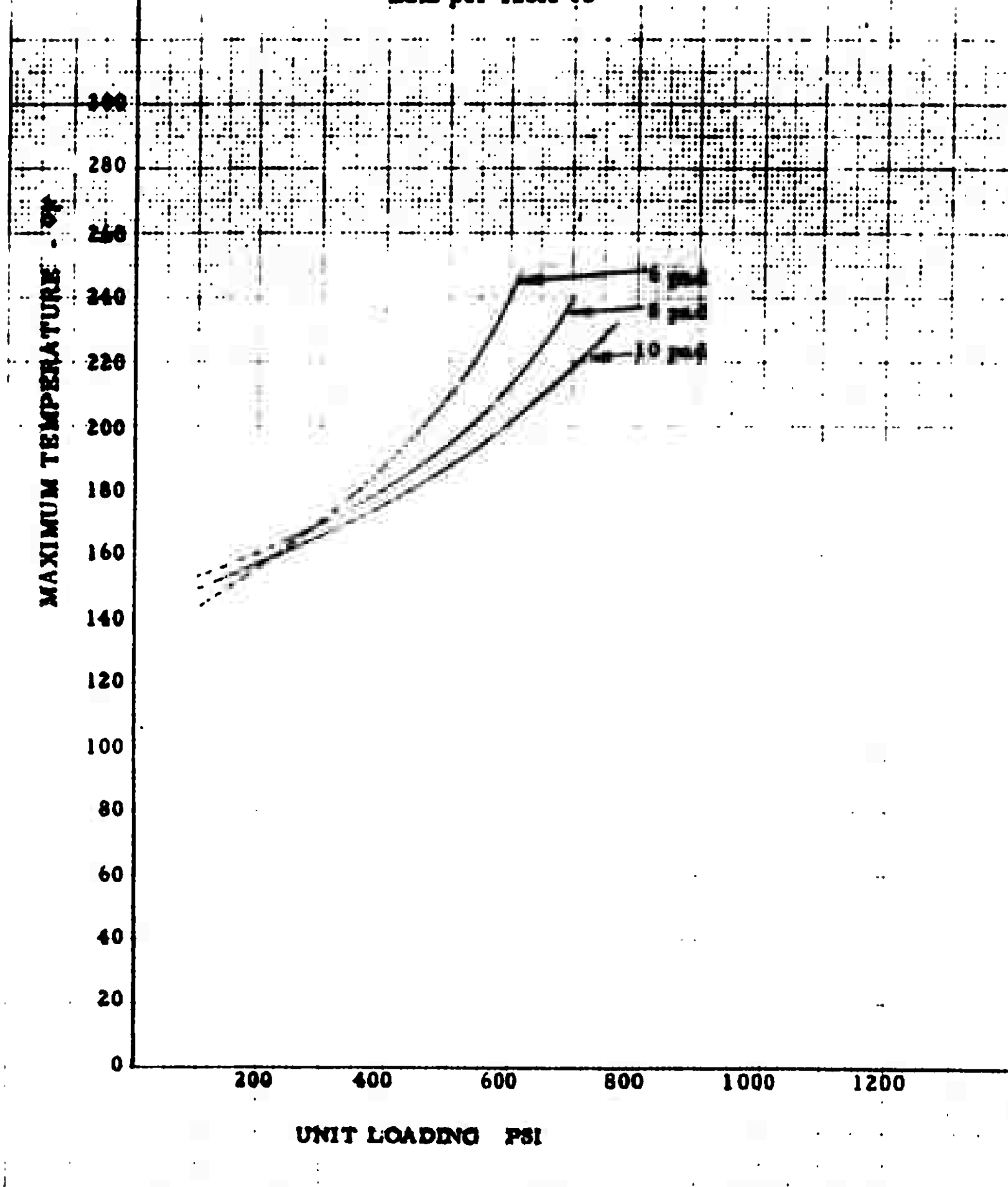

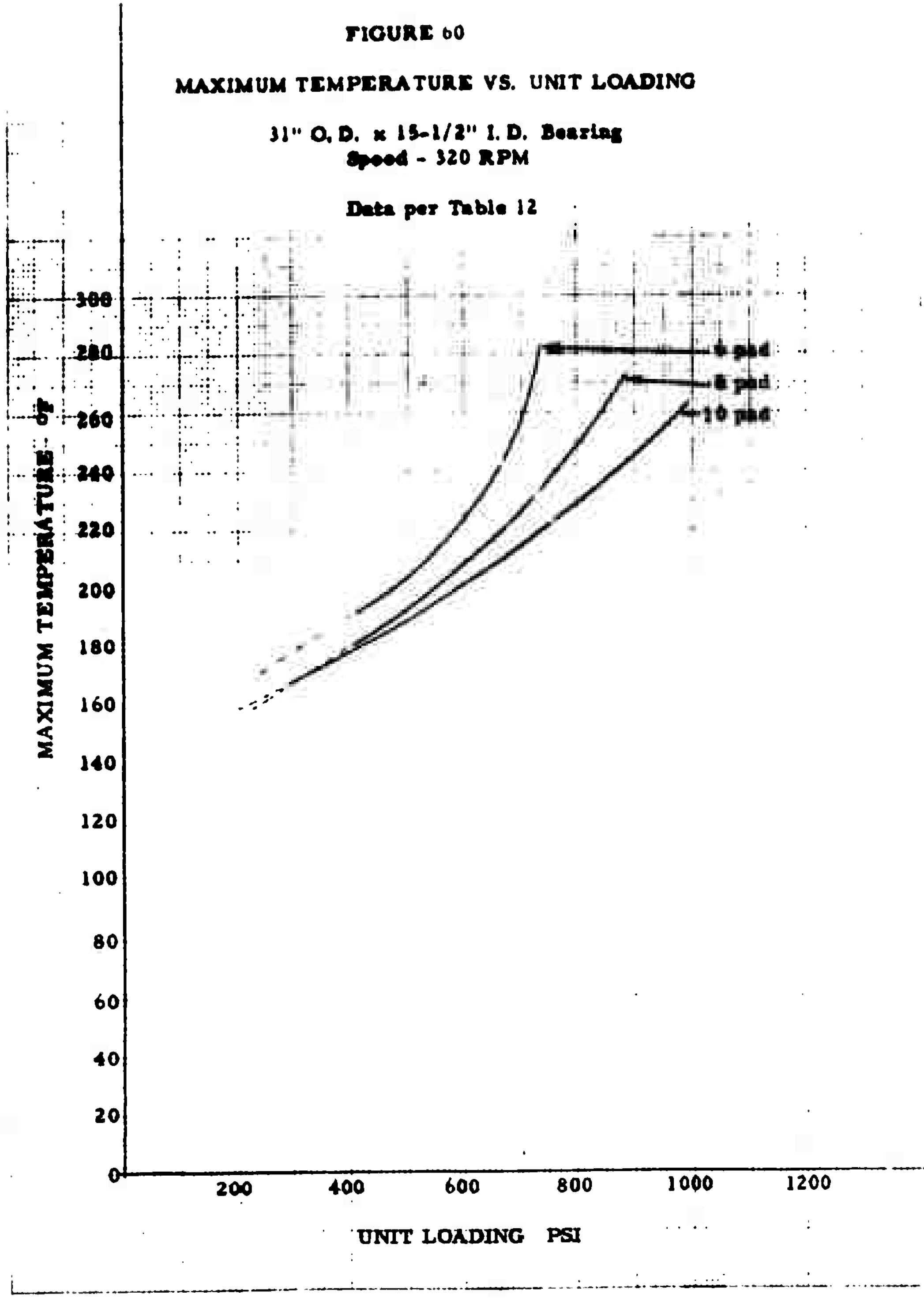
FIGURE 60
MAXIMUM TEMPERATURE VS. UNIT LOADING
31" O.D. x 15-1/2" I.D. Bearing
Speed - 320 RPM
Data per Table 12
MAXIMUM TEMPERATURE °F
300
280
260
240
220
200
180
160
140
120
100
80
60
40
20
0
200
400
600
800
1000
1200
UNIT LOADING PSI
6 pad
8 pad
10 pad

FIGURE 61

MINIMUM FILM THICKNESS VS. UNIT LOADING

31" O.D. x 15-1/2" I.D. Bearing
Speed - 180 RPM

Pad Dimensions and Data per Table 13

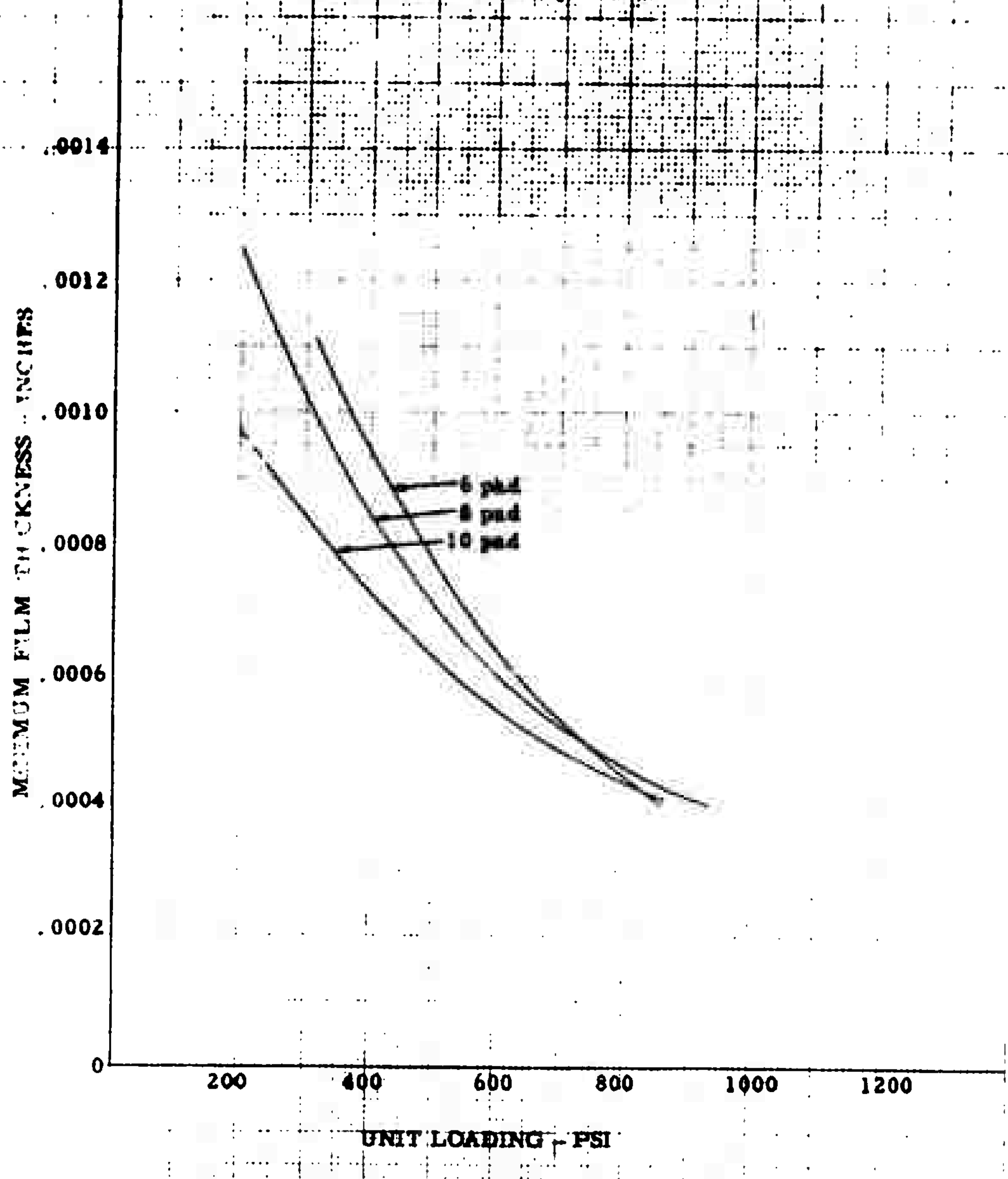

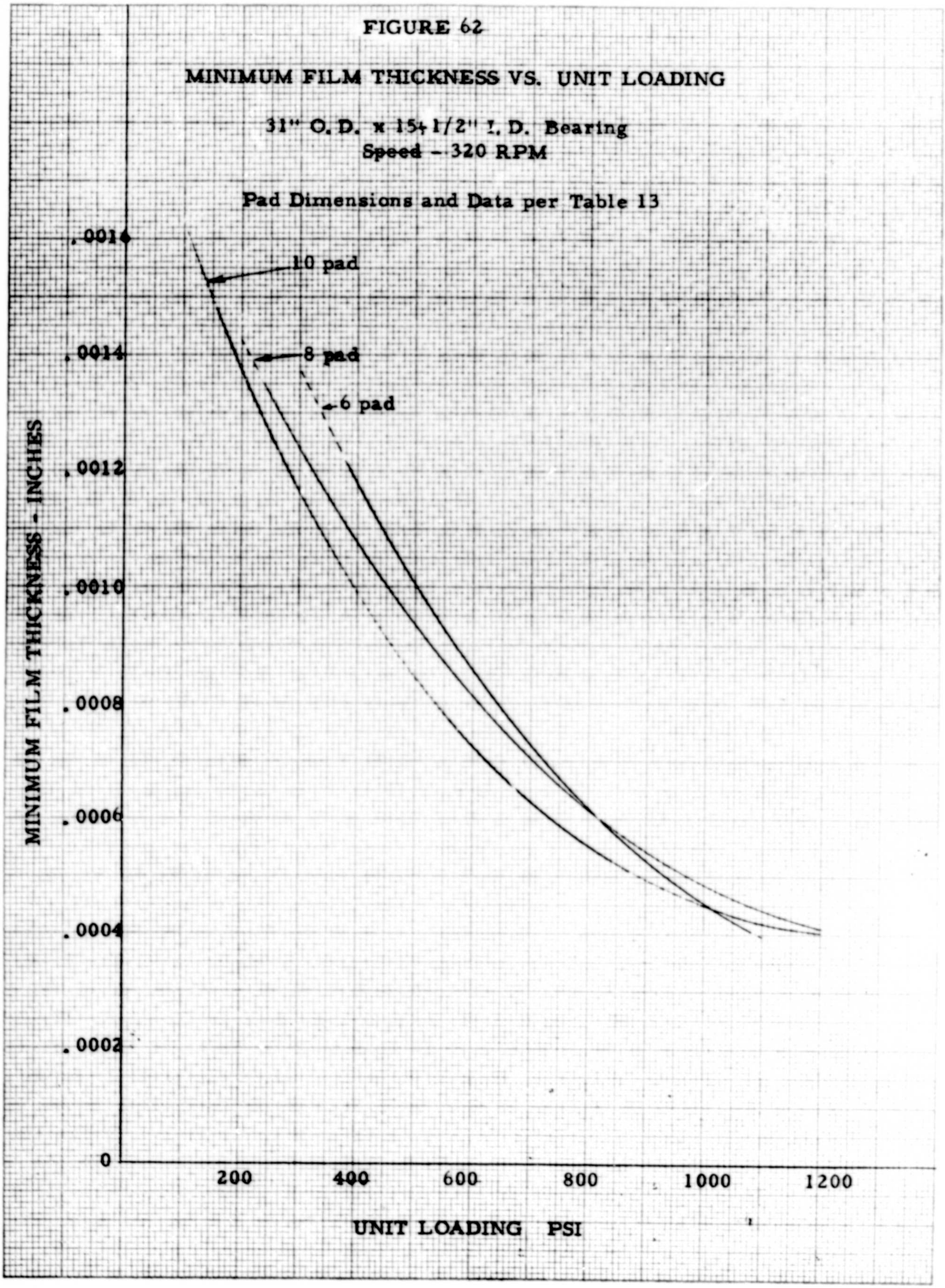

160 x 220 29/64 In. Div.

FIGURE 63

MAXIMUM TEMPERATURE VS. UNIT LOADING

31" O.D. x 15-1/2" I.D. Bearing
Speed - 180 RPM

Data per Table 13

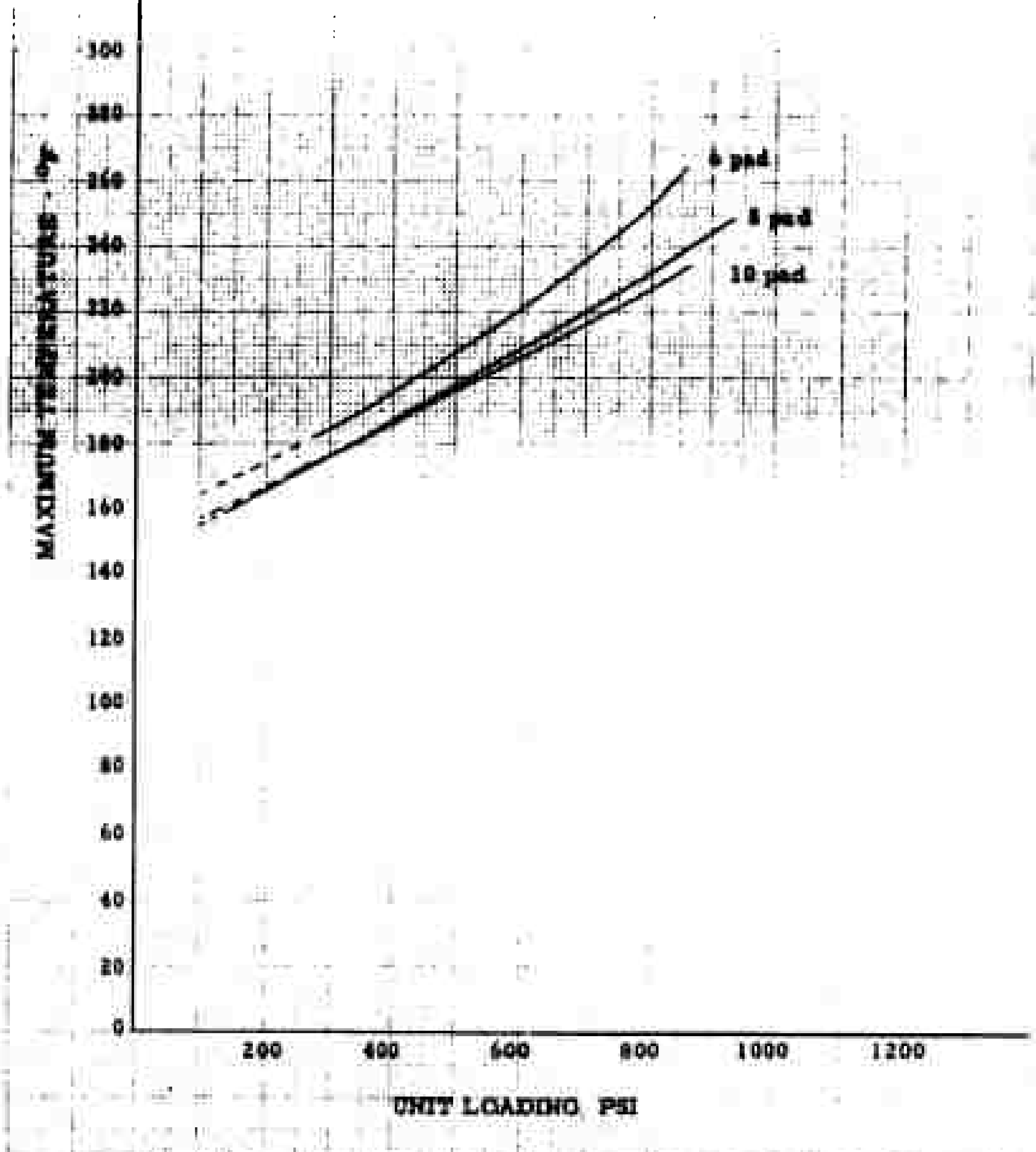

FIGURE 64

MAXIMUM TEMPERATURE VS. UNIT LOADING

31" O.D. x 15-1/2" I.D. Bearing
Speed - 320 RPM

Data per Table 13

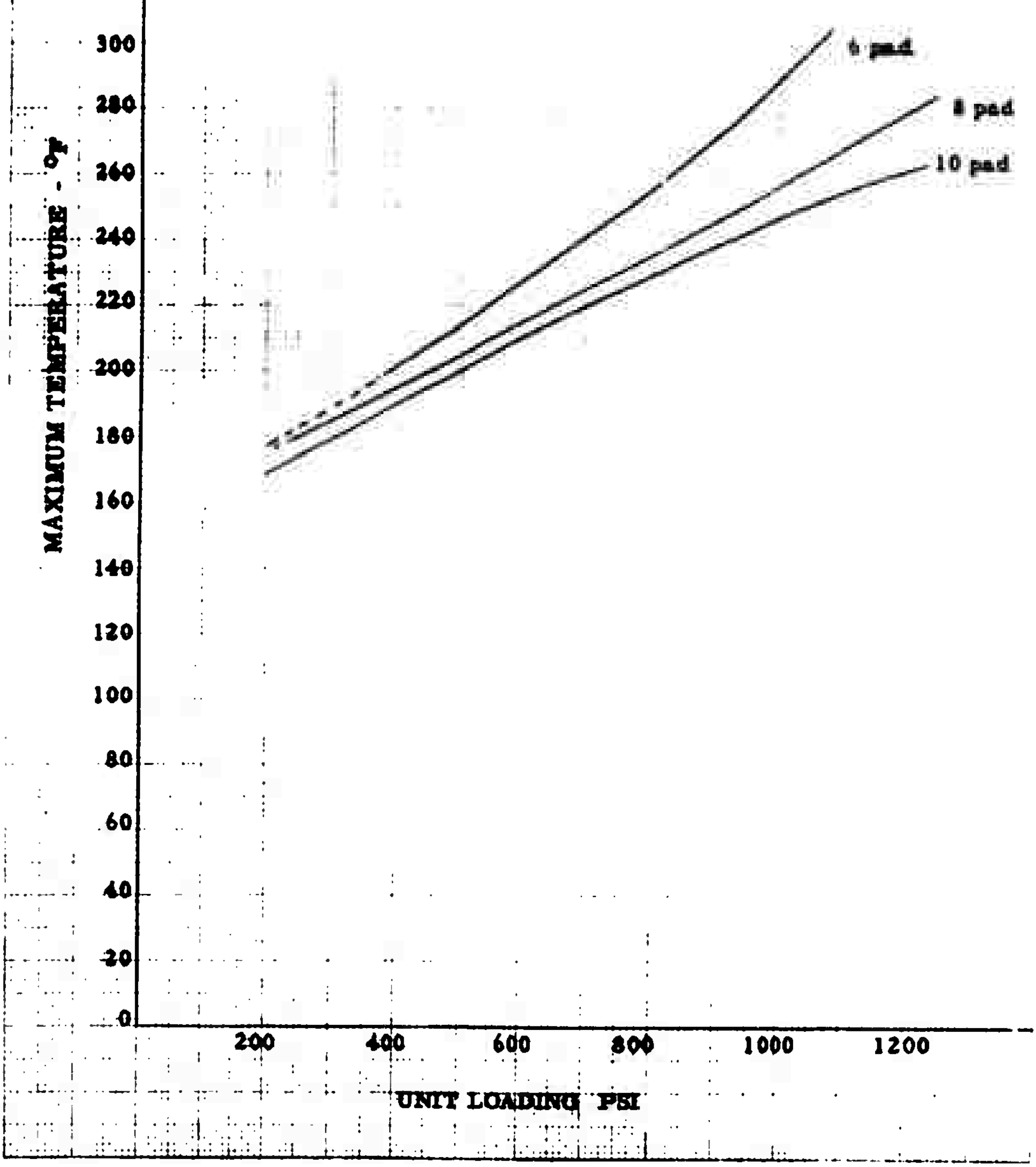

FIGURE 65

HYDRODYNAMIC OIL FLOW VERSUS UNIT LOADING

31" O.D. x 15-1/2 I.D. Bearing
8 Pads

Pad Dimensions and Data per Tables 3, 12, 13

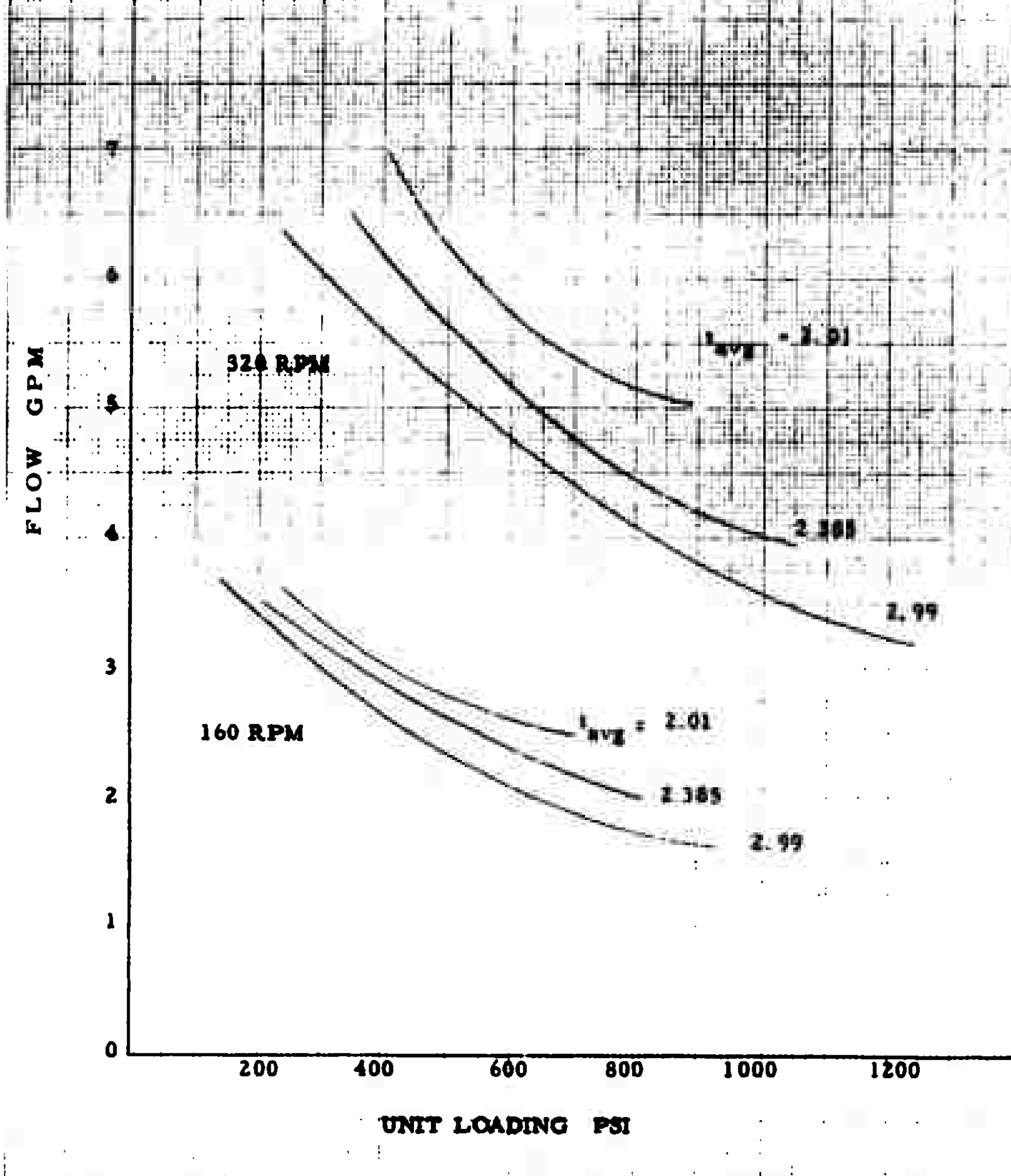

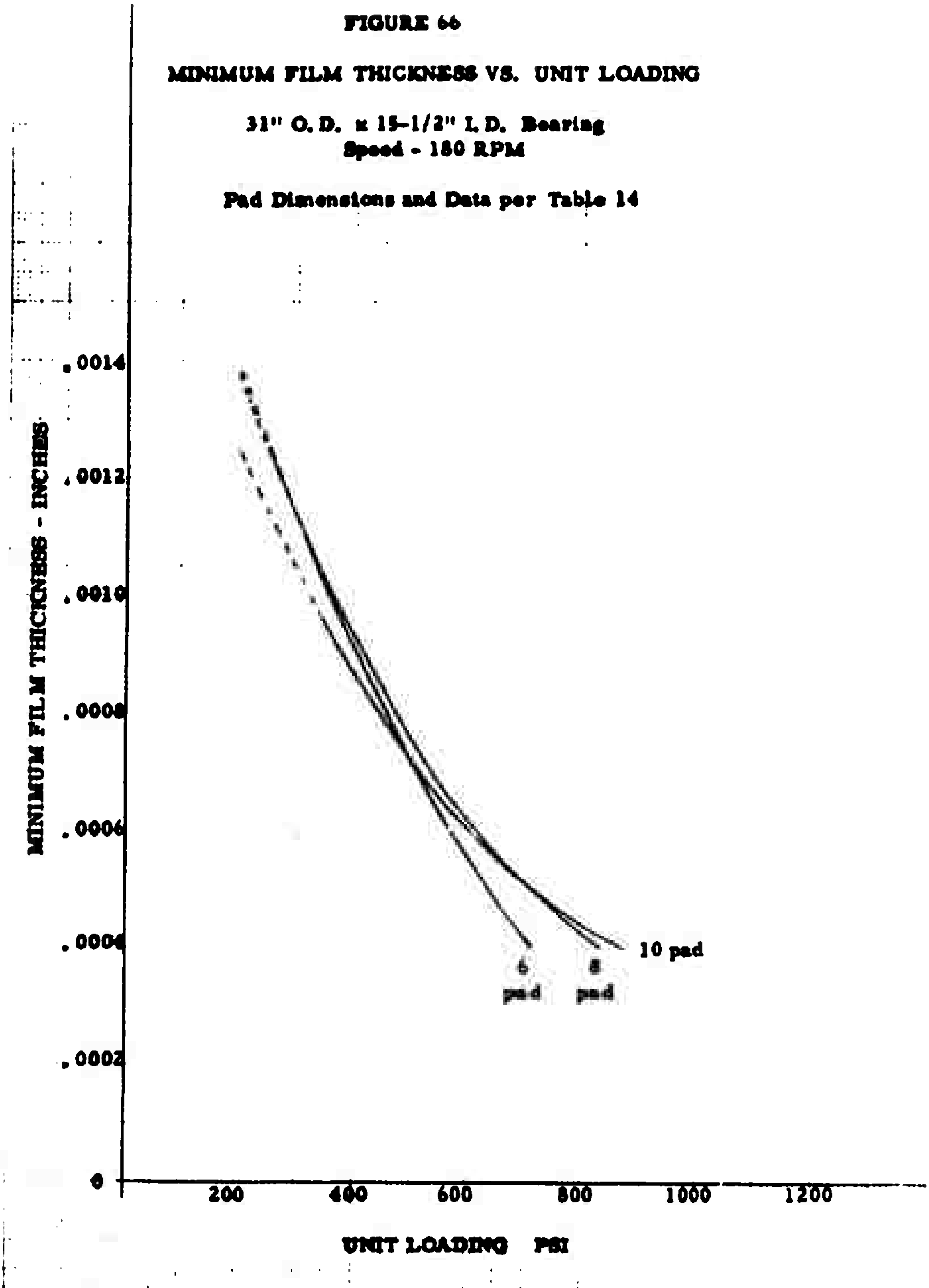
FIGURE 66
MINIMUM FILM THICKNESS VS. UNIT LOADING
31" O.D. x 15-1/2" I.D. Bearing
Speed - 180 RPM
Pad Dimensions and Data per Table 14
MINIMUM FILM THICKNESS - INCHES
.0014
.0012
.0010
.0008
.0006
.0004
.0002
0
200
400
600
800
1000
1200
UNIT LOADING PSI
10 pad
6 pad
8 pad

FIGURE 67

MINIMUM FILM THICKNESS VS. UNIT LOADING

31" O. D. x 15-1/2" I. D. Bearing
Speed - 320 RPM

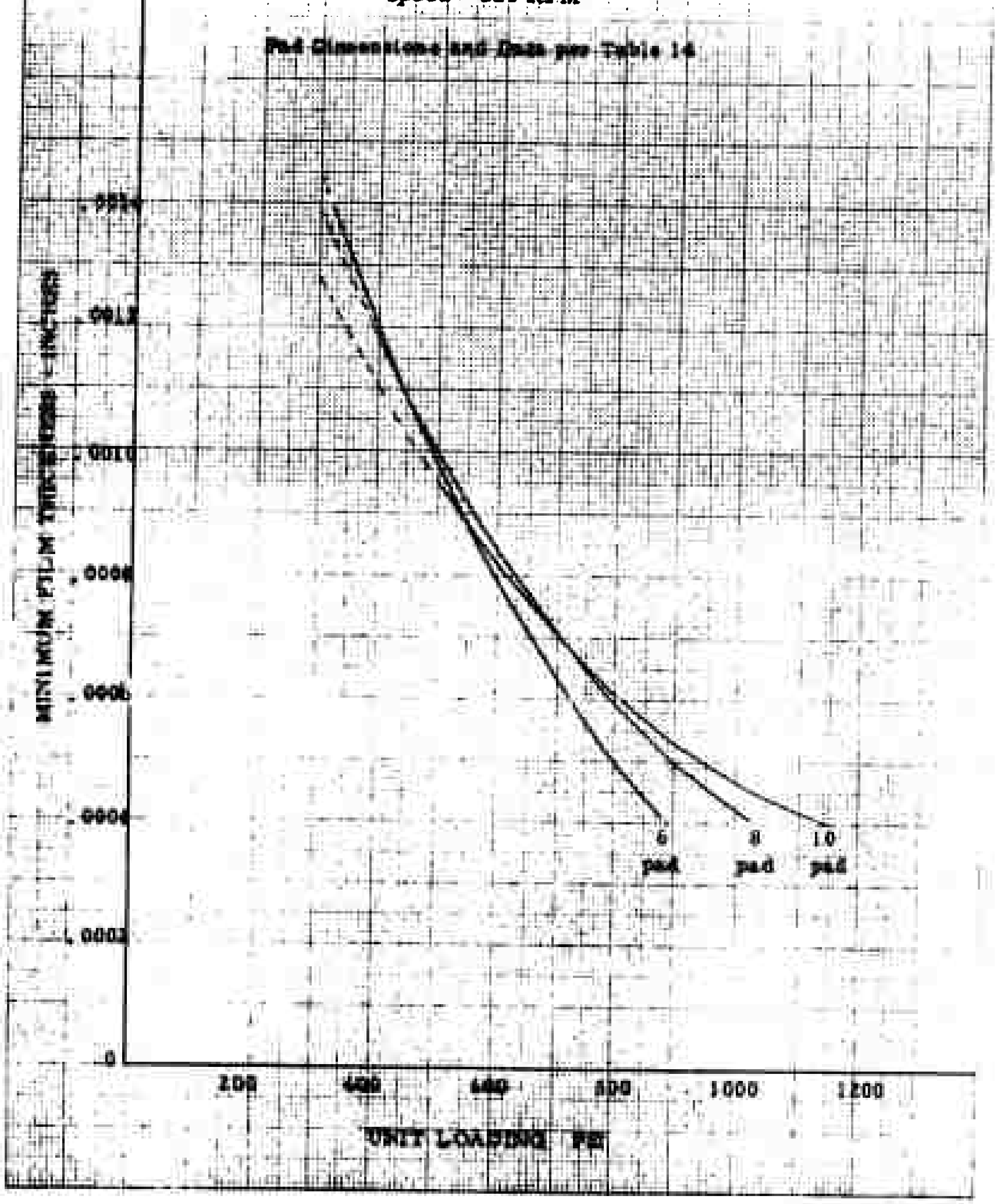

FIGURE 68

MAXIMUM TEMPERATURE VS. UNIT LOADING

31" O.D. x 15-1/2" I.D. Bearing
Speed – 180 RPM

Data per Table 14

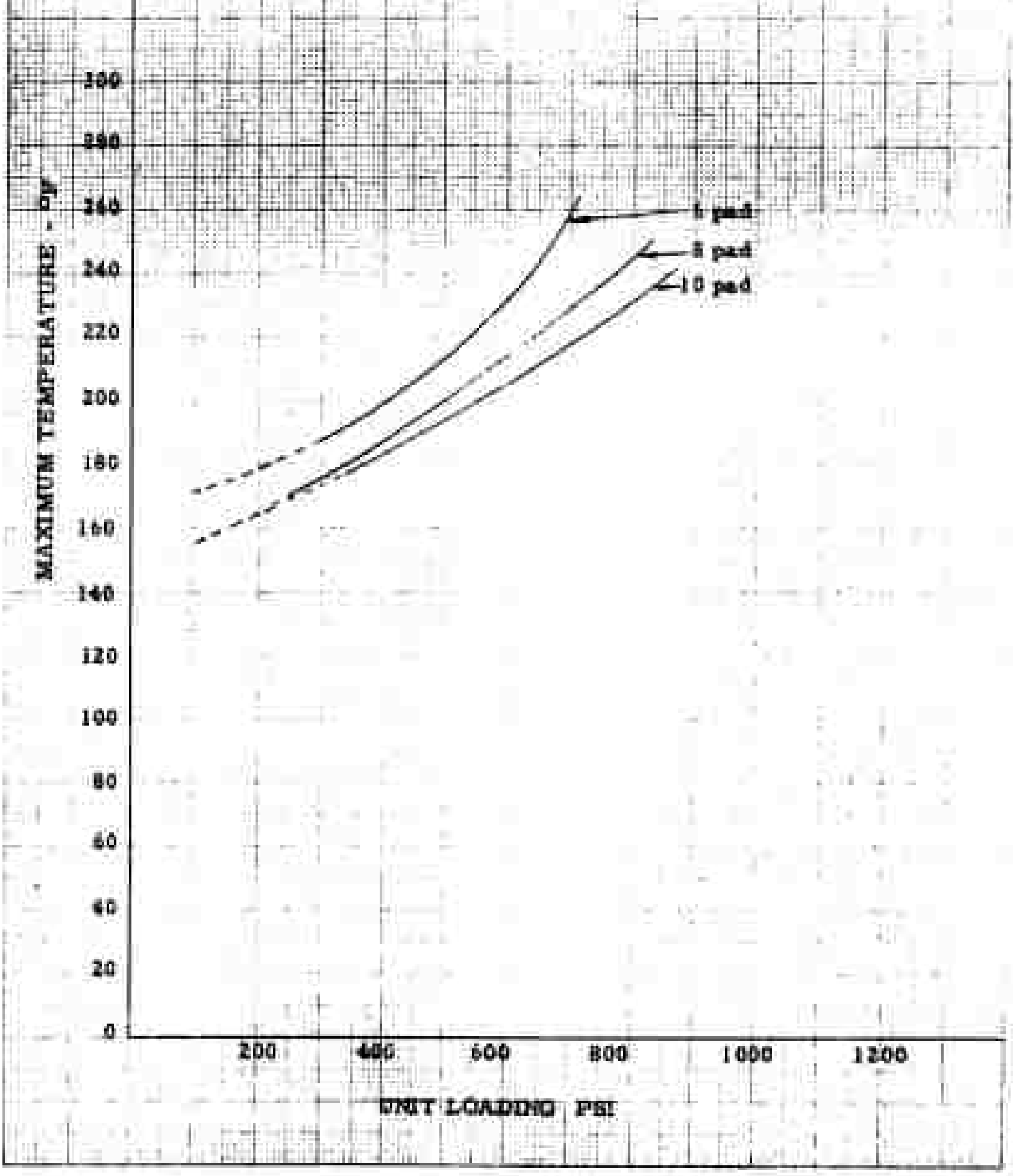

FIGURE 69

MAXIMUM TEMPERATURE VS. UNIT LOADING

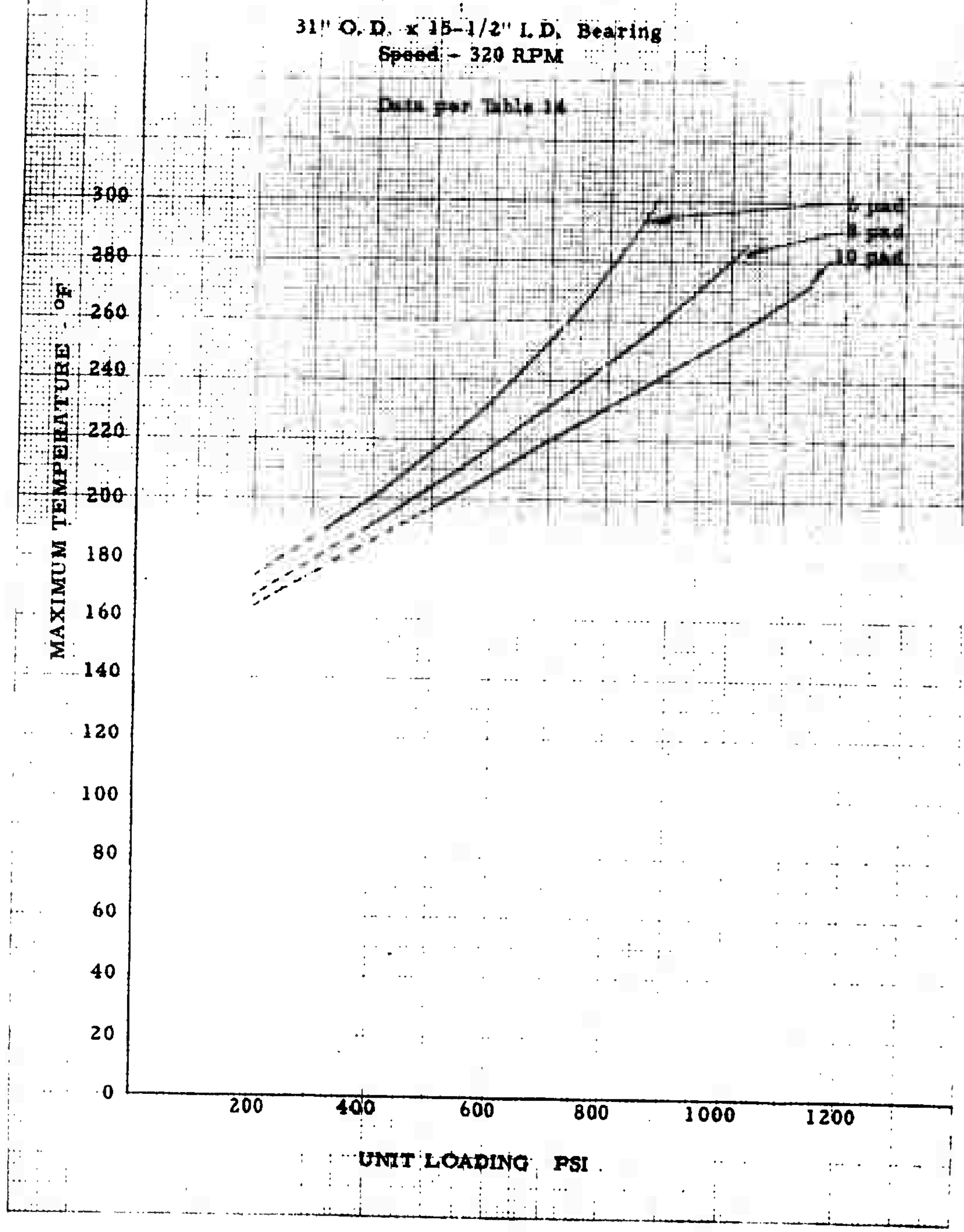

160 x 220 29/64 In. Div

FIGURE 70

MINIMUM FILM THICKNESS VS. UNIT LOADING

31" O.D. x 15-1/2" I.D. Bearing

Speed - [illegible] RPM

Pad Dimensions and Data per Table [illegible]

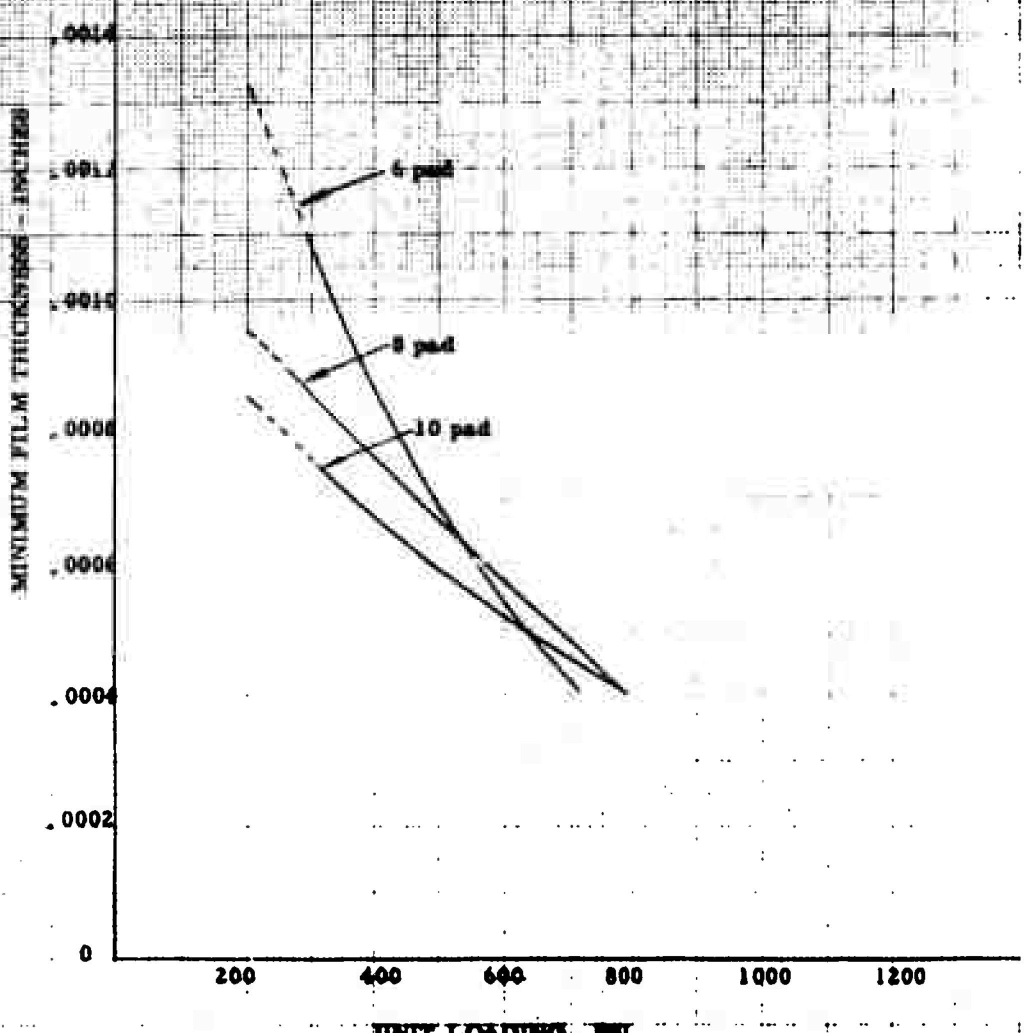

FIGURE 71

MINIMUM FILM THICKNESS VS. UNIT LOADING

31" O. D. x 15-1/2" I. D. Bearing
Speed -- 320 RPM

Pad Dimensions and Data per Table 15

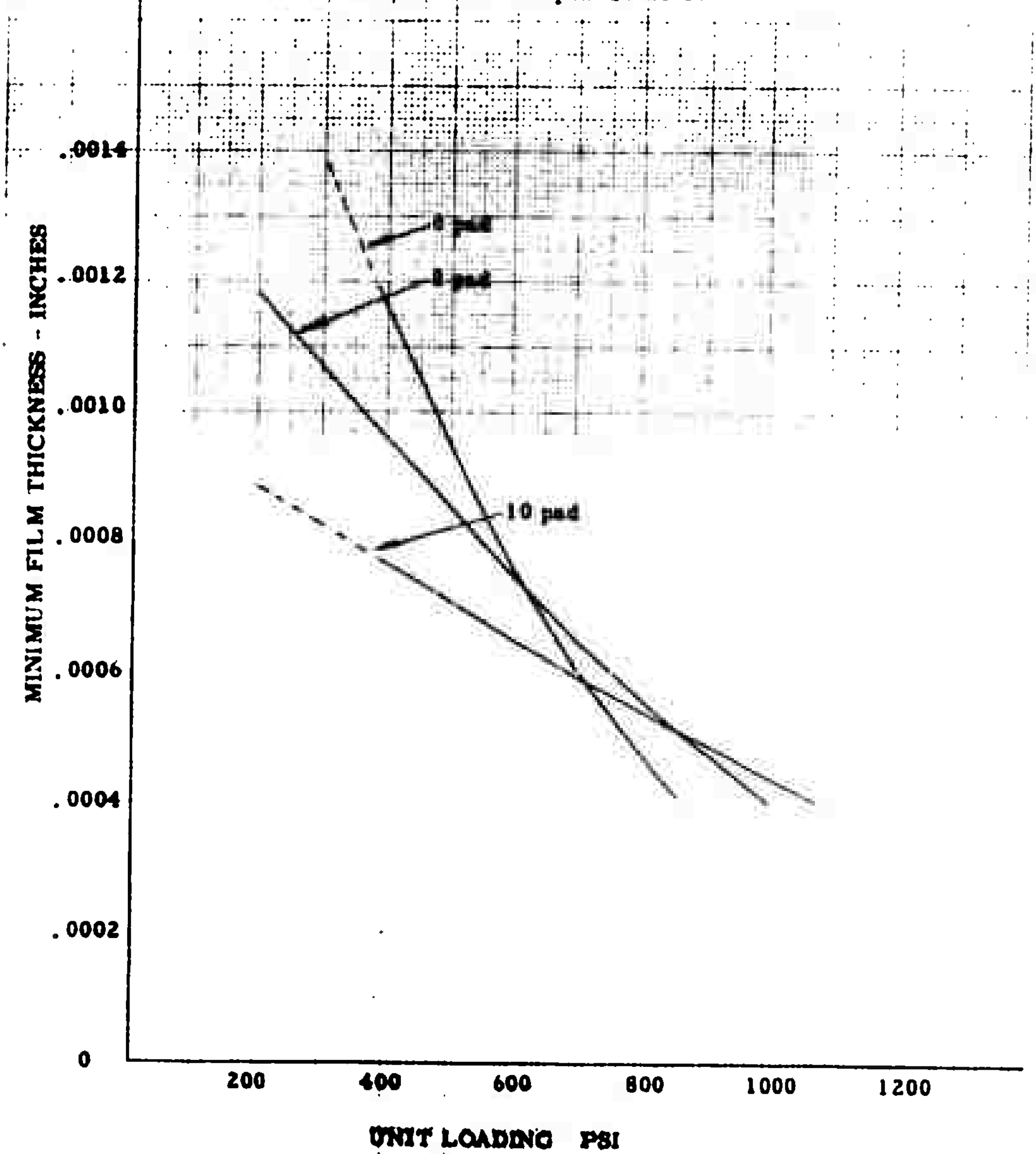

FIGURE 72

MAXIMUM TEMPERATURE VS. UNIT LOADING

31" O.D. x 15-1/2" I.D. Bearing
Speed - 180 RPM

Data per Table 15

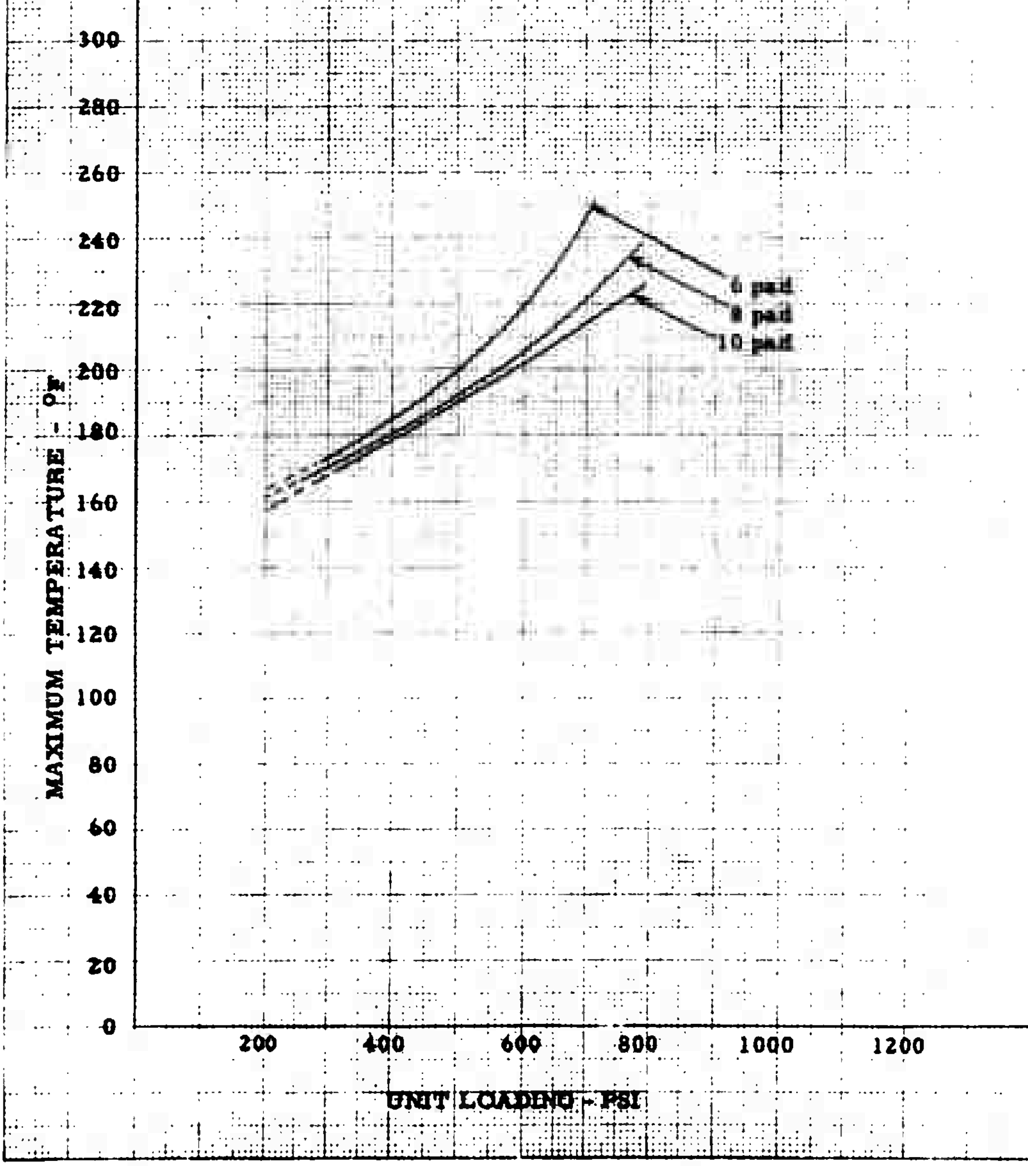

FIGURE 73

MAXIMUM TEMPERATURE VS. UNIT LOADING

31" O.D. x 15-1/2" I.D. Bearing
Speed - 320 RPM

Data per Table 15

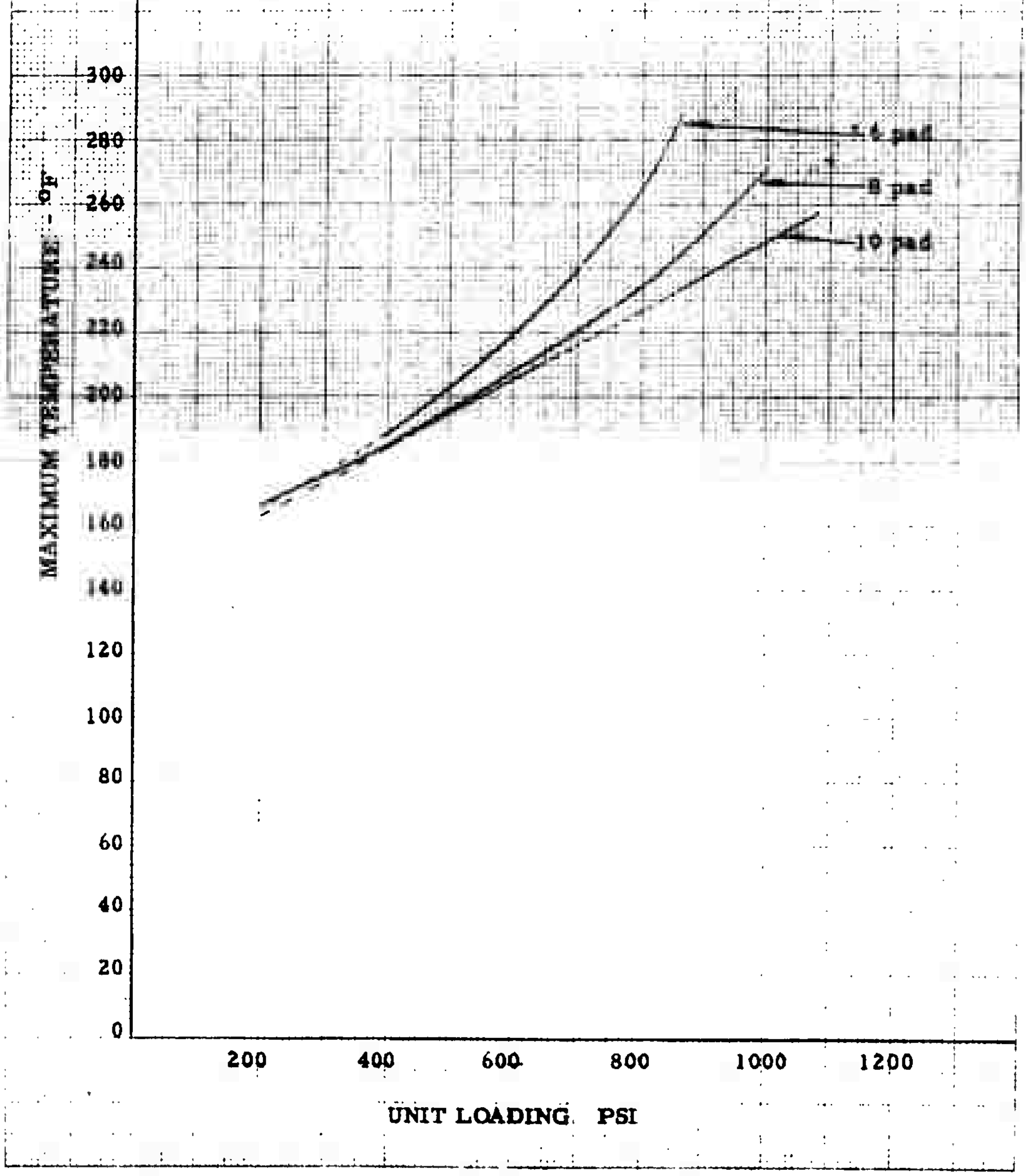

FIGURE 74

HYDRODYNAMIC OIL FLOW VERSUS UNIT LOADING

31" O. D. x 15-1/2" I. D. Bearing
8 Pads

Pad Dimensions and Data per Tables 3, 14 and 15

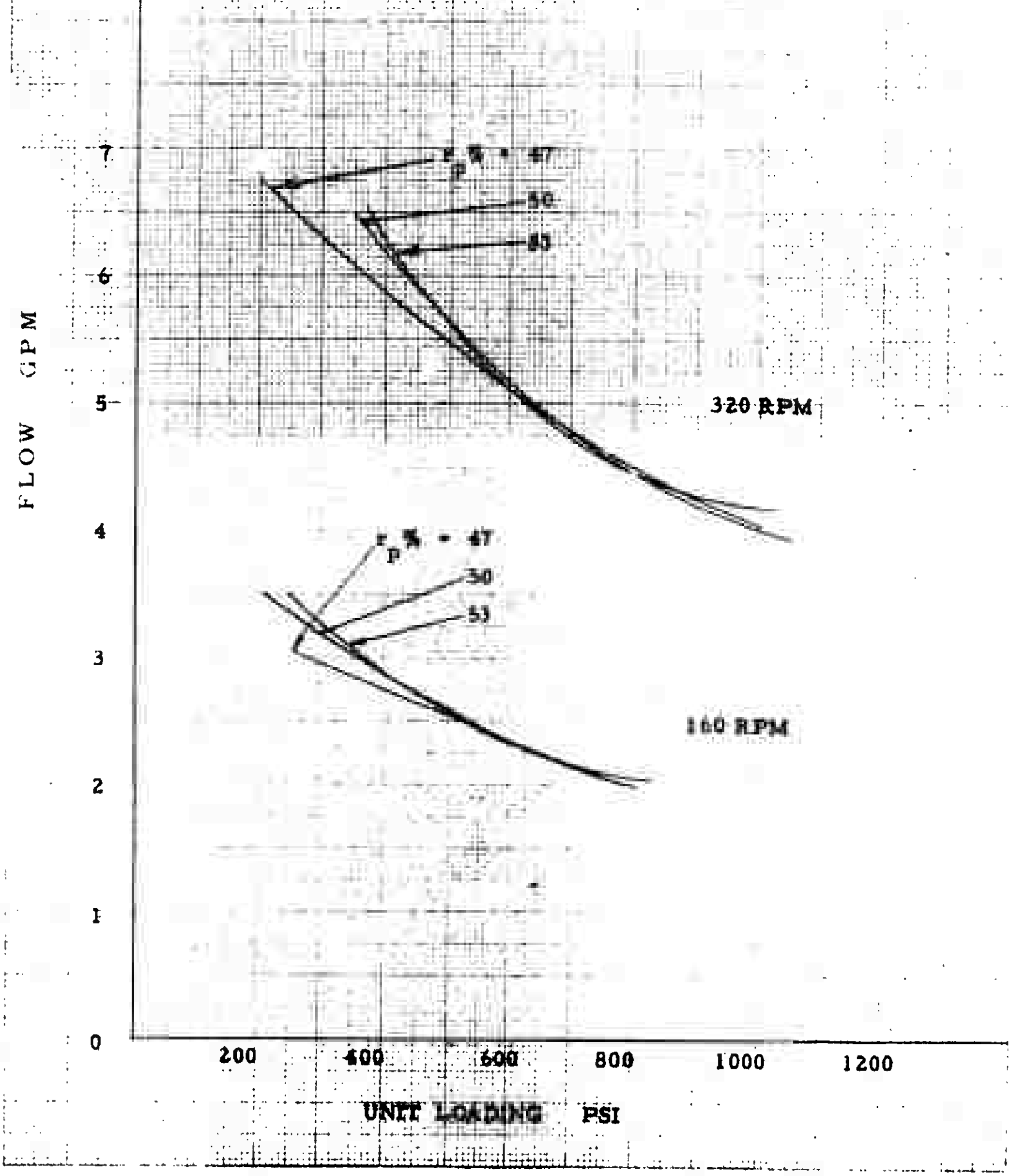

FIGURE 75

MINIMUM FILM THICKNESS VS. UNIT LOADING

31" O.D. x 15-1/2" I.D. Bearing

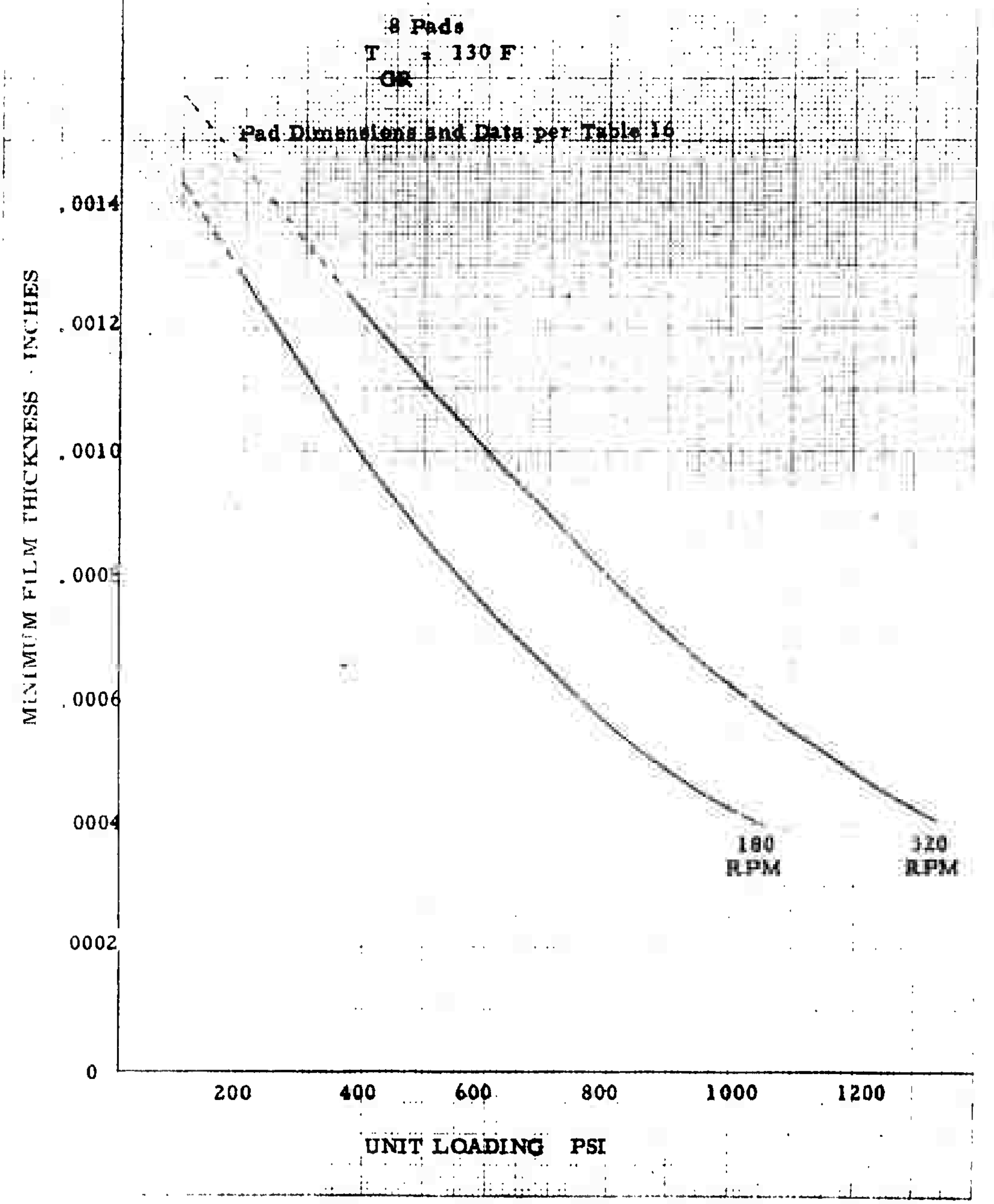

FIGURE 76

MAXIMUM TEMPERATURE VS. UNIT LOADING

31" O.D. x 15-1/2" I.D. Bearing

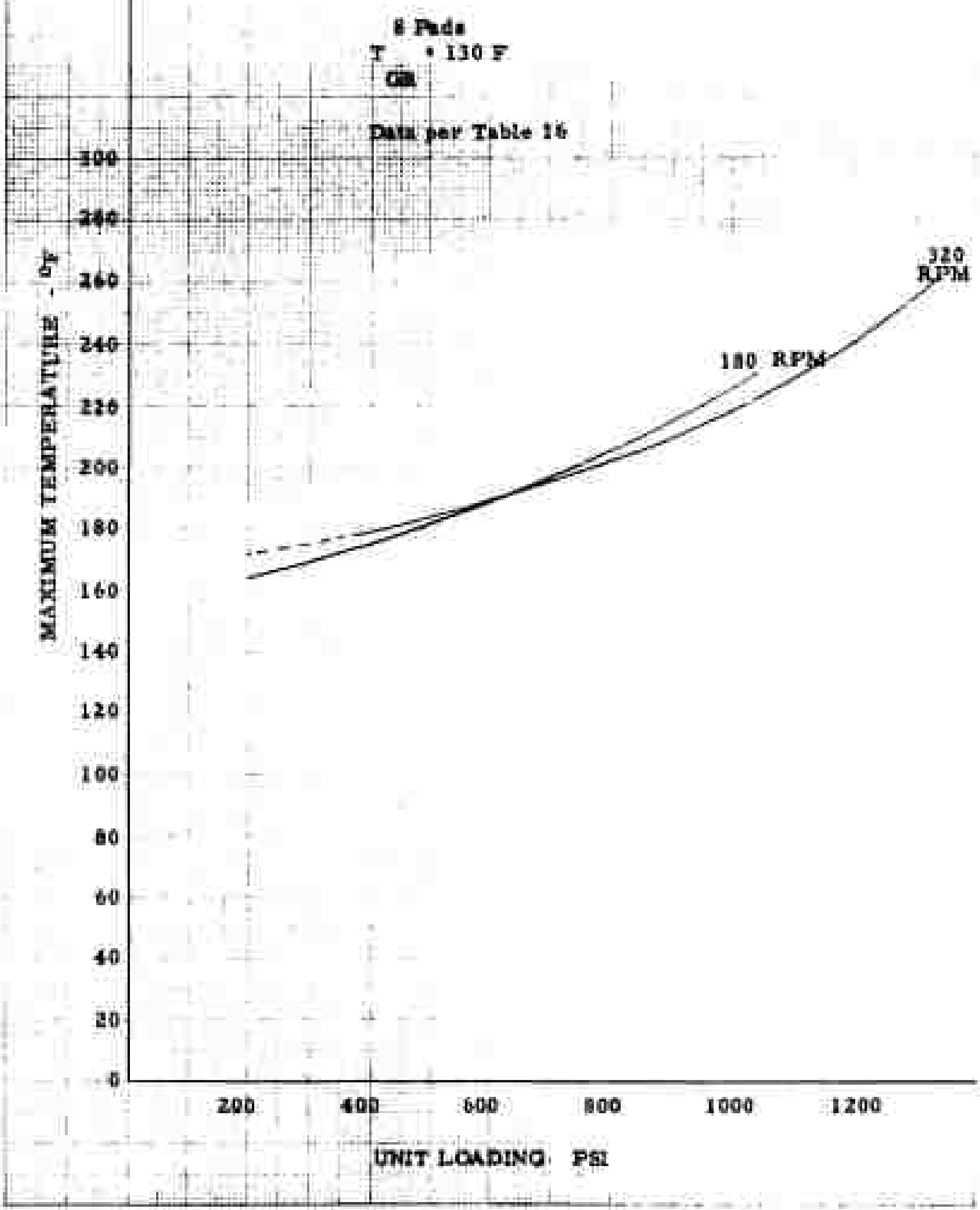

FIGURE 77

HYDRODYNAMIC OIL FLOW VERSUS UNIT LOADING

31" O. D. x 15-1/2" I. D. Bearing

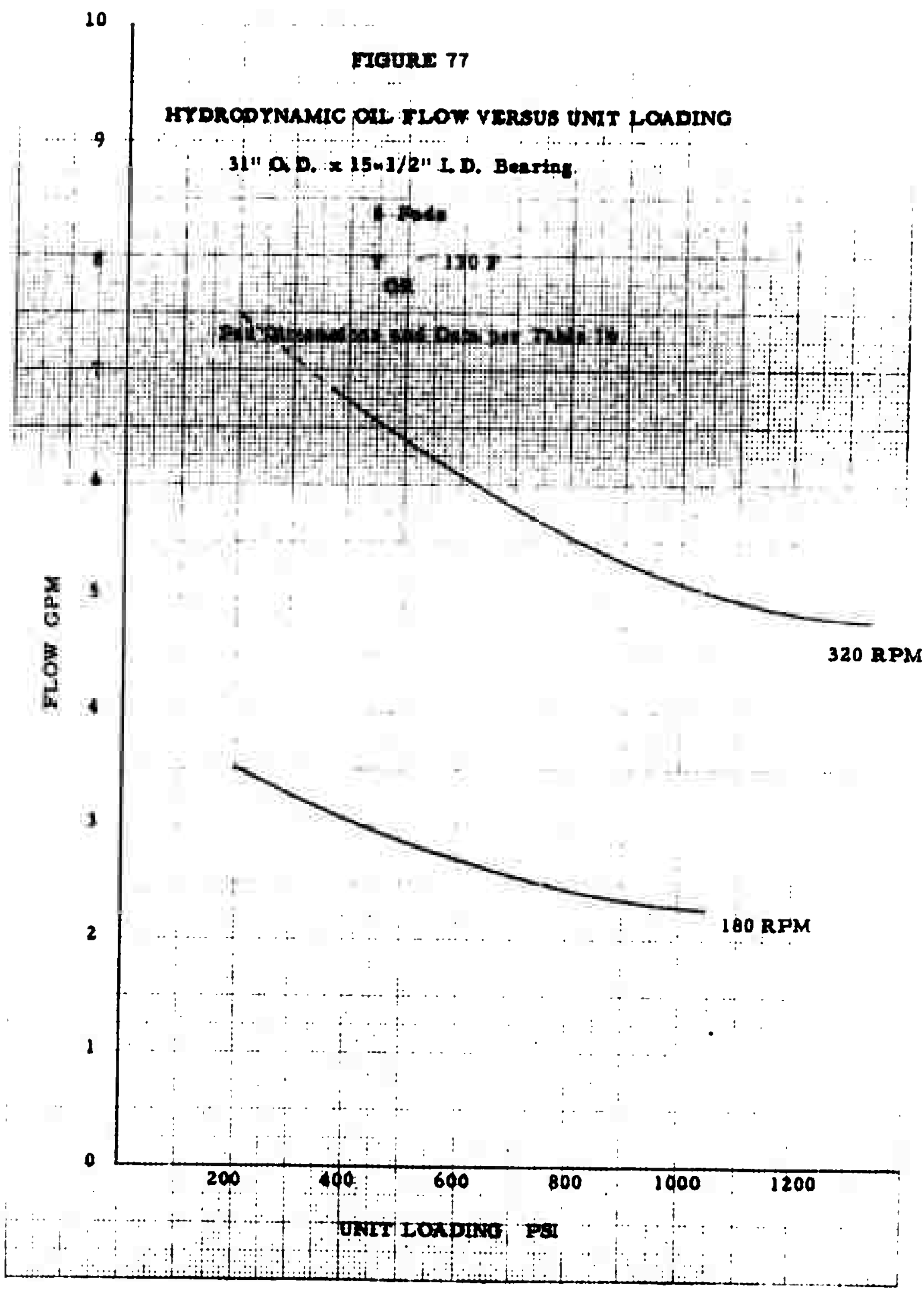

FIGURE 78

MINIMUM FILM THICKNESS VS. UNIT LOADING

39" O. D. x 19-1/2" I. D. Bearing

8 Pads

$T_{GR} = 130$ F

Pad Dimensions and Data per Table 17

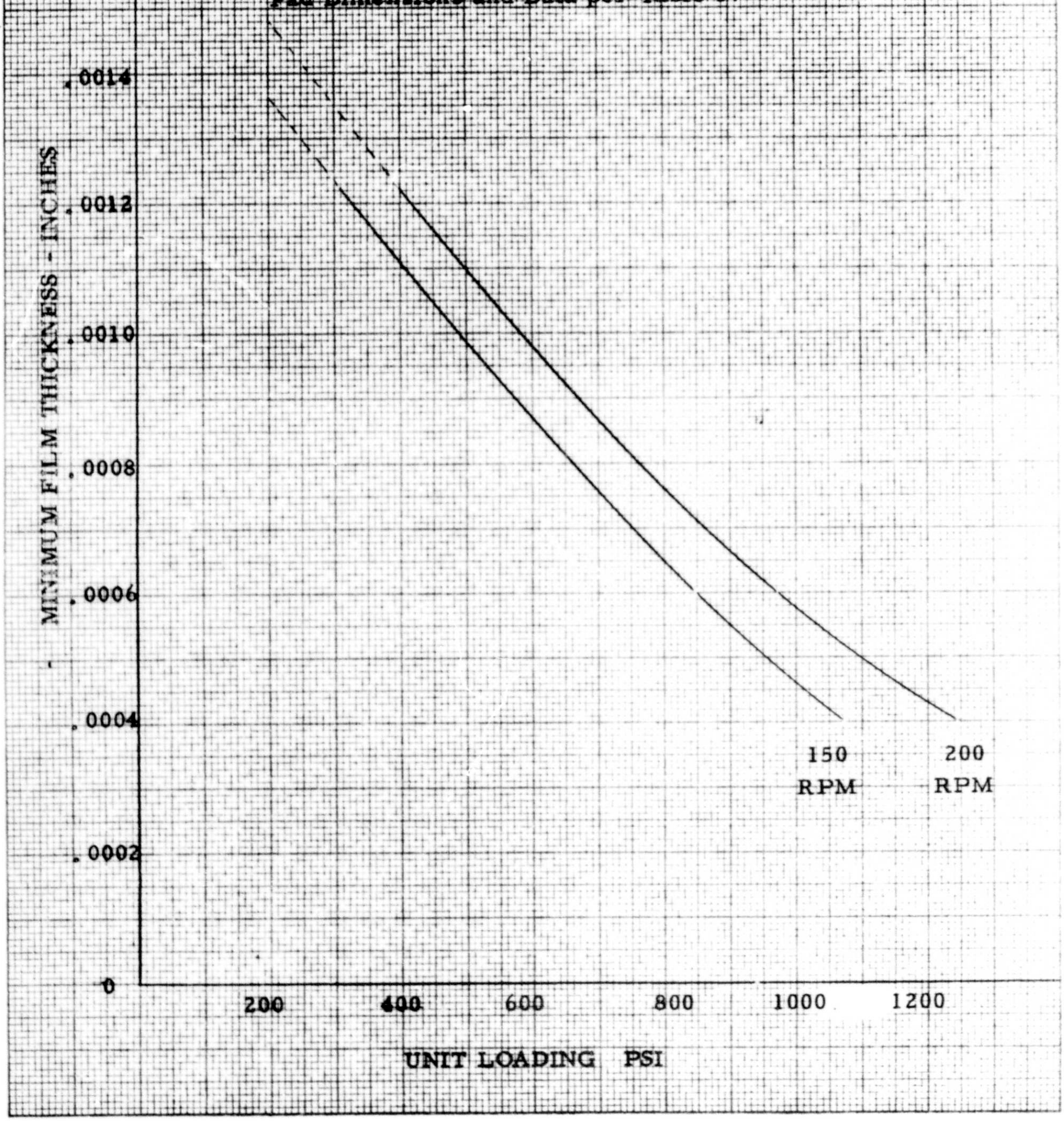

FIGURE 79

MAXIMUM TEMPERATURE VS. UNIT LOADING

39" O. D. x 19-1/2" I. D. Bearing

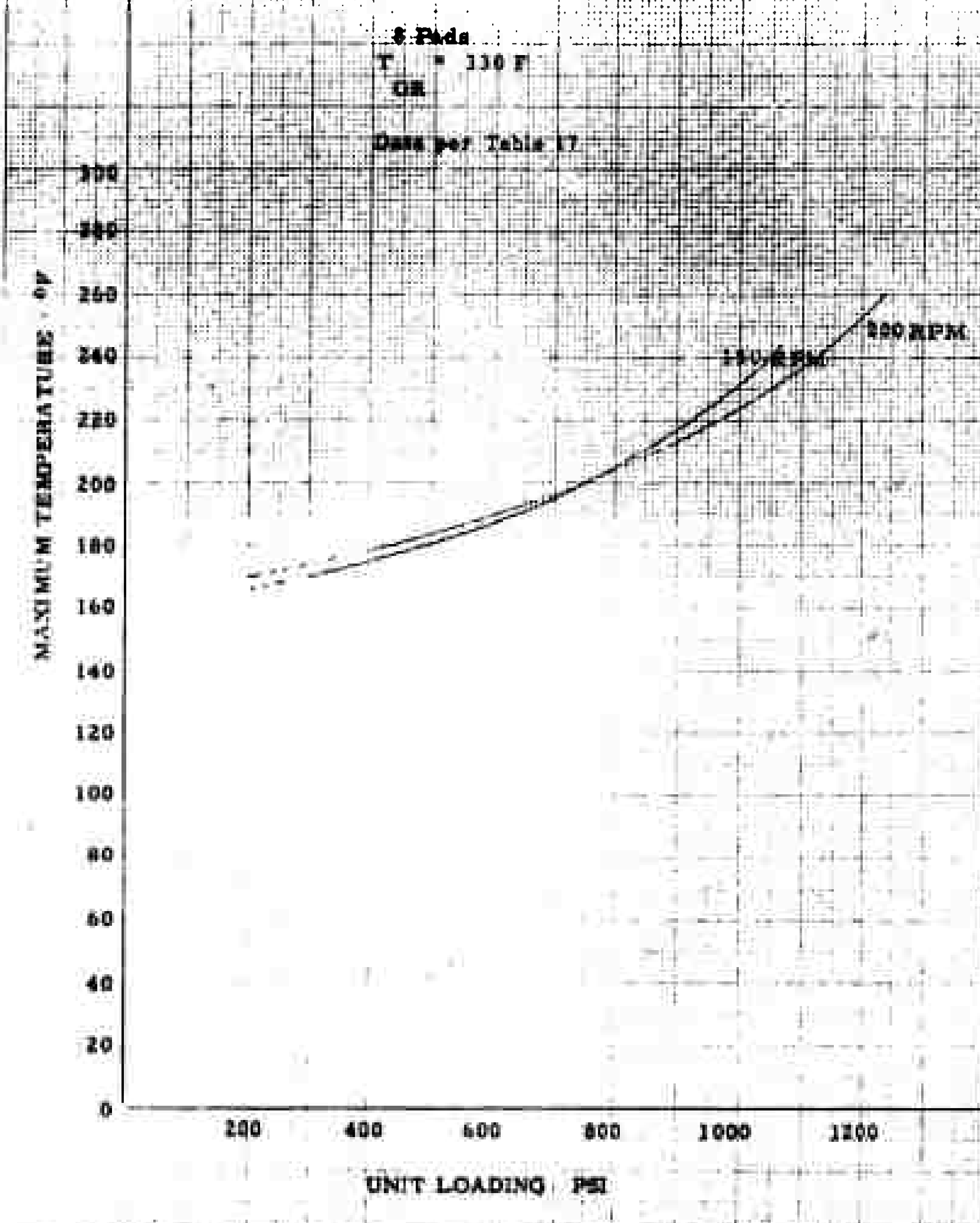

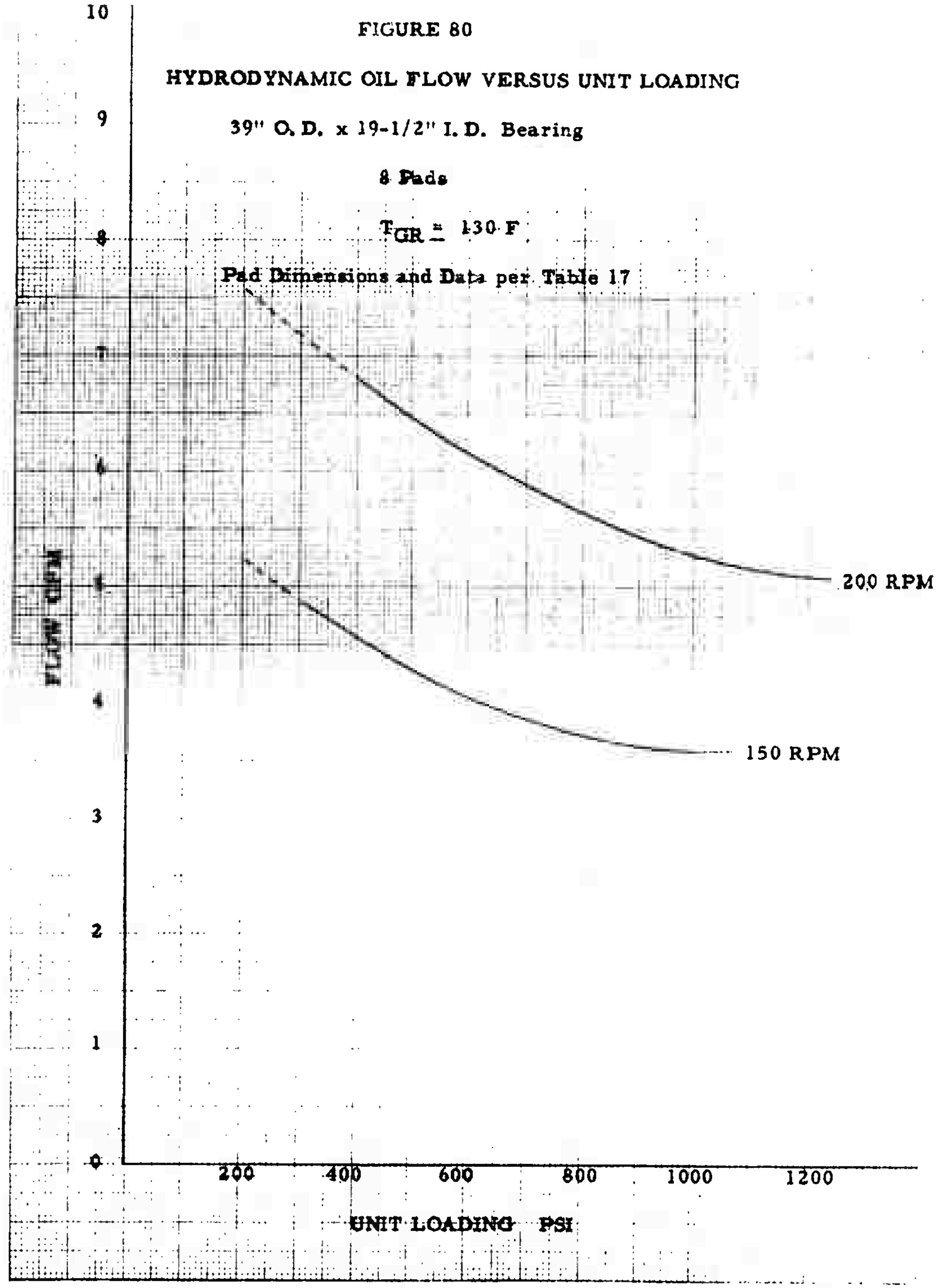
FIGURE 80
HYDRODYNAMIC OIL FLOW VERSUS UNIT LOADING
39" O.D. x 19-1/2" I.D. Bearing
8 Pads
T_{GR} = 130 F
Pad Dimensions and Data per Table 17
200 RPM
150 RPM
FLOW GPM
UNIT LOADING PSI
0
1
2
3
4
5
6
7
8
9
10
200
400
600
800
1000
1200

FIGURE 81

UNIT LOADING VS. BEARING SIZE

Speed - 100 RPM t_{avg} - 0.154 Θ_T - 51^0 $r_{P\%}$ - 50

Data per tables 6, 7, 8, 18, 19 and 20

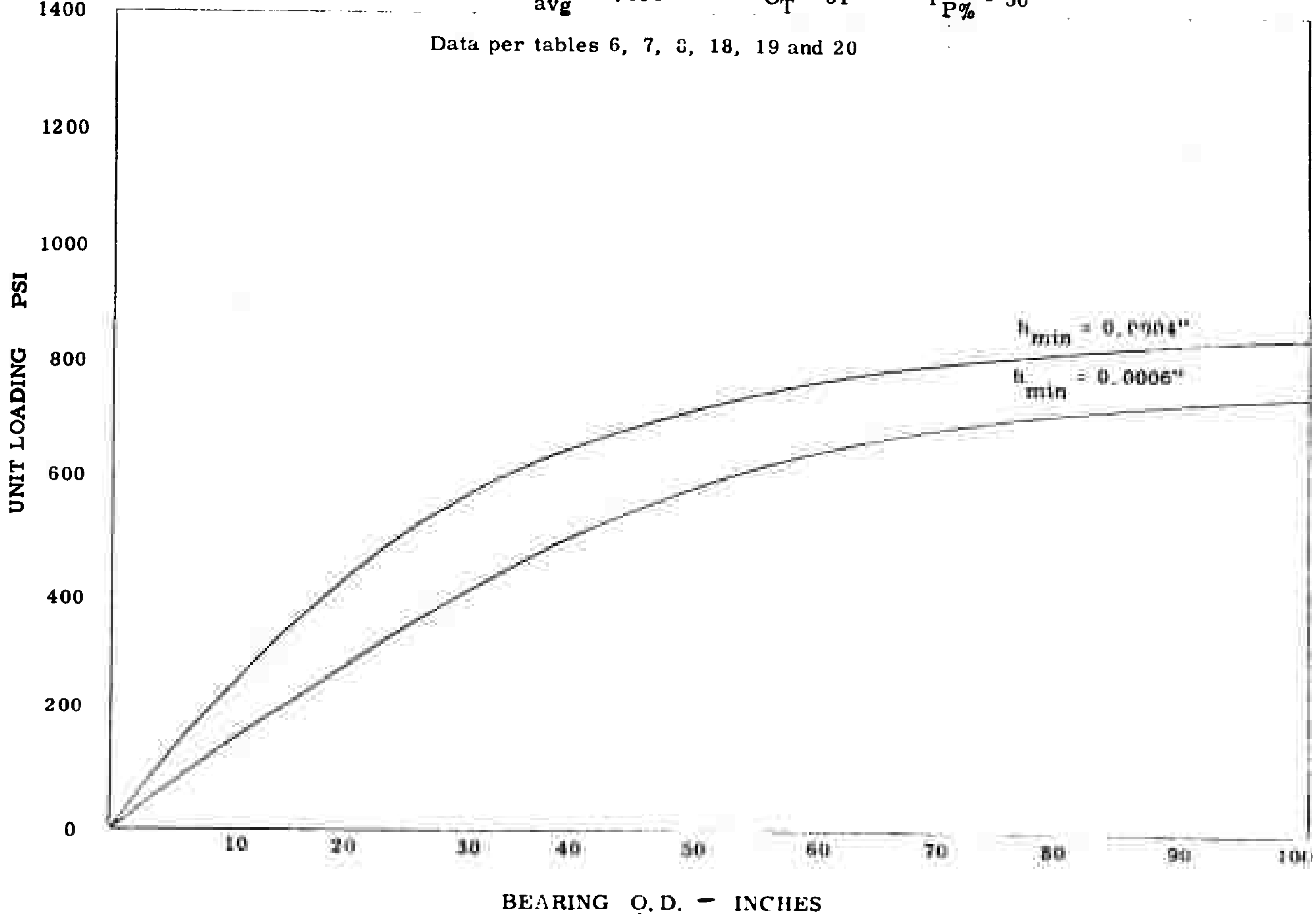

FIGURE 82

MINIMUM FILM THICKNESS VS. UNIT LOADING

51-1/2" O. D x 32" I. D. Bearing
Speed - 200 RPM

Pad Dimensions and Data per Table 22

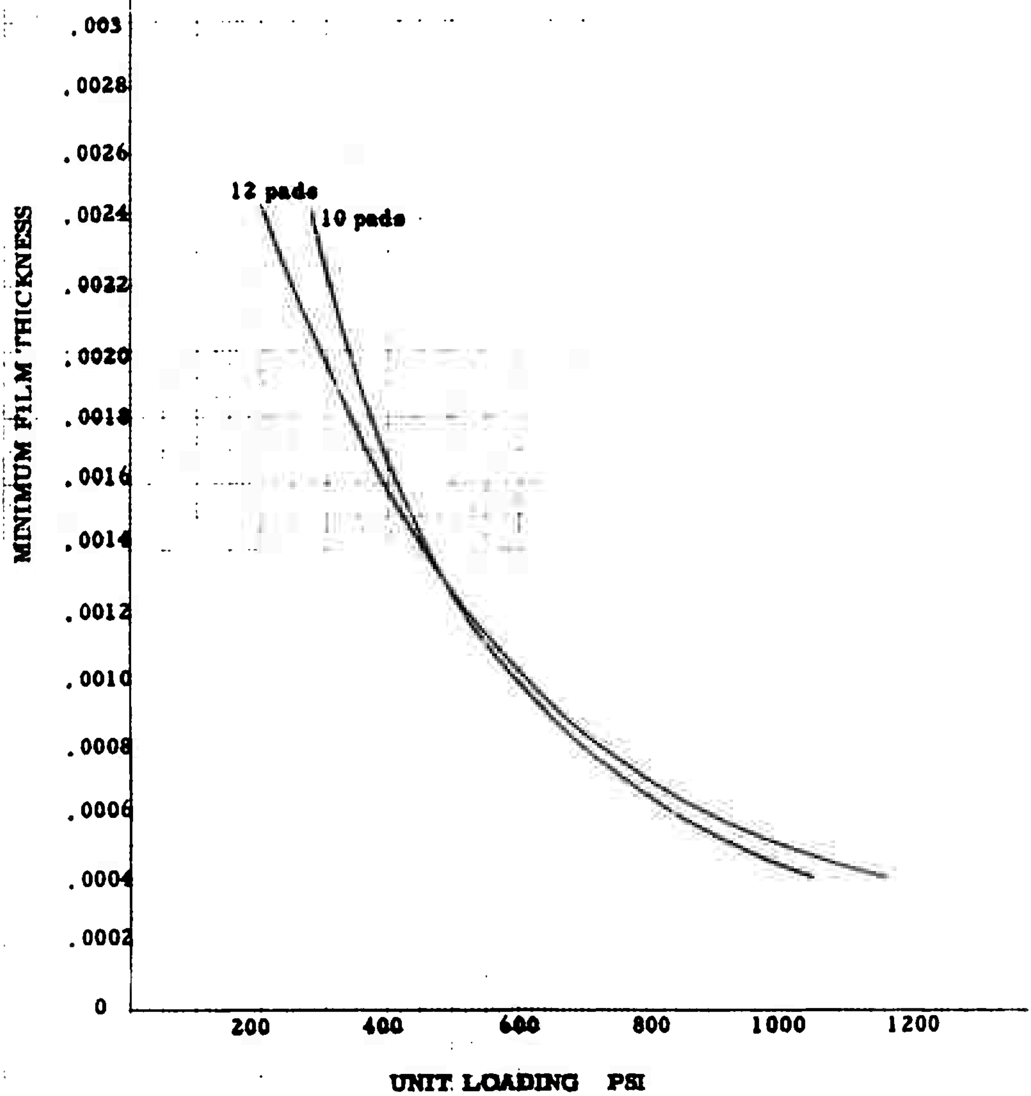

FIGURE 83

MAXIMUM TEMPERATURE VS. UNIT LOADING

51-1/2" O.D. x 32" I.D. Bearing
Speed - 200 RPM

Data per Table 22

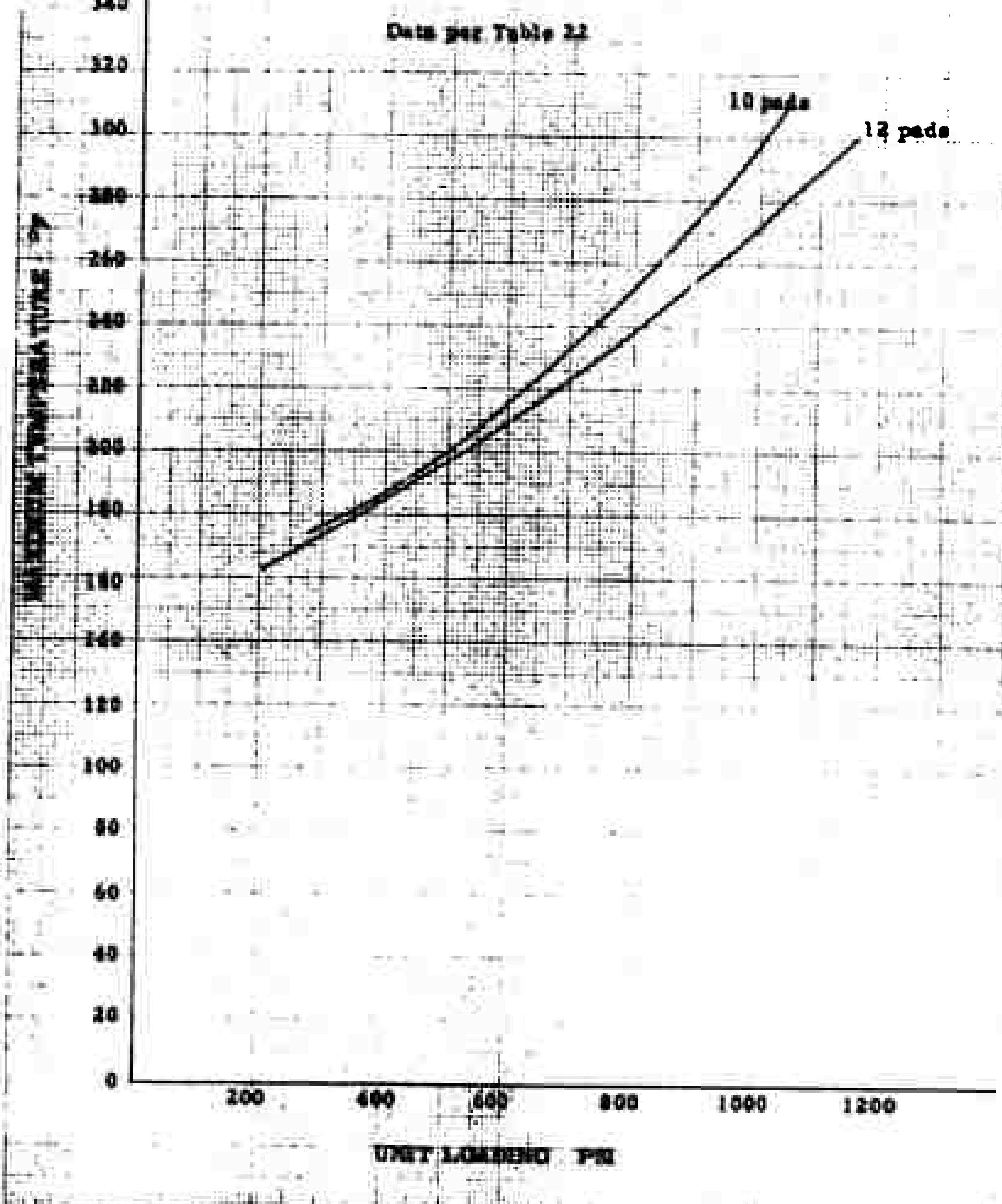

FIGURE 84

MINIMUM FILM THICKNESS VS. UNIT LOADING

51-1/2" O.D. x 32" I.D. Bearing
Speed - 400 RPM

Pad Dimensions and Data per Table 22

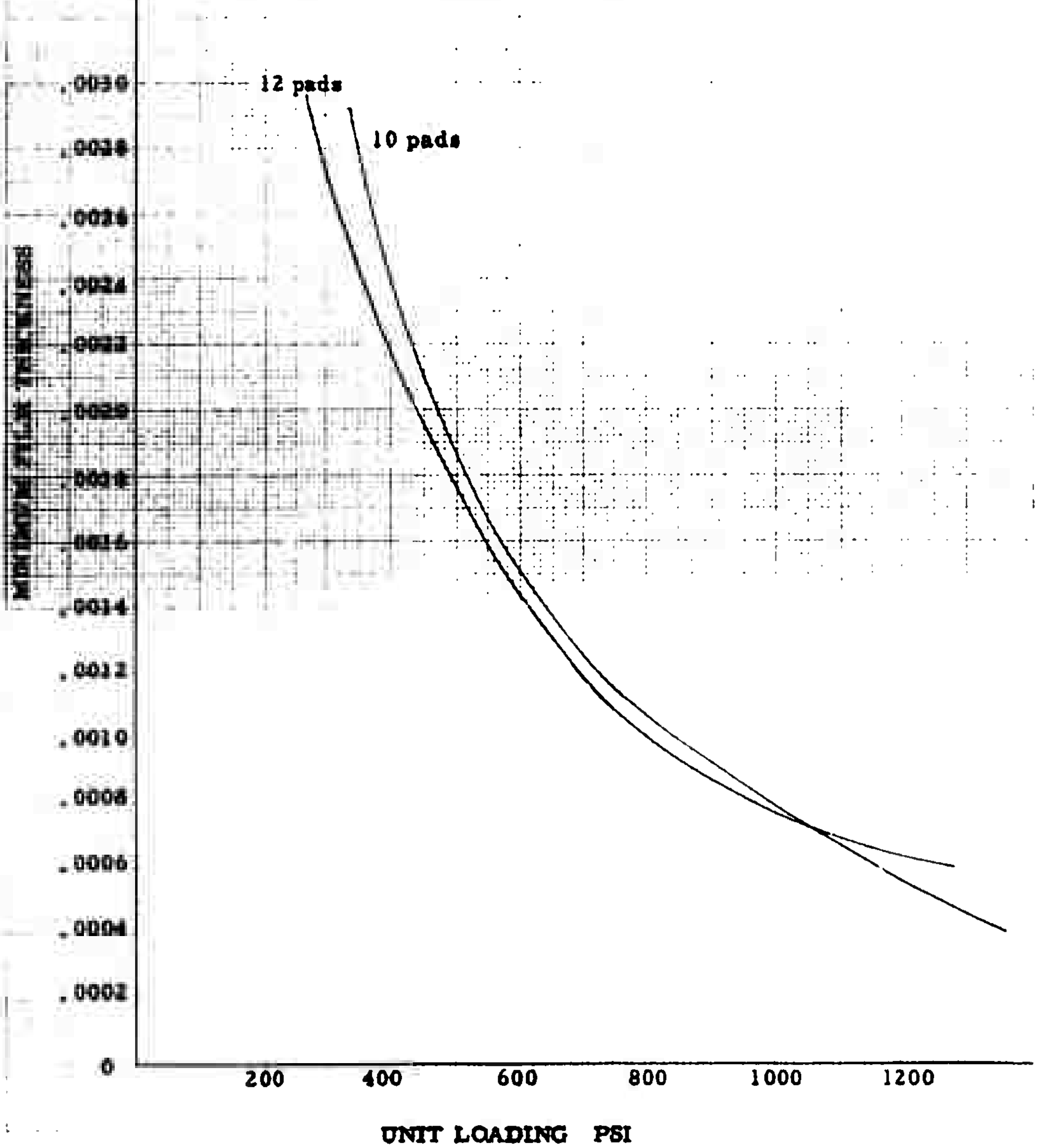

FIGURE 85

MAXIMUM TEMPERATURE VS. UNIT LOADING

51-1/2" O. D. x 32" I. D. Bearing
Speed - 400 RPM

Data per Table 22

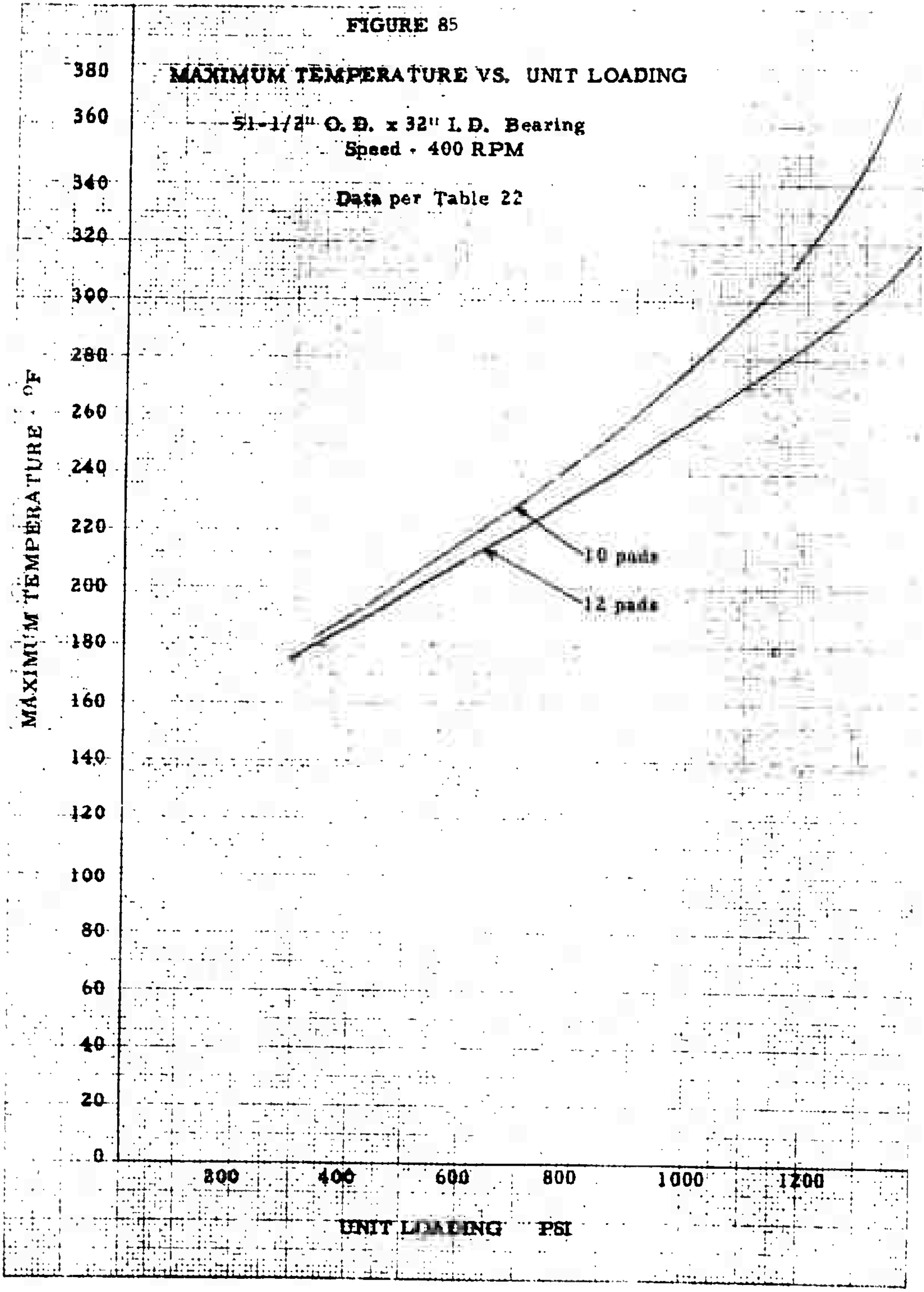

FIGURE 86

HYDRODYNAMIC OIL FLOW VERSUS UNIT LOADING

51-1/2" O. D. x 32" I. D. Bearing
10 Pads

Pad Dimensions and Data per Table 22

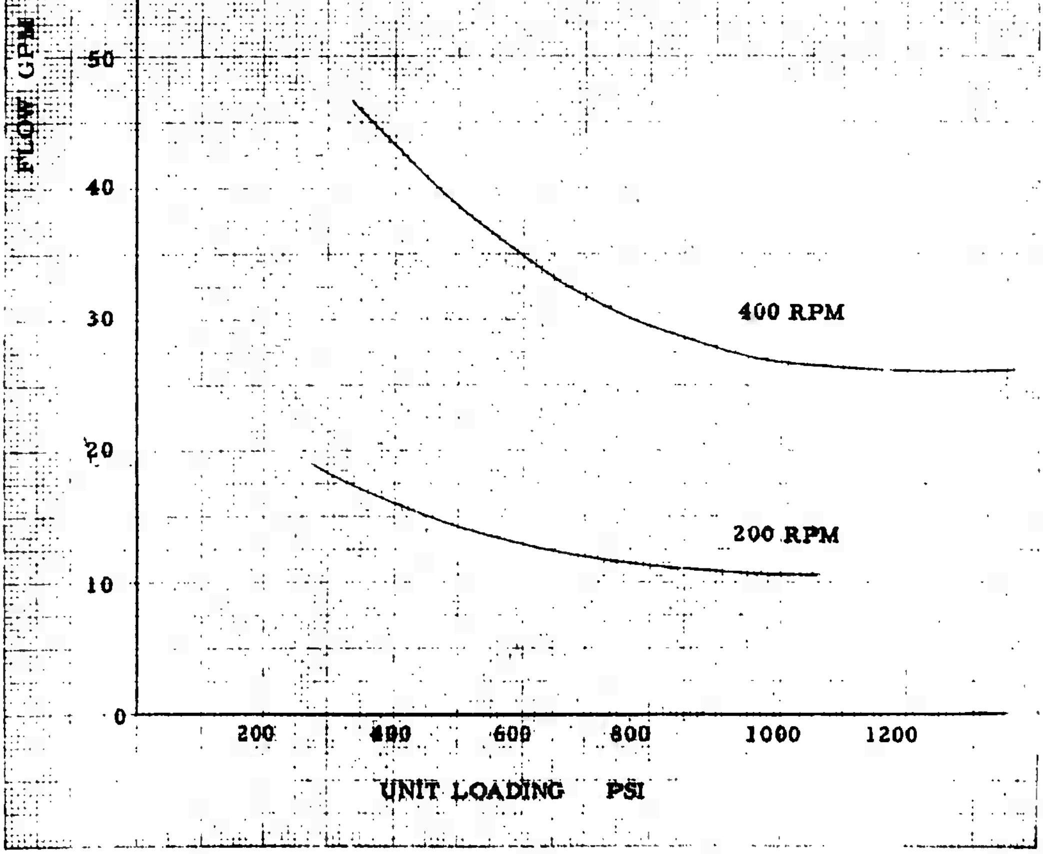

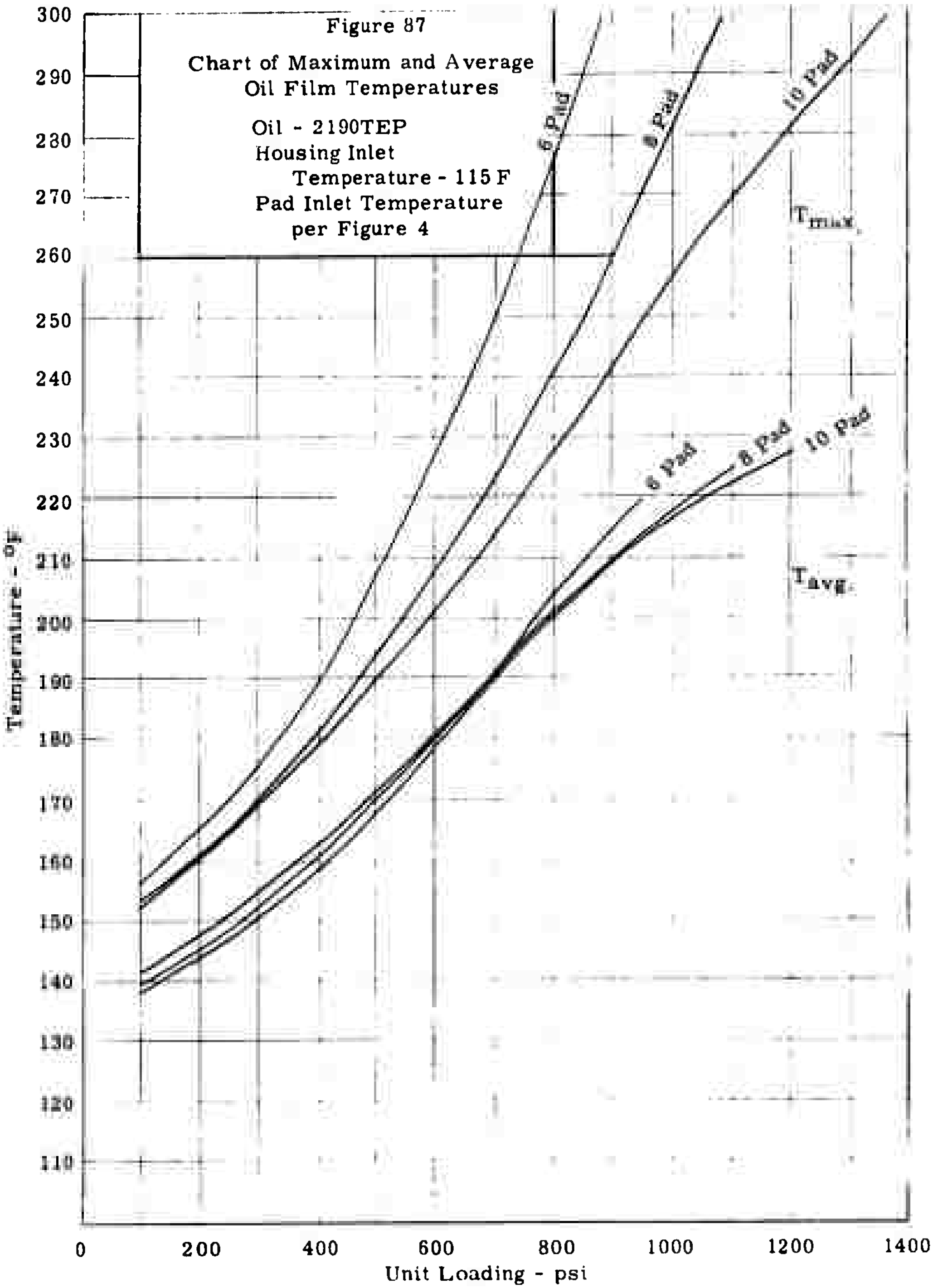
Figure 87
Chart of Maximum and Average
Oil Film Temperatures
Oil - 2190TEP
Housing Inlet
Temperature - 115 F
Pad Inlet Temperature
per Figure 4
6 Pad
8 Pad
10 Pad
Tmax
6 Pad
8 Pad
10 Pad
Tavg
Temperature - °F
300
290
280
270
260
250
240
230
220
210
200
190
180
170
160
150
140
130
120
110
0
200
400
600
800
1000
1200
1400
Unit Loading - psi

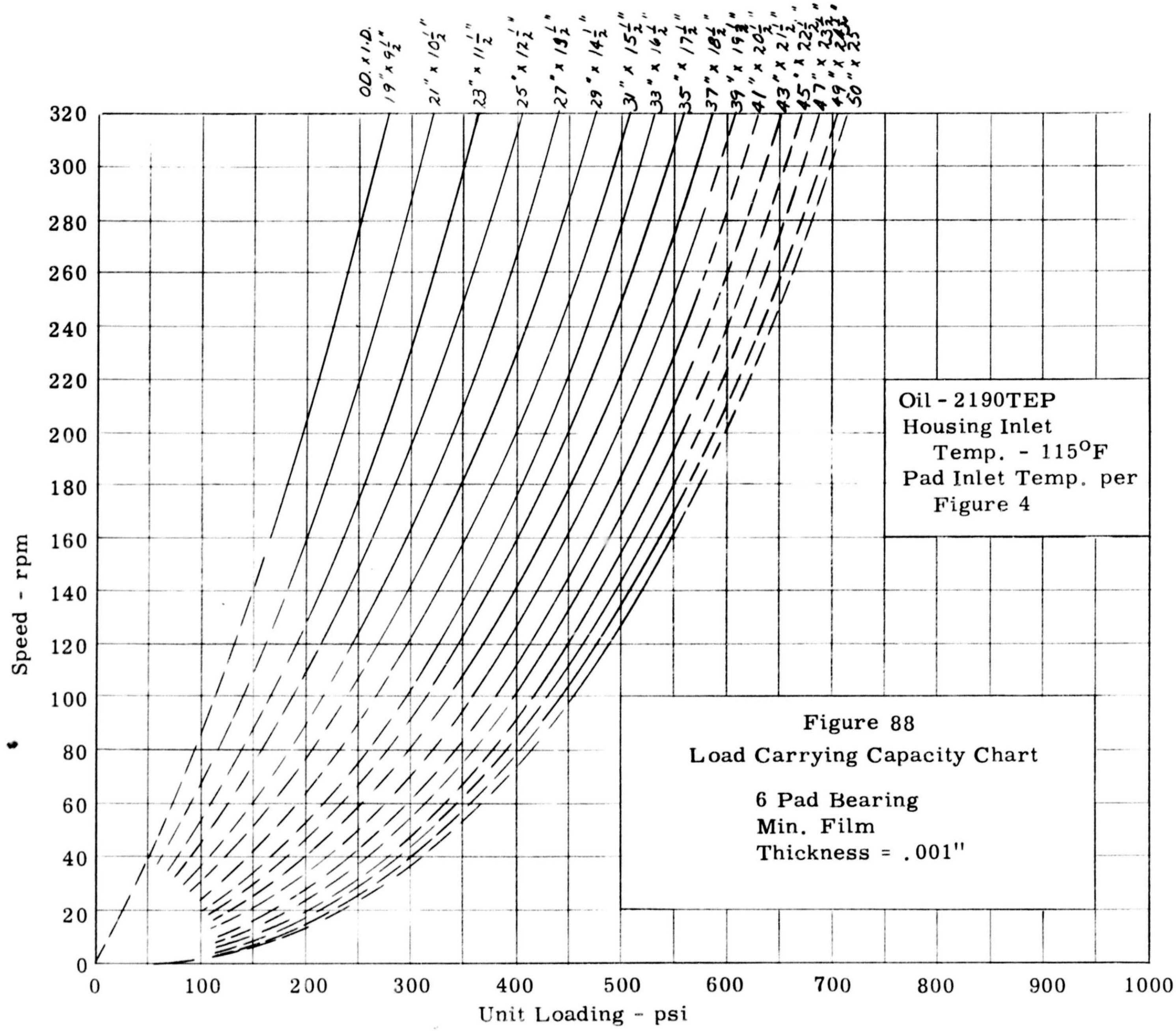

Figure 88
Load Carrying Capacity Chart

6 Pad Bearing
Min. Film
Thickness = .001"

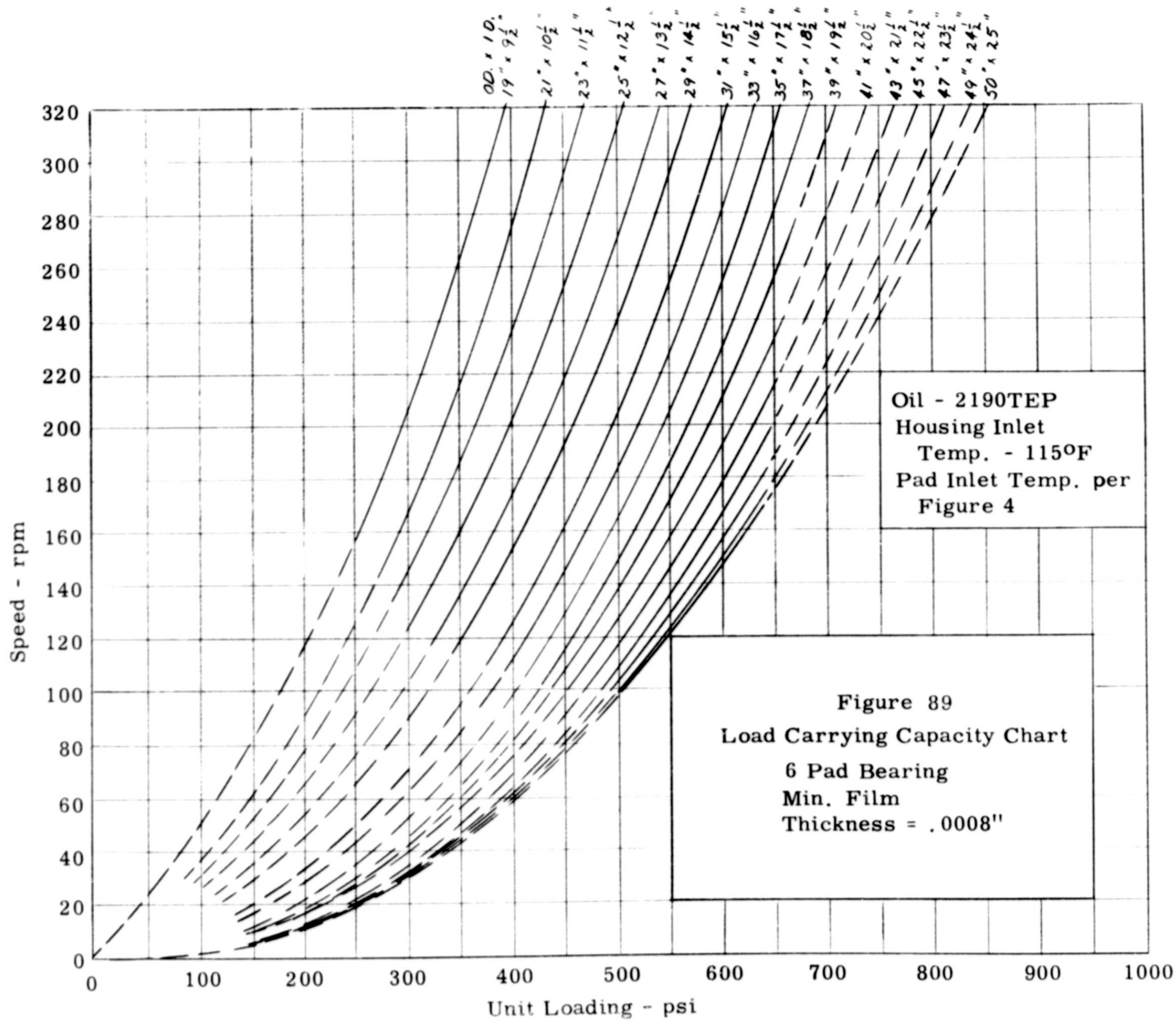

Figure 89
Load Carrying Capacity Chart
6 Pad Bearing
Min. Film
Thickness = .0008"

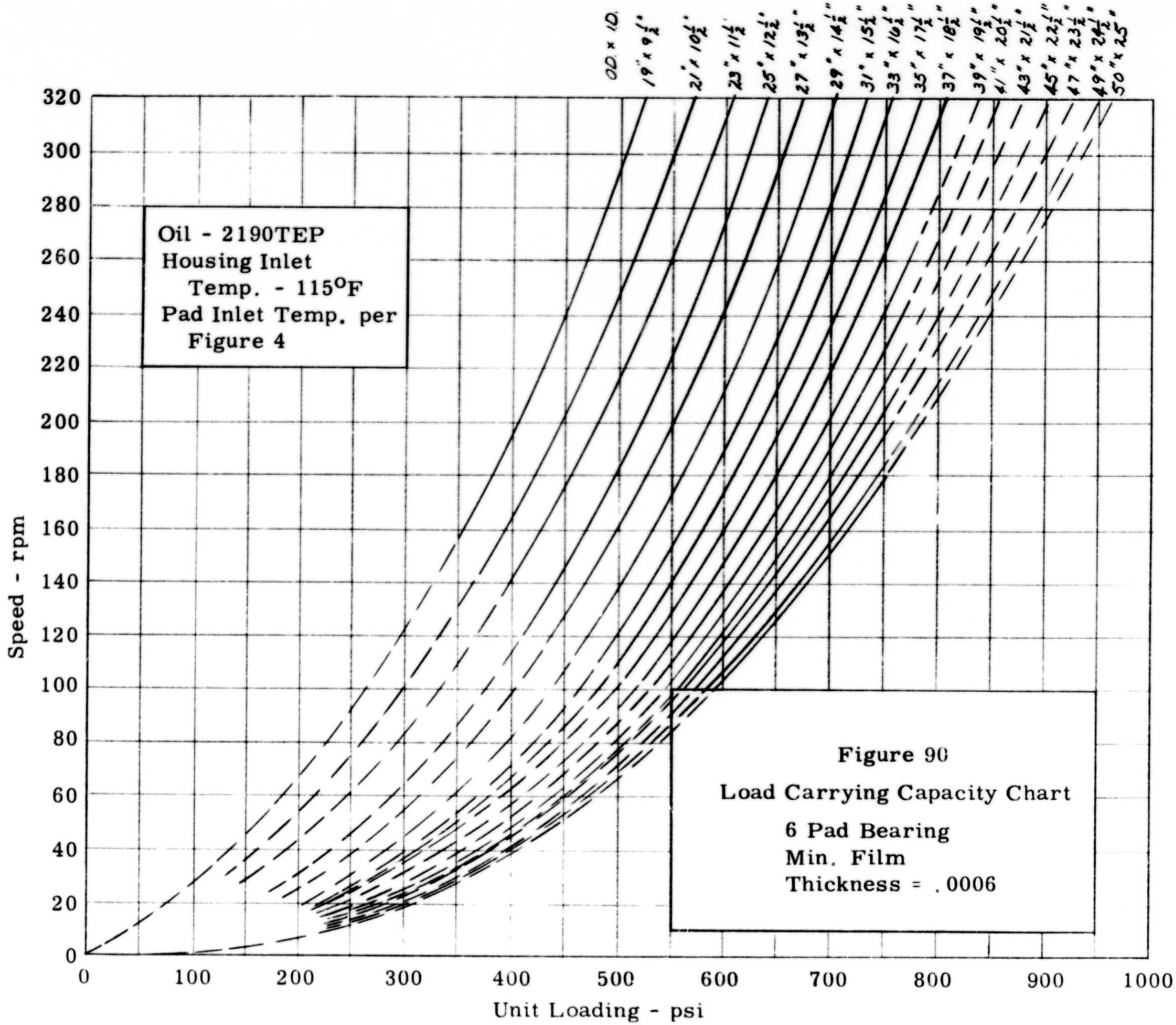

Figure 90

Load Carrying Capacity Chart

6 Pad Bearing

Min. Film

Thickness = .0006

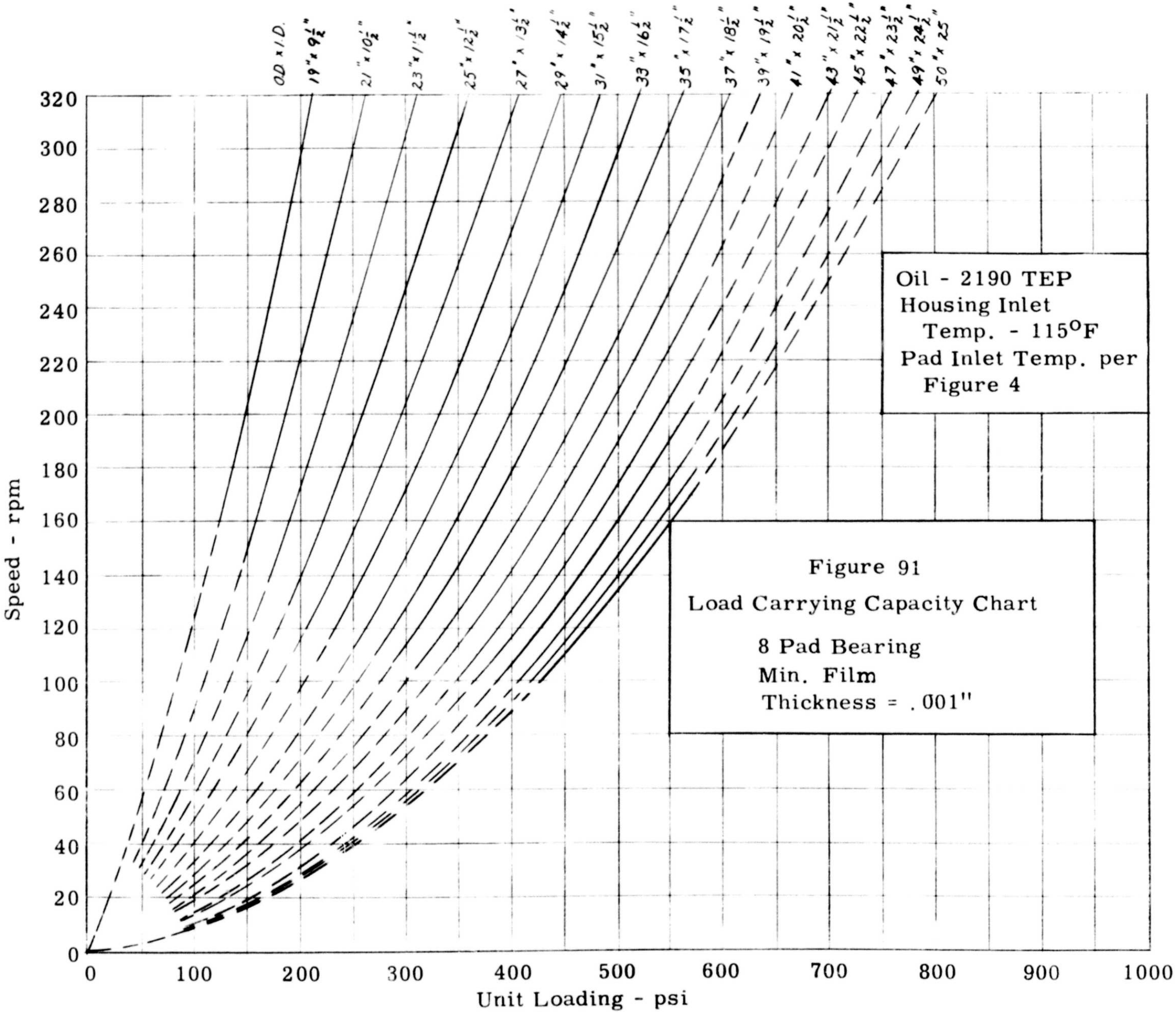

Figure 91

Load Carrying Capacity Chart

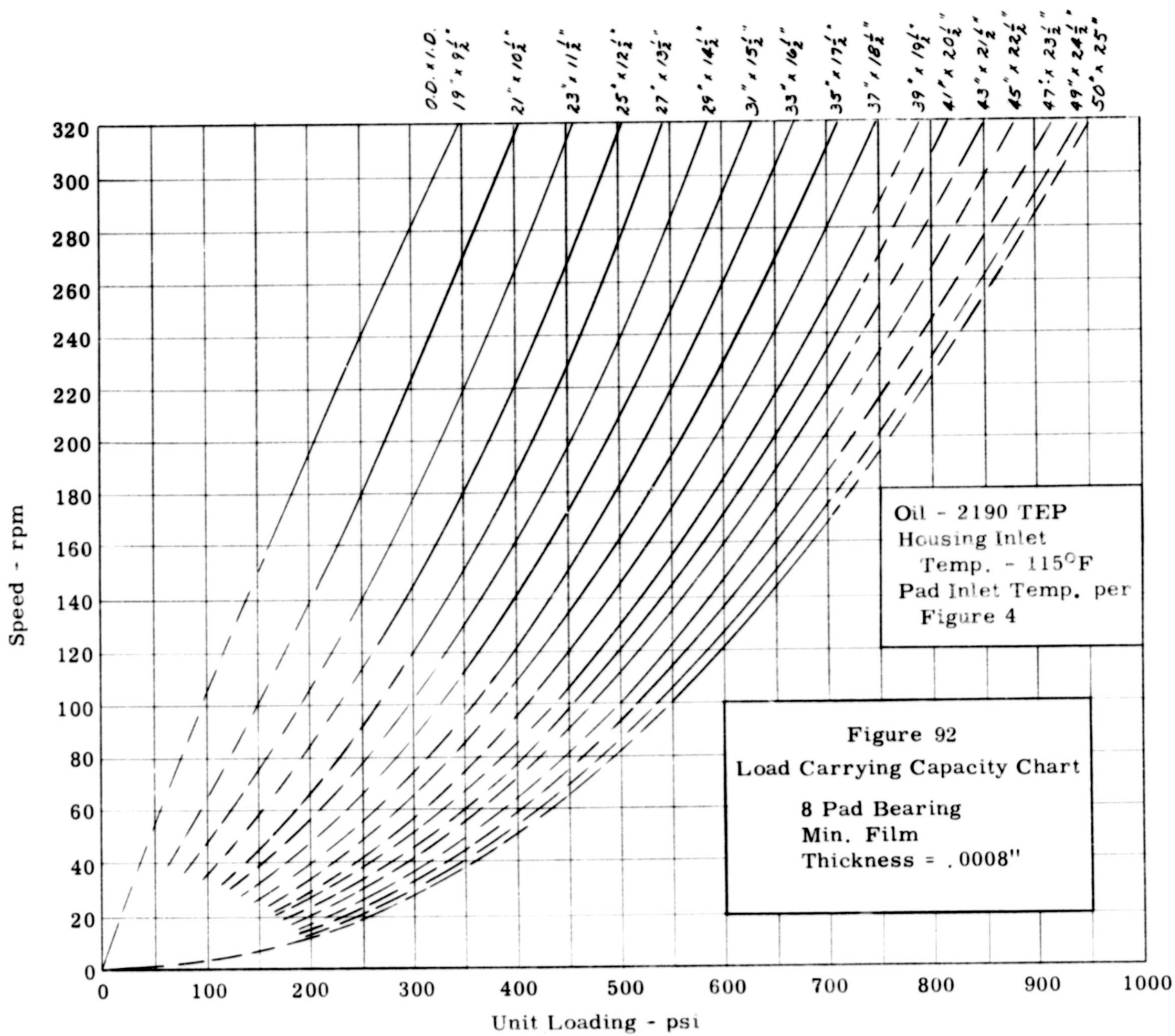

Figure 92
Load Carrying Capacity Chart

8 Pad Bearing
Min. Film
Thickness = .0008"

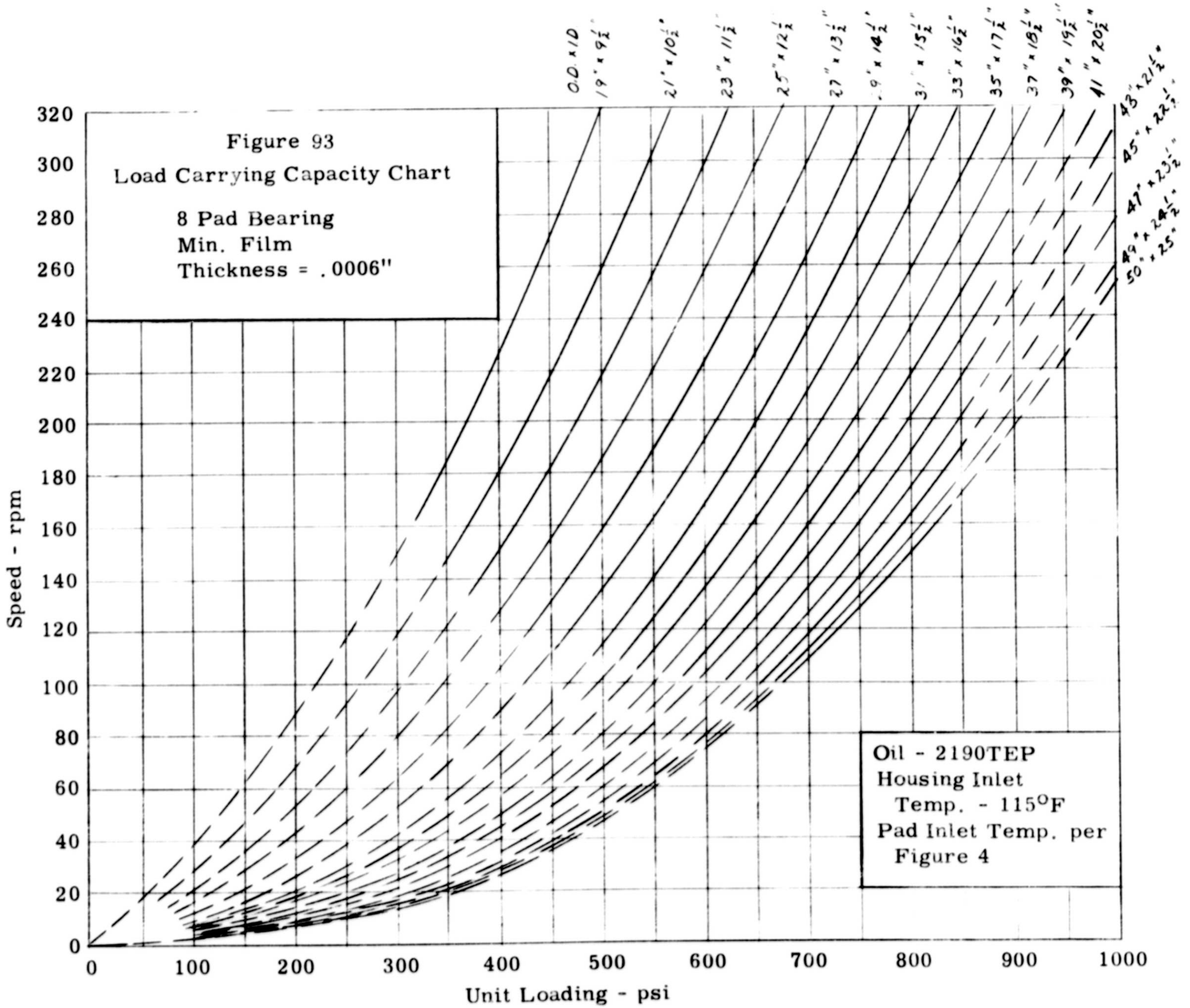
Figure 93
Load Carrying Capacity Chart
8 Pad Bearing
Min. Film
Thickness = .0006"
Oil - 2190TEP
Housing Inlet
Temp. - 115°F
Pad Inlet Temp. per
Figure 4
Speed - rpm
Unit Loading - psi
0
100
200
300
400
500
600
700
800
900
1000
20
40
60
80
100
120
140
160
180
200
220
240
260
280
300
320
O.D. x I.D
19" x 9½"
21" x 10½"
23" x 11½"
25" x 12½"
27" x 13½"
35" x 17½"
37" x 18½"
39" x 19½"
43" x 21½"
45" x 22½"
47" x 23½"
49" x 24½"
50" x 25"

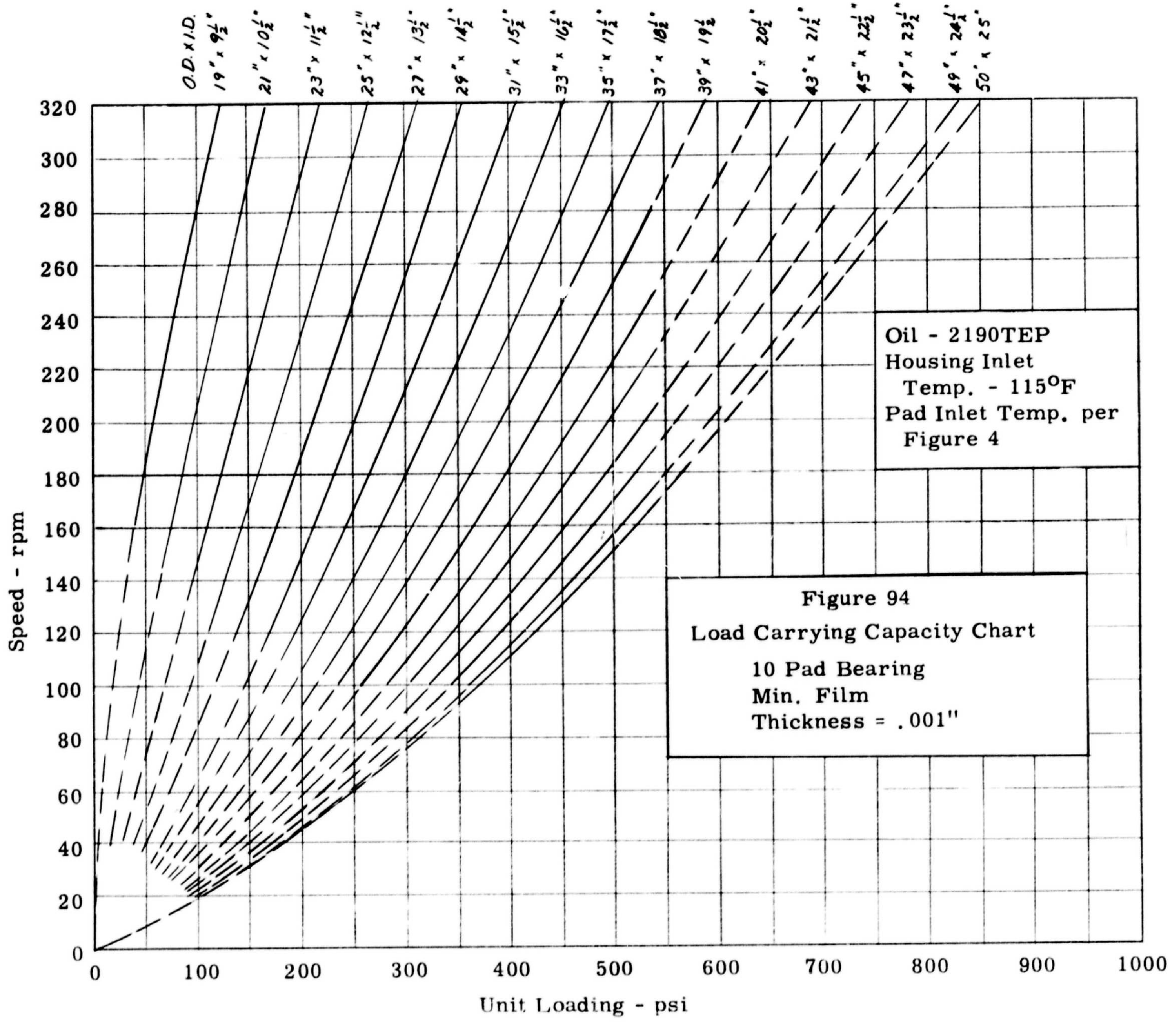

Figure 94
Load Carrying Capacity Chart
10 Pad Bearing
Min. Film
Thickness = .001"

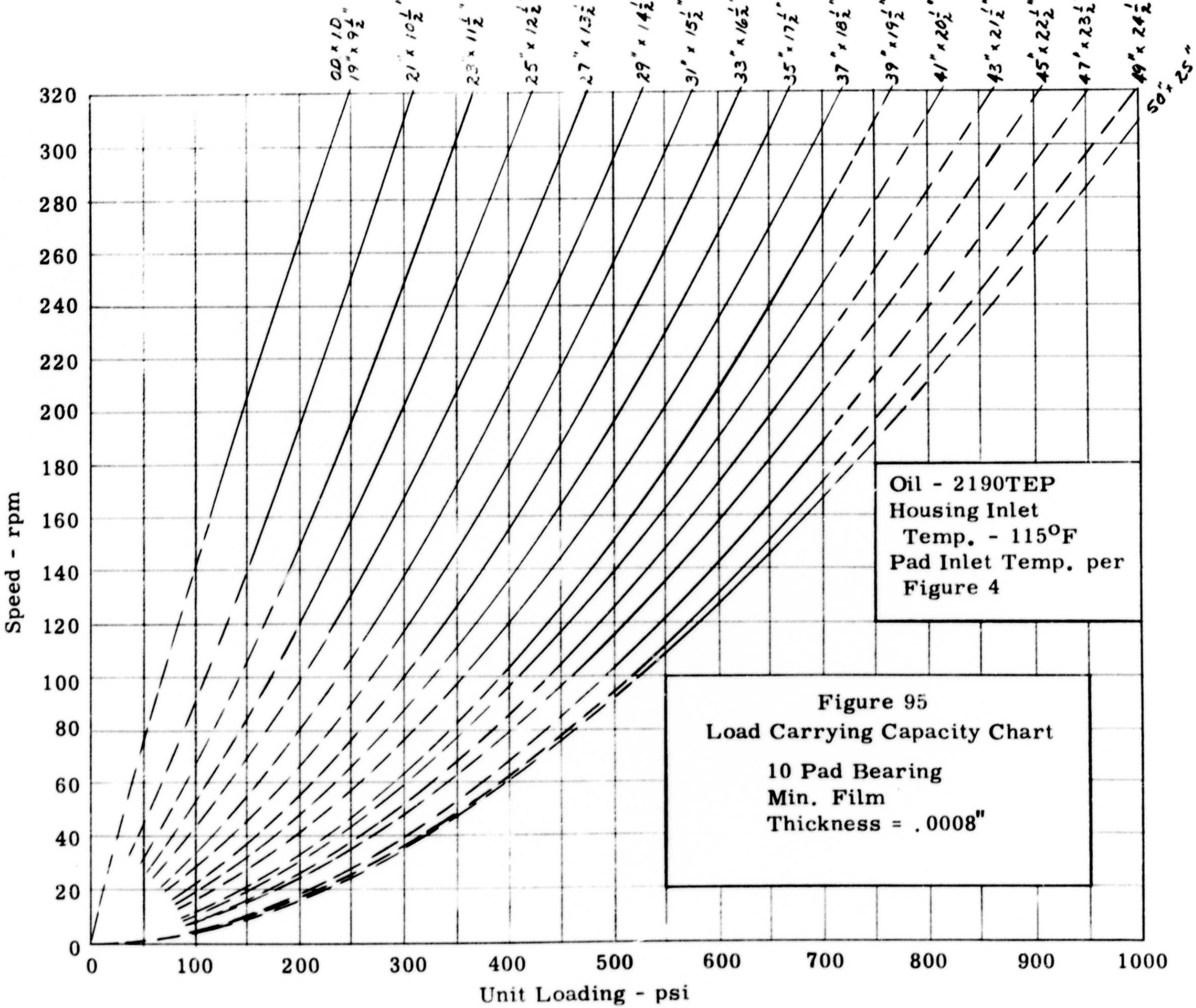

Figure 95
Load Carrying Capacity Chart

10 Pad Bearing
Min. Film
Thickness = .0008"

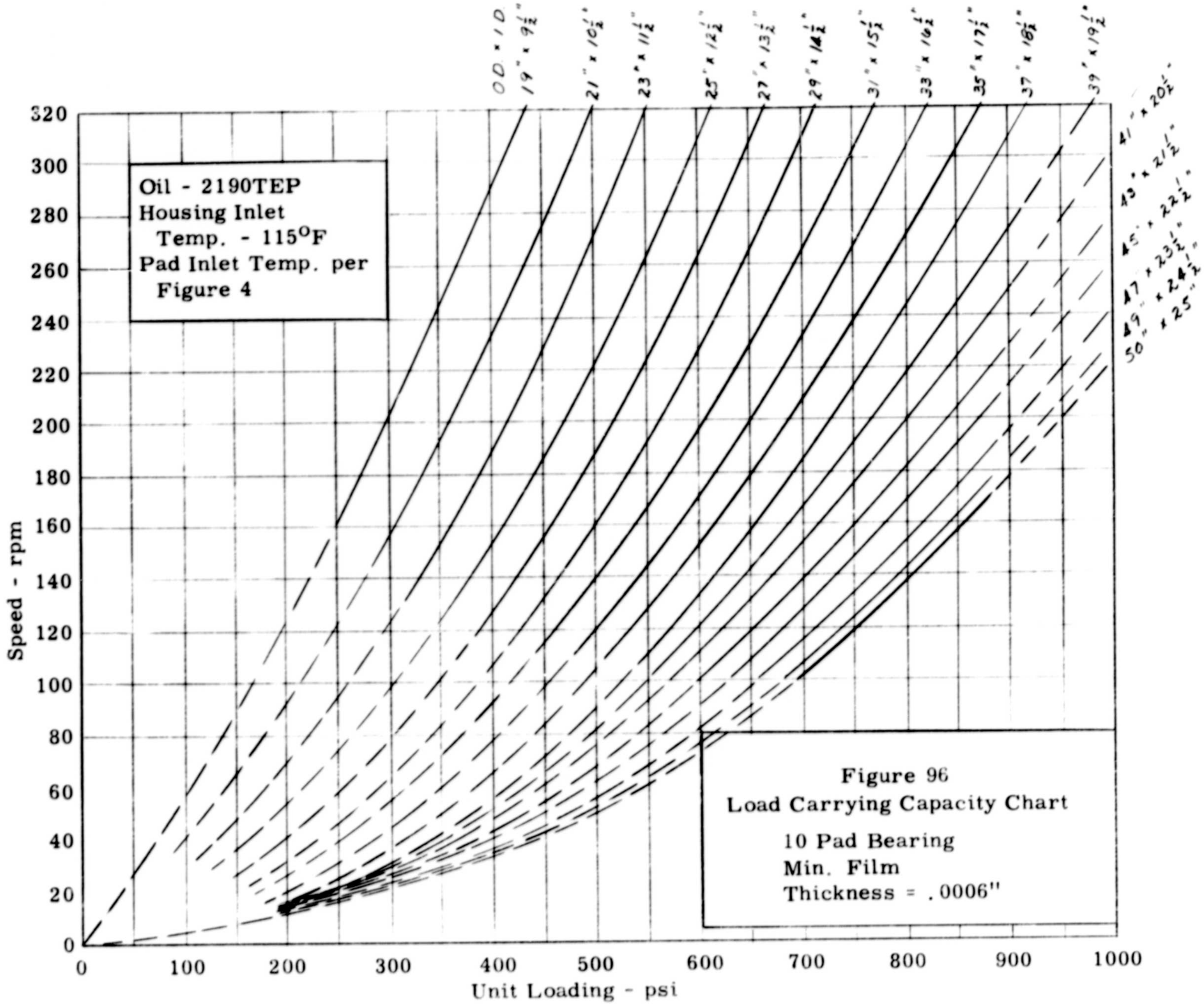

Figure 96
Load Carrying Capacity Chart

10 Pad Bearing
Min. Film
Thickness = .0006"

FIGURE 97

CHART OF HYDRODYNAMIC OIL FLOW PER PAD
OIL - 2190T
Average Film Temperature per Figure 87

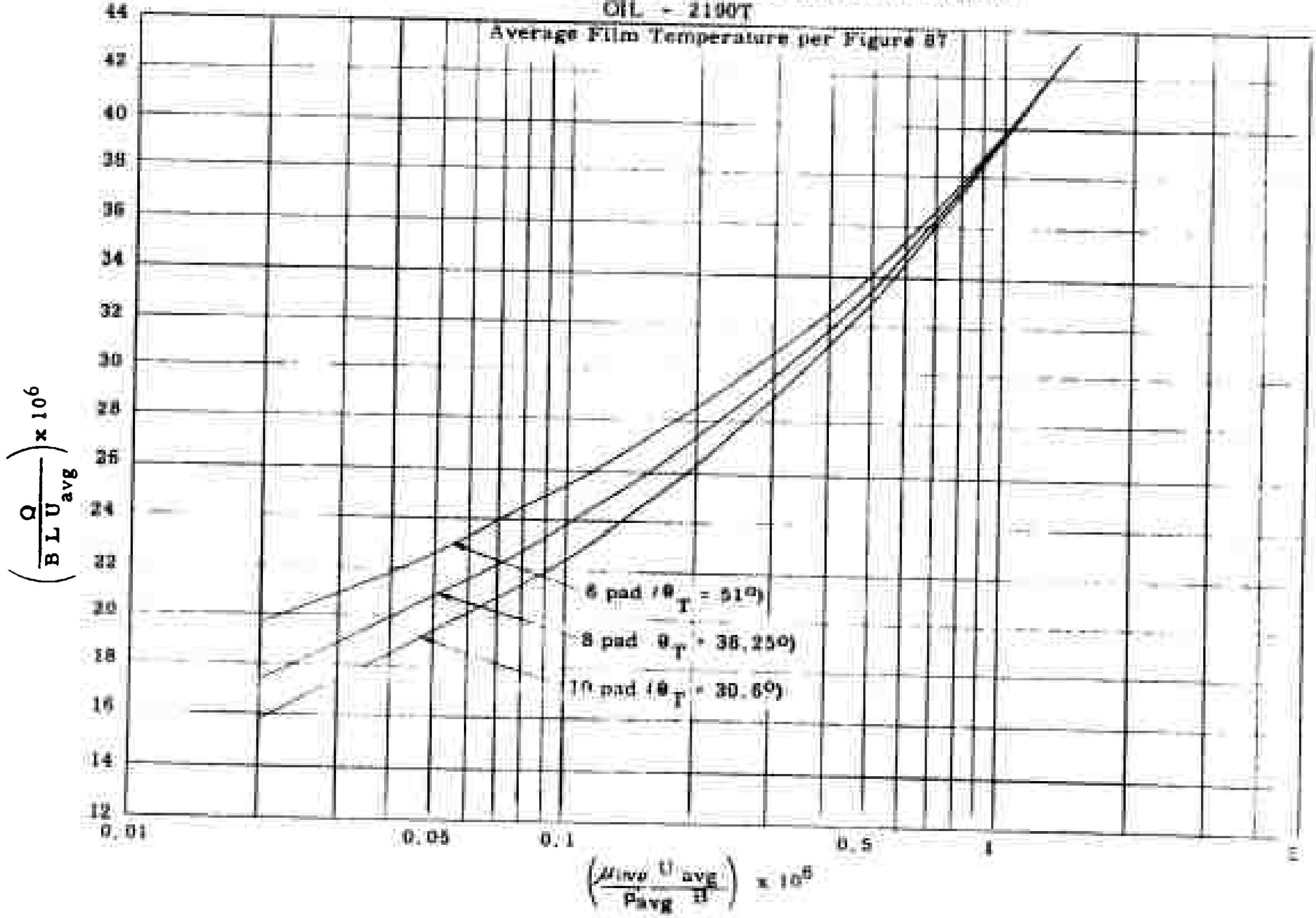

FIGURE 98

CHART OF HORSEPOWER LOSS PER PAD

OIL - 2190T

Average Film Temperatures per Fig. 87

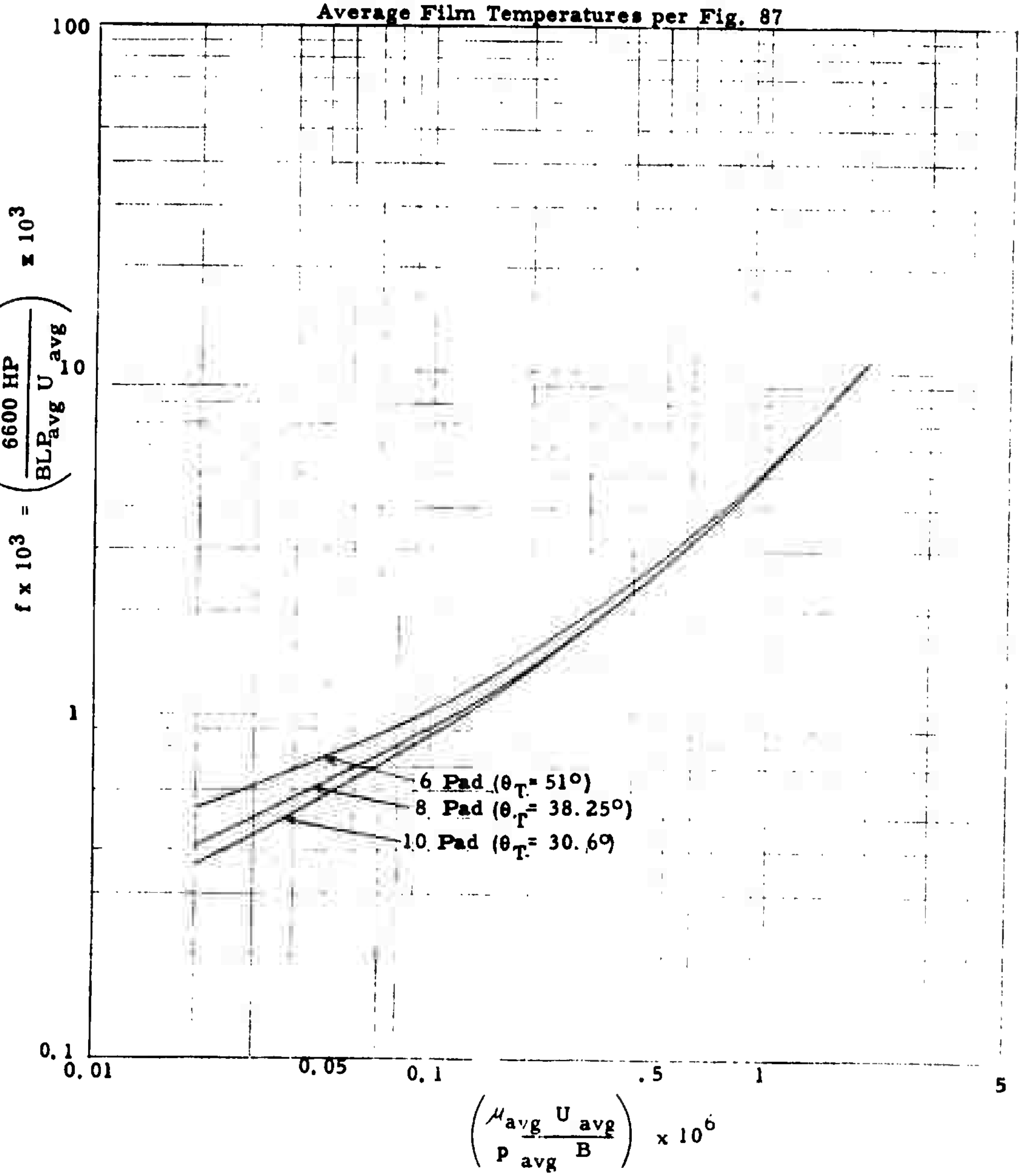

Figure 99
Location of Point of Minimum Film Thickness
31" OD x 15 1/2" ID Bearing At 320 RPM
Data per Table 3

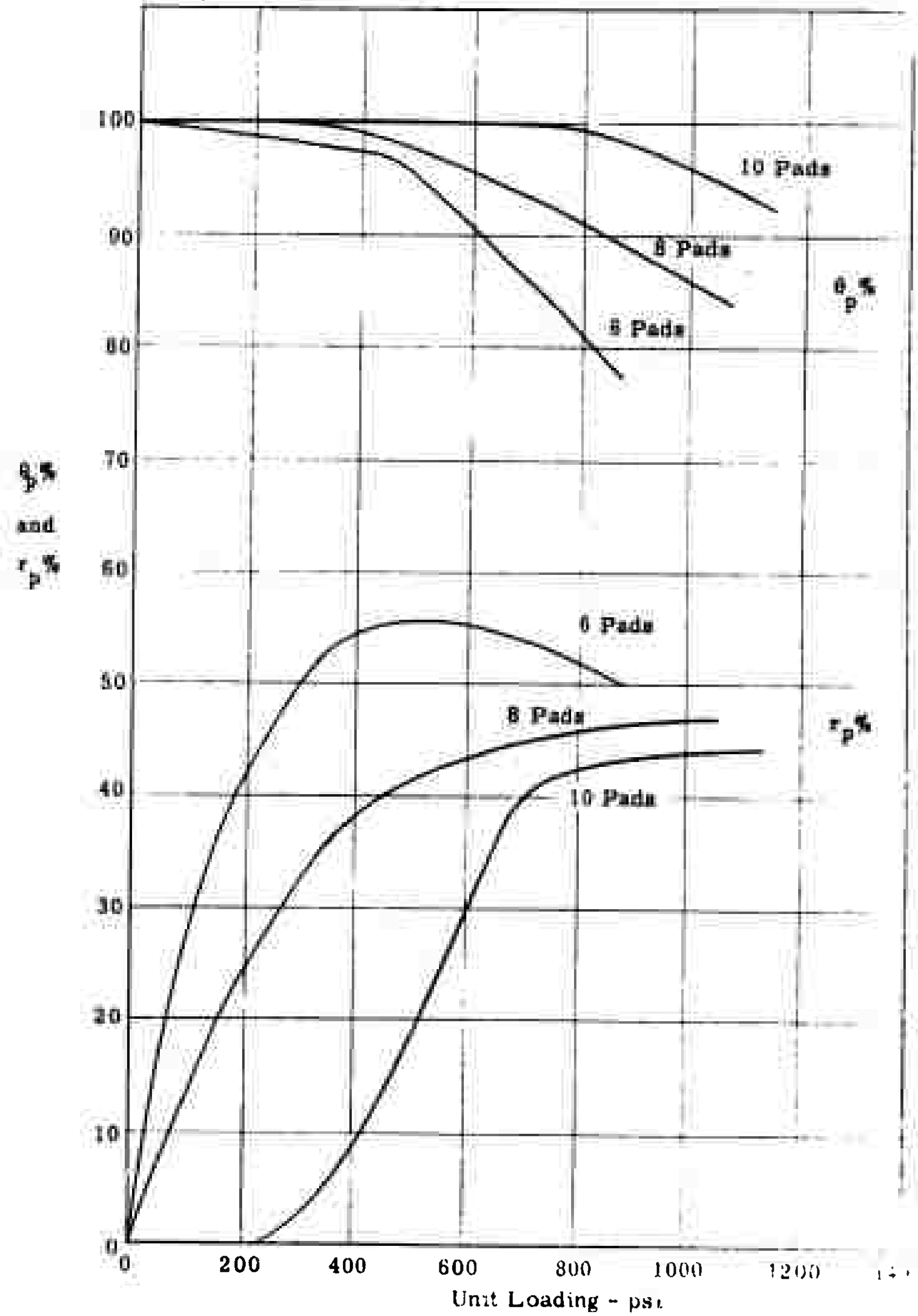

FIGURE 100

FILM THICKNESS VS. LOAD

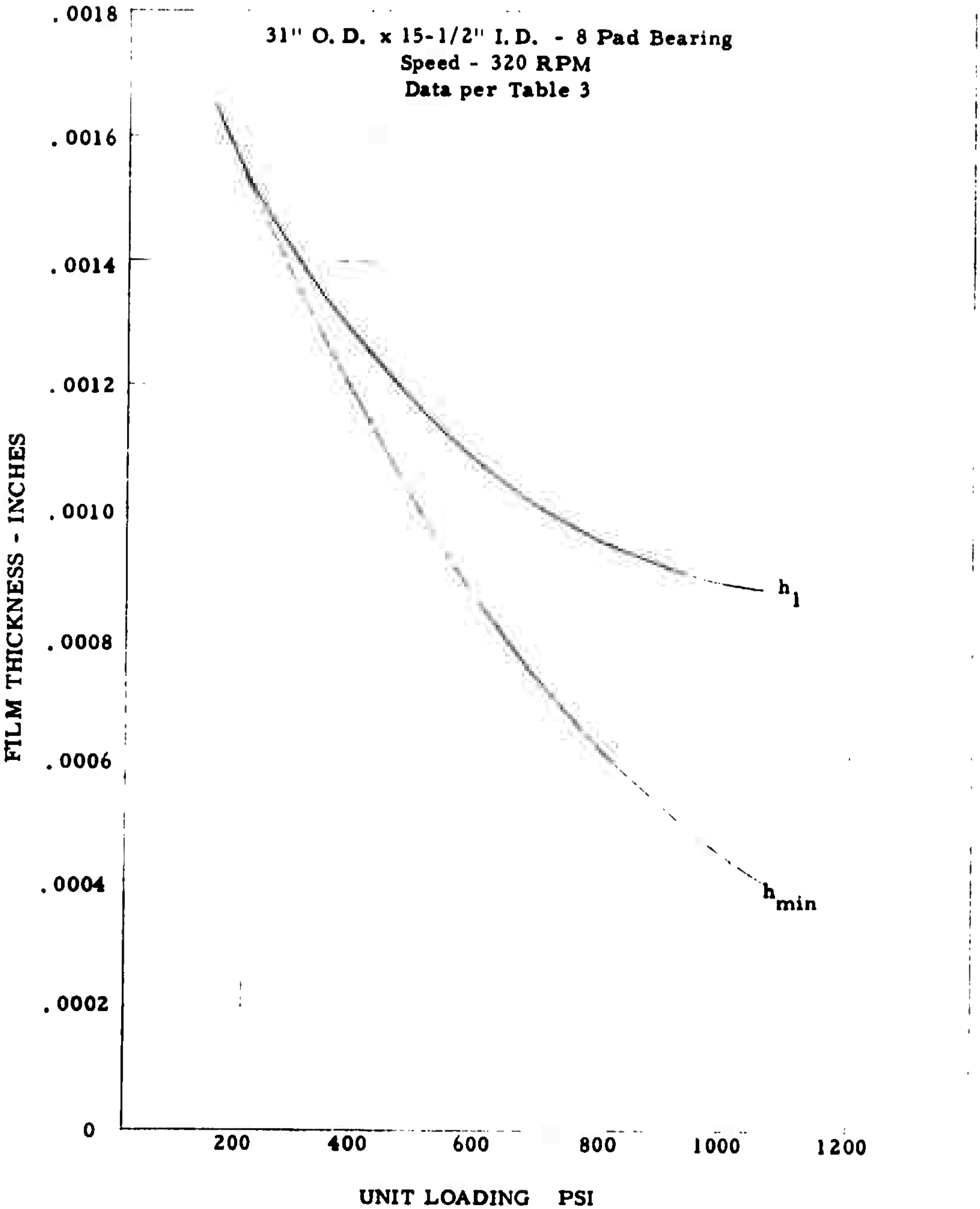

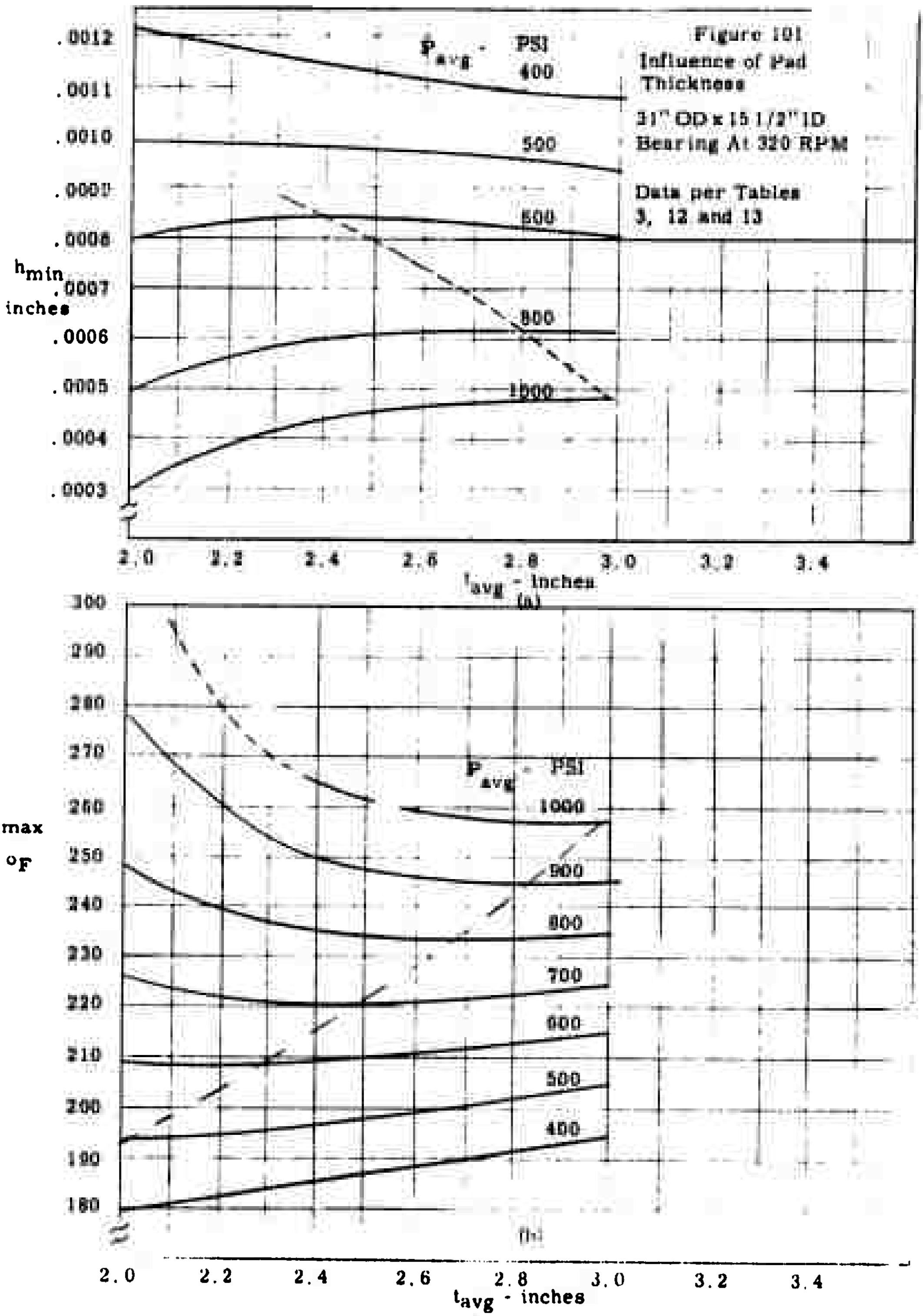

Figure 101
Influence of Pad Thickness

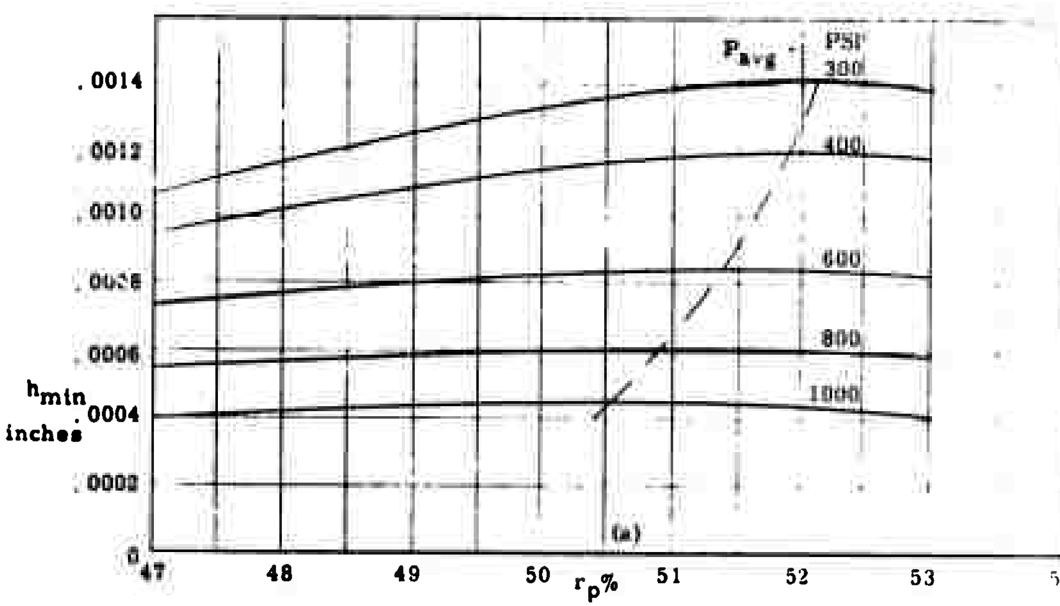

Figure 102
Influence of Radial Pivot Location
31" OD x 15 1/2" ID Bearing
At 320 RPM

Data per Tables 3, 14 and 15

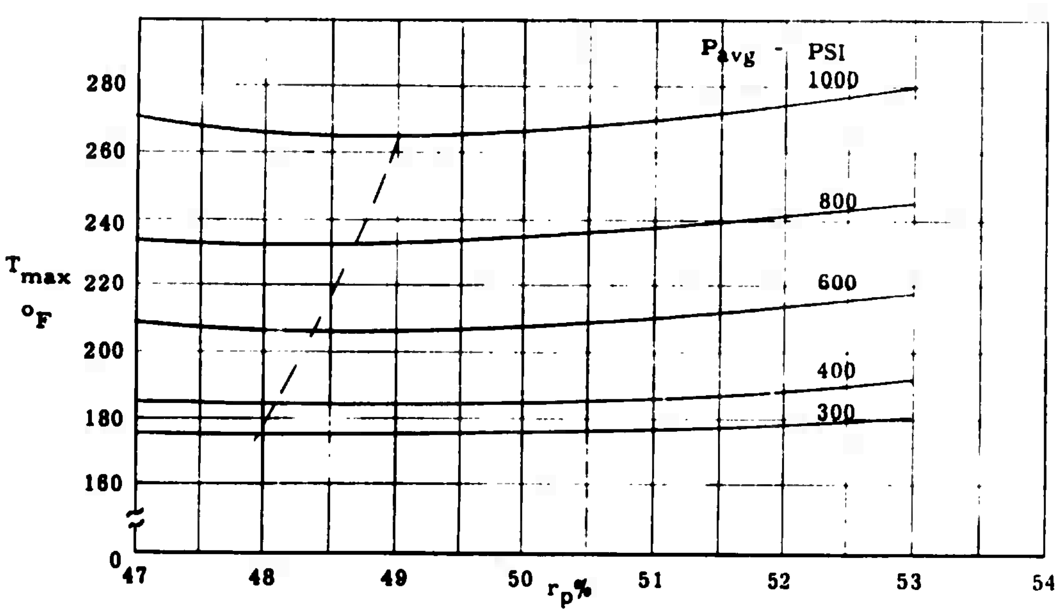

(b)

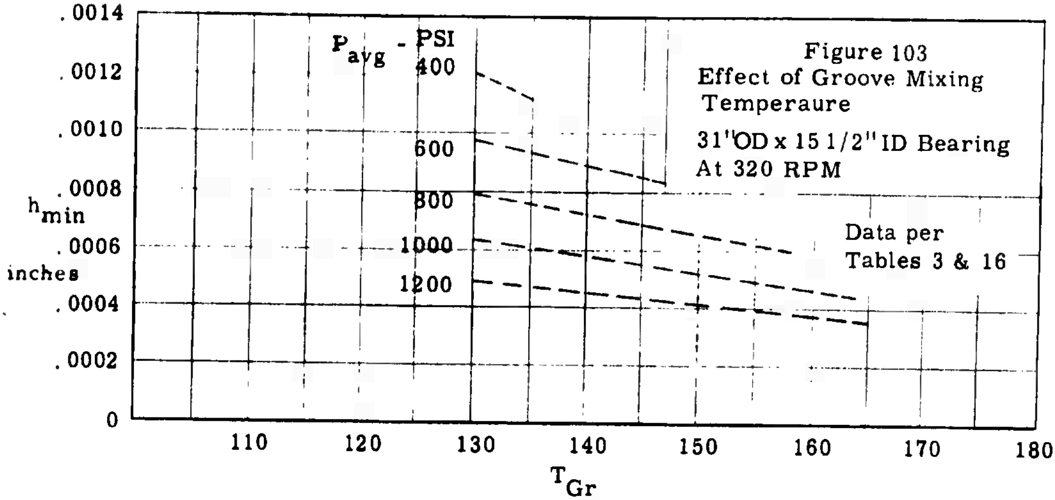

Figure 103
Effect of Groove Mixing Temperaure
31" OD x 15 1/2" ID Bearing
At 320 RPM
Data per Tables 3 & 16
P_{avg} - PSI
400
600
800
1000
1200
h_{min} inches
.0014
.0012
.0010
.0008
.0006
.0004
.0002
0
110
120
130
140
150
160
170
180
T_{Gr}

(a)

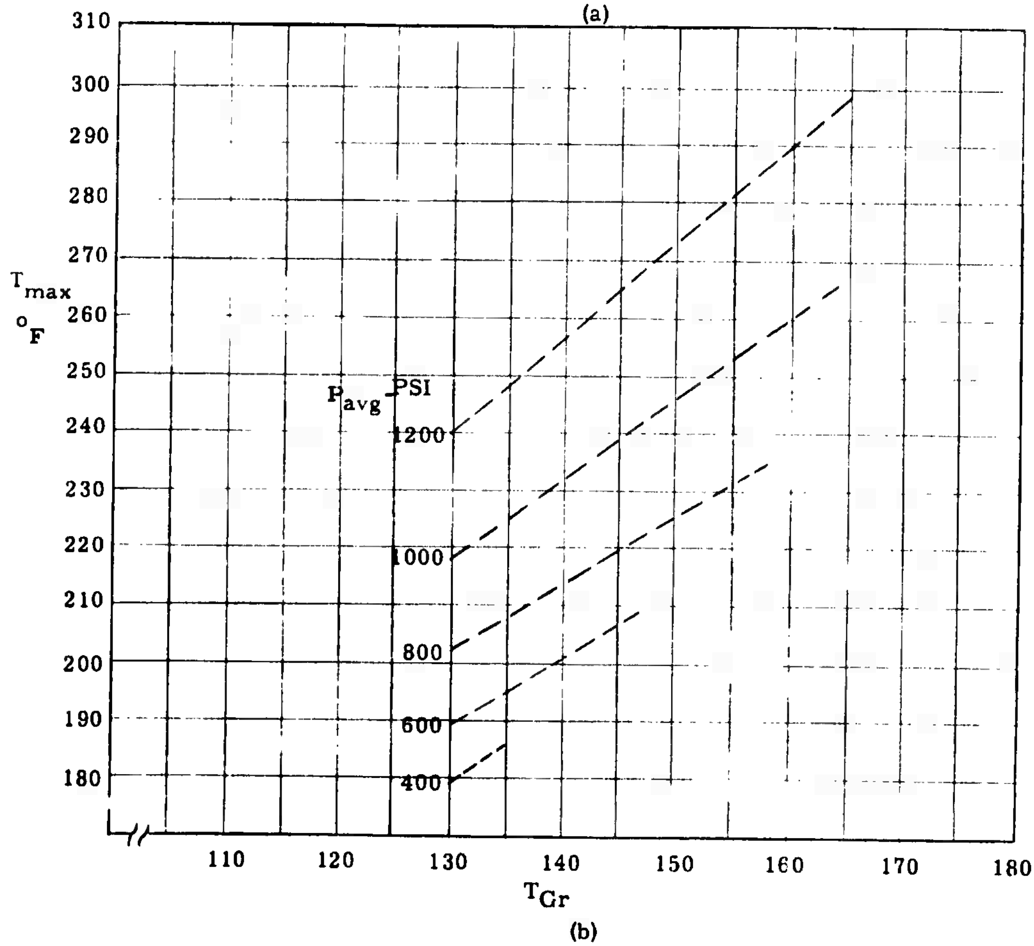

T_{max} ^oF
310
300
290
280
270
260
250
240
230
220
210
200
190
180
P_{avg}-PSI
1200
1000
800
600
400
110
120
130
140
150
160
170
180
T_{Gr}

(b)

FIGURE 104

COMPARISON OF PRESSURE PROFILES

31" OD x 15 1/2" ID Bearing (θ_{tot} = 38.25°)

h_{min} = 0.001" T_{Gr} = 130°F

N = 320 rpm 2190T Oil

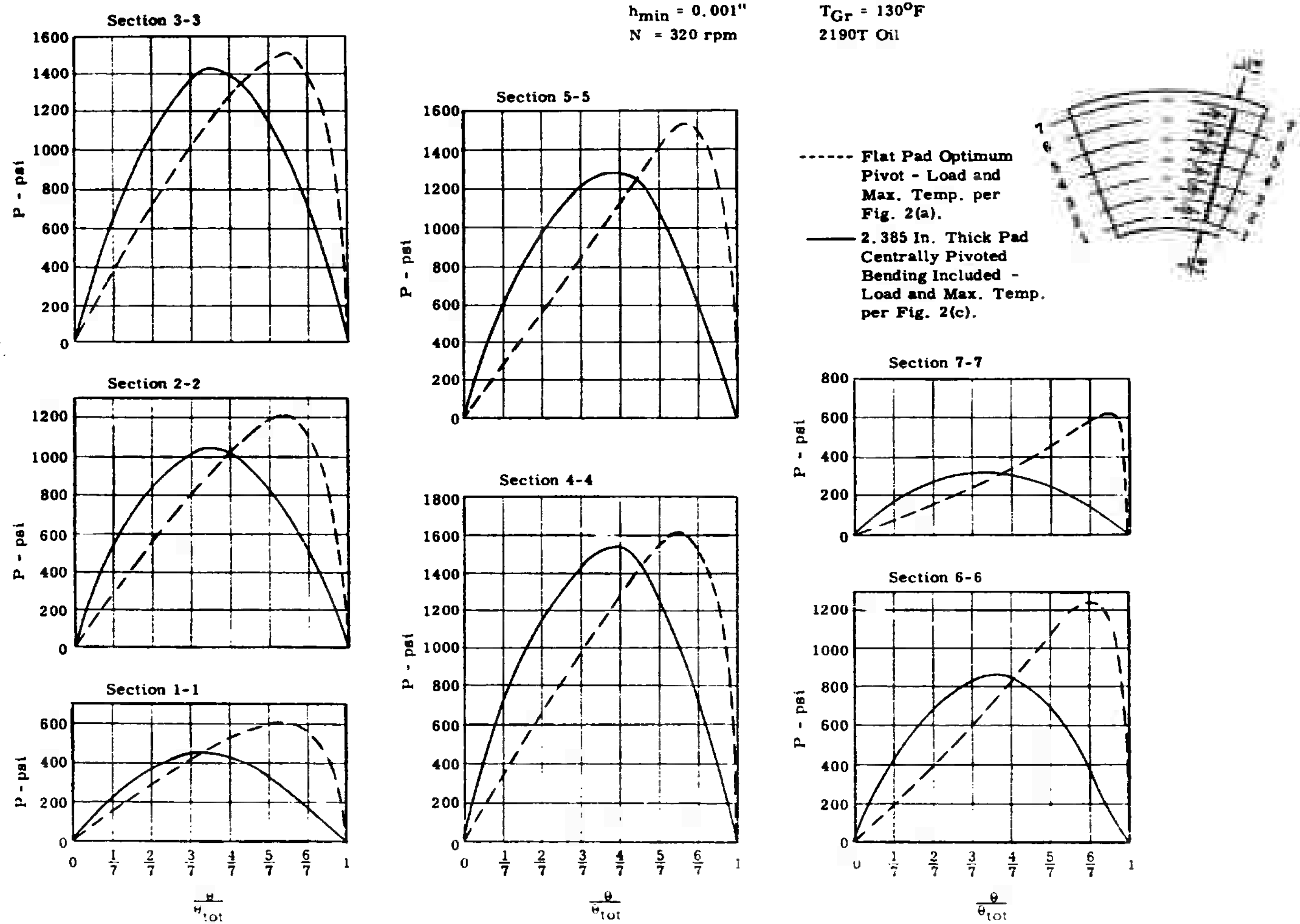

SYMBOLS

a	Radius of equivalent circular plate	inches
B	Average circumferential pad length $\left[= (R - L/2)\ \theta_T\right]$	inches
C_p	Specific heat of oil	BTU/lb. x °F
f	Coefficient of friction	
h	Film thickness	inches
h_i	Film thickness at inside radius of trailing edge	inches
h_a	Film thickness at reference point (r_a, θ_a)	inches
h_{min}	Minimum film thickness	inches
HP	Horsepower loss per pad	H. P.
HP_{tot}	Total horsepower loss in bearing	H. P.
$HP_{2,3,4}$	Components of pad horsepower loss corresponding to $Q_{2,3,4}$	H. P.
J	Mechanical equivalent of thermal energy (= 9339 in. lbs./BTU)	
k	Ratio of effective pad area to total available area $\left(= \dfrac{\text{Area of pads}}{\text{Area of pads + Area of grooves}}\right)$ (Also used as subscript to denote number of iterations.)	
K	Bending coefficient	inches^{-1}
L	Radial length of pad	inches
m_θ	Tangential pad inclination	radians
m_r	Radial pad inclination	radians
n	Number of pads in the bearing (Also used as subscript to denote outermost mesh in radial direction.)	
N	Angular speed	R. P. S.
p	Pressure	psi
p_{avg}	Average pressure (unit loading)	psi
p_{max}	Maximum pressure	psi
Q	Hydrodynamic flow per pad	G. P. M.
$Q_{1,2,3,4}$	Edge flow (see Figure 3)	G. P. M.
Q_{tot}	Hydrodynamic flow per bearing	G. P. M.
r	radial co-ordinate	inches
r_a	radial co-ordinate of reference point	inches
r_{cp}	radial co-ordinate of center of pressure	inches
$r_{cp}\%$	radial co-ordinate of center of pressure $\left\{= 100\left[r_{cp} - (R-L)\right]/L\right\}$	inches
r_m	radial co-ordinate of point of minimum film thickness	inches
r_p	radial co-ordinate of pivot	inches
$r_p\%$	radial co-ordinate of pivot $\left\{= 100\left[r_p - (R-L)\right]/L\right\}$	inches
R	Outer radius of pad	inches
R_c	Radius of curvature of bent pad	inches
t_{avg}	Average pad thickness	inches
T	Temperature	°F
T_{avg}	Average pad temperature	°F
T_{GR}	Groove mixing temperature	°F
T_{max}	Maximum film temperature	°F
U_{avg}	Average surface speed $\left[= 2\pi (R-L/2)\ N\right]$	inches/sec.
W	Load per pad	lbs.
W_{tot}	Total bearing load	lbs.
(x, y)	co-ordinates	inches
(x_a, y_a)	co-ordinates of reference point	inches
δ	Bending deflection	inches
Δ	Increment	
θ	Angular co-ordinate	radians
θ_{cp}	Angular co-ordinate of center of pressure	radians
$\theta_{cp}\%$	Angular co-ordinate of center of pressure $= 100\ (\theta_{cp}/\theta_T)$	radians
θ_m	Angular co-ordinate of point of minimum film thickness	radians
θ_p	Angular co-ordinate of pivot	radians
$\theta_p\%$	Angular co-ordinate of pivot $= 100\ (\theta_p/\theta_T)$	radians
θ_T	Angular extent of pad	radians
ρ	Mass density of oil	lb. sec^2/in^4
μ	Absolute viscosity of oil	lbs. sec./$in.^2$
μ_{GR}	Absolute viscosity of oil at T_{GR}	lb. sec./$in.^2$
μ_{avg}	Absolute viscosity of oil at T_{avg}	lb. sec./$in.^2$
ω	Angular velocity	radians/sec.

SUBSCRIPTS

i	Defines value of r in the thrust bearing pad mesh, running from 1 to n
j	Defines value of θ in the thrust bearing pad mesh, running from 1 to m
k	Iteration number

Bar above symbols denotes dimensionless quantity.